

# Application of super-element theory to crash-worthiness evaluation within the scope of the A.D.N. Regulations

**Hasan Özgür Uzögüten**

**Master Thesis**

presented in partial fulfillment  
of the requirements for the double degree:  
"Advanced Master in Naval Architecture" conferred by University of Liege  
"Master of Sciences in Applied Mechanics, specialization in Hydrodynamics,  
Energetics and Propulsion" conferred by Ecole Centrale de Nantes

developed at West Pomeranian University of Technology, Szczecin  
in the framework of the

**"EMSHIP"**  
**Erasmus Mundus Master Course**  
**in "Integrated Advanced Ship Design"**

Ref. 159652-1-2009-1-BE-ERA MUNDUS-EMMC

Supervisor: Prof. Maciej Taczala, West Pomeranian University of Technology  
Ing. Nzengu Wa Nzengu, Bureau Veritas DNI, Belgium

Reviewer: Prof. Hervé Le Sourne, L'Institut Catholique d'Arts et Métiers, France

Szczecin, February 2016



## **ABSTRACT**

The design requirements for the carriage of dangerous goods by inland waterways include the provisions dealing with vessel survival capability and location of the cargo tank within the vessel, notably:

- tankers are expected to survive the normal effects of flooding following damage externally caused
- cargo tanks are required to be protected from penetration in the event of minor damage to the vessel, e.g. from handling alongside by tugs/pushers, and having as well a degree of protection from damage in the event of collision.
- limitations are imposed to cargo tank size, intended to restrict the amount of cargo which may escape in the event of accidental breaching.

Vessels not complying with the above design requirements shall be protected through a more crashworthy side structure. The crash-worthiness shall be proved by applying the method prescribed in section 9.3.4 of A.D.N., i.e., by comparing the risk of a conventional construction (reference construction), complying with the A.D.N. Regulations with the risk of a crashworthy construction (alternative construction). When the risk of the more crashworthy construction is equal to or lower than the risk of the conventional construction, equivalent or higher safety is proved. The equivalent or higher safety shall be proven using a probabilistic approach.

In this thesis, crash-worthiness evaluation of a Type C inland tanker will be carried out through the instrumentality of the SHARP tool. The difference between the application of super-element and finite-element method will be presented in the light of *Section 9.3.4. Alternative Constructions* of A.D.N.. Finally, the risk of cargo tank rupture of the alternative construction in the aftermath of the collision will be assessed in order to provide a design with the better crash-worthiness by comparing the risk of cargo tank rupture with the conventional (reference) construction.

## **Declaration of Authorship**

I declare that this thesis and the work presented in it are my own and has been generated by me as the result of my own original research.

Where I have consulted the published work of others, this is always clearly attributed.

Where I have quoted from the work of others, the source is always given. With the exception of such quotations, this thesis is entirely my own work.

I have acknowledged all main sources of help.

Where the thesis is based on work done by myself jointly with others, I have made clear exactly what was done by others and what I have contributed myself.

This thesis contains no material that has been submitted previously, in whole or in part, for the award of any other academic degree or diploma.

I cede copyright of the thesis in favour of the West Pomeranian University of Technology.

Date:

Signature

## **Contents**

<b>ABSTRACT</b>	<b>1</b>
<b>1 INTRODUCTION</b>	<b>18</b>
1.1 General . . . . .	18
1.2 Objectives of the study . . . . .	19
1.3 Main steps of the study . . . . .	19
<b>2 CLASSIFICATION AND CARRIAGE OF THE DANGEROUS GOODS</b>	<b>21</b>
2.1 Definition . . . . .	21
2.2 Classification . . . . .	21
2.3 Carriage of Dangerous Goods by Inland Waterways . . . . .	22
2.3.1 Dangerous goods allowed for carriage in inland tank vessels . . . . .	22
2.3.2 Design requirements . . . . .	23
2.3.3 Type of vessels . . . . .	23
<b>3 INVESTIGATED VESSEL WITHIN THE STUDY</b>	<b>25</b>
3.1 General . . . . .	25
3.2 Main features of the vessel . . . . .	26
3.3 Structural Configuration . . . . .	27
3.4 Hull strength check approach . . . . .	29
3.4.1 General . . . . .	29

3.4.2	Partial safety factor . . . . .	29
3.4.3	Net scantling . . . . .	29
3.4.4	Limit states . . . . .	33
3.4.5	Design Loads . . . . .	33
3.5	Strength check . . . . .	35
3.5.1	General . . . . .	35
3.5.2	Hull scantling . . . . .	35
3.5.2.1	MARS Inland Software . . . . .	35
3.5.2.2	Hull girder yielding check . . . . .	38
3.5.2.3	Hull scantling results . . . . .	39
3.5.3	Strength check of primary supporting members . . . . .	40
3.5.3.1	FEMAP Software . . . . .	40
3.5.3.2	Modelling . . . . .	40
3.5.3.3	Loading conditions and load cases . . . . .	40
3.5.3.4	Checking criteria . . . . .	42
3.5.3.5	Results of the direct calculation . . . . .	43
<b>4</b>	<b>A.D.N. ALTERNATIVE DESIGN PROCEDURE</b>	<b>45</b>
4.1	General . . . . .	45
4.2	Approach . . . . .	45
4.3	Calculation Procedure . . . . .	46
4.4	Determination of collision energy absorbing capacity . . . . .	52

4.4.1	Material Properties . . . . .	53
4.4.2	Rupture criteria . . . . .	54
4.4.3	Friction energy . . . . .	55

**5 SHIP COLLISION ANALYSIS 56**

5.1	General . . . . .	56
5.2	Internal Mechanics . . . . .	56
5.2.1	Experimental Methods . . . . .	57
5.2.2	Empirical Methods . . . . .	59
5.2.2.1	Minorsky’s Method (1959) . . . . .	59
5.2.2.2	Enhancements to Minorsky’s Method . . . . .	60
5.2.2.3	Paik’s stiffened plate approach . . . . .	62
5.2.3	Simplified Analytical Methods . . . . .	62
5.2.3.1	Super-element theory . . . . .	62
5.2.4	Numerical Methods . . . . .	71
5.2.4.1	Non-linear Finite Element Analysis . . . . .	71
5.2.4.2	Idealized Structural Unit Method . . . . .	72
5.3	External Dynamics . . . . .	73
5.3.1	Minorsky’s Method . . . . .	73
5.3.2	DAMAGE . . . . .	74
5.3.3	MCOL . . . . .	75
5.4	Coupling of Internal and External Models . . . . .	76

5.4.1	SHARP Tool . . . . .	76
5.4.2	SIMCOL . . . . .	76
5.4.3	LS-DYNA finite element solver (with MCOL) . . . . .	78
<b>6</b>	<b>SHARP TOOL</b>	<b>79</b>
6.1	General . . . . .	79
6.2	FEM versus SHARP Tool . . . . .	81
6.2.1	Material properties . . . . .	81
6.2.2	Rupture Criteria . . . . .	83
6.2.3	Friction energy . . . . .	84
6.2.4	Contribution of shear forces . . . . .	85
6.3	Modelling of struck vessel . . . . .	85
6.4	Handling of the results . . . . .	86
6.5	Determined collision energy values . . . . .	87
<b>7</b>	<b>APPLICATION OF SHARP TO CRASH-WORTHINESS ASSESSMENT OF THE INVESTIGATED VESSEL</b>	<b>91</b>
7.1	General . . . . .	91
7.2	Modelling of struck vessel . . . . .	91
7.2.1	Hull form modelling . . . . .	91
7.2.2	Structural modelling . . . . .	93
7.2.2.1	Definition of the surfaces . . . . .	93
7.2.2.2	Definition of the scantlings . . . . .	95



7.2.2.3	Material properties . . . . .	96
7.3	Modelling of striking vessels . . . . .	98
7.4	Creating the collision scenarios . . . . .	104
7.5	Generating hydrodynamics matrices . . . . .	107
7.5.1	HydroStar . . . . .	107
7.5.2	ARGOS . . . . .	108
7.5.3	Procedure to create .MCO files . . . . .	110
7.6	Simulations . . . . .	113
7.7	Application of A.D.N Alternative Constructions (9.3.4.) . . . . .	117
7.7.1	Calculations . . . . .	117
7.7.2	Results . . . . .	122
<b>8</b>	<b>CONCLUSIONS AND RECOMMENDATIONS</b>	<b>123</b>
<b>9</b>	<b>ACKNOWLEDGEMENTS</b>	<b>125</b>
	<b>REFERENCES</b>	<b>126</b>
<b>A</b>	<b>APPENDIX: RULE STRENGTH CHECK</b>	<b>129</b>
<b>B</b>	<b>APPENDIX: DEFORMATION ENERGIES</b>	<b>142</b>
<b>C</b>	<b>APPENDIX: EQUIVALENT THICKNESS FOR THE PLATINGS WITH HOLES</b>	<b>180</b>
<b>D</b>	<b>APPENDIX: VBA CODES FOR .MCO FILES</b>	<b>185</b>

## List of Figures

Figure 1	Alternative design check . . . . .	20
Figure 2	A type-C tank vessel for inland navigation . . . . .	25
Figure 3	General arrangement plan . . . . .	26
Figure 4	Typical midship section . . . . .	28
Figure 5	MARS Inland main interface . . . . .	36
Figure 6	Basic ship data input . . . . .	37
Figure 7	Modelling of the vessel . . . . .	37
Figure 8	Calculations and rule check . . . . .	38
Figure 9	Applied loads on the FEM model in FEMAP . . . . .	41
Figure 10	Rigid element in the aft part of the model . . . . .	42
Figure 11	Complete FEM model (Non-deformed and deformed) . . . . .	43
Figure 12	Von-Mises stress on web frame . . . . .	43
Figure 13	Von-Mises stress on lateral double bottom girder . . . . .	44
Figure 14	Definition of vertical striking positions . . . . .	47
Figure 15	Full-scale experiment in Germany (Woisin, 1979) . . . . .	58
Figure 16	Full-scale experiment in Netherlands (Zhang, 1999) . . . . .	58
Figure 17	Minorskys linear relation . . . . .	59
Figure 18	Representation of the super-elements in a ship structure . . . . .	65
Figure 19	Deformed configuration of the hull super-element . . . . .	66
Figure 20	Deformed configuration of the vertical bulkhead super-element . . . . .	67

Figure 21	Deformed configuration of the beam super-element . . . . .	68
Figure 22	Deformed configuration of the beam super-element . . . . .	70
Figure 23	Finite element analysis graphical representation . . . . .	71
Figure 24	Graphical user interface (GUI) of the SHARP . . . . .	77
Figure 25	SIMCOL workflow (Brown, 2001) . . . . .	77
Figure 26	LS-Dyna/MCOL collision simulation (Le Sourne et al., 2003) . . . . .	78
Figure 27	SHARP workflow (Paboeuf & Le Sourne et al., 2015) . . . . .	80
Figure 28	Comparison between the true stress-strain relation and SHARP . . . . .	82
Figure 29	Impact locations on side shell . . . . .	86
Figure 30	Results of the Scenario I . . . . .	88
Figure 31	Results of Scenario II . . . . .	88
Figure 32	Results of Scenario III . . . . .	89
Figure 33	Results of Scenario IV . . . . .	90
Figure 34	Building sections . . . . .	92
Figure 35	SHARP complete model . . . . .	93
Figure 36	Structural model from different views (hidden deck and outer shell) . . . . .	94
Figure 37	Striking ship definition interface . . . . .	99
Figure 38	Bow model of striking ship . . . . .	100
Figure 39	Illustration of push barge bow given by the A.D.N. . . . .	101
Figure 40	Modelled push barge striking vessel in SHARP . . . . .	102
Figure 41	Characteristic dimensions of V-bow . . . . .	103

Figure 42	V-Bow striking model in SHARP . . . . .	104
Figure 43	Draft points . . . . .	105
Figure 44	Vertical collision locations . . . . .	106
Figure 45	Created scenarios for each type of construction . . . . .	108
Figure 46	User interface of ARGOS . . . . .	109
Figure 47	Meshed models in HydroStar . . . . .	111
Figure 48	Encounter wave periods in Belgian coast (Zeebrugge) . . . . .	112
Figure 49	Scheldt estuary - Zeebrugge . . . . .	113
Figure 50	Running simulations . . . . .	114
Figure 51	3D model for push barge bow with an impact angle of 55 deg at just below deck . . .	115
Figure 52	3D collision model for v-shape bow with an impact angle of 90 deg at just below deck	115
Figure 53	A.D.N. Alternative design check . . . . .	122
Figure 54	Rule check for stiffeners (Part 1) . . . . .	130
Figure 55	Rule check for stiffeners (Part 2) . . . . .	131
Figure 56	Rule check for stiffeners (Part 3) . . . . .	132
Figure 57	Rule check for stiffeners (Part 4) . . . . .	133
Figure 58	Rule check for stiffeners (Part 5) . . . . .	134
Figure 59	Rule check for stiffeners (Part 6) . . . . .	135
Figure 60	Rule check for stiffeners (Part 7) . . . . .	136
Figure 61	Rule check for stiffeners (Part 8) . . . . .	137
Figure 62	Rule check for stiffeners (Part 9) . . . . .	138

Figure 63	Rule check for strakes (Part 1) . . . . .	139
Figure 64	Rule check for strakes (Part 2) . . . . .	140
Figure 65	Rule check for strakes (Part 3) . . . . .	140
Figure 66	Rule check for strakes (Part 4) . . . . .	141
Figure 67	Rule check for strakes (Part 5) . . . . .	141
Figure 68	Scenario I, Case 1 - at bulkhead . . . . .	144
Figure 69	Scenario I / Case 2 / at bulkhead . . . . .	144
Figure 70	Scenario I / Case 3 / at bulkhead . . . . .	145
Figure 71	Scenario I, Case 1 - at web . . . . .	145
Figure 72	Scenario I / Case 2 / at web . . . . .	146
Figure 73	Scenario I / Case 3 / at web . . . . .	146
Figure 74	Scenario I, Case 1 - between webs . . . . .	147
Figure 75	Scenario I / Case 2 / between webs . . . . .	147
Figure 76	Scenario I / Case 3 / between webs . . . . .	148
Figure 77	Scenario II, Case 1 - at bulkhead . . . . .	148
Figure 78	Scenario II / Case 2 / at bulkhead . . . . .	149
Figure 79	Scenario II / Case 3 / at bulkhead . . . . .	149
Figure 80	Scenario II, Case 1 - at web . . . . .	150
Figure 81	Scenario II / Case 2 / at web . . . . .	150
Figure 82	Scenario II / Case 3 / at web . . . . .	151
Figure 83	Scenario II, Case 1 - between webs . . . . .	151

Figure 84	Scenario II / Case 2 / between webs . . . . .	152
Figure 85	Scenario II / Case 3 / between webs . . . . .	152
Figure 86	Scenario I, Case 1 - at bulkhead . . . . .	153
Figure 87	Scenario I / Case 2 / at bulkhead . . . . .	153
Figure 88	Scenario I / Case 3 / at bulkhead . . . . .	154
Figure 89	Scenario I, Case 1 - at web . . . . .	154
Figure 90	Scenario I / Case 2 / at web . . . . .	155
Figure 91	Scenario I / Case 3 / at web . . . . .	155
Figure 92	Scenario I, Case 1 - between webs . . . . .	156
Figure 93	Scenario I / Case 2 / between webs . . . . .	156
Figure 94	Scenario I / Case 3 / between webs . . . . .	157
Figure 95	Scenario I, Case 1 - at bulkhead . . . . .	157
Figure 96	Scenario I / Case 2 / at bulkhead . . . . .	158
Figure 97	Scenario I / Case 3 / at bulkhead . . . . .	158
Figure 98	Scenario I, Case 1 - at web . . . . .	159
Figure 99	Scenario I / Case 2 / at web . . . . .	159
Figure 100	Scenario I / Case 3 / at web . . . . .	160
Figure 101	Scenario I, Case 1 - between webs . . . . .	160
Figure 102	Scenario I / Case 2 / between webs . . . . .	161
Figure 103	Scenario I / Case 3 / between webs . . . . .	161
Figure 104	Scenario I, Case 1 - at bulkhead . . . . .	162

Figure 105	Scenario I / Case 2 / at bulkhead . . . . .	162
Figure 106	Scenario I / Case 3 / at bulkhead . . . . .	163
Figure 107	Scenario I, Case 1 - at web . . . . .	163
Figure 108	Scenario I / Case 2 / at web . . . . .	164
Figure 109	Scenario I / Case 3 / at web . . . . .	164
Figure 110	Scenario I, Case 1 - between webs . . . . .	165
Figure 111	Scenario I / Case 2 / between webs . . . . .	165
Figure 112	Scenario I / Case 3 / between webs . . . . .	166
Figure 113	Scenario I, Case 1 - at bulkhead . . . . .	166
Figure 114	Scenario I / Case 2 / at bulkhead . . . . .	167
Figure 115	Scenario I / Case 3 / at bulkhead . . . . .	167
Figure 116	Scenario I, Case 1 - at web . . . . .	168
Figure 117	Scenario I / Case 2 / at web . . . . .	168
Figure 118	Scenario I / Case 3 / at web . . . . .	169
Figure 119	Scenario I, Case 1 - between webs . . . . .	169
Figure 120	Scenario I / Case 2 / between webs . . . . .	170
Figure 121	Scenario I / Case 3 / between webs . . . . .	170
Figure 122	Scenario I, Case 1 - at bulkhead . . . . .	171
Figure 123	Scenario I / Case 2 / at bulkhead . . . . .	171
Figure 124	Scenario I / Case 3 / at bulkhead . . . . .	172
Figure 125	Scenario I, Case 1 - at web . . . . .	172

Figure 126	Scenario I / Case 2 / at web . . . . .	173
Figure 127	Scenario I / Case 3 / at web . . . . .	173
Figure 128	Scenario I, Case 1 - between webs . . . . .	174
Figure 129	Scenario I / Case 2 / between webs . . . . .	174
Figure 130	Scenario I / Case 3 / between webs . . . . .	175
Figure 131	Scenario I, Case 1 - at bulkhead . . . . .	175
Figure 132	Scenario I / Case 2 / at bulkhead . . . . .	176
Figure 133	Scenario I / Case 3 / at bulkhead . . . . .	176
Figure 134	Scenario I, Case 1 - at web . . . . .	177
Figure 135	Scenario I / Case 2 / at web . . . . .	177
Figure 136	Scenario I / Case 3 / at web . . . . .	178
Figure 137	Scenario I, Case 1 - between webs . . . . .	178
Figure 138	Scenario I / Case 2 / between webs . . . . .	179
Figure 139	Scenario I / Case 3 / between webs . . . . .	179
Figure 140	Web frame section . . . . .	181
Figure 141	Ordinary frame section . . . . .	183



## List of Tables

Table 1	Examples of design requirements (Bureau Veritas training materials) . . . . .	24
Table 2	Stiffener spacing . . . . .	27
Table 3	Deviation of structural configuration between Reference and Alternative design . . . . .	27
Table 4	Corrosion additions according to BV Rules . . . . .	30
Table 5	Coefficients $\alpha$ and $\beta$ for bulb profiles . . . . .	31
Table 6	Net modulus of longitudinal stiffeners . . . . .	31
Table 7	Net thickness of plate elements . . . . .	32
Table 8	Cross section properties of net scantling . . . . .	32
Table 9	Serviceability limit states . . . . .	33
Table 10	Still water bending moments . . . . .	34
Table 11	Total vertical bending moments . . . . .	34
Table 12	Hull girder stresses . . . . .	39
Table 13	Scantling summary . . . . .	39
Table 14	Boundary Conditions . . . . .	41
Table 15	Speed reduction and weighting factors for different scenarios . . . . .	49
Table 16	Weighting factors for each characteristic collision speed . . . . .	50
Table 17	Uniform strain and necking values in A.D.N. . . . .	54
Table 18	Comparison between the methods for the calculations of internal mechanics . . . . .	72
Table 19	Uniform strain and necking values in A.D.N. . . . .	83
Table 20	Main particulars of the ships in the validation . . . . .	87

Table 21	Collision scenarios for the validation . . . . .	87
Table 22	Applied reinforcements to Alternative Construction - 2 (gross thickness) . . . . .	96
Table 23	Created materials with different rupture strain values . . . . .	98
Table 24	Symbols of parameters of bow model in SHARP . . . . .	100
Table 25	Characteristic dimensions of barge bow . . . . .	101
Table 26	Drafts for the cases of vertical collision location cases . . . . .	106
Table 27	Summary of the energy results from SHARP . . . . .	116
Table 28	Weighting factors of vertical collision locations . . . . .	117
Table 29	Weighting factors of longitudinal collision locations . . . . .	117
Table 30	Total weighting factors corresponding to the respective collision location . . . . .	118
Table 31	A.D.N. probability calculations for Reference construction . . . . .	119
Table 32	A.D.N. probability calculations for Alternative construction - 1 . . . . .	120
Table 33	A.D.N. probability calculations for Alternative construction - 2 . . . . .	121
Table 34	Equivalent thickness calculations for web frame . . . . .	182
Table 35	Equivalent thickness calculations for ordinary frame . . . . .	184

## **Nomenclature**

ADN	: European Agreement concerning the International Carriage of Dangerous Goods by Inland Waterways
BV	: Bureau Veritas
DNI	: Direction de la Navigation Intérieure (Inland Navigation Management)
FEA	: Finite Element Analysis
FEM	: Finite Element Method
GUI	: Graphical User Interface
ICAM	: Institut Catholique dArts et Métiers
ITH	: Ikeda-Tanaka-Himeno
ISUM	: Idealized Structural Unit Method
QTF	: Quadratic Transfer Function
SHARP	: Ship Hazardous Aggression Research Program
SIMCOL	: Simplified Collision Model
SNAME	: Society of Naval Architects and Marine Engineers
UNECE	: United Nations Economic Commission for Europe

# 1 INTRODUCTION

## 1.1 General

Transportation of hazardous and polluting substances can cause risks not only for the limited environs of the vessel but also for a great number of people living near especially in European inland waterways which connect many large and highly populated cities and urban areas. United Nations Economic Commission for Europe (UNECE) has published a set of regulations called A.D.N. Regulations concerning international carriage of dangerous goods by inland waterways, in order to promote the safety of transportation by inland waters. The risks in transporting and handling hazardous substances must be anticipated by appropriate design countermeasures to reduce the eventuality of accidents and the consequences of such accidents which might create severe levels of pollution.

Accidental spillage of a vast amount of dangerous substances may be brought by an external injury caused by the collision. Dealing with the collision problem in inland waters is significantly important as well as in the marine collisions due to possible consequences. According to the World Casualty Statistics, a considerable number of losses results from collisions and grounding in marine field. Statistics show that between 2000 and 2010, 10% of total loss has its source in collisions which corresponds to 15-20 ships per annum.

There are many methods available to evaluate the crashing incident and structural damage. However, some of them are either too simple to describe the phenomena or reliable but time consuming and expensive. In recent years, non-linear finite element methods have widely been used to evaluate the collision problem. However, at the preliminary design phase, finite element analysis may not be feasible due to the required time for computation and its high cost. For that matter, a new simplified analytical tool based on upper bound theorem which implements the intermediate features among those methods, is developed in the research program named SHARP. Super-element approach has been implemented to solve the collision problem. It takes penetration of the collision into account in order to obtain crushing resistance from the expressions representing collision mechanics by using macro-structures so-called super-elements. SHARP tool has an user-friendly and practical graphical user interface, as well as being able to analyse different collision scenarios in a short time comparing to the finite element method.

## **1.2 Objectives of the study**

According to the A.D.N., the collision energy absorption capacity is traditionally determined by means of a finite element analysis (e.g. LS-DYNA, ABAQUS, etc.), which is quite time consuming, especially when a large number of required collision scenarios are simulated. Furthermore, before an optimal alternative design is reached, different alternative designs need to be examined, leading to a huge amount of time for modelling and computation by use of a finite element software program. To reduce this time, a simplified tool based on analytical formulations aiming to predict the collision energy absorption capability of the design is developed. This approach decomposes the ship structure into macro-elements, widely known as super-elements, then evaluates the individual strength of each super-element to collision. This simplified method delivers a quick and efficient procedure for rapid ship collision analysis.

As an objective of this thesis, crash-worthiness evaluation of a Type C inland tanker will be carried out through the instrumentality of the SHARP Tool. The difference between the application of the super-element and the finite-element method will be presented in the light of *Section 9.3.4. Alternative Constructions* of A.D.N. Finally, the risk of cargo tank rupture of the alternative construction in the aftermath of the collision will be assessed in order to provide better crashworthy design by comparing the risk of cargo tank rupture with conventional (reference) construction.

## **1.3 Main steps of the study**

The study has been performed according to the following methodology (see also Fig. 1):

1. Checking structural scantling complying with the BV Rules of Inland Navigation NR 217 for the investigated vessel.
  - Rule scantling check using Mars Inland software
  - Direct calculations using FEMAP-Nastran software
2. Determining necessary adaptations to utilize super-element method within Sec. 9.3.4 Alternative constructions of A.D.N. Regulations.
3. Modelling the struck ship
4. Choosing similar striking vessels from the database of BV and modelling in SHARP

5. Creating the scenarios and running the simulations in SHARP as prescribed in the A.D.N. Regulations
6. Conducting a comparative study between the different constructions

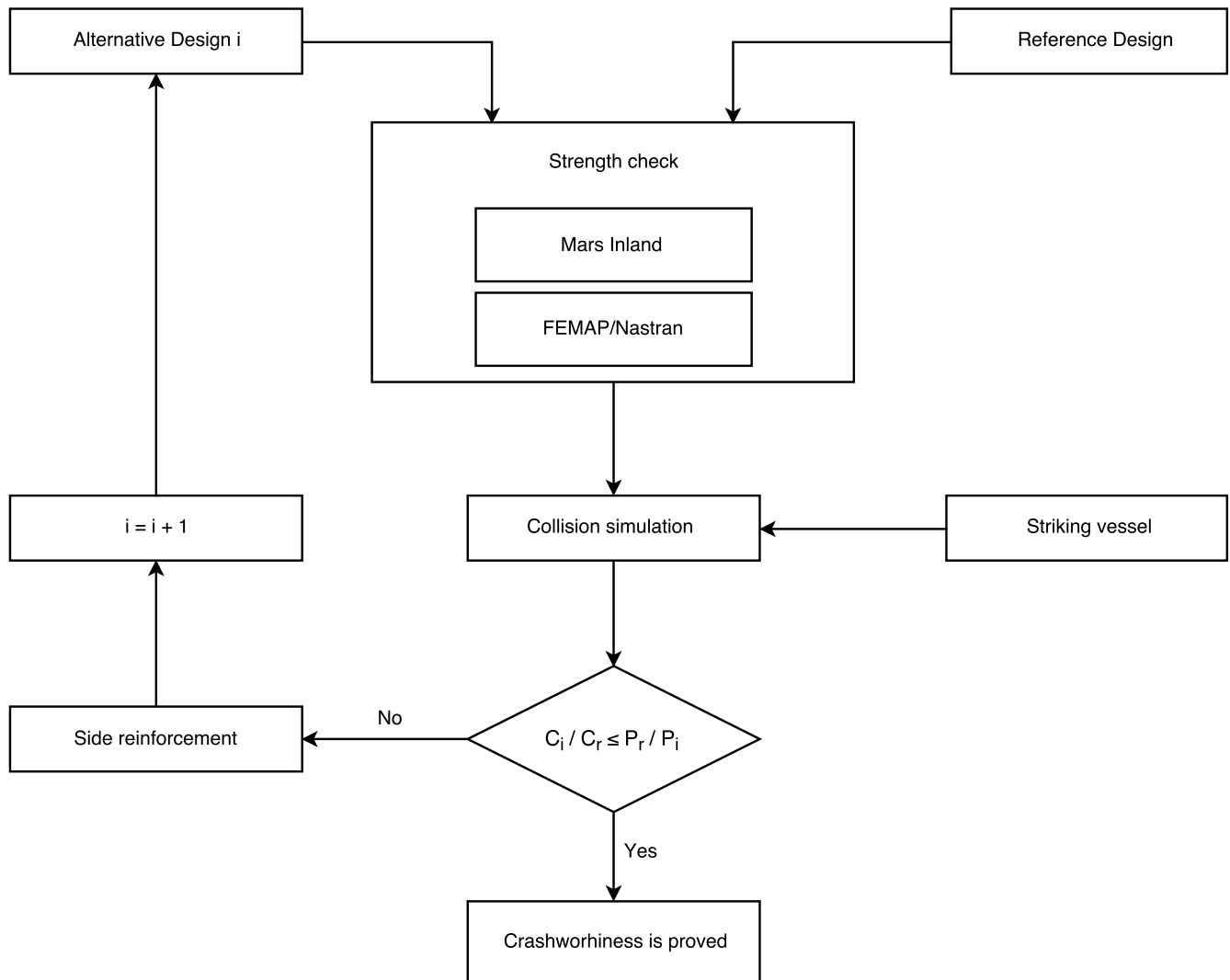


Figure 1: Alternative design check

## **2 CLASSIFICATION AND CARRIAGE OF THE DANGEROUS GOODS**

### **2.1 Definition**

Dangerous goods are substances that can harm people, other living organisms, or the environment.

### **2.2 Classification**

According to The Recommendations Transport of Dangerous Goods by UN, dangerous goods are divided into nine classes. Some of these classes are subdivided into divisions. These are:

#### **Class 1 Explosives**

**Division 1.1** Substances and articles which have mass explosion hazard.

**Division 1.2** Substances and articles which have a projection hazard but not a mass explosion hazard

**Division 1.3** Substances and articles which have a fire hazard and either a minor blast hazard or a minor projection hazard or both, but not a mass explosion hazard

**Division 1.4** Substances and articles which present no significant hazard

**Division 1.5** Very insensitive substances which have a mass explosion hazard

**Division 1.6** Very insensitive substances which do not have a mass explosion hazard

#### **Class 2 Gases**

**Division 2.1** Flammable gases

**Division 2.2** Non-flammable, non toxic gases

**Division 2.3** Toxic gases

#### **Class 3 Flammable liquids**

**Class 4** Flammable solids; substances liable to spontaneous combustion; substances which on contact with water, emit flammable gases

**Division 4.1** Flammable solids, self-reactive substances and solid desensitized explosives

**Division 4.2** Substances liable to spontaneous combustion

**Division 4.3** Substances which in contact with water emit flammable gases

**Class 5** Oxidizing substances and organic peroxides

**Division 5.1** Oxidizing substances

**Division 5.2** Organic peroxides

**Class 6** Toxic and infectious substances

**Division 5.1** Oxidizing substances

**Division 5.2** Organic peroxides

**Class 7** Radioactive materials

**Class 8** Corrosive substances

**Class 9** Miscellaneous dangerous substances and articles, including environmentally hazardous substances

## **2.3 Carriage of Dangerous Goods by Inland Waterways**

### **2.3.1 Dangerous goods allowed for carriage in inland tank vessels**

Not all dangerous goods are allowed to be transported by inland waterways. Transportation of these goods is regulated by the international agreements. In A.D.N. Regulations (Section 3.2.3.2. Table C), a list of dangerous goods which are allowed to be carried by inland navigation is shown associated with the design requirements. The dangerous goods of the classes listed below may be carried by tankers depending on their construction:

- **Class 2** Gases compressed, liquefied or dissolved under pressure;
- **Class 3** Flammable liquids;
- **Class 5.1** Oxidizing substances;
- **Class 6.1** Toxic substances;
- **Class 8** Corrosive substances;



- **Class 9** Miscellaneous dangerous substances and articles.

Table C of A.D.N is made of 20 columns.

- Columns (1) to (5) define identification and classification of the dangerous goods.
- Columns (6) to (20) give the applicable specific requirements to be complied with for the carriage of the dangerous goods, such as, type of tank vessel, cargo tank design, cargo tank type, cargo tank equipment, opening pressure of the high-velocity vent valve.

It is an extensive table with all the required information for carrying dangerous goods by inland vessels. Where a substance is specifically indicated by name in A.D.N., it shall be carried by the vessels complying with certain design requirements mentioned in A.D.N. Regulations.

### **2.3.2 Design requirements**

The rules for the construction of tank vessels intended to carry dangerous goods, are presented in A.D.N. Regulations (Chapter 9.3). It contains the design requirements for aspects such as material of construction, protection against penetration of gases, hold spaces, cargo tanks, ventilation, engine rooms, piping system, fire system, electrical installations and ship stability. Examples of vessel design requirements are given in Table 1 depending on the cargo dangers and physico-chemical properties.

### **2.3.3 Type of vessels**

Dangerous goods can be transported by the tank vessels of types G, C or N depending on the class of the substance. The type of the tank vessel is described in A.D.N. as following:

- **Type G** : tank vessel intended for the carriage of gases. Carriage may be under pressure or under refrigeration.
- **Type C** : tank vessel intended for the carriage of liquids. This type of vessel shall be constructed double hull. The vessel is to be flush deck/double hull type with double bottom. The cargo tanks may be independent tanks installed in the hold spaces, or may be formed by the inner structure.
- **Type N** : tank vessel intended for the carriage of liquids.

Table 1: Examples of design requirements (Bureau Veritas training materials)

<b>Dangers</b>	<b>Physico-chemical properties</b>	<b>Examples of design requirements</b>
	<ul style="list-style-type: none"> <li>- viscosity</li> <li>- freezing temp.</li> <li>- boiling temp.</li> </ul>	cargo temperature control
	<ul style="list-style-type: none"> <li>- density</li> <li>- vapour pressure</li> </ul>	structural strength Cargo tank pressure control
	transport temperature	independent cargo tank
corrosivity		special materials
reactivity - self-reactivity - with water - with other prod.		<ul style="list-style-type: none"> <li>- inerting or stabilizing</li> <li>- cargo tank separation from vessel sides</li> <li>- segregation of cargo tanks and systems.</li> </ul>
flammability		<ul style="list-style-type: none"> <li>- appropriate fire fighting system</li> <li>- Improved cofferdam and pump room ventilation</li> <li>- flammable vapour detection</li> <li>- controlled cargo tank venting</li> <li>- special electrical provisions</li> </ul>
health toxicity	vapour, liquid	<ul style="list-style-type: none"> <li>- toxic vapour detection</li> <li>- Improved cofferdam and pump room ventilation</li> <li>- controlled cargo tank venting</li> <li>- vapour return line to shore</li> <li>- closed sampling devices</li> <li>- high level filling alarm</li> </ul>
pollution		<ul style="list-style-type: none"> <li>- high level filling alarm</li> <li>- tank vessel type N, C, G</li> <li>- survival capability</li> </ul>

### **3 INVESTIGATED VESSEL WITHIN THE STUDY**

#### **3.1 General**

The evaluation of crash-worthiness within the scope of the A.D.N. Regulations is carried out for a Type-C tank vessel complying with the BV Rules for Classification of Inland Navigation Vessels NR 217. Main features of the vessel are given in Section 3.2. The structural configuration of the vessel and the following deviations of the vessel design with respect to the A.D.N. Regulations are represented in Section 3.3.

- Width of the side tank
- Maximum cargo tank volume

The compliance of the vessel design with the BV Rules is shown in Section 3.4.



Figure 2: A type-C tank vessel for inland navigation

### 3.2 Main features of the vessel

In this study, a typical Type C tanker is used as the reference vessel. This vessel is also constructed and equipped with the fulfilment of the requirements of A.D.N. Regulations.

Main particulars of the vessel are given as following:

- Length overall : 125.00 [m]
- Length between perpendiculars : 124.84 [m]
- Rule length : 122.40 [m]
- Breath : 11.42 [m]
- Depth : 6.00 [m]
- Draught : 4.50 [m]
- Block coefficient : 0.90
- Service speed : 11.40 [kn] (= 20 km/h)

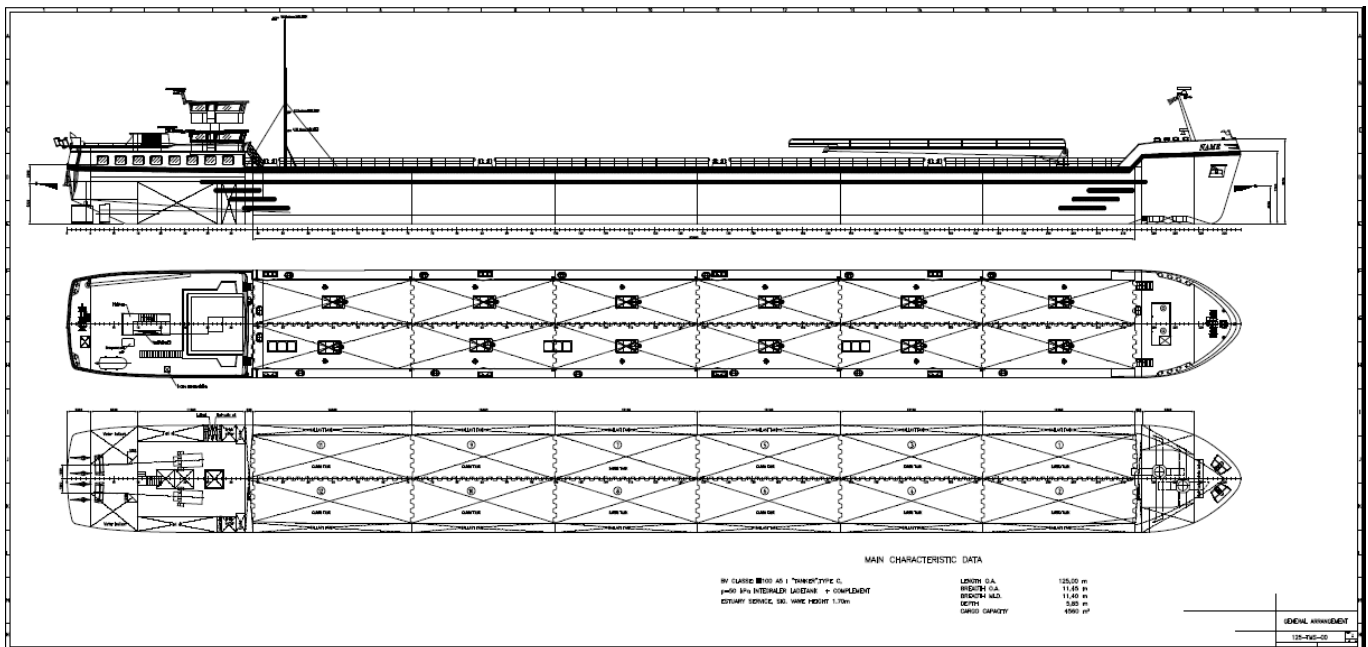


Figure 3: General arrangement plan

**Range of navigation:** IN(1.7)

**Loading sequence:** 2R (2 Runs)

**Propulsion:** Self-propelled

**Material type:** Steel - Grade A ( $R_{eH} = 235 \text{ N/mm}^2$ )

### 3.3 Structural Configuration

Type of the vessel: Tanker vessel Type C, double hull

The vessel is framed longitudinally through the bottom, side and deck. Spacing of longitudinal stiffeners and transverse primary supporting members are given in Table 2.

Table 2: Stiffener spacing

Elements	Spacing [m]
Bottom stiffeners	0.47
Inner bottom stiffeners	0.47
Side stiffeners	0.50
Inner side stiffeners	0.50
Deck stiffeners	0.47
Primary supporting member spacing	1.59

Double bottom heights:

- At side: 0.91 [m]
- At centre: 0.76 [m]

The deviations between the reference and the alternative constructions are summarized in Table 3.

Table 3: Deviation of structural configuration between Reference and Alternative design

	Reference vessel	Alternative design
side tank width [m]	1.0	0.8
cargo tank width [m]	(2 x 4.7) = 9.4	(2 x 4.9) = 9.8
tank capacity [ $m^3$ ]	377.7	390.7



## **3.4 Hull strength check approach**

### **3.4.1 General**

The hull strength check is carried out according to Bureau Veritas Rules for the classification of Inland Vessels NR 217, developed according to the main approaches described in sub-sections 3.4.2 to 3.4.4.

The scantling of structural members, primary supporting members excepted, is carried out using Mars Inland software. The strength check of primary supporting members is performed by direct calculation using FEMAP software

### **3.4.2 Partial safety factor**

The partial safety factors are introduced by the rules due to the uncertainties on some parameters. In BV Rules NR 217, those are defined as:

- $\gamma_{W1}$  : Partial safety factor covering the uncertainties regarding wave hull girder loads
- $\gamma_{W2}$  : Partial safety factor covering the uncertainties regarding wave local loads
- $\gamma_m$  : Partial safety factor covering the uncertainties regarding material
- $\gamma_R$  : Partial safety factor covering the uncertainties regarding resistance

### **3.4.3 Net scantling**

The scantlings obtained by applying the criteria specified in BV Rules are net scantlings, i.e. those which provide the strength characteristics required to sustain the loads, excluding any addition for corrosion.

Exceptions are the scantlings of:

- rudder structures and hull appendages
- massive pieces made of steel forgings, steel castings or iron castings.

The required strength characteristics are:

- thickness, for plating including that which constitutes primary supporting members

- section modulus, shear sectional area, moments of inertia and local thickness, for ordinary stiffeners and, as the case may be, primary supporting members
- section modulus, moments of inertia and single moment for the hull girder.

Table 4: Corrosion additions according to BV Rules

Compartment type		Corrosion addition (1)
Ballast tank		1.00
Cargo tank and fuel oil tank	Plating of horizontal surfaces	0.75
	Plating of non-horizontal surfaces	0.50
	Ordinary stiffeners and primary supporting members	0.75
Dry bulk cargo hold	General	1.00
	Inner bottom plating Side plating for single hull vessel Inner side plating for double hull vessel Transverse bulkhead plating	1.75
	Frames, ordinary stiffeners and primary supporting members	1.00
	Hopper well of dredging vessels	2.00
Accommodation space		0.00
Compartments and areas other than those mentioned above		0.50
(1) Corrosion additions are applicable to all members of the considered item.		

The corrosion addition for each of the two sides of a structural member is  $t_{C1}$  or  $t_{C2}$ . The total corrosion addition  $t_C$ , in mm, for both sides of a structural member, is equal to:

- for a plating with a gross thickness greater than 10 mm:

$$t_C = t_{C1} + t_{C2}$$

- for a plating with a gross thickness less than or equal to 10 mm:

$$t_C = 20\% \text{ of the gross thickness of the plating, or } t_C = t_{C1} + t_{C2}, \text{ whichever is smaller}$$

For an internal member within a given compartment, the total corrosion addition  $t_C$  is to be determined as follows:

- for a plating with a gross thickness greater than 10 mm:

$$t_C = 2t_{C1}$$



- for a plating with a gross thickness less than or equal to 10 mm:

$t_C = 20\%$  of the gross thickness of the plating, or  $t_C = 2 t_{C1}$ , whichever is smaller

The corrosion additions for the structural members of the different compartments are specified in rules (see Table 4).

The net strength characteristics are to be calculated for the net transverse section. As an alternative, the net section modulus of bulb profiles may be obtained from the following formula:

$$w = w_G (1 - \alpha t_C) - \beta t_C \quad (1)$$

where

$w_G$  : Stiffener gross section modulus, in  $cm^3$

$\alpha, \beta$  : Coefficients defined in Table 5.

A summary of the net modulus calculations is given in Table 6. According to BV Rules Part B Ch 2 Sec 5, the calculation of the net thickness of platings is shown in Table 7.

Table 5: Coefficients  $\alpha$  and  $\beta$  for bulb profiles

Range of $w_G$	$\alpha$	$\beta$
$w_G \leq 200 \text{ cm}^3$	0.070	0.4
$w_G > 200 \text{ cm}^3$	0.035	7.4

Table 6: Net modulus of longitudinal stiffeners

Items	Profile [cm]	Gross modulus [ $cm^2$ ]/[ $cm^3$ ]	Corrosion addition [mm]	Net Modulus [ $cm^2$ ]/[ $cm^3$ ]
Bottom longitudinals	(HP 140x8)	58.35 / 84.31	web: MIN(1.00x2; 0.20t) = 1.60	56.11 / 74.51
Inner bottom longitudinals	(HP 160x7)	48.64 / 105.10	web: MIN(1.00x2; 0.20t) = 1.40	46.40 / 94.65
Side longitudinals	(HP 140x7)	59.80 / 78.43	web: MIN(1.00x2; 0.20t) = 1.40	57.84 / 69.71
	(140x10 100x10)	71.50 / 197.42	1.00x2 = 2.00	66.70 / 160.74
Inner side longitudinals	(HP 120x7)	47.91 / 55.79	web: MIN(1.00x2; 0.20t) = 1.40	46.21 / 49.28
	(HP 140x7)	49.80 / 76.58	web: MIN(1.00x2; 0.20t) = 1.40	47.84 / 68.20
	(140x10 100x10)	61.50 / 192.67	1.00x2 = 2.00	56.70 / 157.27
Deck longitudinals	(HP 140x7)	58.12 / 78.43	web: MIN(0.75x2; 0.20t) = 1.40	56.16 / 69.71

Table 7: Net thickness of plate elements

Items	Gross thickness [mm]	Corrosion addition [mm]	Net thickness [mm]
Bottom	11	$1.00 + 0.50 = 1.50$	9.50
Bilge	13	$1.00 + 0.50 = 1.50$	11.50
Side	11	$1.00 + 0.50 = 1.50$	9.05
Sheerstrake	25	$1.00 + 0.50 = 1.50$	23.50
Deck stringer plate	11	$1.00 + 0.50 = 1.50$	9.50
Deck	11	$0.75 + 0.50 = 1.25$	9.75
Inner bottom	9	$\text{MIN}(1.00+0.75; 0.20t) = 1.75$	7.25
Inner side	9	$\text{MIN}(1.00+0.50; 0.20t) = 1.50$	7.50
Lateral double bottom girder	9	$\text{MIN}(1.00+1.00; 0.20t) = 1.80$	7.20
Central double bottom girder	7	$\text{MIN}(1.00+1.00; 0.20t) = 1.40$	5.60
Longitudinal bulkhead	7	$\text{MIN}(0.50+0.50; 0.20t) = 1.00$	6.00
Trans. cargo bulkhead	8	$\text{MIN}(0.50+0.50; 0.20t) = 1.00$	7.00
Web frame	8	$\text{MIN}(1.00+1.00; 0.20t) = 1.60$	6.40
Web frame (partition with manhole)	10	$\text{MIN}(1.00+1.00; 0.20t) = 2.00$	8.00

The geometric properties of the midship section corresponding to the net scantling are shown in Table 8.

Table 8: Cross section properties of net scantling

Geometric area of cross-section	0.6586 [m <sup>2</sup> ]
Effective area	0.6217 [m <sup>2</sup> ]
Single moment above neutral axis ( / neutral axis)	0.6951 [m <sup>3</sup> ]
Single moment of half section ( / centre line)	1.1849 [m <sup>3</sup> ]
Moment of inertia / Gy axis	3.6406 [m <sup>4</sup> ]
Moment of inertia / Gz axis	10.9807 [m <sup>4</sup> ]
Position of neutral axis (above base line)	2.8165 [m]
Modulus at deck (6.000 m)	1.1436 [m <sup>3</sup> ]
Modulus at bottom (0.000 m)	1.2926 [m <sup>3</sup> ]
Transverse sectional area of deck flange	0.1673 [m <sup>2</sup> ]
Transverse sectional area of bottom flange	0.1506 [m <sup>2</sup> ]

### 3.4.4 Limit states

The serviceability limit states adopted for the hull structure (hull girder, primary supporting members, plating, and ordinary stiffeners) are summarised in Table 9.

Table 9: Serviceability limit states

	Yielding	Plate strength under lateral loads	Buckling
Hull girder	x		
Primary supporting members	x		x
Plating		x	x
Stiffener	x		x

### 3.4.5 Design Loads

#### Design local loads

Local loads are pressures and forces which are directly applied to the individual structural members: plating panels, ordinary stiffeners and primary supporting members.

Still water local loads are constituted by the hydrostatic external river pressures and the static pressures and forces induced by the weights carried in the vessel spaces.

Wave local loads are constituted by the external river pressures due to waves and the inertial pressures and forces induced by the vessel accelerations applied to the weights carried in the vessel spaces.

#### Design hull girder loads

Hull girder loads are still water and wave forces and moments which result as effects of local loads acting on the vessel as a whole and considered as a beam.

With respect to the BV Rules NR 217 Part B Ch 3 Sec 2, calculated still water bending moments for different are shown in Table. 10

Table 10: Still water bending moments

	<b>Hogging [<math>kNm</math>]</b>	<b>Sagging [<math>kNm</math>]</b>
Design S.W.B.M. - Navigation condition	52 909	75 219
Design S.W.B.M. - Harbour condition	65 105	95 850
Design vertical wave bending moment	69 022	69 022

(*S.W.B.M.: Still Water Bending Moment*)

The total vertical bending moments at any hull girder transverse section is determined as specified in Table 11. considering the limit states.

Table 11: Total vertical bending moments

<b>Load case</b>	<b>Limit state</b>	<b>Hogging</b>	<b>Sagging</b>
Navigation	Hull girder yielding	$M_{TH} = M_H + M_W$	$M_{TS} = M_S + M_W$
	Other limit states	$M_{TH} = M_H + \gamma_W M_W$	$M_{TS} = M_S + \gamma_W M_W$
Harbour	All limit states	$M_{TH} = M_H$	$M_{TS} = M_S$

$\gamma_W$  : safety factor, taken equal to:

$$\gamma_W = 1.00 \text{ for } H_S = 0.6$$

$$\gamma_W = 0.625 \gamma_{W1} \text{ for } H_S > 0.6$$

## **3.5 Strength check**

### **3.5.1 General**

In this section, the strength check of the structure is carried out according to BV Rule requirements.

Scantlings of the plating and ordinary stiffeners of the midship section according to Bureau Veritas Rules are checked by Mars Inland software. The dimensions of all structural elements in the midship section are given and compared with the rule requirements. See Appendix A for the rule check output file provided by MARS Inland software which represents the results for all longitudinal stiffeners and plate strakes in detail.

The strength check of primary supporting members has been carried out by direct calculation using SIEMENS PLM Software FEMAP™.

### **3.5.2 Hull scantling**

#### **3.5.2.1 MARS Inland Software**

The scantling calculations are performed by using MARS Inland software developed by Bureau Veritas. MARS Inland software is capable of performing scantling calculations of platings and longitudinal stiffeners for any transversal section along the parallel body of the vessel. The strength check of primary supporting members and transversal elements has to be checked through direct calculation or finite element analysis. There are three modules in the main screen of the GUI:

- Basic Ship Data
- Edit
- Rule

In Basic Ship Data (BSD) module, the main particulars of the vessel are defined. This module is divided into seven subsections. Those are:

1. General
2. Notations & Main Data
3. Moment & Draughts

4. Bow Flare
5. Materials
6. Frame Locations
7. Calculations & Print

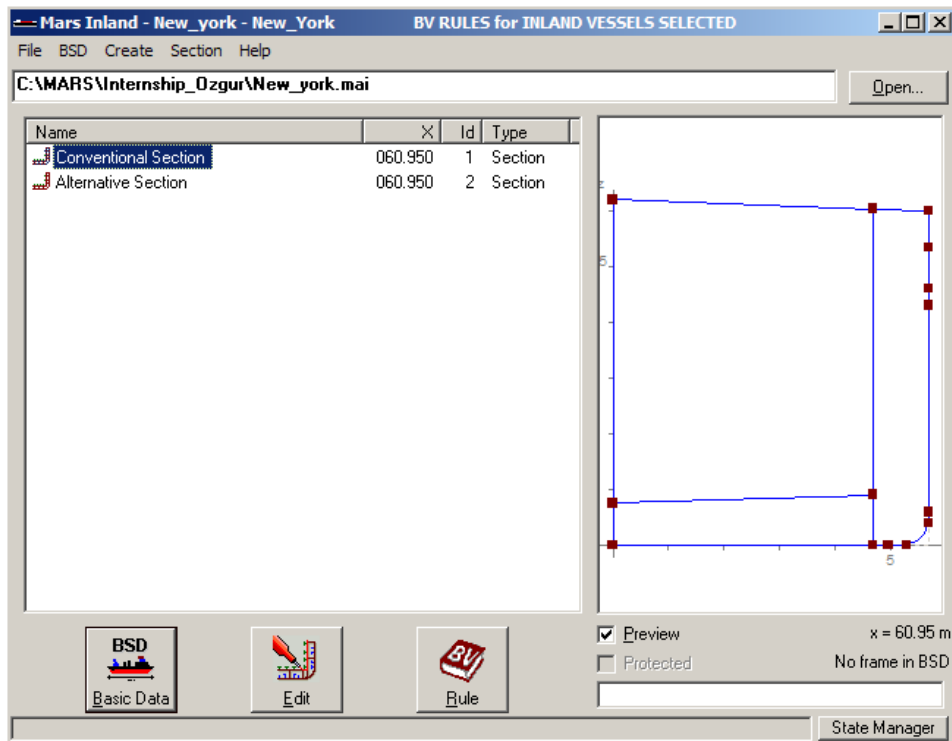


Figure 5: MARS Inland main interface

In *General* tab, general information of the vessel such as name, builder, hull number etc. is defined. In *Notations & Main Data* tab, main particulars and geometrical definitions are specified. In *Moment & Draughts* tab, if calculated a user specified still water bending moment can be entered, otherwise rule values will be used. If applicable, bow flares can be defined in *Bow Flare* tab. In *Materials* tab, material properties of the vessel at different parts can be defined. For investigated vessel, only one type of material has been used. Transverse frame locations is defined in *Frame Locations* tab.

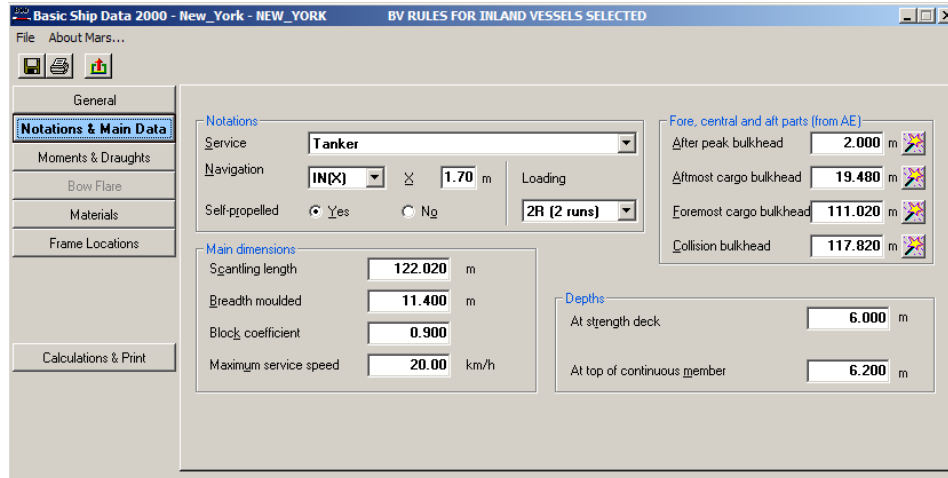


Figure 6: Basic ship data input

After the definition of the basic ship data, the section is modelled in *Edit* module. First, the geometry of the section is defined by nodes and panels. Then, plating strakes, longitudinal stiffeners, transversal stiffeners, compartments are defined. For all elements gross scantlings must be entered as the input dimensions. MARS Inland calculates net scantlings according to the compartment where the element is located as specified in the rules.

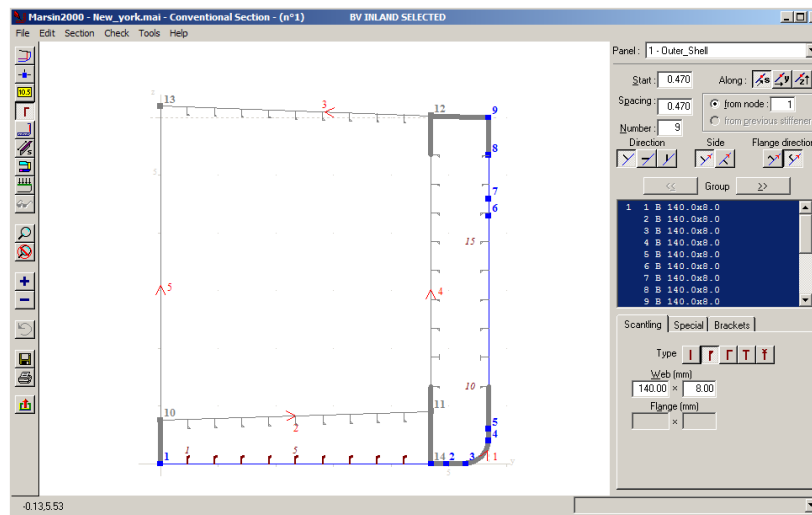


Figure 7: Modelling of the vessel

Finally, in the *Rule* module, yielding check of plates, and yielding, ultimate strength and buckling check of the longitudinal stiffeners are done. Also cross section properties for gross net scantling are given as output.

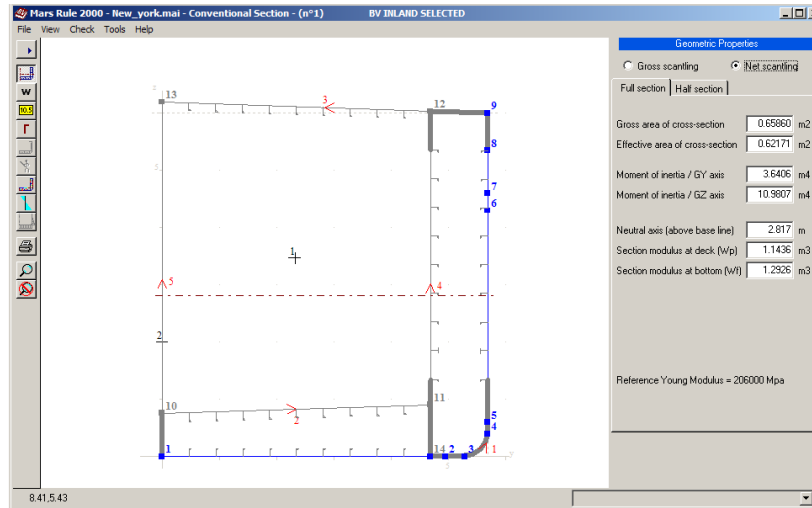


Figure 8: Calculations and rule check

### 3.5.2.2 Hull girder yielding check

The hull girder normal stresses induced by vertical bending moments are obtained from following formulae:

- In hogging condition

$$\sigma_1 = \frac{M_{TH}}{Z} 10^3 \quad [N/mm^2] \quad (2)$$

- In sagging conditions

$$\sigma_1 = \frac{M_{TS}}{Z} 10^3 \quad [N/mm^2] \quad (3)$$

Checking criteria for hull girder stress are given by the following equation:

$$\sigma_1 = MAX(\sigma_H; \sigma_S) \leq 192/k \quad [N/mm^2] \quad (4)$$

$k$  is the material factor, and is equal to 1 for ordinary strength shipbuilding steel ( $R_{eH} = 235 \text{ N/mm}^2$ )

Stresses are to be checked on the deck and the bottom of the section. As it can be seen in Table 12. the stress values for both hogging and sagging conditions are below the limit criteria thus hull girder stresses fulfil the rule requirements.



Table 12: Hull girder stresses

Items	Distance from baseline [m]	Hogging $\sigma_H$ [N/mm <sup>2</sup> ]	Sagging $\sigma_H$ [N/mm <sup>2</sup> ]
Bottom	0.0	111.8	135.6
Deck	6.0	126.3	153.2

### 3.5.2.3 Hull scantling results

Scantlings and the comparison between the rule minimum requirements are shown in Table 13. As it is seen, net scantlings are in compliance with the *Bureau Veritas Rules for the Classification of Inland Vessels NR 217*.

Table 13: Scantling summary

Items	As built net scantling	Rule net scantling
<b>Plating (thickness)</b>	[mm]	[mm]
Bottom	9.50	8.50
Bilge	11.50	8.50
Side	9.05	8.50
Sheerstrake	23.50	19.00
Deck stringer	9.50	9.50
Deck	9.75	6.25
Inner bottom	7.25	5.75
Inner side	7.50	7.50
Lateral double bottom girder	7.20	7.20
Central double bottom girder	5.60	4.60
<b>Stiffeners (area / section modulus)</b>	[cm <sup>2</sup> ] / [cm <sup>3</sup> ]	[cm <sup>3</sup> ]
Bottom stiffeners	56.11 / 74.51	57.90
Inner bottom stiffeners	46.40 / 94.65	69.86
Side stiffeners	57.84 / 69.71	24.89
	66.70 / 160.74	30.12
Inner side stiffeners	46.21 / 49.28	27.32
	47.84 / 68.20	51.53
	56.70 / 157.27	58.05
Deck stiffeners	56.16 / 69.71	47.25

### **3.5.3 Strength check of primary supporting members**

#### **3.5.3.1 FEMAP Software**

With the integration of FEMAP with NX Nastran, it serves as the pre and the post processing tool for Nastran solver. It is able to model complete geometry by using FEMAP interface. On the other hand, the modelling of the geometry can be done by importing geometry files generated by external CAD softwares such as CATIA, Pro/Engineer, AutoCAD, Solidworks.

The most severe condition is considered as the fully loaded case at its maximum draft and computations has been done for only this condition. After computation, Von-Mises equivalent stresses have been evaluated on primary supporting members. Critical stresses are proved to be lower than limit values in accordance with the BV Rules.

#### **3.5.3.2 Modelling**

Three cargo holds have been modelled for the analysis.

In BV Rules, there are some norms which have to be followed for direct calculation:

- The quadrilateral elements are to be defined with an aspect ratio not exceeding 4.
- The quadrilateral element angles are to be greater than 60° and less than 120°.
- The triangular elements angles are to be greater than 30° and less than 120°.
- Primary transversal supporting members, stiffeners and girders are to be modelled with beam elements.

Also the ratio between the shorter and the longer edge of the element should be less than 3 for the regions where higher stress levels are expected. The FEM model aimed at checking the strength of the primary supporting members and stress concentration at discontinuities is composed of 195 514 elements whose size is about 120 x 120 mm. Only one symmetric half of three cargo tanks is modelled.

#### **3.5.3.3 Loading conditions and load cases**

The definition of the loads give by the rules is presented in Section 3.4.5.

In the model, the local loads and applied locations are listed below:

- Side plating : River hydrostatic pressure + wave pressure
- Bilge plating : River hydrostatic pressure + wave pressure
- Bottom plating : River hydrostatic pressure + wave pressure
- Inner bottom plating : Tank hydrostatic pressure + Inertial pressure + Tank design pressure
- Inner side plating : Tank hydrostatic pressure + Inertial pressure + Tank design pressure
- Deck plating : Tank setting pressure

Aforementioned loads are illustrated by the red arrows in Fig. 141. The hull girder bending moment as the global load is applied on the rigid nodes at the aft and the fore extremities of the model. A symmetry

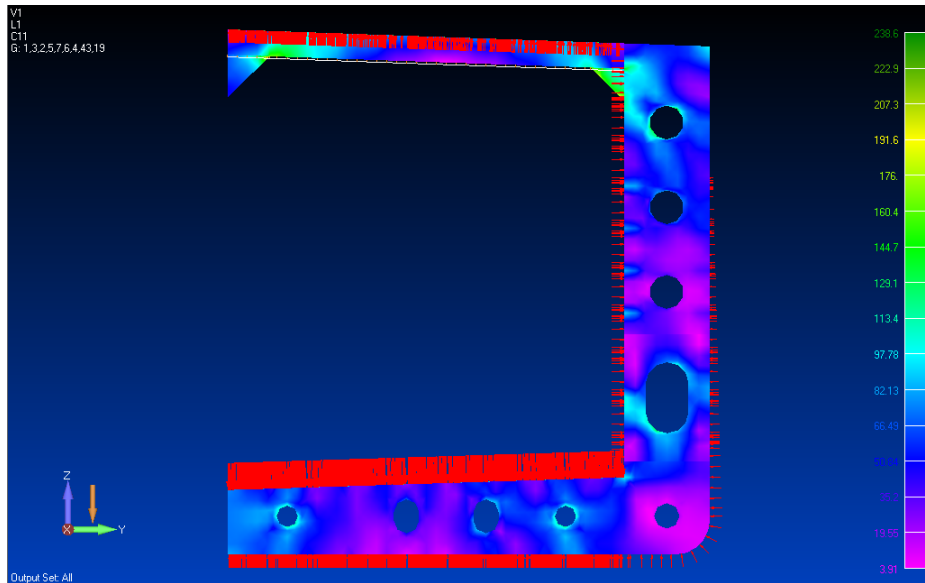


Figure 9: Applied loads on the FEM model in FEMAP

boundary condition is applied to the plane passing through the centreline along the ship. Two rigid nodes are defined aft and fore extremity of the model and connected to the corresponding nodes at the limits. Model is constrained as simply supported at those points by one direction as shown in Table 14.

Table 14: Boundary Conditions

<b>Boundary Conditions</b>	Translation in directions			Rotation around axes		
	x	y	z	x	y	z
Node at fore end	fixed	fixed	fixed	fixed	free	fixed
Node at aft end	fixed	fixed	fixed	fixed	free	fixed

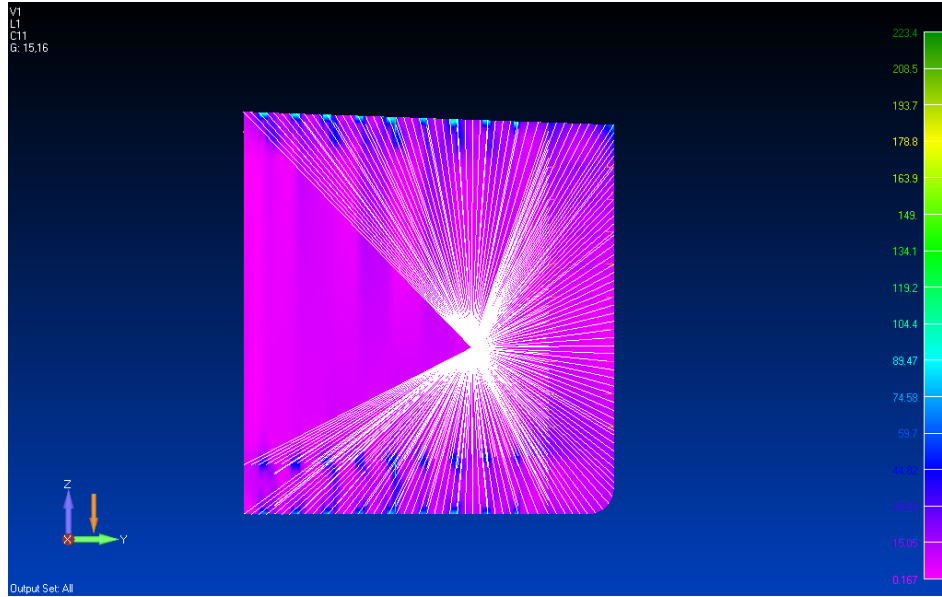


Figure 10: Rigid element in the aft part of the model

### 3.5.3.4 Checking criteria

The master allowable stress,  $\sigma_{MASTER}$ , in  $N/mm^2$ , is obtained from the following formula:

$$\sigma_{MASTER} = \frac{R_y}{\gamma_R \gamma_m} \quad (5)$$

where

$R_y$  : yielding stress,

$\gamma_R$  : resistance partial safety factor

$\gamma_m$  : material partial safety factor

The master allowable stress,  $\sigma_{MASTER}$  is calculated as  $219.42 N/mm^2$

For the all types of analysis, it is to be checked that the equivalent Von-Mises stress  $\sigma_{VM}$  is in compliance with the following formula:

$$\sigma_{VM} \leq \sigma_{MASTER} \quad (6)$$

### 3.5.3.5 Results of the direct calculation

In order to fulfil the strength checking criteria, Von-Mises equivalent stress in critical areas is shown as lower than the master allowable stress. In following figures, critical stress values are indicated which are lower than the master allowable stress.

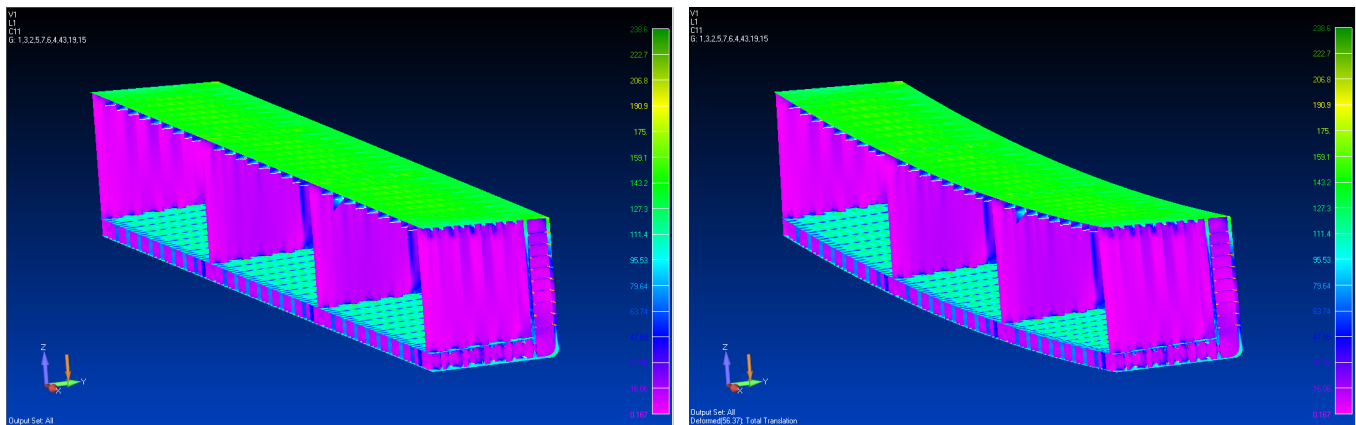


Figure 11: Complete FEM model (Non-deformed and deformed)

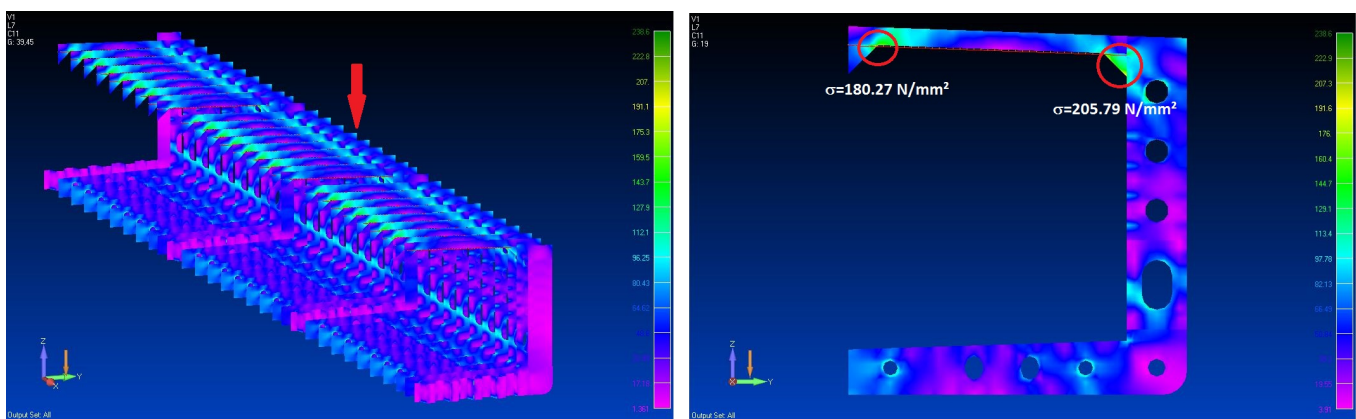


Figure 12: Von-Mises stress on web frame

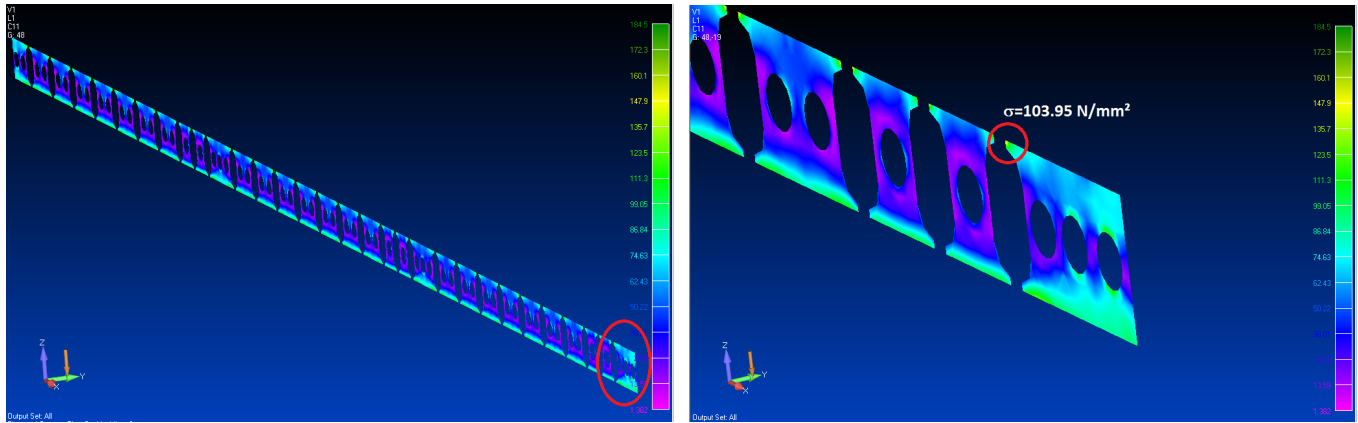


Figure 13: Von-Mises stress on lateral double bottom girder

## 4 A.D.N. ALTERNATIVE DESIGN PROCEDURE

### 4.1 General

Within the scope of the A.D.N. Regulations, tankers fitted with cargo tanks of capacity exceeding the maximum allowable one (but not greater than 1000  $m^3$ ) and/or deviating from the minimum distance between outer hull and cargo tank, may be permitted if the ship is protected through a more crash-worthy side wall. This shall be done by comparing the risk of cargo tank failure of the conventional construction complying with the A.D.N. Regulations to one of the alternative construction. When the risk of the alternative construction does not exceed that of the conventional construction, equivalent or higher safety is proven. This shall be proven according to the A.D.N calculation procedure summarized in Section 4.3.

### 4.2 Approach

Referring to the A.D.N. Regulations the risk is described as following:

$$R = P \cdot C \quad (7)$$

where

$R$  : risk [ $m^2$ ]

$P$  : probability of cargo tank rupture

$C$  : consequence (measure of damage) of cargo tank rupture [ $m^2$ ]

It is derived with respect to the spillage of dangerous goods through the size of the damaged compartment. The probability of cargo tank rupture  $P$  depends on the probability distribution of the impact energy of the collision. It is described by the energy absorbing capability of the structure of the struck ship without any damage to the cargo tanks. This probability can be reduced by improving the crash-worthiness of the struck ship. The consequence  $C$  of cargo spillage is described as the affected area around the struck ship.

### 4.3 Calculation Procedure

Calculation procedure for Type C vessel is defined in the A.D.N. by 13 steps.

#### Step 1

Besides the alternative design, a conventional design which is used as the reference for the improvements, must be provided. The reference design must have the same dimensions with the alternative design and fulfil all the requirements of the A.D.N.. In addition, it must comply with the rules of a recognized classification society.

#### Step 2

The typical collision positions and the number of possible locations must be determined depending on the type of the ship. A recognized classification society shall agree with the proposed locations.

#### Vertical collision locations:

To determine the vertical striking locations, the minimum and the maximum drafts of the collided ships must be known. The draft combinations are shown in Fig. 14. Point  $P_1$  is the point where the lower edge of the flat transom of the push barge or the V-bow strikes at the deck level.

It should be noted that the probability of each draft combination is equal. Each inclined line represents the same draft difference. To assess the case of maximum collision energy, the case with the same draft difference but the highest displacement must be selected. (highest point on each respective diagonal  $\Delta T_i$  )

Classification societies may require different impact positions than aforementioned cases depending on the design of the vessel.



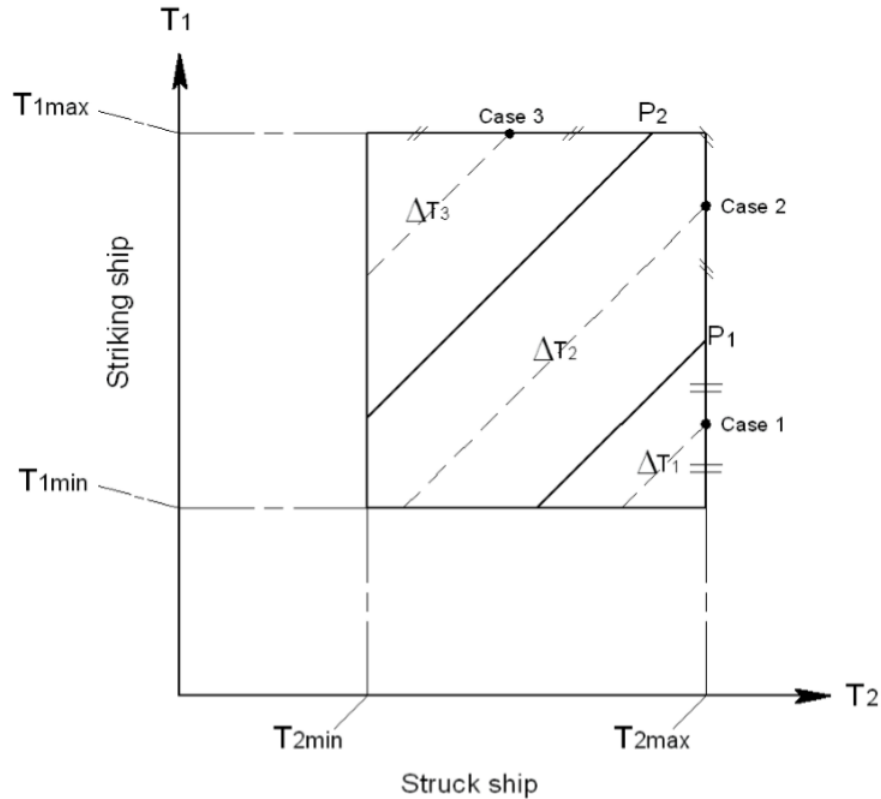


Figure 14: Definition of vertical striking positions

### Longitudinal collision locations:

At least three possibilities are advised to specify longitudinal striking locations for tankers. Those are:

- at bulkhead
- at web
- between two webs

### Number of collision locations:

The number of collision locations results from the combination of chosen vertical and longitudinal collision locations. In default case, the number of locations is  $3 \cdot 3 = 9$ .

### Step 3

A weighting factor shall be introduced which specifies relative probability of certain impact locations.

These factors are named  $w_{f_{loc}(i)}$ . Assumptions to obtain these factors must be agreed by a recognized classification society. The total weighting factor is calculated by the product of the weighting factors of the vertical and the longitudinal positions.

#### **Vertical collision locations:**

The weighting factors of vertical locations are obtained by the ratio between the partial area of the collision case and the total area of the rectangle as shown in Fig. 14.

#### **Longitudinal collision locations:**

For the longitudinal locations, the weighting factor is defined as the ratio between the calculational span length and tank length. The calculational span length can be obtained as follows:

- collision on bulkhead:  
0.2 \* distance between web frame and bulkhead (not larger than 450 mm)
- collision on web frame:  
0.2 \* web frame spacing forward (not larger than 450 mm)  
+ 0.2 \* web frame spacing aft (not larger than 450 mm)
- collision between web frames:  
cargo tank length, minus the length of "collision on bulkhead", and minus the length of "collision on web frame"

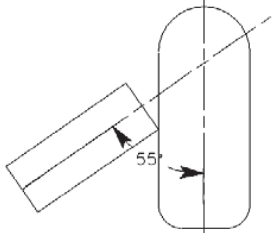
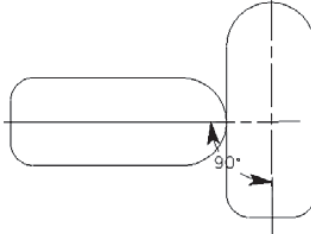
#### **Step 4**

For each collision location, the collision energy absorbing capacity  $E_{loc(i)}$  shall be determined. It is defined as the total energy absorbed by the structure until the moment that the cargo tank ruptures. To obtain these values, a finite element analysis must be performed. These calculations must be carried out for two collision scenarios described by A.D.N.:

Collision scenario I: Push barge bow shape as striking bow

Collision scenario II: V-shaped bow as striking bow

Table 15: Speed reduction and weighting factors for different scenarios

Worst case scenarios		Causes			
		Communication error and poor visibility	Technical error	Human error	
		0,50	0,20	0,30	
I		0,80	0,66	0,50	1,00
		0,20	0,30		1,00

### Step 5

Probability of exceedance is to be calculated for each collision energy absorbing capacity  $E_{loc(i)}$ . To calculate this probability, cumulative probability density functions (CPDF) are used. For the tables of CPDF, refer to A.D.N. Section 9.3.4.3.1.5.6. The probability of exceedance is given by the equation:

$$P_{x\%} = C_1 \left( E_{loc(i)} \right)^3 + C_2 \left( E_{loc(i)} \right)^2 + C_3 E_{loc(i)} + C_4 \quad (8)$$

wherein:

$P_{(x\%)}$  : probability of exceedance (tank rupture)

$C_{(1-4)}$  : coefficients from the table

$E_{loc(i)}$  : collision energy absorbing capacity

This formula is valid only in given energy ranges in the tables of CPDF coefficients. If  $E_{loc(i)}$  value is below the given range, the probability  $P_{(x\%)}$  equals 1.0. If else,  $E_{loc(i)}$  value is above the given range probability  $P_{(x\%)}$  equals 0.

Effective mass should be taken equal to the maximum displacement of the vessels multiplied by a factor of 1.4 in both collision scenarios.

In Scenario I (push barge bow at  $55^\circ$ ) three CPDF formulas shall be used:

CPDF 50%, CPDF 66%, CPDF 100%.

In Scenario II (V-shaped bow at  $90^\circ$ ) two CPDF formulas shall be used:

CPDF 30%, CPDF 100%.

### Step 6

The weighted probabilities of cargo tank rupture  $P_{wx\%}$  are calculated by multiplying each cargo type rupture probability  $P_{x\%}$  by the weighting factors corresponding to each characteristic collision speed.

Table 16: Weighting factors for each characteristic collision speed

			weighting factor
<b>Scenario I</b>	CPDF 50%	wf 50%	0.2
	CPDF 66%	wf 66%	0.5
	CPDF 100%	wf 100%	0.3
<b>Scenario II</b>	CPDF 30%	wf 30%	0.7
	CPDF 100%	wf 100%	0.3

### Step 7

For each collision location, the total probabilities of cargo tank rupture  $P_{loc(i)}$  must be calculated as the summation of weighted probabilities of cargo tank rupture  $P_{wx\%}$ .

### Step 8

The weighted total probabilities of cargo tank rupture  $P_{wloc(i)}$  is calculated by the multiplication of the total probabilities of cargo tank rupture  $P_{loc(i)}$  by the weighting factors  $wf_{loc(i)}$ .

### Step 9

The scenario specific total probabilities of cargo tank rupture  $P_{scenI}$  and  $P_{scenII}$  (according to table in Section 9.3.4.3.1. in A.D.N.) are calculated.

### Step 10

In this step, the weighted value of the overall probability of cargo tank rupture  $P_w$  is calculated by given formula:

$$P_w = 0.8 P_{scenI} + 0.2 P_{scenII} \quad (9)$$

### Step 11

The overall probability of cargo tank rupture  $P_w$  for the alternative design is called  $P_n$ . The overall probability of cargo tank rupture  $P_w$  for the reference design as  $P_r$ .

### Step 12

The ratio between the consequence related to alternative and reference designs ( $C_n/C_r$ ) is calculated by the formula below:

$$C_n/C_r = V_n/V_r \quad (10)$$

where

$V_n$  : maximum capacity of the largest cargo tank in the alternative design

$V_r$  : maximum capacity of the largest cargo tank in the reference design

It is assumed that magnitude of consequence increases linearly (proportionality factor 1.0) depending on the tank size for the capacities between  $380 m^2$  and  $1000 m^2$ . If the proportionality factor is expected to be more than 1.0, the affected area must be calculated separately.

**Step 13**

Finally, the ratio  $P_r/P_n$  between the overall total probability of cargo tank rupture, where  $P_r$  is for the reference design and  $P_n$  for the alternative design, shall be compared with the ratio  $C_n/C_r$  between the consequence related to the alternative design, and the consequence related to the reference design. If  $C_n/C_r \leq P_r/P_n$  is fulfilled, alternative design is accepted.

**4.4 Determination of collision energy absorbing capacity**

The collision energy absorbing capacity shall be determined by using a finite element analysis (FEA). Finite elements codes which are capable of taking into account geometrical and non-linear effects, shall be used such as LS-DYNA, PAM-CRASH, ABAQUS etc. The chosen solver must be able to simulate realistic rupture. Moreover, the level of detail of the program must be accepted by a recognized classification society.

In the step of creation of the finite element models, both reference and alternative designs are modelled. Cargo area sections subjected to collision are to be generated under supervision of the recognized classification society. The modelled section is restrained for all three translational motions at the both ends. Most of the collision cases, global hull girder bending does not participate in collision mechanics. In those cases, modelling the half of the section which is symmetric about the centreline may be sufficient and constraints are also defined at the centreline. A trial simulation must be performed in order to be sure that there is no plastic deformation near constraint boundaries. If a plastic deformation is observed, limits of the model must be extended.

In structural zones which are subjected to impact, a fine meshing must be applied. A coarse meshing may be used in the other parts. The fineness of the mesh must be sufficient to show the real behaviour of structural rupture. Also, the maximum element size shall not exceed the value of 200 mm in collision area. The ratio between the lengths of the longer and the shorter edges of the shell element cannot be more than the value of three. In addition to that, the ratio between the element length and element thickness shall be larger than five.

Plate structures (shell, webs stringers etc.) can be modelled as shell elements and stiffeners as beam elements. Cut outs and manholes in collision areas must be taken into consideration in modelling.

In the calculation phase, node on segment penalty method in contact option has to be enabled. Names of this option in some commercial codes are: *contact\_automatic\_single\_surface* (LS DYNA), *self-impacting* (PAMCRASH) etc.

#### 4.4.1 Material Properties

According to A.D.N., due to the extreme behaviour of the material and the structure during a collision, and non-linear effects caused by the geometry and material, true stress-strain relation must be used:

$$\sigma = C \epsilon^n \quad (11)$$

and,

$$n = \ln(1 + A_g) \quad (12)$$

$$C = R_m \left( \frac{e}{n} \right)^n \quad (13)$$

where

$A_g$  : maximum uniform strain related to the ultimate tensile stress  $R_m$

$e$  : natural logarithmic constant

The values  $A_g$  and  $R_m$  are determined by tensile tests.

In the case that only the ultimate tensile stress result  $R_m$  is available, following approximation can be used in order to obtain the  $A_g$  value from the  $R_m$  value. This approximation is valid for shipbuilding steel with a yield stress  $R_eH$  less than  $355 [N/mm^2]$ .

$$A_g = \frac{1}{0.24 + 0.01395 R_m} \quad (14)$$

If tensile test results are not available in the calculation phase, minimum values of  $A_g$  and  $R_m$  should be used which are defined by a recognized classification society. For other material or shipbuilding steel with higher yield stress ( $> 355 N/mm^2$ ), material properties must be agreed upon with a recognized classification

society.

#### 4.4.2 Rupture criteria

In A.D.N., rupture of the element is defined by the failure strain value for FEA. If the strain in the thickness direction exceeds the failure strain limit of the element, this element must be removed from the model and cannot contribute to the deformation energy at further time steps. The following expression is to be used for the calculation of rupture strain:

$$\varepsilon_f(l_e) = \varepsilon_g + \varepsilon_e \frac{t}{l_e} \quad (15)$$

where

$\varepsilon_g$  : uniform strain

$\varepsilon_e$  : necking

$t$  : plate thickness

$l_e$  : individual element length

Uniform strain and necking values for shipbuilding steel with a yield stress  $R_{eH}$  of less than 355 N/mm<sup>2</sup> must be taken from the table given below:

Table 17: Uniform strain and necking values in A.D.N.

Stress states	1-D	2-D
$\varepsilon_g$	0.079	0.056
$\varepsilon_e$	0.76	0.54
Element type	Truss beam	Shell plate

Strain values other than the specified above, which are taken from measurements from some cases, can be used in agreement with the recognized classification society. Furthermore, other rupture criteria can also be applied if it is proven by the tests and accepted by the recognized classification society.



#### **4.4.3 Friction energy**

An energy absorption mechanism other than deformation of structural elements in collision phenomenon is the friction. The Coulomb friction coefficient  $\mu_c$  is given by A.D.N. as follows:

$$\mu_c = FD + (FS - FD) e^{-DC |\nu_{rel}|} \quad (16)$$

with the values of

$$FD = 0.1$$

$$FS = 0.3$$

$$DC = 0.01$$

$|\nu_{rel}|$ : relative friction velocity

## 5 SHIP COLLISION ANALYSIS

### 5.1 General

Ship collisions are governed by the kinetic energy possessed by the motion. After the impact, a part of this kinetic energy is transformed into deformation energy in structural elements of both striking and struck ships. This transition continues until the speed of the striking ship is equal to the struck ship. It also includes the hydrodynamic effects such as added mass and damping. In most cases the impact energy results in large deformations on struck ship.

Mechanics of ship collision are divided into two main parts: (Pedersen, 1995)

- Internal Mechanics
- External Dynamics

Internal mechanics involve structural deformation and failure in ship structures subjected to the effect of collision forces. External dynamics is the physical interpretation of the motion of colliding bodies under the effects of collision and hydrodynamics forces. Those parts will be explained in detail in following sections.

### 5.2 Internal Mechanics

In this section some methods are discussed in the matter of structural response in collisions. To understand the behaviour of the side structure on collision, it is better to divide the whole structure into composing structural elements. The complex arrangement of side structure becomes even more complex when elements start deforming or being destroyed. It can be examined as an assembly of plated structures with attached reinforcing profiles. Main energy absorbing structural elements and crushing modes for the side impact on collisions are listed below: (Pedersen & Zhang, 2010)

- Membrane deformation of shell plating and attached stiffeners
- Folding and crushing of transverse frames and longitudinal stringers
- Folding, cutting and crushing of horizontal decks
- Cutting or crushing of bottom of the ship

- Crushing of transversal bulkheads

This approach can also be used for a mechanical interpretation of the striking bow. The evaluation of the energy absorbing capacity of the striking bow can vary and should be taken into consideration. This is important to assess the real physical behaviour on the impact.

A part of the energy is also absorbed by the striking bow. The energy absorption of large ships with a longitudinally stiffened bow is relatively small, vice versa small ships with a transversally stiffened bow is expected to be higher. (Sajdak & Brown, 2005)

Up to the present, internal mechanics of the collisions have been evaluated by making use of several kinds of methods and approaches. Each of them has their own competitive edge and disadvantages depending on the needs and expectations. Those can be categorized as:

- Experimental methods
- Empirical methods
- Simplified analytical methods
- Numerical methods

### **5.2.1 Experimental Methods**

Due to the complex nature of collision mechanics, it is necessary to acquire real collision data in order to comprehend the mechanics behind the collisions. Many different types of tests are conducted to explain the behaviour of the ship structures in collision starting from 1960s. The main purpose of those initial experiments was to make crashworthy designs for nuclear-powered vessels in order to protect reactors from the collision damage. In scope of this objective, some investigators in Italy, Germany and Japan examined the ship collisions by performing physical model tests.

Since 1990s, also full scale model tests are performed. Concerning the subject of inland tankers, a set of full-scale experiments has been conducted in the Netherlands collaboration with Japan in 1991. Two inland tankers with the length of 80 metres have been tested. Following to this, two 1500 tons tankers were tested in the Netherlands again as a joint project of the Netherlands, Germany and Japan. Two different conventional and alternative side structures have been constructed and penetration depths have been compared.

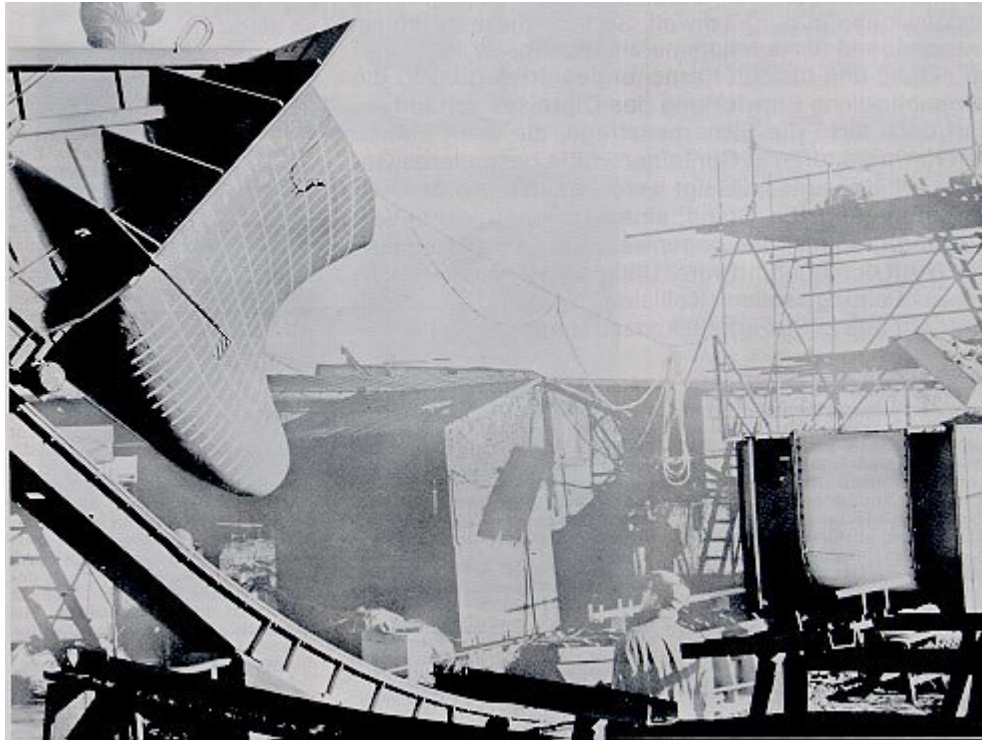


Figure 15: Full-scale experiment in Germany (Woisin, 1979)

Results of experiments are reliable but performing physical tests are quite expensive due to the necessity of production of the side structure and striking bow.



Figure 16: Full-scale experiment in Netherlands (Zhang, 1999)

## 5.2.2 Empirical Methods

### 5.2.2.1 Minorsky's Method (1959)

One of the earliest attempts to analyse ship collisions has been done by Minorsky in a purpose to investigate collisions on ships carrying nuclear materials. Minorsky derived a formulation based on statistical data of twenty-seven cases of collisions. From these collisions nine of them are used to fit a straight line which is represented as the following relation: (Minorsky, 1959)

$$\Delta KE = 47.2 R_T + 37.7 \quad (17)$$

where

$\Delta KE$  : energy absorbed by the struck ship [MJ]

$R_T$  : Resistance factor [m<sup>3</sup>]

A relation between the volume of damaged steel structure and absorbed energy is developed.  $R_T$  is basically equal to damaged volume of steel structure of the struck ship. This may not be true for every case.

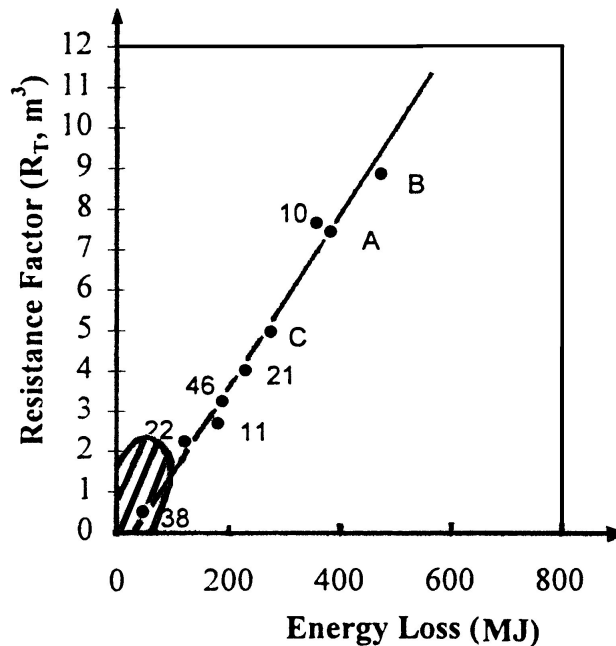


Figure 17: Minorskys linear relation

Minorsky's equation gives accurate results for the collisions cases with large deformations. The main advantage of this method can be obviously seen as its simplicity. On the other hand, material properties, side structural arrangement and mode of deformation have no influence to determination of the total absorbed energy. This approach which is dependant a single variable is not accurate on collisions with low-energy without the rupture of the shell plating. The results for impact energy lower than 80 MJ are not reliable.

### 5.2.2.2 Enhancements to Minorsky's Method

In order to improve Minorsky's formulation for low-energy collisions, a couple of developments have been made afterwards.

Jones proposed an improvement to Minorsky's formula that energy absorption behaviour of shell plating is described by beam theory. It is indicated that membrane energy of shell plating is more significant in minor collisions with low-energy. In low-energy collisions, absorbed energy is defined as following: (Giannotti, & Johns et al. 1979)

$$E_T = 0.030288 \sigma_0 \left( \frac{w}{L} \right)^2 R_T \quad (18)$$

$$R_T = \frac{2LBt}{144}$$

where

$w$  : displacement

$B$  : beam breadth

$t$  : beam thickness

$2L$  : beam length

Thereafter Van Mater has improved Jones formulation by analysing collision at off-centre. The formula has

become:

$$E_{(a,b)} = E_{center} \frac{a}{b} \quad (19)$$

$$w_{max} = 0.453 a$$

where

$E_{(a,b)}$  : displacement

$E_{center}$  : beam breadth

$a$  : beam thickness

$b$  : beam length

$w_{max}$  : maximum deformation of the side plating

Furthermore, Minorsky's approach has been developed by adding some mechanical failure modes into the equation by Pedersen and Zhang (1998). Three deformation modes are introduced with a reference to full scale tests and accidents. Absorbed energy is defined for different types of deformation modes which are plate stretching (for side shell), plate crushing (for deck, stiffeners), plate cutting (for deck, bottom). Representing formulae are given below:

1. Plate stretching (side shell)

$$E_1 = 0.77 \epsilon_c \sigma_0 R_{T1}$$

2. Plate crushing (deck, stiffeners)

$$E_1 = 0.77 \epsilon_c \sigma_0 R_{T1}$$

3. Plate cutting (deck, bottom)

$$E_1 = 0.77 \epsilon_c \sigma_0 R_{T1}$$

This approach enables the formulation to be sensitive to the structural scantling not only the damaged volume of structural steel. As can be seen by the preceding information, Minorsky's method is a useful tool to analyse ship collisions in a practical way. However, it cannot be applied to unique designs or double hull structure. Therefore, in the purpose of developing an alternative structure this approach has strict limitations.

### 5.2.2.3 Paik's stiffened plate approach

Paik (1994) has also performed a set of experiments by cutting stiffened panels using non-deformable wedges. The total absorbed energy calculated by using an equivalent thickness method and formulation is given as following:

$$E = C_{1.5} \sigma_0 l^{1.5} t_{eq}^{1.5} \quad (20)$$

where

$$C_{1.5} = 1.112 - 1.156 \theta + 1.760 \theta^2$$

$\theta$  : half angle of the wedge [rad]

$t_{eq}$  : equivalent plate thickness

In this approach, structural response of stiffened deck plates to the impact force has been investigated.

## 5.2.3 Simplified Analytical Methods

Simplified analytical methods in ship collisions are generally based on the upper-bound theorem. In upper bound theorem the principle basically defined by Jones (2012): "If the work rate of a system of applied loads during any kinematically admissible collapse of the structure is equated to the corresponding internal energy dissipation rate, then the system of loads will cause collapse or be at the point of collapse." One of the main assumptions is the neglect of the interactions between structural elements within the response to the load. Each element contributes independently to the collision resistance.

### 5.2.3.1 Super-element theory

The basic idea of the super-element method is to split the vessel into structural macro-components so-called the super-elements. Each super-element (Lutzen, 2000) is characterized by a closed-form expression giving the crushing resistance with respect to the penetration of the striking ship. As the impacting vessel is moving forward into the struck structure, these super-elements are successively activated and their contribution to the total collision force is evaluated.



In the super-element theory, the ship structure is split into macro components which are expected to present the same behaviour as the actual model. Each component is defined by its own mathematical expression to obtain crushing resistance in respect to the penetration caused by the striking ship. While collision is progressing, the elements which are associated with the striking ship in the impact region are activated and the total force is calculated by means of the contribution of each super element to the absorption of impact energy.

In the basis of this theorem, the external and the internal energy rates must be given. The external energy rate is expressed by

$$\dot{E}_{ext} = F \cdot \dot{\delta} \quad (21)$$

where  $F$  is required resistance of the super-element,  $\delta$  is the penetration of the striking ship into the struck ship.  $\dot{E}_{ext}$  stands for the time derivative of the external energy.

The internal energy rate for a solid body is given as

$$\dot{E}_{int} = \iiint_V \sigma_{ij} \cdot \dot{\epsilon}_{ij} \cdot dV \quad (22)$$

Finally for a structural component, force is defined in upper-bound theorem as follows:

$$F \cdot \dot{\delta} = \iiint_V \sigma_{ij} \cdot \dot{\epsilon}_{ij} \cdot dV \quad (23)$$

where

- $\dot{\delta}$  : striking ship surge velocity
- $\sigma_{ij}$  : stress tensor of the super element
- $\dot{\epsilon}_{ij}$  : strain rate tensor
- $V$  : component volume to derive the force  $F$  analytically

Some assumptions made to simplify the solution are:

- Material is considered perfect rigid plastic.
- Shear effects is neglected on the surface thus the internal energy is calculated by only bending and membrane effects.

The total internal energy rate is assumed to be composed of bending and membrane effects. In bending energy, the flexional effects are confined in a certain number of  $m$  of plastic hinge lines. Therefore, bending energy rate  $\dot{E}_b$  is written as

$$\dot{E}_b = M_0 \sum_{k=1}^m \dot{\theta}_k l_k \quad (24)$$

In order to calculate membrane energy rates  $\dot{E}_m$  of a plate element, the formulae are given by

$$\dot{E}_m = t_p \iint_A \sigma_{ij} \cdot \dot{\epsilon}_{ij} \cdot dA \quad (25)$$

By using Von-Mises yield criterion for the bending plate, it is derived as

$$\dot{E}_b = \frac{2\sigma_0 t_p}{\sqrt{3}} \iint_A \sqrt{\dot{\epsilon}_{11}^2 + \dot{\epsilon}_{22}^2 + \dot{\epsilon}_{12}^2 + \dot{\epsilon}_{11}\dot{\epsilon}_{11}} dA \quad (26)$$

where

$M_0$  : fully plastic bending moment

$A$  : area of the plate

$t_p$  : thickness of the plate

$\dot{\theta}_k$  : rotation of the hinge number  $k$

$l_k$  : length of the hinge number  $k$

The total energy rate is calculated by summing the bending and membrane energy rates:

$$\dot{E}_{int} = \dot{E}_b + \dot{E}_m \quad (27)$$

In the following figure, collision scenario is represented and possible components of the ships are shown as super-elements. Super-elements which are depicted in Fig. 18 are:

### 1. Hull super-element

2. Vertical bulkhead super-element
3. Beam super-element
4. Horizontal deck super-element

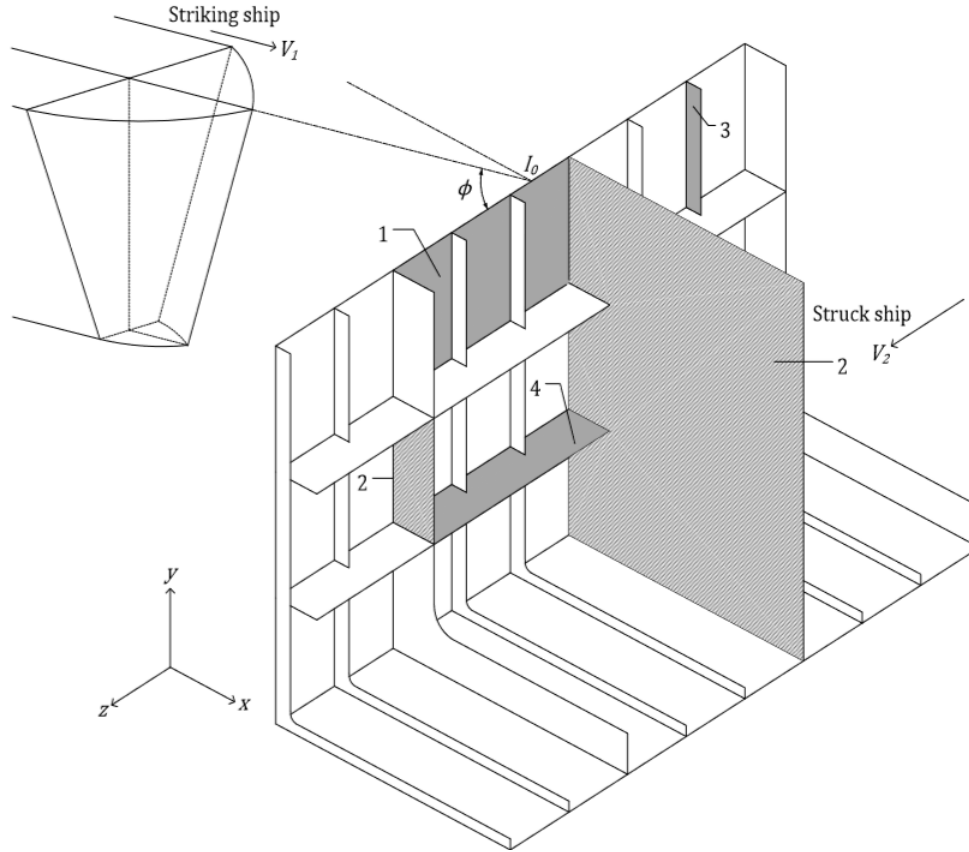


Figure 18: Representation of the super-elements in a ship structure

$V_1$  and  $V_2$  stand for respectively the speed of striking and the struck ship.

### Hull super-element (1)

The hull super element is defined as a simply supported plate on its four edges subjected to an out-of-plane impact. This element is divided into four zones shown in Fig. 19. The displacements fields  $w(y, z)$  is derived for these four zones oriented along the normal direction of the plate surface. For plate number I, the displacement field is given by:

$$w(y, z) = \left( \frac{z}{a_1 + \delta \cos \phi} \right)^n \left( \frac{y}{b_1} \right)^n \delta \sin \phi \quad (28)$$

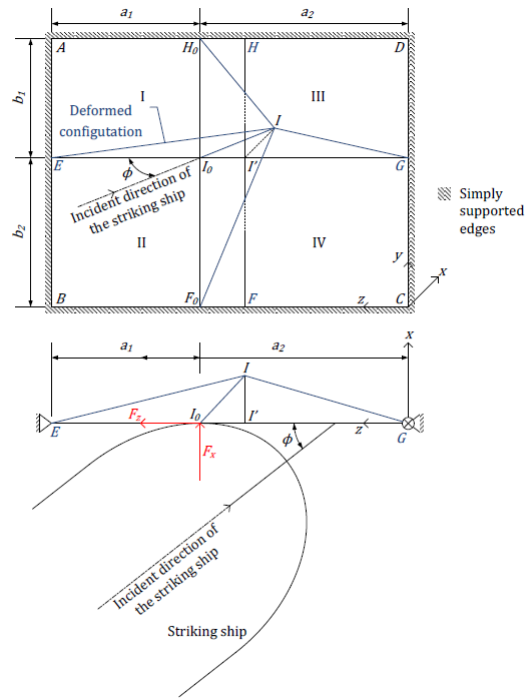


Figure 19: Deformed configuration of the hull super-element

where  $n$  is a natural number assumed equal to 2 on the purpose of providing a close agreement between numerical and analytical results. The compatibility at the junctions between each surface is maintained by introducing four plastic hinges  $HI, EI, FI$  and  $GI$ . The strain rates tensor for four zones is derived by applying the Green's formulae. Consequently, the total membrane energy rate  $\dot{E}_m$  of the super element is defined by:

$$\dot{E}_m = \dot{E}_I + \dot{E}_{II} + \dot{E}_{III} + \dot{E}_{IV} \quad (29)$$

In consideration of the thin plate, the total bending energy rate  $\dot{E}_m$  is small comparing to the membrane effects and can be neglected. Then the total membrane energy rate  $\dot{E}_m$  is considered equal to the total internal energy rate. Using the virtual work principle, it can be expressed by:

$$\dot{E}_m = F_x \cdot \dot{\delta} \sin \phi \quad (30)$$

Assuming that the  $F_z$  acting in the plate is created by the friction between impacted element and striking geometry. Then this force can be given by  $F_z = \mu F_x$  where  $\mu$  is the Coulomb friction coefficient of the

material. Finally, the total crushing force of hull super-element is obtained by:

$$\dot{E}_m = \sqrt{F_x^2 + F_z^2} = \frac{\dot{E}_m}{\delta \sin \phi} \sqrt{1 + \mu^2} \quad (31)$$

### Vertical bulkhead super-element (2)

Vertical bulkhead super-element is developed to obtain crushing resistance of transversal bulkheads or vertical frames. It is modelled as a plate simply supported on three edges. The impact is considered to be from the free edge. The deformation pattern is given by two plastic hinges which is shown in Fig.20 The

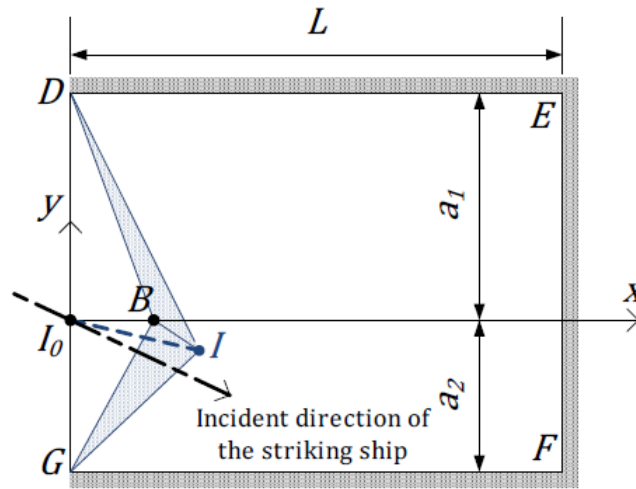


Figure 20: Deformed configuration of the vertical bulkhead super-element

plate is supposed to rotate around the plastic hinges of  $BD$  and  $BG$ . Thus, the edges of  $I_0BD$  and  $I_0BG$  have only axial extension along the  $y$  axis. The displacement fields  $v(x, y)$  oriented along  $y$  axis are given by

$$\text{For } I_0BD \quad v(x, y) = \frac{1}{2} \cdot \frac{p^2}{a_1} \cdot \frac{b-x}{b} \cdot \frac{a_1-y}{a_1} \quad (32)$$

$$\text{For } I_0BG \quad v(x, y) = \frac{1}{2} \cdot \frac{p^2}{a_2} \cdot \frac{b-x}{b} \cdot \frac{a_2-y}{a_2}$$

where  $p = \overline{I_0I}$  and  $b = \overline{I_0B}$

Applying Green's formulae to Eq.32, the membrane energy  $E_m$  is obtained. The bending energy as a component of the internal energy can be calculated using the rotation angles  $\theta_1$  and  $\theta_2$  in respect to the

plane  $(x, y)$  with the surfaces  $IBG$  and  $IBD$ .  $\theta_1$  and  $\theta_2$  is given as follows:

$$\text{For } I_0BD \quad \theta_1 = \arccos\left(\frac{a_1(2b^2 - p^2)}{2b^2\sqrt{a_1^2 + b^2}}\right) \quad (33)$$

$$\text{For } I_0BD \quad \theta_2 = \arccos\left(\frac{a_1(2b^2 - p^2)}{2b^2\sqrt{a_1^2 + b^2}}\right)$$

Then applying the virtual velocities principle, the crushing resistance is derived:

$$F = \frac{\sigma_0 t_p}{2} \cdot \frac{a_1 + a_2}{a_1 a_2} \cdot p \left( b \frac{\partial p}{\partial \delta} + \frac{p}{2} \frac{\partial b}{\partial \delta} \right) + \frac{\sigma_0 t_p^2}{4} \left( \sqrt{a_1^2 + b^2} \frac{\partial \theta_1}{\partial \delta} + \sqrt{a_2^2 + b^2} \frac{\partial \theta_2}{\partial \delta} \right) \quad (34)$$

where  $a_1$  and  $a_1$  are the distances between the impact point and the fixed edges and  $t_p$  is the plate thickness. The parameters  $b$  and  $p$  are given previously.

### Beam super-element (3)

The crushing resistance of the longitudinal and the vertical secondary stiffeners is evaluated by the beam super-element. It is considered to be clamped at both extremities.

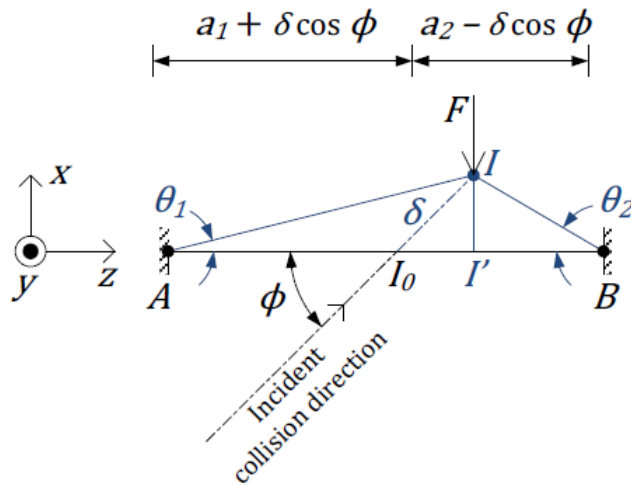


Figure 21: Deformed configuration of the beam super-element

In the moment of the impact, the horizontal distances to the supports from the actual contact point between the super element and striking geometry  $I$  for a given penetration  $\delta$  is given:

$$a_1 + \delta \cos \phi, \quad a_2 - \delta \sin \phi \quad \text{with } \delta = \bar{I}_0 \quad (35)$$

By using the sectional properties of the super-element, the yield locus between the normal force  $N$  and the bending moment  $M$  can be developed where the behaviour is fully plastic:

$$M = L(N) \quad (36)$$

where  $L$  is the mathematical expression of the yield locus.

Applying the virtual work principle, the crushing resistance  $F$  is derived. Then, the external and the internal works rates can be found by:

$$\begin{aligned} \dot{E}_{ext} &= F \dot{\delta} \sin \phi \\ \dot{E}_{int} &= 2M (\dot{\theta}_1 + \dot{\theta}_2) + N (\dot{\Delta}_1 + \dot{\Delta}_2) \end{aligned} \quad (37)$$

where  $\dot{\theta}_1$  and  $\dot{\theta}_2$  are the rotations defined in Fig. 21 and  $\dot{\Delta}_1$  and  $\dot{\Delta}_2$  are the axial extensions of  $AI'$  and  $BI'$ .

Using the Eq. 36 and 37, the following expression is obtained:

$$F \dot{\delta} \sin \phi = 2 (\dot{\theta}_1 + \dot{\theta}_2) L(N) + N (\dot{\Delta}_1 + \dot{\Delta}_2) \quad (38)$$

The crushing force  $F$  is described by two expressions in respect to the normal force  $N$

$$\begin{aligned} F &= 2M_0 \cdot (a_1 a_2 + \delta^2 \cos^2 \phi) \quad \text{if } N < N_0 \\ F &= N_0 (a_1 + a_2) \cdot \delta \sin \phi \cdot \frac{a_1 a_2 + \delta^2 \cos^2 \phi - \delta \cos \phi (a_1 - a_2) / 2}{(a_1 + \delta \cos \phi)^2 (a_2 - \delta \cos \phi)^2} \quad \text{if } N = N_0 \end{aligned} \quad (39)$$

where  $M_0$  and  $N_0$  are respectively the bending and axial capacities of the cross section. It should be noted that this formulation is valid until the rupture of the beam. When the deformation of the super element reaches the rupture value, the resistance of subjected element is assumed to be zero.

### Horizontal deck super-element (4)

The horizontal deck super-element is modelled as a plate with three simply supported and one free edges. The height of the one deformation fold defined as  $H$  so that the length of the complete deformation pattern is given as  $4H$ . The horizontal distances between the contact point and the supporting edges are  $a_1 + \delta \cos \phi$  and  $a_2 - \delta \cos \phi$  as shown in Fig. 22.

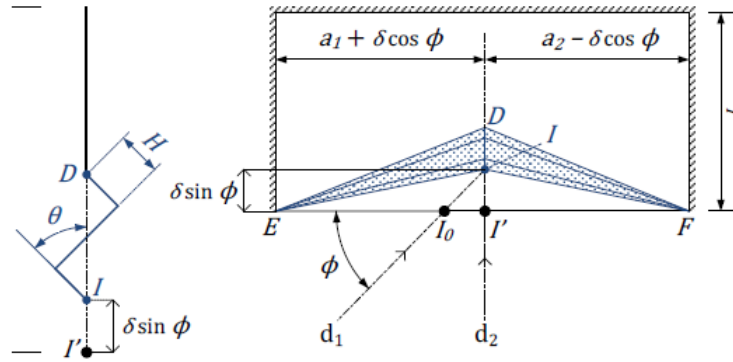


Figure 22: Deformed configuration of the beam super-element

The bending effects are associated with the triangular surfaces rotating around four plastic hinges of folding. A part of bending energy is created by the rotations  $\theta$  around the hinges. This folding surfaces does not relocate rigidly, but with the straining along the  $z$ -direction. By introducing the displacement field  $u(x, z)$  along this direction, the membrane energy dissipation  $E_m$  can be obtained.

By applying the procedure of Simonsen and Ocakli(1999), the crushing resistance of the deck super-element is obtained by using the following formula:

$$F_i(\delta) = \frac{2a_1 + \delta \cos \phi + 4(i-1)H \cot \phi}{(a_1 + \delta \cos \phi)^2} + \frac{2a_2 - \delta \cos \phi - 4(i-1)H}{(a_2 + \delta \cos \phi)^2} \quad (40)$$

However, the crushing resistance cannot be assumed to be the same during the entire crushing length. After the certain a value, a concertina tearing occurs. Therefore, in this mechanism the procedure of Wierzbicki(1995) is used, and crushing force is described by:

$$F = 4.33 \sigma_0 t_p^{5/3} (a_1 + a_2)^{1/3} + \frac{8}{3} R_m t_p \quad (41)$$

where  $R_m$  is the tearing resistance of the material (typically  $500 \text{ N/m}$ ).



## 5.2.4 Numerical Methods

### 5.2.4.1 Non-linear Finite Element Analysis

The finite element method is a powerful tool for the computation of structural and collision problems. Several commercial finite element solver software sophisticated for collision analysis, exist such as LS-Dyna, ABAQUS/Explicit, MSC/DYTRAN, PAM-CRASH. Acquired results using the finite element method are considered quite accurate and in some cases it may replace the model experiments. On the other hand, to obtain reliable results the mesh size must be much smaller, and consequently a large number of elements is needed. It results in a very long computational time. Equations must be solved for each time step. Due to the complex nature of the ship structure and the vast number of elements, modelling and computation may take hundreds of hours (Zhang, 1999). Critical values of the results are directly dependent on the mesh resolution at the collided region. Therefore, the quality of the mesh is crucial to achieve good accuracy for the results.

A graphical representation of collision analysis performed with finite element method (FEM) can be seen in the figure below.

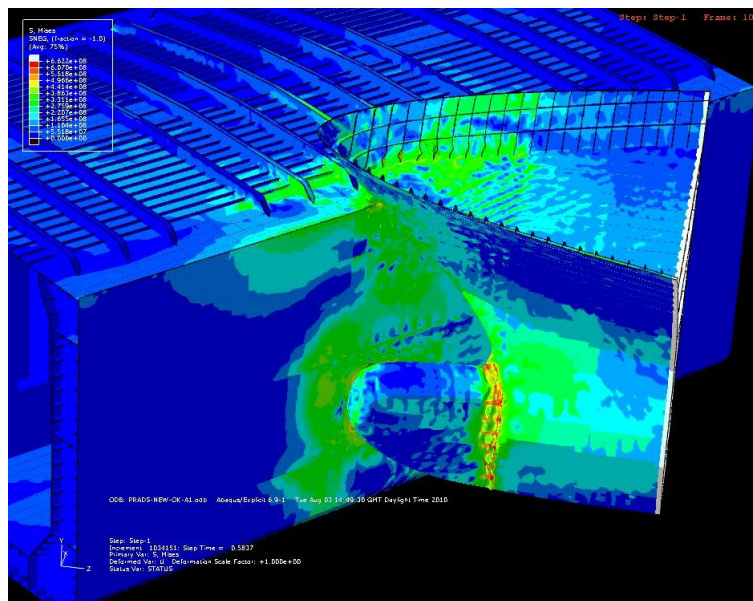


Figure 23: Finite element analysis graphical representation

It is obviously expected that developments of processor technology may enable computers to perform

analyses faster in next years. FEM algorithm also can take many properties and nonlinearities into account such as material properties, friction, rupture of elements.

#### 5.2.4.2 Idealized Structural Unit Method

Because of the time requirements of non-linear FEA, Paik (1999) developed a method based on the finite element approach so-called Idealized Structural Unit Method (ISUM). Concordantly, collision simulation software ALPS/SCOL is developed by Paik. In this method, structural elements of the ship are evaluated as macro components similarly to super-element approach but expressions are solved in finite element matrix. In ISUM, local and global deformation and failure modes are taken into account at the same time. (Paik & Pedersen, 1996. Paik et al., 1999)

Consequently, a significant decline in computational time is achieved by this method. A single scenario can be simulated in less than an hour. Despite its advantages, ISUM is not widely being used in industry. (16th International Ship And Offshore Structures Congress, 2006)

In the following table, a comparison of different methods can be seen in terms of efforts and results.

Table 18: Comparison between the methods for the calculations of internal mechanics  
(The 16th International Ship And Offshore Structures Congress, 2006)

Methods	Analysis Efforts		Available results			
	Modeling efforts	Computation efforts	Stress	Loads	Penetration	Energy
Experimental Methods	Some	Difficulty of data acquisition	✓	✓	✓	✓
Empirical Methods	Fewest	Hand calculation				✓
Simplified Analytical Methods	Few	Hand calculation, simple tools		✓	✓	✓
Non-linear FEM	Extensive	Complex, sophisticated software	✓	✓	✓	✓

## 5.3 External Dynamics

In this section, different models to calculate ship dynamics in collision are discussed.

### 5.3.1 Minorsky's Method

Since the type of material is highly dangerous, assumptions have been made for the worst case scenario. Those are listed below:

- Kinetic energy at the longitudinal direction of struck ship is neglected.
- Collision is fully inelastic.
- Rotations are assumed to be small and neglected for both colliding ships.

With those assumptions, the problem is treated in a more conservative perspective and it may be sufficient in preliminary design step. Considering the assumptions given above, the problem becomes one-dimensional. From the conservation of the momentum principle, velocities of striking and struck ship can be written:

$$\begin{aligned} (M_A + M_B + m_{sway}) \nu &= M_B \nu_B \\ \nu &= \frac{M_B \nu_B}{M_A + M_B + m_{sway}} \end{aligned} \tag{42}$$

where

- $M_A$  : mass of struck ship
- $M_B$  : mass of striking ship
- $m_{sway}$  : added mass of struck ship in sway motion
- $\nu$  : final velocity in y-direction
- $\nu_B$  : initial velocity of the striking ship in y-direction

Total energy absorbed in the collision, which is equal to the kinetic energy lost by striking ship, is defined as:

$$\Delta KE = \frac{1}{2} M_B \nu_B^2 - \frac{1}{2} (M_A + M_B + m_{sway}) \nu^2 \quad (43)$$

$$\Delta KE = \frac{M_B (M_A + m_{sway})}{2 (M_A + M_B + m_{sway})} \nu_B^2$$

Also, Minorsky assumed added mass of the sway to be equal to  $0.4M_A$ . For the collisions with an impact angle different than 90, the transversal component of the velocity of the striking ship must be introduced. After these modifications the absorbed kinetic energy by struck ship becomes:

$$\Delta KE = \frac{M_A M_B}{2M_A + 1.43M_B} (\nu_B \sin \phi)^2 \quad (44)$$

### 5.3.2 DAMAGE

DAMAGE is the collision analysis software developed by Massachusetts Institute of Technology (MIT). In its external dynamics model, another degree of freedom is added to the model by including the yaw motion of the struck ship. It is useful when the impact position of the collision is not at the centre of gravity of the struck ship. It enables the model to take into account energy losses resulted from the yaw motion (Simonsen, 1999). This model is not applicable for the cases of oblique collisions or struck ships with initial surge velocity.

By using the principles of conversation of linear and angular momentum, final velocity can be obtained as following:

$$\begin{aligned} M_{Ay} \nu_A + M_{Bx} \nu_B &= M_{Bx} \nu_B^i \\ I_{Az} \omega_A + M_{Bx} \nu_B x_A &= M_{Bx} \nu_B^i x_A \\ \nu_B &= \nu_A + x_A \omega_A \end{aligned} \quad (45)$$

and the final linear and angular velocities of the struck ship become:

$$\nu_A = \nu_B^i \frac{1}{\left(1 + \frac{M_{Ay} x_A^2}{I_{Az}} + \frac{M_{Ay}}{M_{Bx}}\right)} \quad (46)$$

$$\omega_A = \nu_B^i \frac{\left( \frac{M_{Ay} x_A}{I_{Az}} \right)}{\left( 1 + \frac{M_{Ay} x_A^2}{I_{Az}} + \frac{M_{Ay}}{M_{Bx}} \right)} \quad (47)$$

Furthermore, the kinetic energy absorbed by struck ship can be found by using following expression:

$$\Delta KE = \frac{1}{2} M_{Ay} \nu_A^2 + \frac{1}{2} M_{Bx} \nu_B^2 + \frac{1}{2} I_{Az} \omega_A^2 - \frac{1}{2} M_{Bx} (\nu_B^i)^2 \quad (48)$$

where

- $M_{Ay}$  : total mass of struck ship (including added mass in sway directions)
- $M_{Bx}$  : total mass of striking ship (including added mass in surge directions)
- $I_{Az}$  : total inertia about yaw axis of struck ship (including added inertia in yaw)
- $\nu_B^i$  : initial velocity of striking ship
- $\nu_B$  : final velocity of striking ship in sway direction of the struck ship
- $\nu_A$  : final velocity of the struck ship in the sway direction
- $\omega_A$  : final angular velocity of the struck ship
- $x_A$  : longitudinal impact position to the centre of gravity of the struck ship

### 5.3.3 MCOL

MCOL is developed in 1980 by Mitsubishi to deal with rigid body dynamics in ship collisions. Le Sourné improved MCOL and made it possible to assess large displacements considering gyroscopic effects and viscous damping (Le Sourné et al. 2001). Also, it may be coupled as a hydrodynamic sub-routine to evaluate external dynamics. It takes 6-degrees of freedom into account therefore it is applicable to solving advanced problems. The hydrodynamics coefficients along with the added mass and restoring stiffness are necessary to be calculated by using a hydrodynamics/seakeeping code (e.g. Hydrostar) for MCOL.

Currently, MCOL code is used by coupling with a commercial non-linear finite element software so-called LS-DYNA/MCOL and also utilized as an external dynamics subroutine for SHARP Tool (Le Sourné 2012). For further details refer to Le Sourné H et al (2001).

## 5.4 Coupling of Internal and External Models

Previously, the majority of the internal mechanics methods evaluate ship collisions uncoupled with the external dynamics. This type of methods directly consider the final velocities of both striking and struck ships estimated by the external model to determine absorbed kinetic energy by the deforming structural elements. A significant variance may be observed in accuracy of the results depending on the collision scenario.

There are some other methods which are used to simulate the collision with a fully coupled solution. In those methods, velocities and transformed energy are computed at each time-step and the collision problem is investigated progressively. The simulation lasts until the velocities of the striking and struck ship converge to a certain equal value. After that time, forces acting on the ships become zero, and no further deformation occurs.

### 5.4.1 SHARP Tool

SHARP tool has been developed to simulate and analyse the collision incidents. It is able to assess the collision of ships with deformable structures for both striking and struck vessels. Crash force is calculated at each time step coupled with the hydrodynamic forces to imply the influence of the external dynamics.

The software has user-friendly and practical graphical user interface to define all the physical parameters. Graphical user interface (GUI) of the SHARP software is shown in the following Fig. 24.

Since the importance of the tool in this study, detailed information regarding the SHARP software is given in Section 6.

### 5.4.2 SIMCOL

The Simplified Collision Model (SIMCOL) has been developed with the support of the Society of Naval Architects and Marine Engineers (SNAME) and Ship Structure Committee. SIMCOL provides simultaneous time domain solution of external dynamics and internal mechanics models.

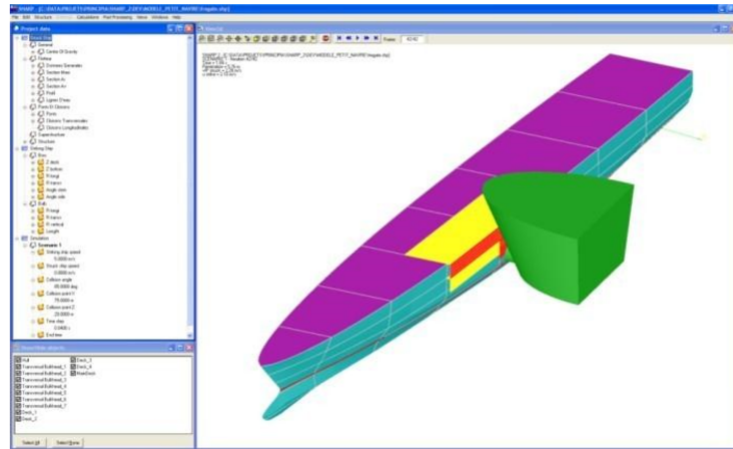


Figure 24: Graphical user interface (GUI) of the SHARP

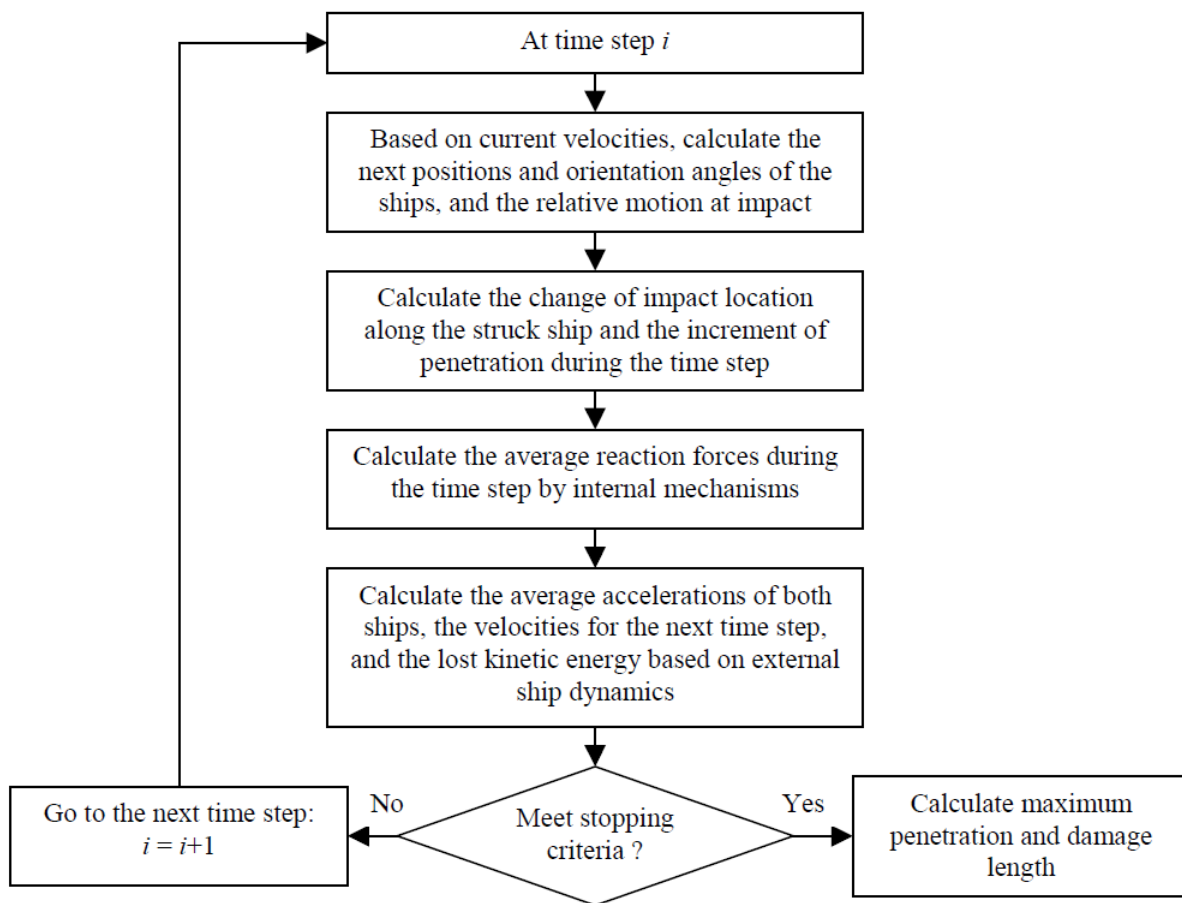


Figure 25: SIMCOL workflow (Brown, 2001)

In Fig. 25, the workflow of SIMCOL is presented. The internal mechanics model computes the deformation with respect to the relative motions of the colliding ships at each time-step. For different types of vertical

components, all have an individually defined deformation mechanism. Those are: membrane tension, shell rupture, web frame bending, shear and compression and friction. For the horizontal components (decks, stringers), it calculates the energy by using Minorsky (1959) correlation.

### 5.4.3 LS-DYNA finite element solver (with MCOL)

LS-DYNA is an advanced multiphysics simulation software package developed by the Livermore Software Technology Corporation (LSTC). It is a general-purpose finite element code for analysing the large deformation static and dynamic response of structures including structures coupled to fluids. While the package continues to contain more and more possibilities for the calculation of many complex, real world problems, its origins and core-competency lie in highly nonlinear transient dynamic finite element analysis (FEA) using explicit time integration.

The problem of internal mechanics of the collision, which is governed by buckling, yielding and rupture of assemblies and materials, is solved by LS-DYNA explicit finite element code. Collision forces and absorbed energies are computed in this step. External dynamics of the collision i.e. global motions of two bodies under collision forces and hydrodynamic forces, are calculated by MCOL algorithm and coupled with LS-DYNA (Le Sourne et al., 2003).

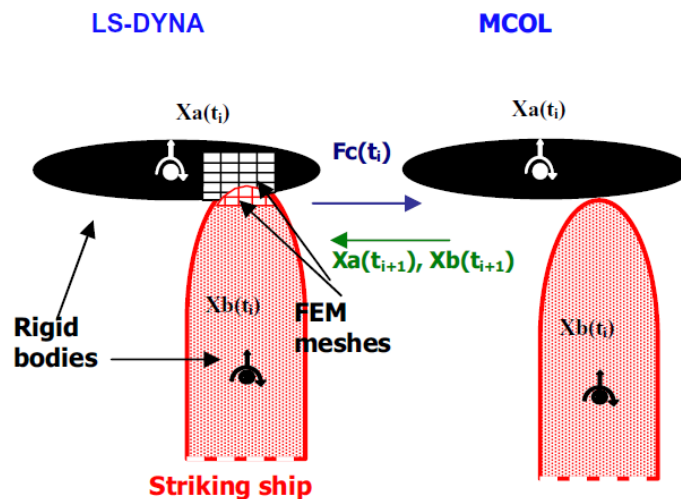


Figure 26: LS-Dyna/MCOL collision simulation (Le Sourne et al., 2003)



## **6 SHARP TOOL**

### **6.1 General**

The crash force is calculated at each time step coupled with the hydrodynamic forces to imply the influence of the external dynamics. Those hydrodynamic forces are in the form of inertia, damping and restoring forces which directly act on the dynamic behaviour of the ship hull in the simulation. Hydrodynamic matrices are obtained from external software such as HydroStar developed by Bureau Veritas. The crushing forces are determined using the super-element method. Crushing forces and corresponding moments are then transmitted to the external dynamics program which calculates the new acceleration, velocity and position of each ship. In Fig. 27, the algorithm of the program is represented in a flowchart.

When the surge velocity of the striking ship equals the sway velocity of the struck ship at the impact point, the program stops and the graphical user interface allows post-treating simulation results like:

- the crushing force and the absorbed energy given as a function of the penetration
- the hydrodynamic forces acting on the ship side
- graphical views of the collision event

In the definition of the striking ship, only the bow part of the ship, which is related to the collision, is modelled in order to simplify the problem. Moreover, there is no need to define transversal stiffeners, since the method considers only longitudinal elements of the ship structure to compute the crushing strength. The striking ship bow is modelled without transversal elements. Striking ship can be defined to have rigid or deformable structure.

Generating the models is simple and super-elements are modelled automatically by the program. The most notable strength of the tool is its effortless modelling and fast computational time comparing to the FEA.

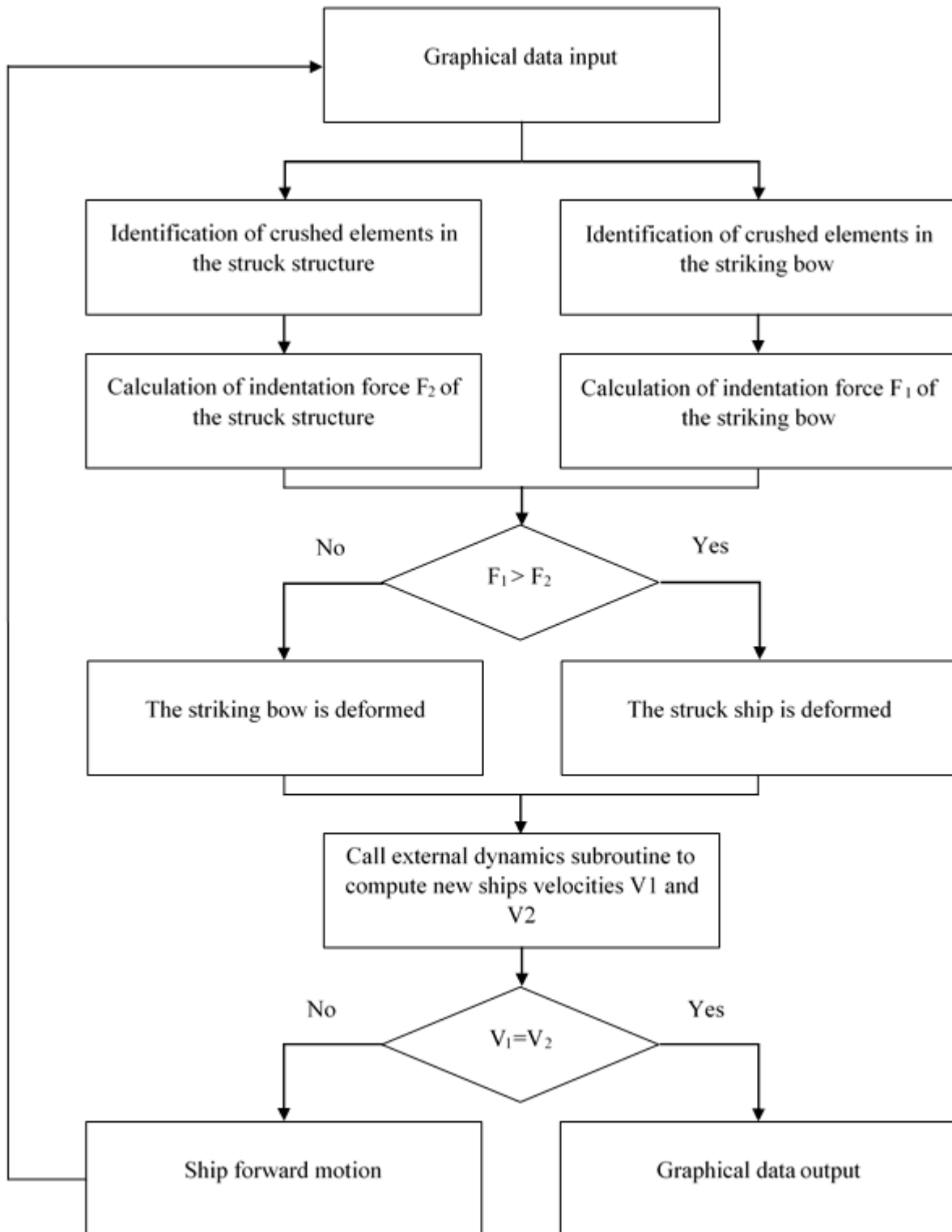


Figure 27: SHARP workflow (Paboeuf & Le Sourne et al., 2015)

## 6.2 FEM versus SHARP Tool

According to the A.D.N. Regulations Section 9.3.4.4, the collision energy absorbing capacity shall be determined by means of a finite element analysis (FEA). In this study, instead of finite-elements, super-elements by using SHARP are utilized to obtain collision energy absorbing capacities. In this section, the differences between the two approaches are discussed and possible adaptations are suggested.

### 6.2.1 Material properties

#### FEM

According to A.D.N., due to the extreme behaviour of the material and the structure during a collision, and non-linear effects caused by the geometry and material, the true stress-strain relation must be used:

$$\sigma = C \epsilon^n \quad (49)$$

and,

$$n = \ln(1 + A_g) \quad (50)$$

$$C = R_m \left( \frac{e}{n} \right)^n \quad (51)$$

where

$A_g$  : the maximum uniform strain related to the ultimate tensile stress  $R_m$

$e$  : natural logarithmic constant

The values  $A_g$  and  $R_m$  are determined by tensile tests.

In case that the only ultimate tensile stress result  $R_m$  is available, following approximation can be used in order to obtain the  $A_g$  value from the  $R_m$  value. This approximation is valid for shipbuilding steel with a yield stress  $R_eH$  less than 355 [ $N/mm^2$ ].

$$A_g = \frac{1}{0.24 + 0.01395 R_m} \quad (52)$$

If tensile test results are not available in the calculation phase, minimum values of  $A_g$  and  $R_m$  should be used which are defined by a recognized classification society. For other material or shipbuilding steel with higher yield stress ( $> 355 N/mm^2$ ), material properties must be agreed upon with a recognized classification society.

## SHARP

In SHARP, the true stress-strain relation is not applicable. A rigid-plastic material assumption is used to define material behaviour. An average yield stress  $\sigma_0$  is introduced in material properties in SHARP algorithm.

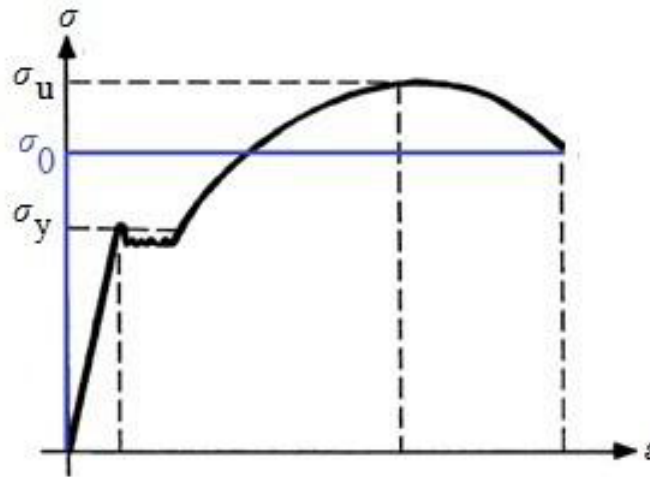


Figure 28: Comparison between the true stress-strain relation and SHARP

In Fig. 28, the black and the blue line represent the true stress-strain relation and assumed relation in SHARP respectively.  $\sigma_u$  and  $\sigma_y$  are denoted for the ultimate stress and yield stress.  $\sigma_0$  is calculated by arithmetic mean value of  $\sigma_u$  and  $\sigma_y$  as shown below:

$$\sigma_0 = \frac{\sigma_u + \sigma_y}{2} \quad (53)$$

According to this approach, a constant stress is maintained until the strain level reaches rupture strain. After that moment, it is assumed that the element cannot contribute to the impact resistance and is eliminated from the calculation.

## 6.2.2 Rupture Criteria

### FEM

In A.D.N. rupture of the element is defined by the failure strain value for FEA. If the strain in the thickness direction exceeds the failure strain limit of the element, this element must be removed from the model and cannot contribute to the deformation energy at next time steps. The following expression is to be used for the calculation of rupture strain:

$$\varepsilon_f(l_e) = \varepsilon_g + \varepsilon_e \frac{t}{l_e} \quad (54)$$

where

$\varepsilon_g$  : uniform strain

$\varepsilon_e$  : necking

$t$  : plate thickness

$l_e$  : individual element length

Uniform strain and necking values for shipbuilding steel with a yield stress  $R_{eH}$  of less than 355 N/mm<sup>2</sup> must be taken from the table given below:

Table 19: Uniform strain and necking values in A.D.N.

Stress states	1-D	2-D
$\varepsilon_g$	0.079	0.056
$\varepsilon_e$	0.76	0.54
Element type	Truss beam	Shell plate

Strain values other than specified above, which are taken from measurements from some cases, can be used in agreement with the recognized classification society. Furthermore, other rupture criteria can also be applied if this criteria are proven by the tests and accepted by the recognized classification society.

### SHARP

Application of the rupture criteria has to be done with some assumptions because of the algorithm of SHARP and the super-element theory. Firstly, there is no individual input for the rupture strain of beam

elements in the software. Those elements are classified into the groups within their attached plating, so rupture strain has the same value with the plate element. Secondly, the individual element length  $l_e$  is mentioned in Eq. 54 cannot be applicable due to the methodology of the super-element theory which introduces macro-elements instead of small elements in FEM.

### 6.2.3 Friction energy

#### FEM

Another energy absorption mechanism other than deformation of structural elements in collision phenomenon is the friction. The Coulomb friction coefficient  $\mu_c$  is given by A.D.N. as follows:

$$\mu_c = FD + (FS - FD) e^{-DC |\nu_{rel}|} \quad (55)$$

with the values of

$$FD = 0.1$$

$$FS = 0.3$$

$$DC = 0.01$$

$|\nu_{rel}|$ : relative friction velocity

For two scenarios of 55° and 90° collision angles which is prescribed by the A.D.N., friction coefficients are calculated as follows:

- for 90°

$$|\nu_{rel}| = 0 \text{ m/s} \quad \implies \quad \mu_c = 0.3$$

- for 55°

$$|\nu_{rel}| = 5.736 \text{ m/s} \quad \implies \quad \mu_c = 0.289$$

#### SHARP

In SHARP, the Coulomb friction coefficient  $\mu_c$  is predefined as a constant value ( $\mu_c=0.3$ ). In this version, no option is available to modify this coefficient. However, in the collision angles between 30° and 150°, the

contribution of this coefficient is expected to be insignificant. In addition to that, for the collision scenario of  $90^\circ$ , the friction coefficient value is 0.3 which is the exact value required by the A.D.N. And for the collision scenario of  $55^\circ$ , the difference of the Coulomb friction coefficients between A.D.N. and SHARP is small and thus the effect of the difference can easily be neglected.

#### **6.2.4 Contribution of shear forces**

In the super-element theory, shear force on plates is neglected. Therefore, bending and membrane effects are the contributors for determination of the internal energy rate. It must also be also noted that those effects are calculated uncoupled.

Elastic strain and sliding are not taken into account in the formulations which are used in order to obtain the crushing force of the striking vessel. Small angles of impact may lead to erroneous results since the effect of those properties will be more significant. Therefore, it is suggested that the collision angles between  $30^\circ$  and  $150^\circ$  are to be considered (Paboeuf. et al. 2015).

### **6.3 Modelling of struck vessel**

SHARP has a simple fast toolbox for modelling. On the other hand, it is not possible to model all the structural details. Those limitations are listed below:

- Brackets cannot be modelled
- Lightening, sloshing holes or manholes cannot be modelled
- Corrugated plates cannot be modelled
- Inner bottom can only be defined as horizontal surface
- If there is more then one type of stiffeners on a single plate, only one of the stiffener property can be chosen

## 6.4 Handling of the results

Due to the theory of super-element behind the algorithm of SHARP, elements are activated and taken into account in the calculation of the impact resistance only when they are in physical contact with the striking bow geometry. The independence of super-element behaviour from their boundary conditions is the main assumption of the super-element theory. Therefore, SHARP does not consider any interaction between neighbouring elements. However in reality, neighbouring structural elements also contribute to the impact resistance. In order to obtain more accurate results, the absorbed energy is calculated by averaging the values of the energy absorbing capacities of 9 impact positions around the real impact position.

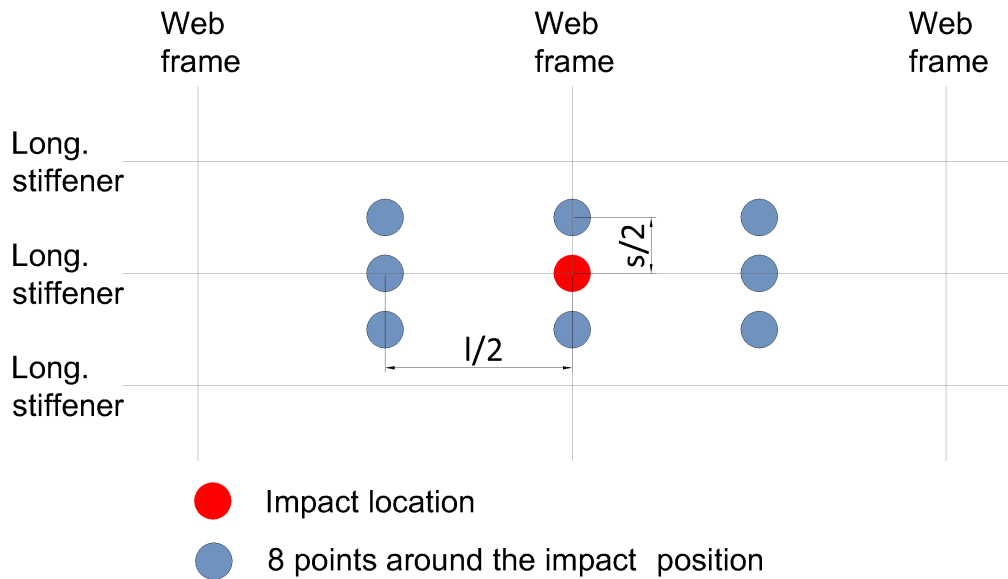


Figure 29: Impact locations on side shell

In Fig. 29. suggested positions on side shell are shown for the case of collision on web frame, where

$s$  : stiffener spacing

$l$  : web frame spacing

To overcome this drawback, total energy absorbing capacity is calculated as in Eq. 56.

$$E_{total} = \frac{\sum_{i=1}^9 E_i}{9} \quad (56)$$



## 6.5 Determined collision energy values

The validation tests of SHARP are performed by Paboeuf et al. (2015). The results are validated by comparing the energy values of SHARP with LS-Dyna finite element solver. The two cases with different impact angles are investigated:

- A FPSO impacted by a tanker (T1) → Scenario I & II
- A cargo carrier impacted by a tanker (T2) → Scenario III & IV

In these simulations, the striking ships are considered to have a deformable bow on impact which means a portion of the collision energy is absorbed by the deformation of the striking bow as well.

(a) Struck ships

	FPSO	Cargo carrier
<b>Length [m]</b>	280.00	274.00
<b>Breadth [m]</b>	60.00	43.00
<b>Draft [m]</b>	23.00	14.90
<b>Depth [m]</b>	33.00	26.25
<b>Displacement [tons]</b>	345000	107180

(b) Striking ships

	Tanker T1	Tanker T2
<b>Length [m]</b>	274.00	274.00
<b>Breadth [m]</b>	48.00	48.00
<b>Depth [m]</b>	25.40	26.25
<b>Displacement [tons]</b>	142800	140000

Table 20: Main particulars of the ships in the validation

The drafts of the striking vessels are determined by the vertical positions of the impact. 4 scenarios are created to present the comparison of the energy and the penetration values. Each scenario has the results from FEA and from SHARP for the nine impact locations around the real location which is previously mentioned in Sec 6.4. The created scenarios are given in Table 21.

Table 21: Collision scenarios for the validation

Parameters	Scenario I	Scenario II	Scenario III	Scenario IV
<b>Longitudinal position [m]</b>	137.5	137.5	127.6	127.6
<b>Vertical position [m]</b>	34.00	14.00	26.25	26.25
<b>Struck vessel speed [m/s]</b>	0	0	0	0
<b>Striking vessel speed [m/s]</b>	2.0	4.0	2.5	2.5
<b>Collision angle [deg]</b>	75	30	90	45

In the Scenario I, the more conservative results are observed for SHARP, with +9.3% discrepancy on the penetration into the struck ship and around +3.5% discrepancy on the struck ship deformation energy.

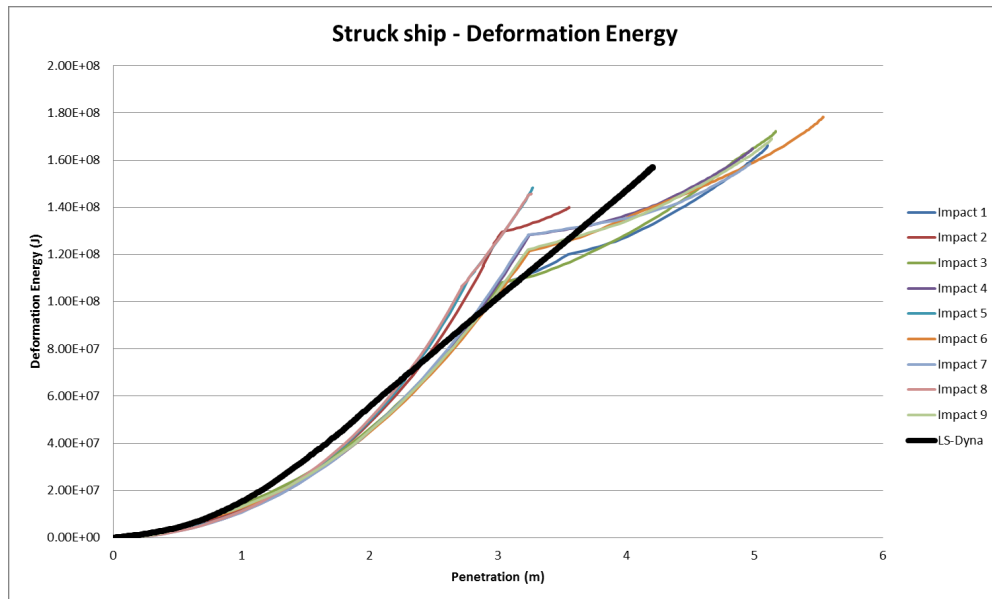


Figure 30: Results of the Scenario I

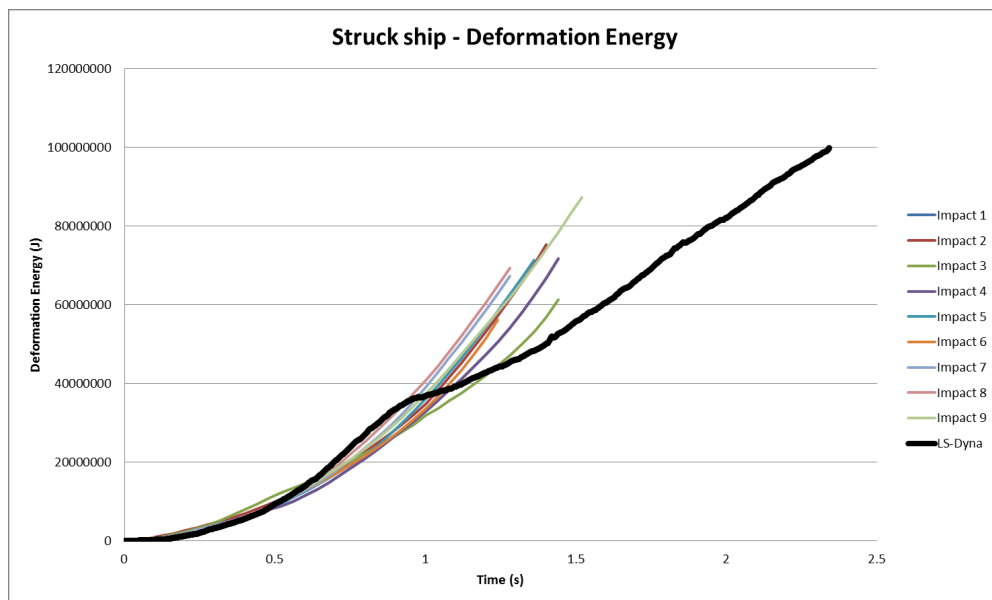


Figure 31: Results of Scenario II

In the Scenario II, the results indicate a discrepancy of +7.7% on the penetration into the struck ship. On the other hand, the struck ship deformation energy is determined with -28% discrepancy. This underestimation can be explained by the reason of the neglect of the overall bending of the bulb occurs during the collision

in SHARP. The deformation energy is absorbed by the struck ship in SHARP and by the striking bulb in LS-Dyna.

The Scenario III results analysis (perpendicular collision) shows that the struck ship deformation energy is underestimated in SHARP. The discrepancy regarding the average penetration remains acceptable when comparing with LS-Dyna results. SHARP computations lead to +8.5% discrepancy on the penetration into the struck ship and -18% discrepancy on the struck ship deformation energy. The difference of the results can be explained by the geometrical simplification made for the inner hull when building the SHARP model. The bottom part of the inner hull which is near the bulb impact is inclined and modelled in LS-Dyna accurately. However, in SHARP it is assumed to be vertical and straight. So that the penetration and the energy values deviate for SHARP and LS-Dyna.

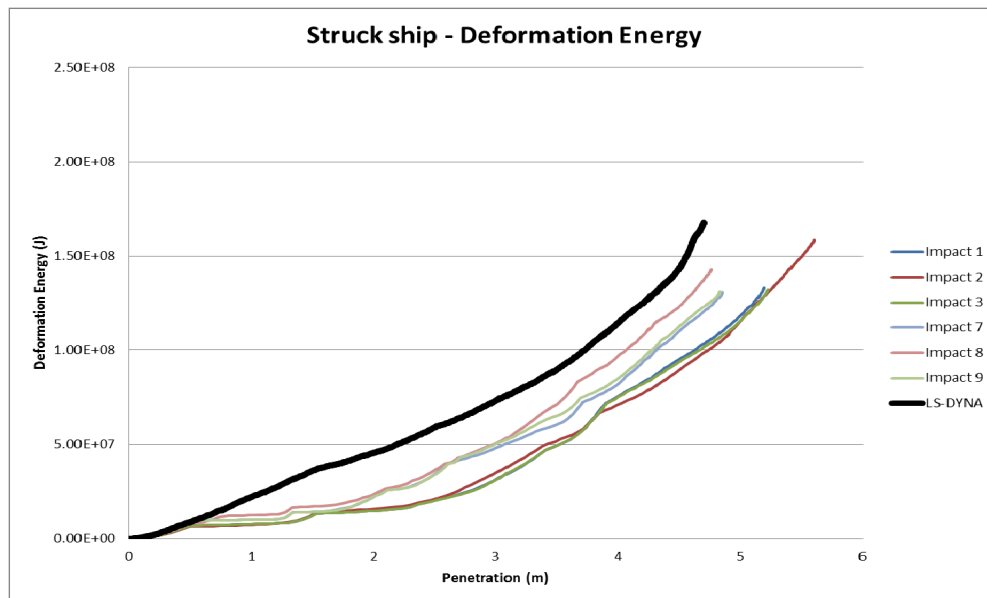


Figure 32: Results of Scenario III

In the scenario IV, the inner hull is not impacted by the bulb and the SHARP results has a discrepancy of +3.1% for the struck ship deformation energy and +11% for the penetration in comparison with LS-Dyna.

According to Paboef et. al.(2015), the discrepancy in penetration into the struck ship is around 10% and generally conservative. The difference between the deformation energies is less than 5%. With these results, it is seen that the obtained results in SHARP is close to the LS-Dyna results.

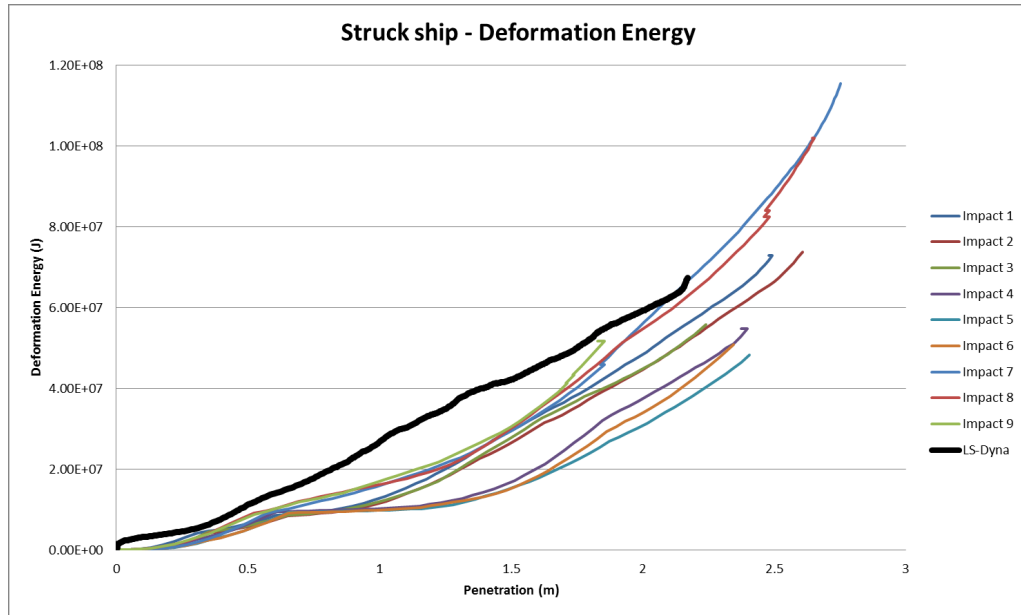


Figure 33: Results of Scenario IV

## **7 APPLICATION OF SHARP TO CRASH-WORTHINESS ASSESSMENT OF THE INVESTIGATED VESSEL**

### **7.1 General**

In this section, the application of the super- element theory through the instrumentality of the SHARP software is demonstrated on the investigated vessel represented in Section 3. The SHARP based procedure is detailed in regard to the application.

### **7.2 Modelling of struck vessel**

Three struck vessels are modelled within the study. Those are:

1. Reference construction
2. Alternative construction 1 (reduced double hull spacing without any reinforcements)
3. Alternative construction 2 (reduced double hull spacing with reinforcements)

#### **7.2.1 Hull form modelling**

Since only the structural arrangements and scantling is modified on the vessels, hull lines will be common for all three type of constructions.

The hull form is defined by a parametric model based on the definition of three sections (aft perpendicular, fore perpendicular and midship section) and longitudinal lines. Each section is defined by 6 control points which are connected through corresponding points between the sections through the longitudinal lines. In the data tree of the SHARP, firstly main particulars of the vessel are defined. These parameters are:

- **LPP** length between perpendiculars, also called L
- **L/B** ratio between the length between perpendiculars and the width at the waterline (B)
- **B/T** ratio between the width at the waterline and the draught (T)
- **B/D** ratio between the width at the waterline and the depth (D)

- **Longeur prismatique** length of the prismatic section of the ship in % of LPP
- **Centre section prismatique** longitudinal position of the prismatic section in % of LPP

Then control points are defined by defining the coordinate of point in the building sections window.

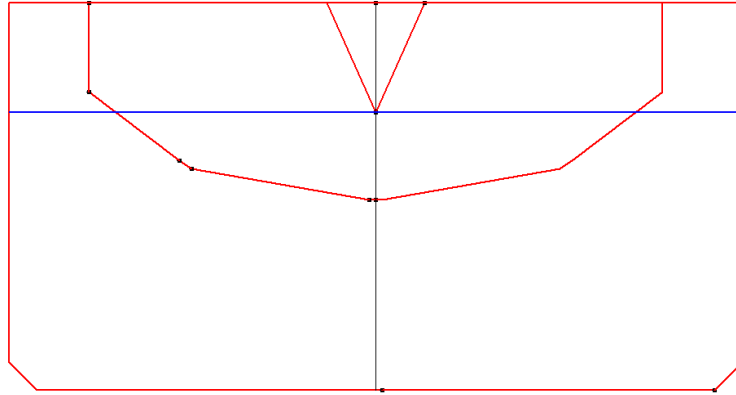


Figure 34: Building sections

In the next step, the longitudinal lines, which pass through the control points in the sections, are defined. Those are:

- centreline
- 4 lines for knuckles
- deck contour

The profile view can be edited in "Profile" chapter in the tree. Parameters that can be edited:

- **Pente d'étrave:** slope of the bow
- **Pente de quille:** slope of the keel starting from the fore section of prismatic section, or from the mid-section if no prismatic section is defined.
- **Pente de voute arrière:** slope of the keel above horizontal, on the aft perpendicular

It must be noted that SHARP is not a tool for advanced definition of hull shape, and as such is not equipped with advanced line or surface functions. However, the hydrodynamic matrix, used for the ship motions, is obtained from fine hull shape description in HydroStar.

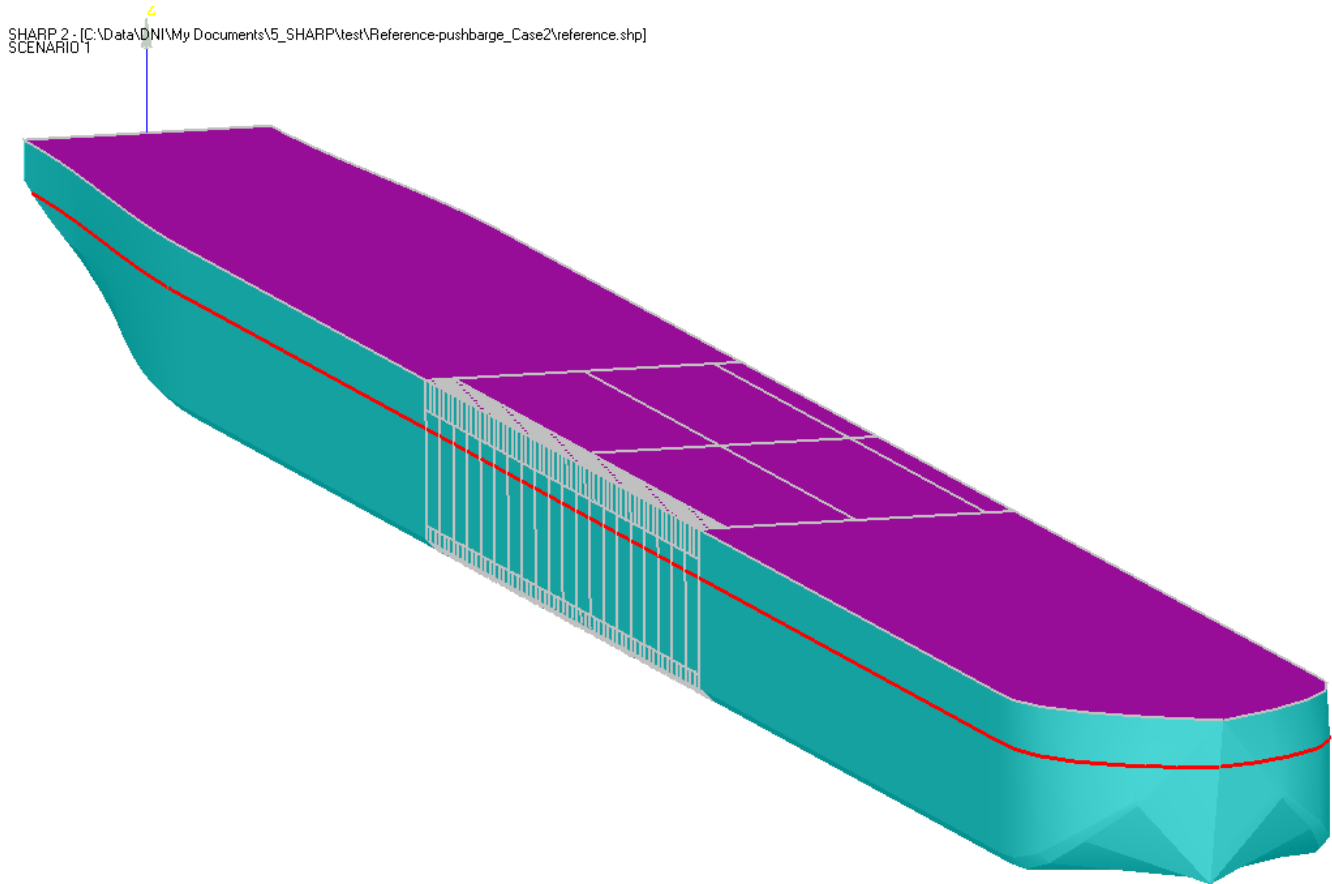


Figure 35: SHARP complete model

## 7.2.2 Structural modelling

In SHARP, the modelling of the ship structure comprises the definition of the ship surfaces (decks, bulkheads, hull) and scantlings including the stiffeners. Also, a fixed frame spacing in meters must be defined before starting the modelling. Only the starboard side must be modelled. The software will automatically create the symmetrical surfaces about the centreline at the port side.

### 7.2.2.1 Definition of the surfaces

Surfaces can be limited in X, Y and Z and other surfaces can be used as the limits. The position of the surfaces is defined by the following reference locations:

- Decks: vertical position with respect to the base line in meters
- Transversal bulkheads: longitudinal position with respect to the aft perpendicular in number of frames
- Longitudinal bulkhead: transversal position with respect to the centreline in meters

In the modelling phase of the vessel, transversal bulkheads are created first. Two cargo tanks are modelled limiting by the transversal bulkheads for this case. Secondly horizontal surfaces such as the decks, the inner bottom plate is modelled. Apart from these, a virtual horizontal surface (later on the thickness will be defined zero) is created to use it as the function of a geometrical limit to create other elements. In our case it is created in order to define the vertical limit for plate brackets at the ordinary frames. In the next step, longitudinal bulkheads such as the centreline bulkhead, central bottom girder, lateral bottom girder and inner side plating are modelled. Finally, other transversal elements are modelled such as floors, web frames, ordinary frame brackets.

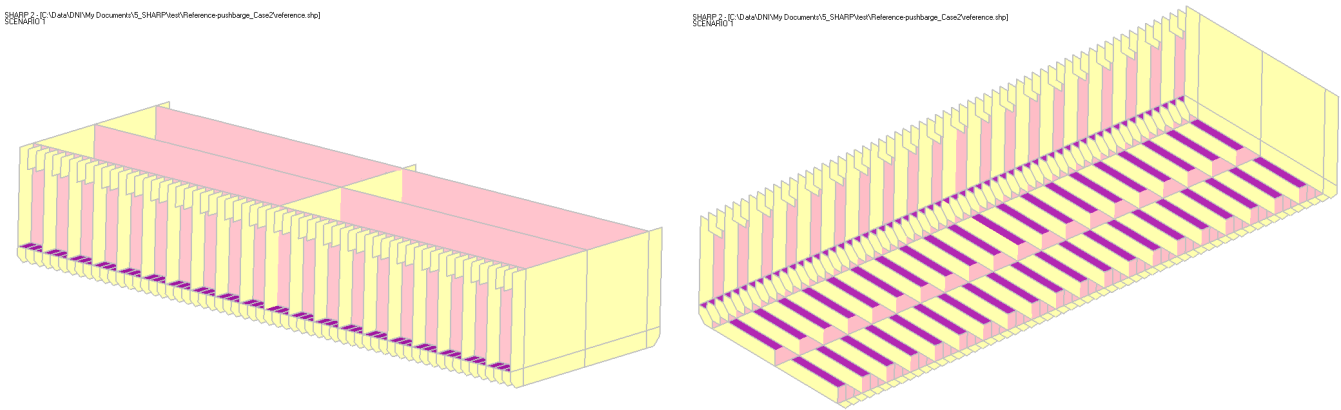


Figure 36: Structural model from different views (hidden deck and outer shell)

In terms of surface definition, the only difference between reference and alternative constructions is the position of the inner side shell. Y coordinates of the inner side bulkhead in respect to the centerline:

for Reference construction: 4.692 m (width of side tank: 1 m)

for Alternative constructions 1 & 2: 4.892 m (width of side tank: 0.8 m)



### 7.2.2.2 Definition of the scantlings

The scantlings are defined by editing the parameters in *Physical Properties* tab in the tree for subjected elements. In this tab, the thicknesses of the plates and the supporting member profiles are entered. Profile types either may be chosen from the SHARP library, or created in *Materials...* window.

In SHARP, in order to model the profiles, first the surface, on which the profiles will be located, is selected. Then, the desired profile type and the spacing are defined. Stiffeners are automatically created on the selected surface. The description of the profiles in SHARP:

1. **Frames:** primary transversal supporting member
2. **Stiffeners:** secondary longitudinal supporting member (can be vertical or horizontal at only transversal bulkhead)
3. **Girders:** primary longitudinal supporting member at deck

Net plate thickness values, which are represented in Section 3, are used to define the surfaces. There can be defined only one thickness value for each surface except the hull shell. By using *Patch* command, the hull shell can be divided into different regions with desired thickness and stiffener configurations. On the other hand, there is no option within the theory to model the holes on platings. To overcome this issue, the subjected elements are modelled without holes but with the equivalent plate thicknesses. It is assumed to maintain the same structural behaviour on impact resistance. Equivalent plate thicknesses are calculated by using following formula:

$$t_{eq} = \frac{A_{actual} t_{actual}}{A_{actual} + A_{hole}} \quad (57)$$

where

- $t_{eq}$  : equivalent plate thickness  
 $t_{actual}$  : actual plate thickness  
 $A_{actual}$  : actual area of the plating  
 $A_{hole}$  : total area of the holes on plating

The formula given in Eq. 57 is derived from the material volume equality of the actual and equivalent plate.

For the details of these calculations see Appendix C.

In some cases, some virtual horizontal surfaces may be needed to use as a limit for other surfaces. When the thickness of a surface is defined zero, the contribution of this surface is not taken into account in the computation.

When there is more than one type of stiffeners on a single plate, individual properties of this stiffener is neglected and assumed to be the same as the other stiffeners. For the instance of the investigated ship, a T-profile longitudinal stiffener is neglected which can be seen in Fig. 4 in Section 3.

The scantlings of the Reference and Alternative construction - 1 is defined in exactly the same as the conventional side structure. Applied reinforcements to Alternative Construction - 2 can be seen in the Table 22.

Table 22: Applied reinforcements to Alternative Construction - 2 (gross thickness)

<b>Reinforcements</b>	Conventional [mm]	Reinforced [mm]	Increase %
deck stringer plate thickness	11.0	15.0	36%
side plating thickness	11.0	15.0	36%
web frame thickness	8.0	10.0	25%
brackets at ordinary frame	8.0	10.0	25%
sheerstrake thickness	25.0	32.5	30%

### 7.2.2.3 Material properties

In the *Physical Properties* tab in the tree, either the default material properties can be selected, or they can be assigned individually for each surface. Profiles on the surfaces share the same material properties with their subjected surface.

Material properties are defined by editing the following parameters:

1. Name
2. Young modulus [ $MPa$ ]
3. Yield stress [ $MPa$ ]
4. Rupture toughness [ $N/mm$ ]

## 5. Rupture strain

In case of this application, *shipbuilding steel - Grade A*, which has stress limits  $\sigma_u$  and  $\sigma_y$  of 400 and 235 [MPa] respectively, is considered. By using Eq.58 which is explained in Section 6.2.1 in a more detailed way,  $\sigma_0$  is calculated as 317.5 [MPa]. Young modulus is taken as 210000 [MPa].

$$\sigma_0 = \frac{\sigma_u + \sigma_y}{2} \quad (58)$$

A.D.N. requires individual rupture strain values for each element concerning their thicknesses. With regard to the this criteria, rupture strain values are calculated for each surface according to the A.D.N. formula (see Sec. 4.4.2, Eq. 15 ) as shown in Table 23. The parameter of *individual element length* in the rupture strain formulation is introduced for the case of a finite element analysis. For this reason, the individual element length is assumed to be 200 mm in order to adapt the formulation to the super-element method. On the other hand, it is not possible to assign an individual rupture strain to the beam elements. In SHARP, the beam elements share the same rupture strain with the subjected plating.

Table 23: Created materials with different rupture strain values

<b>Conventional Vessel Scantling (Reference, Alternative Construction - 1)</b>			
<b>Items</b>	<b>Defined thickness [mm]</b>	<b>Rupture strain</b>	<b>Assigned material name</b>
Bottom plating	9.50	0.0817	S1
Bilge plating	11.50	0.0871	S2
Side shell	9.50	0.0817	S3
Sheerstrake	23.50	0.1195	S4
Deck plating	9.75	0.0823	S5
Inner bottom	7.25	0.0756	S6
Inner side	7.50	0.0763	S7
Transversal tank bulkhead	7.00	0.0749	S8
Floors*	5.94	0.0720	S9
Web frames*	5.78	0.0716	S10
Ordinary bracket (deck)	6.40	0.0733	S11
Ordinary bracket (bottom)*	5.50	0.0709	S12
<b>Reinforcements applied to Alternative construction - 2</b>			
Side shell	13.50	0.0925	S3_alt
Sheerstrake	31.00	0.1397	S4_alt
Deck stringer plate	13.50	0.0925	S5_alt
Web frame	6.78	0.0743	S10_alt
Ordinary bracket (deck)	8.00	0.0776	S11_alt

\* *equivalent thickness of the plate with the holes - see Appendix C*

### 7.3 Modelling of striking vessels

In SHARP, the bow part of the striking ships subjected to impact are modelled. In spite of the possibility to model striking vessels with their structural configurations, since A.D.N. requires a rigid striking bow, only the geometry of the bow is modelled in the case of this study. On the other hand, SHARP is able to perform the simulations with the deformable striking bow.

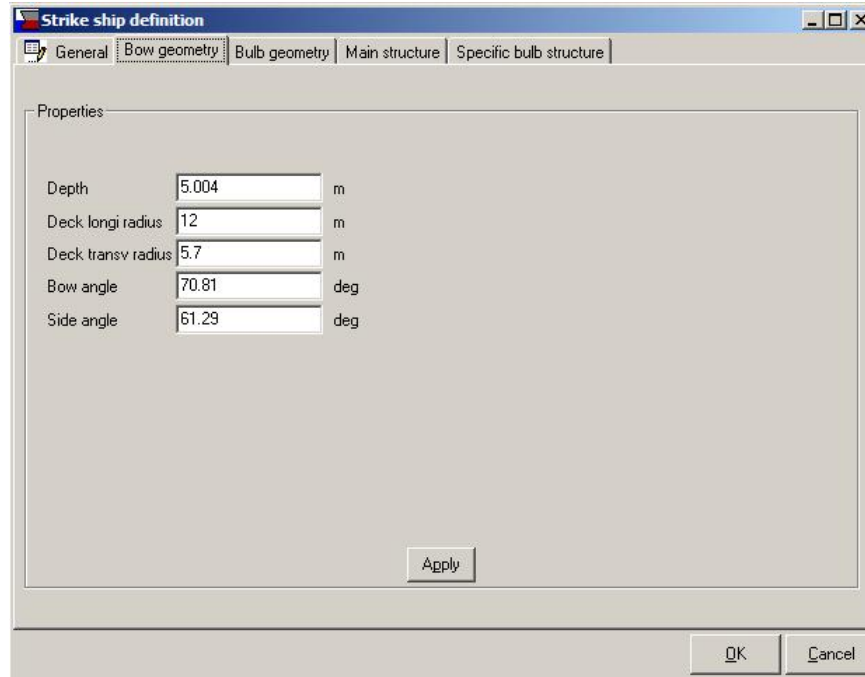


Figure 37: Striking ship definition interface

In the interface, the input parameters of a striking bow geometry are:

1. Semi major and minor radius of ellipse describing the deck
2. bow depth
3. bow angle
4. side angle

SHARP defines the bow geometry by using geometrical inputs and creates the bow model as shown in Fig. 38. Depending on the minor ( $a$ ) and major ( $b$ ) radius, geometry is created by applying the ellipse equation:

$$\frac{x^2}{a^2} + \frac{y^2}{b^2} = 1 \quad (59)$$

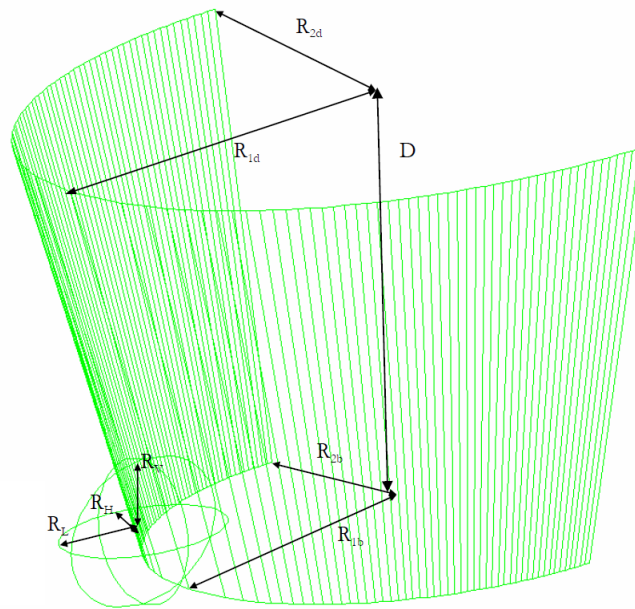


Figure 38: Bow model of striking ship

Table 24: Symbols of parameters of bow model in SHARP

Identification of the parameter	Notation
Semi major axis of the deck	$R_{1d}$
Semi minor axis of the deck	$R_{2d}$
Semi major axis of the bottom	$R_{1b}$
Semi minor axis of the bottom	$R_{2b}$
Depth	$D$
Length of the bulb	$R_L$
Vertical radius of the bulb	$R_V$
Horizontal radius of the bulb	$R_H$
Distance between the bulb tip and the foremost part of the bow	$R_D$

Two types of bow geometry are modelled in SHARP as prescribed in detail by A.D.N..

### Push barge bow

Characteristic dimensions of the bow of the push barge vessel, which is instructed by the A.D.N., are given in Table 25.

Table 25: Characteristic dimensions of barge bow

Half breadths				Heights			
fr	Knuckle 1	Knuckle 2	deck	stem	Knuckle 1	Knuckle 2	deck
145	4.173	5.730	5.730	0.769	1.773	2.882	5.084
146	4.100	5.730	5.730	0.993	2.022	3.074	5.116
147	4.028	5.730	5.730	1.255	2.289	3.266	5.149
148	3.955	5.711	5.711	1.559	2.576	3.449	5.181
149	3.883	5.653	5.653	1.932	2.883	3.621	5.214
150	3.810	5.555	5.555	2.435	3.212	3.797	5.246
151	3.738	5.415	5.415	3.043	3.536	3.987	5.278
152	3.665	5.230	5.230	3.652	3.939	4.185	5.315
transom	3.600	4.642	4.642	4.200	4.300	4.351	5.340

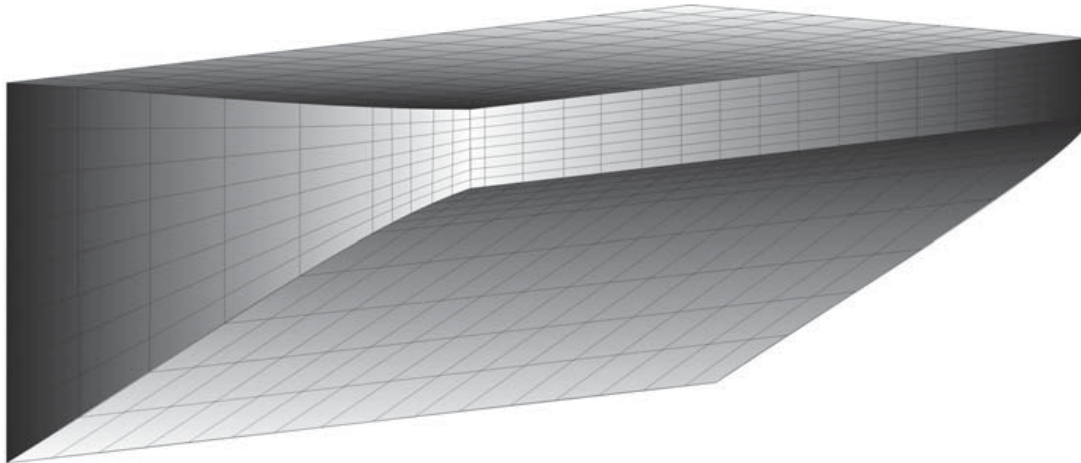


Figure 39: Illustration of push barge bow given by the A.D.N.

The defined parameters for the striking bow model are given as follows:

- Depth : 4.20 m
- Deck longi. radius : 2.00 m
- Deck trans. radius : 5.73 m
- Bow angle : 65 deg
- Side angle : 38 deg

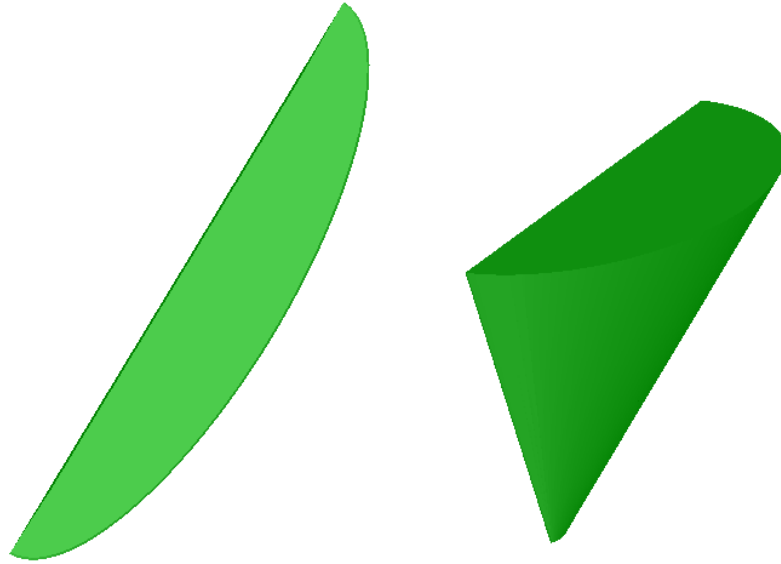


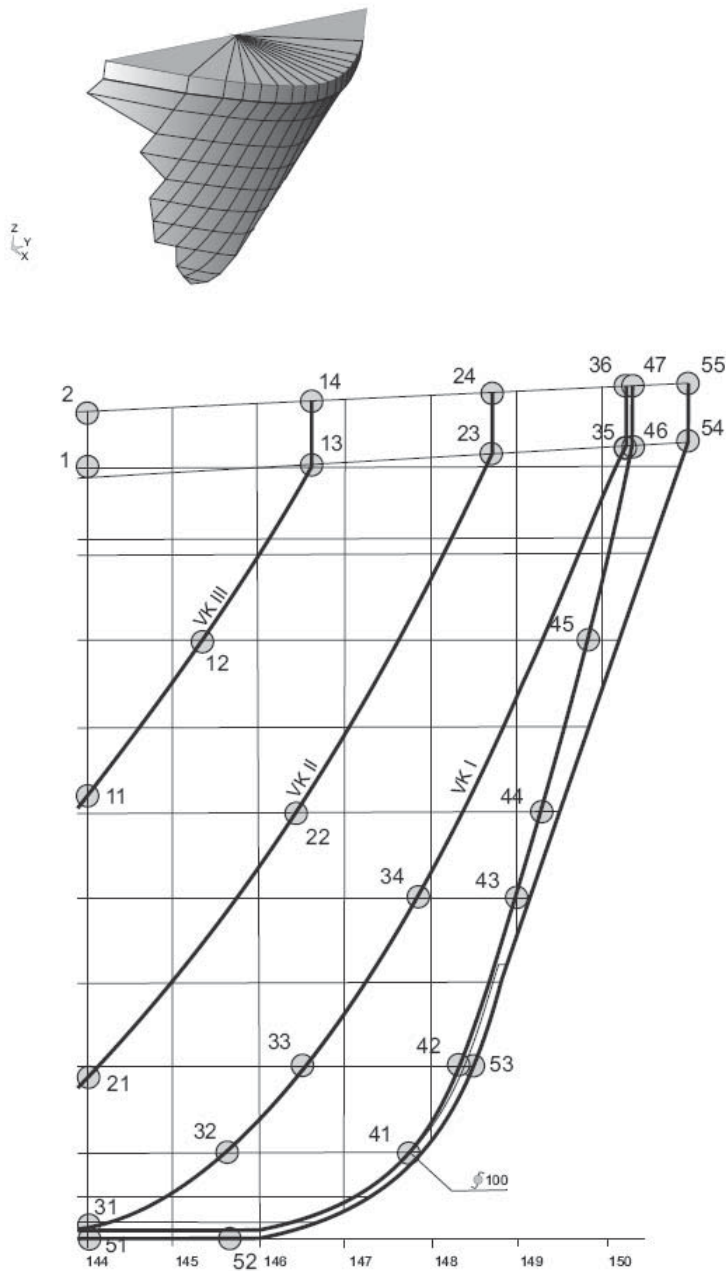
Figure 40: Modelled push barge striking vessel in SHARP

In the modelling tool of SHARP, it is not possible to have a straight stem without curvature. In order to obtain a similar push barge bow geometry given by the A.D.N., the longitudinal curvature of the ellipse is reduced as much as possible to have a flattened shape of ellipse which defines the deck geometry. Moreover, due to the limitation of the modelling of the knuckles, only one side angle can be defined. This angle is assumed to be the initial angle of side of the A.D.N. model on the impact moment.



**V-shape bow (without bulb)**

The characteristic dimensions of the V-bow are given by the A.D.N. in the following figure:



Reference no	x	y	z
1	0.000	3.923	4.459
2	0.000	3.923	4.852
11	0.000	3.000	2.596
12	0.652	3.000	3.507
13	1.296	3.000	4.535
14	1.296	3.000	4.910
21	0.000	2.000	0.947
22	1.197	2.000	2.498
23	2.346	2.000	4.589
24	2.346	2.000	4.955
31	0.000	1.000	0.085
32	0.420	1.000	0.255
33	0.777	1.000	0.509
34	1.894	1.000	1.997
35	3.123	1.000	4.624
36	3.123	1.000	4.986
41	1.765	0.053	0.424
42	2.131	0.120	1.005
43	2.471	0.272	1.997
44	2.618	0.357	2.493
45	2.895	0.588	3.503
46	3.159	0.949	4.629
47	3.159	0.949	4.991
51	0.000	0.000	0.000
52	0.795	0.000	0.000
53	2.212	0.000	1.005
54	3.481	0.000	4.651
55	3.485	0.000	5.004

Figure 41: Characteristic dimensions of V-bow

The V-bow striking ship modelled in SHARP is represented in Fig. 42.

The defined parameters for the striking bow model are given as follows:

Depth	: 4.65 m
Deck longi. radius	: 12.00 m
Deck trans. radius	: 5.70 m
Bow angle	: 70.81 deg
Side angle	: 61.29 deg

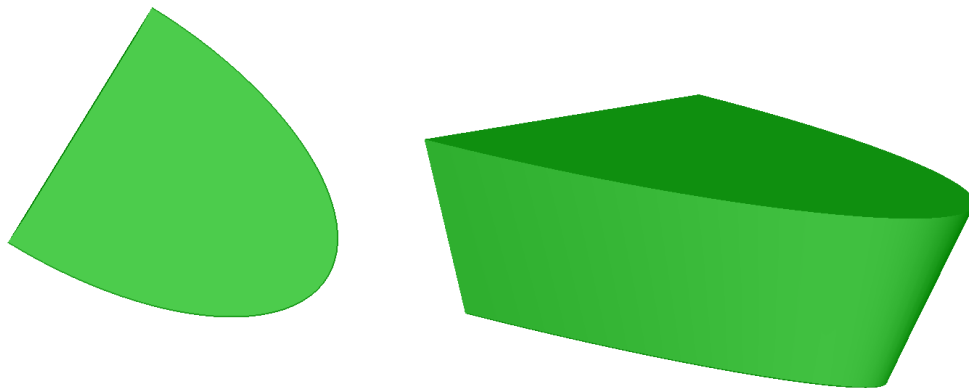


Figure 42: V-Bow striking model in SHARP

In conclusion, both aforementioned striking ships have flat stem transom. Unfortunately, there is no option to implement a flat stem transom to the striking vessel model in SHARP. For that reason, the geometry above the lower edge of vertical part of stem transom is neglected. The knuckles, and angle changes also cannot be modelled. In conclusion, it is not possible to model the exact striking ship which is described by A.D.N., but it is possible to achieve a similar geometry in SHARP.

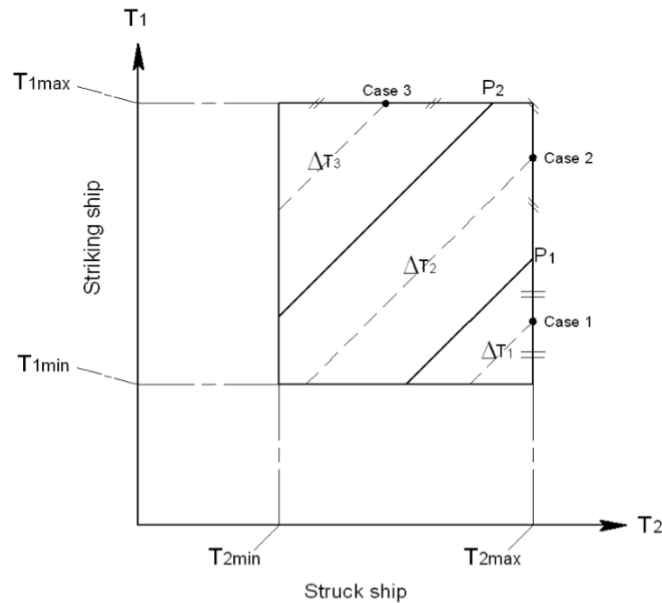
## 7.4 Creating the collision scenarios

In order to determine the vertical impact locations for the given scenarios, there is a necessity to select two real ships with similar bow dimensions. In this context, *Touax* vessel data for push barge bow and *Odina* for V-shaped bow from the BV database, are used as references for striking vessels. Minimum and maximum

drafts are taken to calculate the vertical impact locations.

For vessel *Touax* (Push-barge bow) :  
 Minimum draft : 0.564 m  
 Maximum draft : 3.400 m

For vessel *Odina* (V-shaped bow) :  
 Minimum draft : 0.807 m  
 Maximum draft : 3.650 m



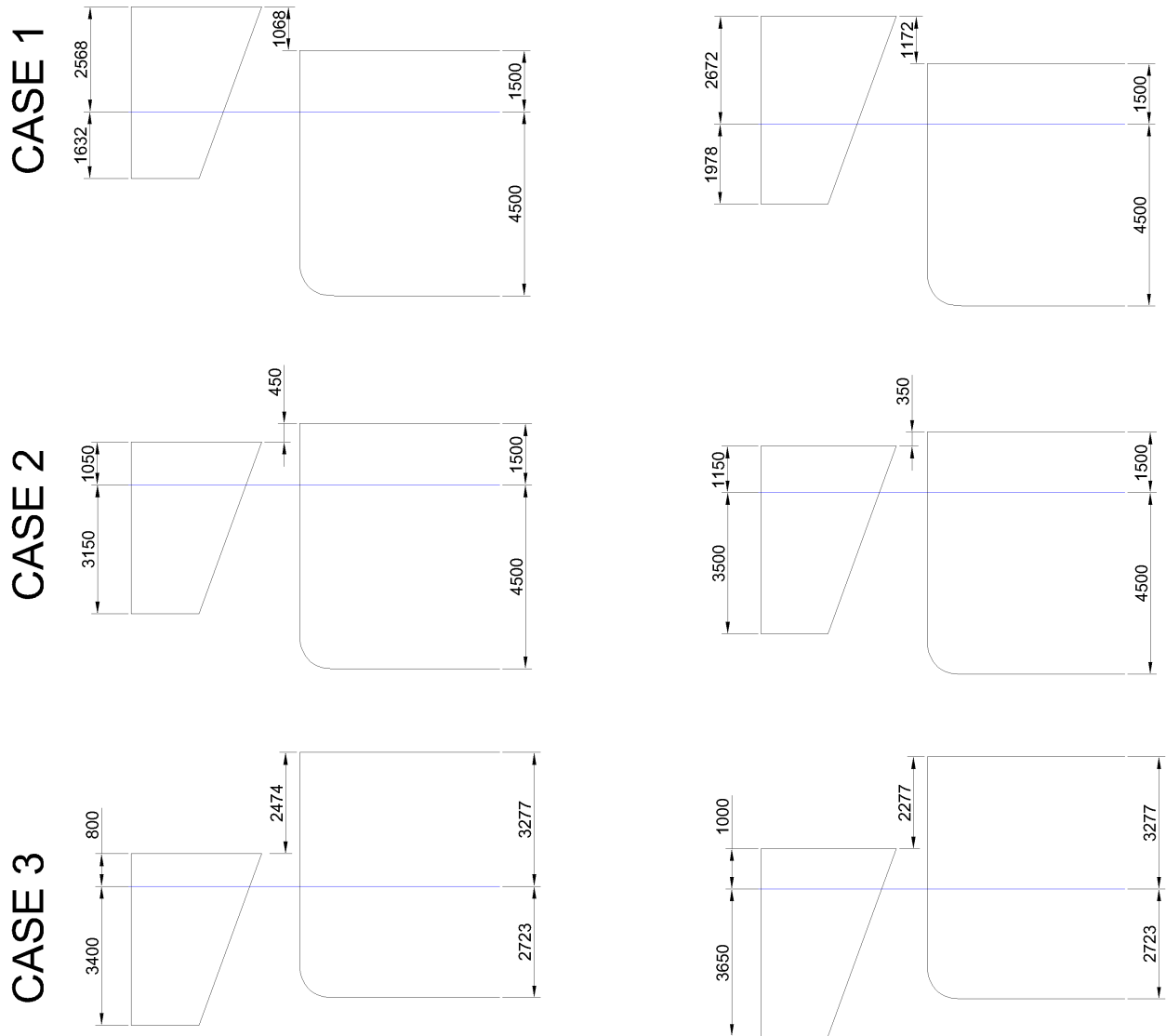
Drafts [m]	Push barge bow	V-shaped bow
$T_{1min}$	0.564	0.807
$T_{1max}$	3.400	3.650
$T_{2min}$	1.147	1.147
$T_{2max}$	4.500	4.500
$P_1$	2.700	3.150
$P_2$	4.300	4.300

Figure 43: Draft points

According to the Fig. 43, drafts of Scenario I and II for three cases of vertical collision locations are calculated. A summary of the drafts can be seen in Tab. 26. In Fig. 47, an illustration of the vertical locations with detailed dimensions for the both scenarios is shown.

Table 26: Drafts for the cases of vertical collision location cases

Drafts [m]	Scenario I (Push barge bow)		Scenario II (V-bow)	
	Striking ship	Struck ship	Striking ship	Struck ship
Case 1	1.632	4.500	1.978	4.500
Case 2	3.150	4.500	3.500	4.500
Case 3	3.400	2.723	3.650	2.723



(a) Scenario I (Push barge bow)

(b) Scenario II (V-shaped bow)

Figure 44: Vertical collision locations

The longitudinal collision locations remain the same for Scenario I and II and the distances from aft perpendicular are defined as follows:

- at bulkhead : 66.780 m
- between two webs : 59.625 m
- at web : 58.830 m

Three vertical and three longitudinal positions, a total number of nine collision locations is determined for both striking vessels. As mentioned before in A.D.N. Procedure in Sec. 4, the push barge striking bow scenarios are created with a collision angle of 55 deg, and the V-shaped striking bow with 90 deg. As it is explained in Section 6.4, in order to obtain more accurate results, nine simulation must be performed for a single collision location. In conclusion, the total number of 162 simulations has been created for one type of construction. This process has been repeated for constructions of Reference, Alternative-1 and Alternative-2. Finally, the grand total of 486 simulations have been prepared in the scope of this application.

## 7.5 Generating hydrodynamics matrices

SHARP simulations require hydrodynamic properties of both struck and striking bodies in order to take the ship motions into consideration in the computations. The energy absorption by motions is also calculated to acquire more realistic results. To obtain the hydrostatic properties, a hydrodynamic analysis by *HydroStar* software is used. In order to prepare the input files for the *HydroStar* computations, an additional software called ARGOS is used.

### 7.5.1 HydroStar

*HydroStar* is the hydrodynamic software developed in Bureau Veritas since 1991, which provides a complete solution of first order problem of wave diffraction and radiation and also the Quadratic Transfer Functions (QTF) of second order low-frequency wave loads for a floating body with or without forward speed in deep water and in finite water depth. In this study, *HydroStar* is used to obtain added mass, damping, and hydrostatic stiffness matrix for 6-degrees of freedom in order to create .mco files which are

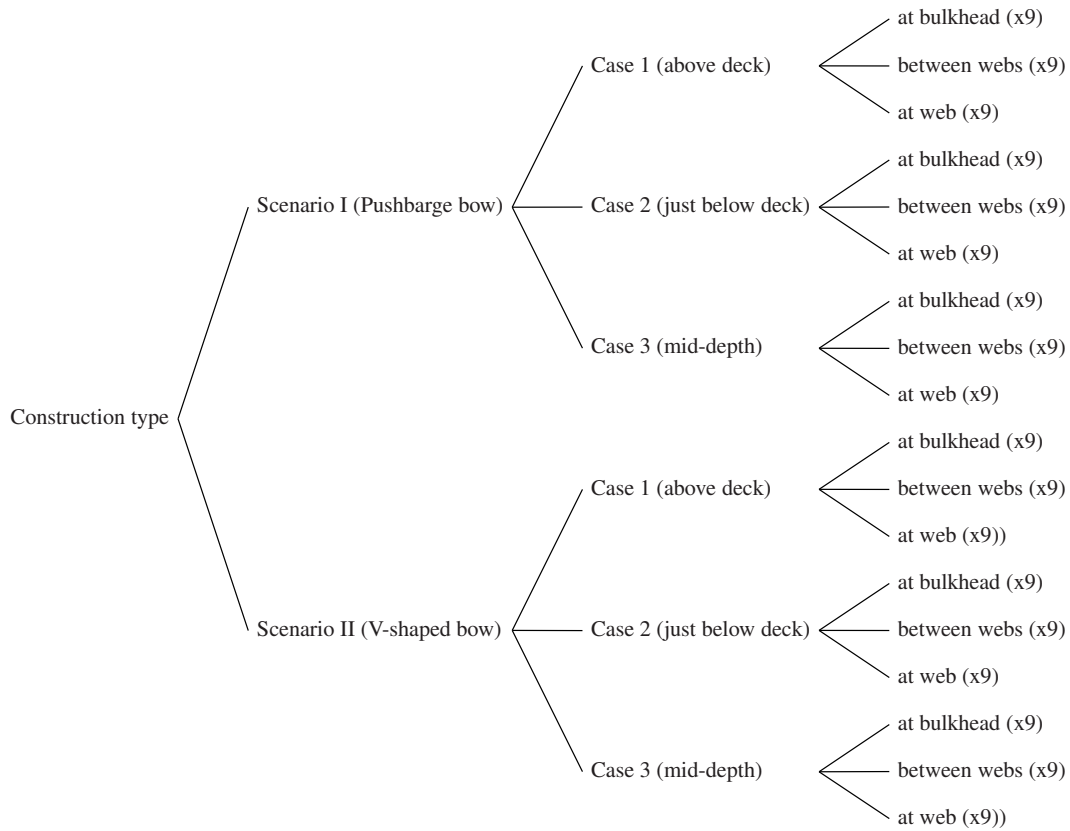


Figure 45: Created scenarios for each type of construction

required by the computations in SHARP.

### 7.5.2 ARGOS

ARGOS software is a naval architecture system for ship hydrostatics, stability and longitudinal strength calculations developed by Bureau Veritas. It is a modular software made of a standard package and some additional modules related to particular applications. Modules in the program can be seen in the user interface shown in Fig. 46

Some modules of the software which are related to the needs of the study are briefly explained below.

#### Basic Ship Data

This module allows the user to enter the identification and the main dimensions of the ship. Also, the

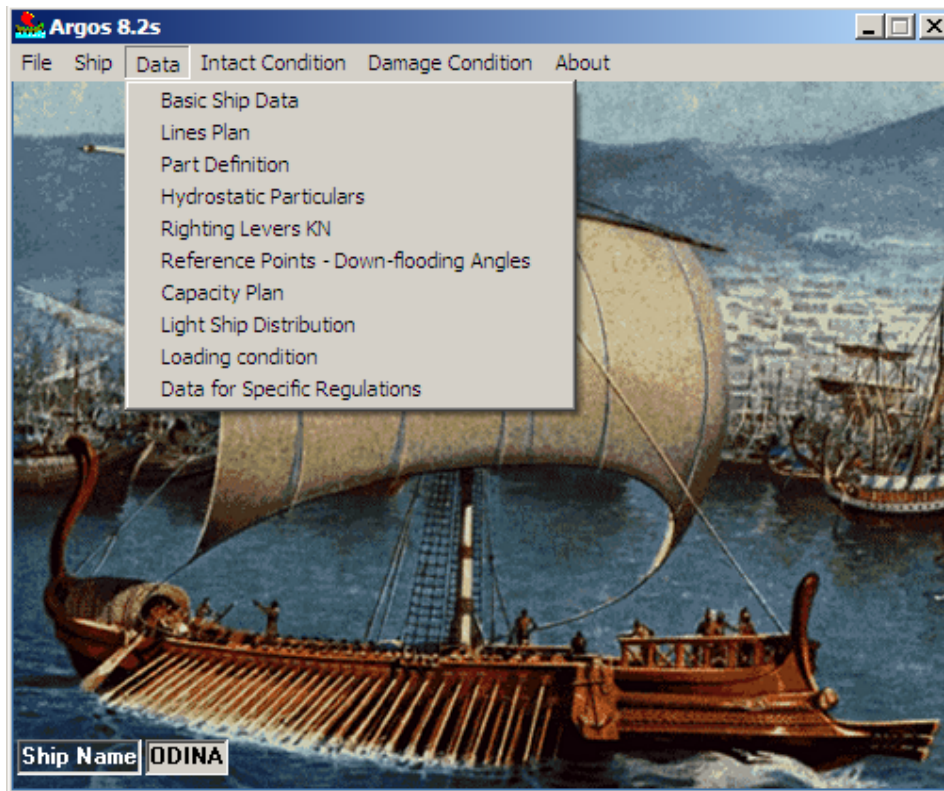


Figure 46: User interface of ARGOS

location of the hull frames is defined.

### **Lines Plan**

This module performs the ship hull geometry description by vertical sections drawn in the transverse plan. Each section is described by points defined by Y and Z coordinates. The geometry can be completed by appendages to be added or deducted to the main hull.

### **Part Definition**

This module is to enter the definition of the parts (sets of sections) which are used to describe the compartments, capacities and floodable lengths. The parts are elementary volumes defined by the transverse sections which can be directly entered by keyboard.

### **Hydrostatic Particulars**

In this module, the results of the hydrostatic calculations of the vessel can be displayed. Moreover, hydrostatic curves can be plotted.

## Capacity Plan

In this module, capacities of the tanks and the compartments can be displayed considering the permeability of the part. The user has the opportunity to select the order of the tasks. If the selected operation needs a previous definition of data or an intermediate calculation which has not been executed yet, a message appears to inform the user regarding the necessity of some previous operations to perform the selected one.

In this study, ARGOS is used to obtain hydrostatic curves of the struck and the striking vessels for the draft calculations corresponding displacements. In addition to that, tank capacities are provided by the software for calculation of consequence of rupture according to A.D.N. Section 9.3.4.

### 7.5.3 Procedure to create .MCO files

In regard to the A.D.N. procedure, three different vertical positions are required within two scenarios (V-bow 90° and Push barge bow 55°). For the calculated draft combinations shown in Sec. 7 Table 26, hydrodynamic coefficients are needed for following struck and striking vessels at indicated drafts:

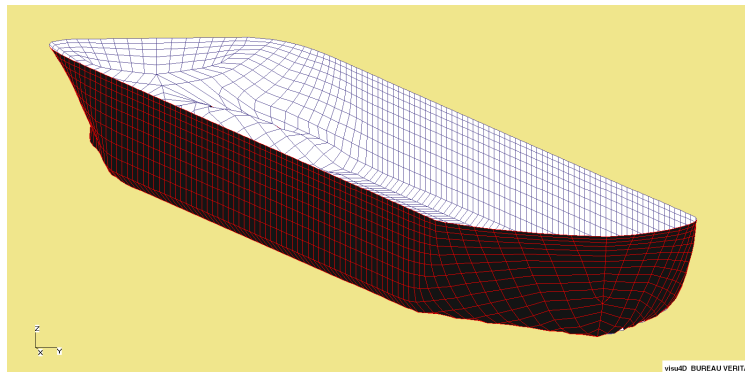
- Struck ship at T = 4.500 m
- Struck ship at T = 2.723 m
- Push barge bow at T = 3.400 m
- Push barge bow at T = 3.150 m
- Push barge bow at T = 1.632 m
- V-bow at T = 3.650 m
- V-bow at T = 3.500 m
- V-bow at T = 1.978 m

Input files to be prepared for the hydrodynamics calculations in HydroStar are:

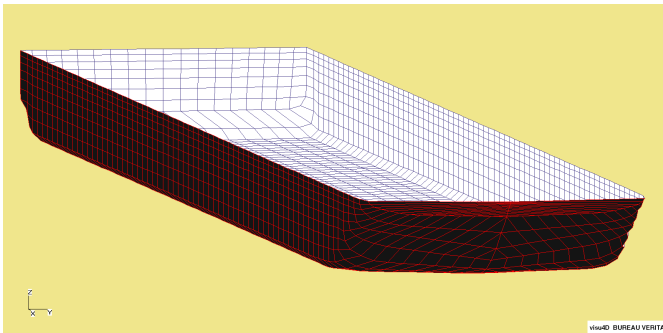
- *ship\_name.hul* - hull coordinates of the vessel  
All nodes on the ship hull is defined by their X, Y and Z coordinates.
- *ship\_name.mri* - main characteristics of the vessel (draft, trim etc.)  
At each draft, parameters in this file are re-edited.



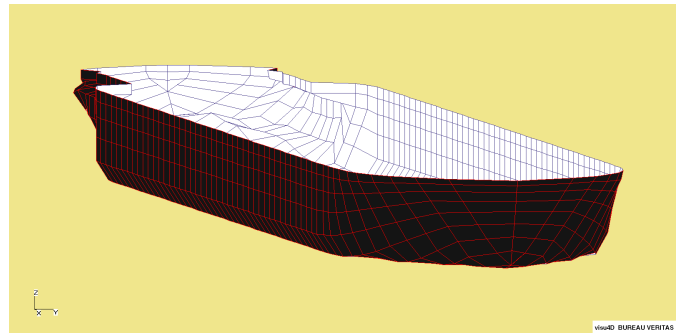
- *ship\_name.rdf* - wave conditions (frequencies, headings and water depth)  
Heading direction is assumed  $0^\circ$  without forward speed for struck vessel. The water depth is considered 10 m in the coastal area.
- *ship\_name.wld* - weight load distribution along the vessel  
With the assistance of ARGOS, weight distribution are defined for each vessel.
- *ship\_name.mcn* - center of gravity, center of gyration, additional stiffness and damping matrices for motion calculations



(a) Struck ship



(b) Push barge striking ship



(c) V-shaped bow striking ship

Figure 47: Meshed models in HydroStar

The functions of HydroStar are used in the following order to perform the analysis.

1. *pwd* - show directory command
2. *cd* - change directory command
3. *lsproj* - list projects in current directory
4. *proj project\_name* - create project or activate existing project with defined name

5. *hsmsh -ship ship\_name* - mesh generator for simple geometries
6. *hslec ship\_name.hst* - reading the mesh
7. *hschk* - verification of the mesh (inconsistency, normal orientation, etc.)
8. *hsvisu* - visualization of the mesh model
9. *hstat* - hydrostatic calculations and inertia matrices computation through the weight distribution
10. *hsrdf ship\_name.rdf* - radiation and diffraction computations for elementary solutions including added-mass, radiation damping and wave excitation loads.
11. *hsmcn ship\_name.mcn* - motions computations for mechanic properties (such as additional stiffness and additional damping matrices)
12. *hswld project\_name\_wld.don* - computation of global wave loads
13. *hsrao ship\_name.rao* - creation of the transfer functions for motions, velocities, accelerations and second order loads.
14. *hsdmp ship\_name.rao* - critical roll damping computation by using ITH formulation

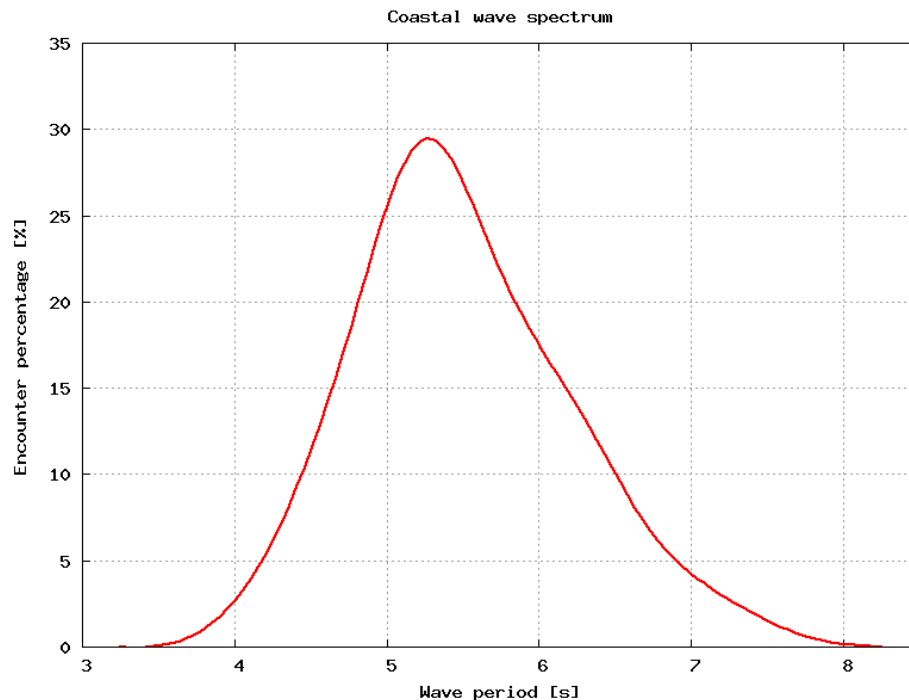


Figure 48: Encounter wave periods in Belgian coast (Zeebrugge)

In the content of the .MCO file, damping matrices are defined for each frequency. However, for hydrostatic restoring force and added mass matrices, MCOL subroutine requires values for a single frequency. The



Figure 49: Scheldt estuary - Zeebrugge

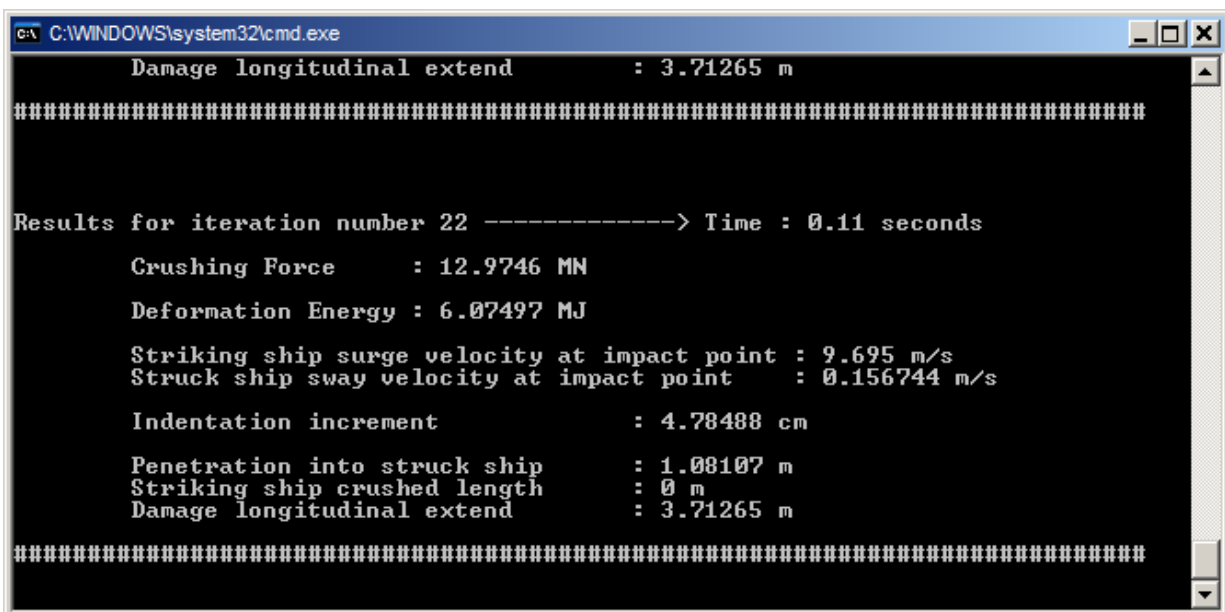
investigated incident location is assumed to be the coastal area of Belgium (Scheldt estuary - Zeebrugge). Therefore, by processing the wave data in this region, the most probable wave period is obtained as approximately 5.25 seconds which equals the frequency of 1.197 *rad/s* among the number of 12875 measured waves (See Fig. 48). Hence, values of hydrostatic restoring force and added mass matrices are taken for this wave period. A macro is programmed by using Visual Basic to handle the output files of HydroStar and to create .mco files. for the VBA codes, refer to Appendix D.

## 7.6 Simulations

Project files are categorized by the scenarios and sub-grouped by the cases of vertical locations. By doing this, the simulations which share the same hydrodynamics coefficients (.mco files) are combined into the same project files. Each project file includes 27 simulations, 9 for each longitudinal location (at bulkhead, web and between webs). While simulations are running, the every time step is displayed in a command prompt window on the screen (Fig. 50).

The simulation time can be defined to end the computation at a preferred duration. Otherwise it will be automatically terminated by the software at the time step that no more penetration occurs. After finishing the 27 simulations for one project file, results can be plotted and a 3D model can be displayed for the desired time step. The super-elements in red colour in the 3D-model are the elements destroyed and removed from

the computation. The elements in yellow are activated and continue to contribute in following time steps until their rupture. Furthermore, the results can be displayed not only through SHARP interface, but they are also available as the output files in a .CSV (Comma separated values) format in the target directory. It may enable to perform an advanced post-processing of the results by using the external data handling tools.



```

C:\WINDOWS\system32\cmd.exe
Damage longitudinal extend      : 3.71265 m
#####

Results for iteration number 22 -----> Time : 0.11 seconds

Crushing Force      : 12.9746 MN
Deformation Energy  : 6.07497 MJ

Striking ship surge velocity at impact point : 9.695 m/s
Struck ship sway velocity at impact point    : 0.156744 m/s

Indentation increment      : 4.78488 cm

Penetration into struck ship : 1.08107 m
Striking ship crushed length : 0 m
Damage longitudinal extend   : 3.71265 m
#####

```

Figure 50: Running simulations

SHARP performs the simulation and generates output of the total energy absorbing capacity of the structure until the moment in which the velocities of the striking and the struck ships become equal. The final velocity can be zero or can converge a certain value that the ships move together at that velocity without any further penetration after that moment. A.D.N. requires the value of the energy absorbing capability of the side structure until the rupture of cargo tank plating. For this reason result files must be examined and when the strain of inner side plating reaches its rupture strain, absorbed energy up to that time step must be considered.



in the case of collision at bulkhead in every analysis.

In Scenario I (push barge bow) differently from the Scenario II (V-bow), energy absorbing capacity values of the "just below deck" collision are higher than "above deck" collision. Some reasons for this dissimilarity are:

1. At the moment of the cargo tank rupture, side shell super-element is not yet activated in the case of "above deck" collision.
2. Because of the striking bow geometry and the collision angle, a larger number of transversal elements contribute to the impact resistance at below deck.
3. Although the contribution of the deck stringer plate is significant at "above deck" collision, still not enough energy is absorbed comparing with the "just below deck" collision.

Table 27: Summary of the energy results from SHARP

			Energy absorbing capacity [MJ]		
			Reference	Alternative-1	Alternative-2
<b>Scenario I</b>	<b>Case 1</b>	<b>at bulkhead</b>	3.790	3.284	5.425
		<b>between webs</b>	3.702	3.217	5.260
		<b>at web</b>	3.688	3.206	5.230
	<b>Case 2</b>	<b>at bulkhead</b>	5.108	4.092	5.968
		<b>between webs</b>	4.594	3.547	5.504
		<b>at web</b>	4.526	3.470	5.407
	<b>Case 3</b>	<b>at bulkhead</b>	1.287	1.010	1.436
		<b>between webs</b>	1.167	0.878	1.301
		<b>at web</b>	1.068	0.810	1.228
<b>Scenario II</b>	<b>Case 1</b>	<b>at bulkhead</b>	8.136	6.103	8.285
		<b>between webs</b>	7.719	5.714	7.822
		<b>at web</b>	7.711	5.669	7.763
	<b>Case 2</b>	<b>at bulkhead</b>	7.011	5.183	7.296
		<b>between webs</b>	5.693	3.961	5.564
		<b>at web</b>	5.685	3.945	5.542
	<b>Case 3</b>	<b>at bulkhead</b>	0.894	0.697	1.177
		<b>between webs</b>	0.730	0.519	0.802
		<b>at web</b>	0.738	0.521	0.806

## 7.7 Application of A.D.N Alternative Constructions (9.3.4.)

### 7.7.1 Calculations

By processing the result files, energy absorbing capacities of the side structures of Reference, Alternative Construction-1 and Alternative Construction-2 up to the cargo tank rupture are obtained as the outputs of the simulation in SHARP as required by the A.D.N. Except the energy values, all the other steps are in compliance with the procedure in A.D.N. Alternative Constructions (9.3.4) which is also referred to previously in Section 4 in this study.

Location weighting factors are calculated as explained in Section 4.3. The weighting factors of the vertical positions for given draft differences of Scenario I & II which have been previously mentioned in Sec.7.4 are calculated by means of the ratio of the areas, and the results are as follows:

Table 28: Weighting factors of vertical collision locations

	Scenario I		Scenario II	
	Area [m <sup>2</sup> ]	weighting factor	Area [m <sup>2</sup> ]	weighting factor
$\Delta_{T1}$	2.281	0.240	2.745	0.288
$\Delta_{T2}$	2.257	0.237	1.817	0.191
$\Delta_{T3}$	4.971	0.523	4.971	0.521
<b>Total</b>	9.510	1.000	9.534	1.000

The longitudinal weighting factors are shared for Scenario-I & II, since the longitudinal position is the same in both cases. By using parameters of frame spacing and tank length for the tanker vessel type C, The longitudinal weighting factors with following parameters are shown in Table 29.

- Frame spacing : 1.59 m
- Tank length : 15.9 m

Table 29: Weighting factors of longitudinal collision locations

	calculational span length	weighting factor
<b>at bulkhead</b>	0.318	0.02
<b>at web</b>	0.636	0.04
<b>between webs</b>	14.946	0.94

The total weighting factors of the impact positions are calculated by multiplying the vertical location weighting factors by the longitudinal location weighting factors. A summary of weighting factor calculations is given in Table 30.

Table 30: Total weighting factors corresponding to the respective collision location

			<b>at bulkhead</b>	<b>between webs</b>	<b>at web</b>
			0.020	0.940	0.040
<b>Scenario I</b>	<b>Case 1 (Above deck)</b>	0.240	0.005	0.225	0.010
	<b>Case 2 (right below deck)</b>	0.237	0.005	0.223	0.009
	<b>Case 3 (mid-depth)</b>	0.523	0.010	0.491	0.021
<b>Scenario II</b>	<b>Case 1 (Above deck)</b>	0.288	0.006	0.271	0.012
	<b>Case 2 (right below deck)</b>	0.191	0.004	0.179	0.008
	<b>Case 3 (mid-depth)</b>	0.521	0.010	0.490	0.021

Following tables are the summary of all calculation steps of the A.D.N. alternative construction procedure (9.3.4.). The grey cells in the tables denote for the energy absorbing capacity of the side structure by indicated location in  $[MJ]$  which is acquired within the use of the SHARP Tool. In the next step, the worksheet obtains CPDF coefficients and the energy range for the corresponding displacement by linear interpolation, and checks if the energy absorbing values are in the range of CPDF tables for the concerning speeds. Next, it applies the CPDF formulation given in Section.4.3. Eq.8 to calculate the probability of exceedance  $P_{(x\%)}$ . In the next column the calculated probabilities are multiplied by the weighting factors for each characteristic collision speed  $wf_{x\%}$  to calculate the weighted probabilities of the cargo tank rupture  $P_{wx\%}$ . To calculate the weighted total probabilities of cargo tank rupture  $P_{wloc(i)}$ , the calculated weighted probabilities of the cargo tank rupture  $P_{wx\%}$  are multiplied by weighting factors  $wf_{loc(i)}$  corresponding to the respective collision location (see Table 30. for the weighting factors). Finally, the scenario specific total probabilities of cargo tank rupture  $P_{scenI}$  and  $P_{scenII}$  are calculated by the summation of all the weighted total probabilities of the cargo tank rupture  $P_{wloc(i)}$  for each scenario. Finally the overall total probability of the cargo tank rupture  $P_w$  is calculated by using the formula indicated in the tables below.



Table 31: A.D.N. probability calculations for Reference construction

SCENARIO I (Push barge)		Energy absorbing capacity (E loc)	CPDF	P %	wf %	Pw%	wf loc	Pw loc
ABOVE DECK	Location 1 (bulkhead)	3.790	50% Vmax (Energy range 2-7.04)	0.6696	0.2000	0.1339		
			66% Vmax (Energy range 2-13.08)	0.9220	0.5000	0.4610		
			100% Vmax (Energy range 4-31.08)	1.0000	0.3000	0.3000		
						SP loc 0.8949	0.0048	0.0043
	Location 2 (betw. webs)	3.702	50% Vmax (Energy range 2-7.04)	0.6855	0.2000	0.1371		
			66% Vmax (Energy range 2-13.08)	0.9273	0.5000	0.4637		
			100% Vmax (Energy range 4-31.08)	1.0000	0.3000	0.3000		
						SP loc 0.9008	0.2255	0.2031
	Location 3 (web)	3.688	50% Vmax (Energy range 2-7.04)	0.6880	0.2000	0.1376		
66% Vmax (Energy range 2-13.08)			0.9282	0.5000	0.4641			
100% Vmax (Energy range 4-31.08)			1.0000	0.3000	0.3000			
					SP loc 0.9017	0.0096	0.0087	
DECK	Location 4 (bulkhead)	5.108	50% Vmax (Energy range 2-7.04)	0.4164	0.2000	0.0833		
			66% Vmax (Energy range 2-13.08)	0.8233	0.5000	0.4116		
			100% Vmax (Energy range 4-31.08)	0.9914	0.3000	0.2974		
						SP loc 0.7923	0.0047	0.0038
	Location 5 (betw. webs)	4.594	50% Vmax (Energy range 2-7.04)	0.5167	0.2000	0.1033		
			66% Vmax (Energy range 2-13.08)	0.8653	0.5000	0.4327		
			100% Vmax (Energy range 4-31.08)	0.9966	0.3000	0.2990		
						SP loc 0.8350	0.2231	0.1863
	Location 6 (web)	4.526	50% Vmax (Energy range 2-7.04)	0.5298	0.2000	0.1060		
66% Vmax (Energy range 2-13.08)			0.8705	0.5000	0.4353			
100% Vmax (Energy range 4-31.08)			0.9972	0.3000	0.2992			
					SP loc 0.8404	0.0095	0.0080	
MID-DEPTH	Location 7 (bulkhead)	1.287	50% Vmax (Energy range 2-7.04)	1.0000	0.2000	0.2000		
			66% Vmax (Energy range 2-13.08)	1.0000	0.5000	0.5000		
			100% Vmax (Energy range 4-31.08)	1.0000	0.3000	0.3000		
						SP loc 1.0000	0.0105	0.0105
	Location 8 (betw. webs)	1.167	50% Vmax (Energy range 2-7.04)	1.0000	0.2000	0.2000		
			66% Vmax (Energy range 2-13.08)	1.0000	0.5000	0.5000		
			100% Vmax (Energy range 4-31.08)	1.0000	0.3000	0.3000		
						SP loc 1.0000	0.4914	0.4914
	Location 9 (web)	1.068	50% Vmax (Energy range 2-7.04)	1.0000	0.2000	0.2000		
66% Vmax (Energy range 2-13.08)			1.0000	0.5000	0.5000			
100% Vmax (Energy range 4-31.08)			1.0000	0.3000	0.3000			
					SP loc 1.0000	0.0209	0.0209	

P scen I  
0.9369

SCENARIO I (V-bow)		Energy absorbing capacity (E loc)	CPDF	P %	wf %	Pw%	wf loc	Pw loc
ABOVE DECK	Location 1 (bulkhead)	8.136	30% Vmax (Energy range 1-2.04)	0.000	0.7000	0.0000		
			100% Vmax (Energy range 4-31.08)	0.933	0.3000	0.2800		
						SP loc 0.2800		
	Location 2 (betw. webs)	7.719	30% Vmax (Energy range 1-2.04)	0.000	0.7000	0.0000		
			100% Vmax (Energy range 4-31.08)	0.944	0.3000	0.2832		
						SP loc 0.2832		
	Location 3 (web)	7.711	30% Vmax (Energy range 1-2.04)	0.000	0.7000	0.0000		
			100% Vmax (Energy range 4-31.08)	0.944	0.3000	0.2833		
						SP loc 0.2833		
DECK	Location 4 (bulkhead)	7.011	30% Vmax (Energy range 1-2.04)	0.000	0.7000	0.0000		
			100% Vmax (Energy range 4-31.08)	0.960	0.3000	0.2880		
						SP loc 0.2880		
	Location 5 (betw. webs)	5.693	30% Vmax (Energy range 1-2.04)	0.000	0.7000	0.0000		
			100% Vmax (Energy range 4-31.08)	0.984	0.3000	0.2951		
						SP loc 0.2951		
	Location 6 (web)	5.685	30% Vmax (Energy range 1-2.04)	0.000	0.7000	0.0000		
			100% Vmax (Energy range 4-31.08)	0.984	0.3000	0.2952		
						SP loc 0.2952		
MID-DEPTH	Location 7 (bulkhead)	0.894	30% Vmax (Energy range 1-2.04)	1.000	0.7000	0.7000		
			100% Vmax (Energy range 4-31.08)	1.000	0.3000	0.3000		
						SP loc 1.0000		
	Location 8 (betw. webs)	0.730	30% Vmax (Energy range 1-2.04)	1.000	0.7000	0.7000		
			100% Vmax (Energy range 4-31.08)	1.000	0.3000	0.3000		
						SP loc 1.0000		
	Location 9 (web)	0.738	30% Vmax (Energy range 1-2.04)	1.000	0.7000	0.7000		
			100% Vmax (Energy range 4-31.08)	1.000	0.3000	0.3000		
						SP loc 1.0000		

P scen II  
0.6592

$$P_w = 0.8 \cdot P_{scenI} + 0.2 \cdot P_{scenII} \rightarrow P_w = 0.8813$$

Table 32: A.D.N. probability calculations for Alternative construction - 1

SCENARIO I (Push barge)		Energy absorbing capacity (E loc)	CPDF	P %	wf %	Pw%	wf loc	Pw loc	
ABOVE DECK	Location 1 (bulkhead)	3.284	50% Vmax (Energy range 2-7.04)	0.7585	0.2000	0.1517			
			66% Vmax (Energy range 2-13.08)	0.9510	0.5000	0.4755			
			100% Vmax (Energy range 4-31.08)	1.0000	0.3000	0.3000			
						SP loc	0.9272	0.0048	0.0044
	Location 2 (betw. webs)	3.217	50% Vmax (Energy range 2-7.04)	0.7697	0.2000	0.1539			
			66% Vmax (Energy range 2-13.08)	0.9544	0.5000	0.4772			
			100% Vmax (Energy range 4-31.08)	1.0000	0.3000	0.3000			
						SP loc	0.9311	0.2255	0.2100
	Location 3 (web)	3.206	50% Vmax (Energy range 2-7.04)	0.7714	0.2000	0.1543			
66% Vmax (Energy range 2-13.08)			0.9549	0.5000	0.4774				
100% Vmax (Energy range 4-31.08)			1.0000	0.3000	0.3000				
					SP loc	0.9317	0.0096	0.0089	
DECK	Location 4 (bulkhead)	4.092	50% Vmax (Energy range 2-7.04)	0.6133	0.2000	0.1227			
			66% Vmax (Energy range 2-13.08)	0.9021	0.5000	0.4511			
			100% Vmax (Energy range 4-31.08)	1.0003	0.3000	0.3001			
						SP loc	0.8738	0.0047	0.0041
	Location 5 (betw. webs)	3.547	50% Vmax (Energy range 2-7.04)	0.7132	0.2000	0.1426			
			66% Vmax (Energy range 2-13.08)	0.9365	0.5000	0.4683			
			100% Vmax (Energy range 4-31.08)	1.0000	0.3000	0.3000			
						SP loc	0.9109	0.2231	0.2032
	Location 6 (web)	3.470	50% Vmax (Energy range 2-7.04)	0.7268	0.2000	0.1454			
66% Vmax (Energy range 2-13.08)			0.9409	0.5000	0.4705				
100% Vmax (Energy range 4-31.08)			1.0000	0.3000	0.3000				
					SP loc	0.9158	0.0095	0.0087	
MID-DEPTH	Location 7 (bulkhead)	1.010	50% Vmax (Energy range 2-7.04)	1.0000	0.2000	0.2000			
			66% Vmax (Energy range 2-13.08)	1.0000	0.5000	0.5000			
			100% Vmax (Energy range 4-31.08)	1.0000	0.3000	0.3000			
						SP loc	1.0000	0.0105	0.0105
	Location 8 (betw. webs)	0.878	50% Vmax (Energy range 2-7.04)	1.0000	0.2000	0.2000			
			66% Vmax (Energy range 2-13.08)	1.0000	0.5000	0.5000			
			100% Vmax (Energy range 4-31.08)	1.0000	0.3000	0.3000			
						SP loc	1.0000	0.4914	0.4914
	Location 9 (web)	0.810	50% Vmax (Energy range 2-7.04)	1.0000	0.2000	0.2000			
66% Vmax (Energy range 2-13.08)			1.0000	0.5000	0.5000				
100% Vmax (Energy range 4-31.08)			1.0000	0.3000	0.3000				
					SP loc	1.0000	0.0209	0.0209	

P scen I  
0.9622

SCENARIO I (V-bow)		Energy absorbing capacity (E loc)	CPDF	P %	wf %	Pw%	wf loc	Pw loc
ABOVE DECK	Location 1 (bulkhead)	6.103	30% Vmax (Energy range 1-2.04)	0.000	0.7000	0.0000		
			100% Vmax (Energy range 4-31.08)	0.977	0.3000	0.2932		
						SP loc		
	Location 2 (betw. webs)	5.714	30% Vmax (Energy range 1-2.04)	0.000	0.7000	0.0000		
			100% Vmax (Energy range 4-31.08)	0.983	0.3000	0.2950		
						SP loc		
	Location 3 (web)	5.669	30% Vmax (Energy range 1-2.04)	0.000	0.7000	0.0000		
			100% Vmax (Energy range 4-31.08)	0.984	0.3000	0.2952		
						SP loc		
DECK	Location 4 (bulkhead)	5.183	30% Vmax (Energy range 1-2.04)	0.000	0.7000	0.0000		
			100% Vmax (Energy range 4-31.08)	0.991	0.3000	0.2972		
						SP loc		
	Location 5 (betw. webs)	3.961	30% Vmax (Energy range 1-2.04)	0.000	0.7000	0.0000		
			100% Vmax (Energy range 4-31.08)	1.000	0.3000	0.3000		
						SP loc		
Location 6 (web)	3.945	30% Vmax (Energy range 1-2.04)	0.000	0.7000	0.0000			
		100% Vmax (Energy range 4-31.08)	1.000	0.3000	0.3000			
					SP loc			0.3000
MID-DEPTH	Location 7 (bulkhead)	0.697	30% Vmax (Energy range 1-2.04)	1.000	0.7000	0.7000		
			100% Vmax (Energy range 4-31.08)	1.000	0.3000	0.3000		
						SP loc		
	Location 8 (betw. webs)	0.519	30% Vmax (Energy range 1-2.04)	1.000	0.7000	0.7000		
			100% Vmax (Energy range 4-31.08)	1.000	0.3000	0.3000		
						SP loc		
Location 9 (web)	0.521	30% Vmax (Energy range 1-2.04)	1.000	0.7000	0.7000			
		100% Vmax (Energy range 4-31.08)	1.000	0.3000	0.3000			
					SP loc			1.0000

P scen II  
0.6636

$$P_w = 0.8 \cdot P_{scenI} + 0.2 \cdot P_{scenII}$$

P\_w  
0.9025

Table 33: A.D.N. probability calculations for Alternative construction - 2

SCENARIO I (Push barge)		Energy absorbing capacity (E loc)	CPDF	P %	wf %	Pw%	wf loc	Pw loc	
ABOVE DECK	Location 1 (bulkhead)	5.425	50% Vmax (Energy range 2-7.04)	0.3551	0.2000	0.0710			
			66% Vmax (Energy range 2-13.08)	0.7953	0.5000	0.3977			
			100% Vmax (Energy range 4-31.08)	0.9875	0.3000	0.2962			
						SP loc	0.7649	0.0048	0.0037
	Location 2 (betw. webs)	5.260	50% Vmax (Energy range 2-7.04)	0.3870	0.2000	0.0774			
			66% Vmax (Energy range 2-13.08)	0.8101	0.5000	0.4051			
			100% Vmax (Energy range 4-31.08)	0.9896	0.3000	0.2969			
						SP loc	0.7793	0.2255	0.1757
	Location 3 (web)	5.230	50% Vmax (Energy range 2-7.04)	0.3928	0.2000	0.0786			
66% Vmax (Energy range 2-13.08)			0.8127	0.5000	0.4064				
100% Vmax (Energy range 4-31.08)			0.9900	0.3000	0.2970				
					SP loc	0.7819	0.0096	0.0075	
DECK	Location 4 (bulkhead)	5.968	50% Vmax (Energy range 2-7.04)	0.2541	0.2000	0.0508			
			66% Vmax (Energy range 2-13.08)	0.7445	0.5000	0.3723			
			100% Vmax (Energy range 4-31.08)	0.9795	0.3000	0.2938			
						SP loc	0.7169	0.0047	0.0034
	Location 5 (betw. webs)	5.504	50% Vmax (Energy range 2-7.04)	0.3402	0.2000	0.0680			
			66% Vmax (Energy range 2-13.08)	0.7883	0.5000	0.3941			
			100% Vmax (Energy range 4-31.08)	0.9864	0.3000	0.2959			
						SP loc	0.7581	0.2231	0.1691
	Location 6 (web)	5.407	50% Vmax (Energy range 2-7.04)	0.3587	0.2000	0.0717			
66% Vmax (Energy range 2-13.08)			0.7970	0.5000	0.3985				
100% Vmax (Energy range 4-31.08)			0.9877	0.3000	0.2963				
					SP loc	0.7666	0.0095	0.0073	
MID-DEPTH	Location 7 (bulkhead)	1.436	50% Vmax (Energy range 2-7.04)	1.0000	0.2000	0.2000			
			66% Vmax (Energy range 2-13.08)	1.0000	0.5000	0.5000			
			100% Vmax (Energy range 4-31.08)	1.0000	0.3000	0.3000			
						SP loc	1.0000	0.0105	0.0105
	Location 8 (betw. webs)	1.301	50% Vmax (Energy range 2-7.04)	1.0000	0.2000	0.2000			
			66% Vmax (Energy range 2-13.08)	1.0000	0.5000	0.5000			
			100% Vmax (Energy range 4-31.08)	1.0000	0.3000	0.3000			
						SP loc	1.0000	0.4914	0.4914
	Location 9 (web)	1.228	50% Vmax (Energy range 2-7.04)	1.0000	0.2000	0.2000			
66% Vmax (Energy range 2-13.08)			1.0000	0.5000	0.5000				
100% Vmax (Energy range 4-31.08)			1.0000	0.3000	0.3000				
					SP loc	1.0000	0.0209	0.0209	

P scen I  
0.8895

SCENARIO I (V-bow)		Energy absorbing capacity (E loc)	CPDF	P %	wf %	Pw%	wf loc	Pw loc	
ABOVE DECK	Location 1 (bulkhead)	8.285	30% Vmax (Energy range 1-2.04)	0.000	0.7000	0.0000			
			100% Vmax (Energy range 4-31.08)	0.930	0.3000	0.2789			
						SP loc			0.2789
	Location 2 (betw. webs)	7.822	30% Vmax (Energy range 1-2.04)	0.000	0.7000	0.0000			
			100% Vmax (Energy range 4-31.08)	0.941	0.3000	0.2824			
						SP loc			0.2824
	Location 3 (web)	7.763	30% Vmax (Energy range 1-2.04)	0.000	0.7000	0.0000			
			100% Vmax (Energy range 4-31.08)	0.943	0.3000	0.2829			
						SP loc			0.2829
DECK	Location 4 (bulkhead)	7.296	30% Vmax (Energy range 1-2.04)	0.000	0.7000	0.0000			
			100% Vmax (Energy range 4-31.08)	0.954	0.3000	0.2862			
						SP loc	0.2862	0.0038	0.0011
	Location 5 (betw. webs)	5.564	30% Vmax (Energy range 1-2.04)	0.000	0.7000	0.0000			
			100% Vmax (Energy range 4-31.08)	0.986	0.3000	0.2957			
						SP loc	0.2957	0.1792	0.0530
Location 6 (web)	5.542	30% Vmax (Energy range 1-2.04)	0.000	0.7000	0.0000				
		100% Vmax (Energy range 4-31.08)	0.986	0.3000	0.2958				
					SP loc	0.2958	0.0076	0.0023	
MID-DEPTH	Location 7 (bulkhead)	1.177	30% Vmax (Energy range 1-2.04)	0.621	0.7000	0.4349			
			100% Vmax (Energy range 4-31.08)	1.000	0.3000	0.3000			
						SP loc	0.7349	0.0104	0.0077
	Location 8 (betw. webs)	0.802	30% Vmax (Energy range 1-2.04)	1.000	0.7000	0.7000			
			100% Vmax (Energy range 4-31.08)	1.000	0.3000	0.3000			
						SP loc	1.0000	0.4902	0.4902
Location 9 (web)	0.806	30% Vmax (Energy range 1-2.04)	1.000	0.7000	0.7000				
		100% Vmax (Energy range 4-31.08)	1.000	0.3000	0.3000				
					SP loc	1.0000	0.0209	0.0209	

P scen II  
0.6563

$$P_w = 0.8 \cdot P_{scenI} + 0.2 \cdot P_{scenII}$$

P\_w 0.8429

### 7.7.2 Results

According to A.D.N. the consequence of the cargo tank rupture is not to be determined individually but relatively to the reference and alternative constructions. The ratio of the consequence is obtained by the ratio between the tank volume of the alternative construction and the reference construction. Therefore, in order to prove the crash-worthiness of the alternative structure, the comparison in Fig. 53 shall be made. Tank volumes are obtained by using defined compartment volumes of the vessel in the ARGOS software.

<p><b>Reference design</b></p> <p><math>P_r</math>            0.8813</p> <p><math>V_{\text{tank}}</math>    377.740 m<sup>3</sup></p>	$\frac{C_n}{C_r} \leq \frac{P_r}{P_n}$	
<p><b>Alternative design-1</b></p> <p><math>P_{n1}</math>           0.9025</p> <p><math>V_{\text{tank}}</math>    393.203 m<sup>3</sup></p>	<p><u>Check</u></p> <p><b>1.0409</b>        ≤        <b>0.9766</b></p> <p><b>(FALSE)</b></p>	<p>Result:</p> <p><b>Reinforcements are required.</b></p>
<p><b>Alternative design-2</b></p> <p><math>P_{n2}</math>           0.8429</p> <p><math>V_{\text{tank}}</math>    393.203 m<sup>3</sup></p>	<p><u>Check</u></p> <p><b>1.0409</b>        ≤        <b>1.0457</b></p> <p><b>(TRUE)</b></p>	<p>Result:</p> <p><b>Alternative design is provided.</b></p>

Figure 53: A.D.N. Alternative design check

As it can be seen in the figure above, alternative design -1 (without reinforcements) has a higher risk than the reference design as a matter of course. The alternative design-2 is proved to have a lower risk than the reference design due to the reinforced side structure. See Appendix B for the energy absorbing capacities for the different constructions. In the alternative construction, reducing the double hull spacing results in an increase of the cargo tank capacity of a single tank from 377.7 m<sup>3</sup> to 393.7 m<sup>3</sup>. In conclusion, an increase of 185.5 m<sup>3</sup> of total cargo tank capacities is achieved for the subjected vessel within the alternative design.

## **8 CONCLUSIONS AND RECOMMENDATIONS**

In this master thesis, an application of the super-element theory to the crash-worthiness evaluation is demonstrated through the instrumentality of the SHARP Tool. The strength check of the investigated vessel is carried out in compliance with the BV Rules for Classification of Inland Navigation Vessels NR 217. It is shown that the super-element method is applicable to the A.D.N. procedure considering the necessity of the adaptations such as the definition of the rupture criteria and some structural simplifications. Thanks to the simplicity of the modelling and the super-element method, SHARP allows to generate a structural model in a few days and simulates one scenario in less than a minute. Furthermore, SHARP makes it possible to simulate the collisions with the rigid or the deformable striking ship bow that is also required in certain conditions described by the A.D.N. Regulations.

Suitability of the investigated vessel made of an alternative design fitted with an improved side shell crash-worthiness is demonstrated by applying the procedure prescribed by the A.D.N Regulations. The crash-worthiness of the side structure is improved by increasing the thicknesses of side plating and stringer plate by 36%, web frame and ordinary frame brackets by 25% and sheerstrake by 30%. Consequently, the alternative construction-2 with reinforcements is proved to possess a lower risk than the reference design.

From an economic point of view, SHARP enables the designer to test many structural arrangement solutions and to select the most efficient crashworthy design without excessive investment. Moreover, SHARP will help ship owners to have a better insight into how to maximize the tank capacity of their vessels by decreasing the distance between the cargo tank wall and the outer shell while fully respecting the criteria related to crash-worthiness. This may be applied not only to new constructions but also to conversions from a single hull vessel to a double hull one in which the best compromise between the cargo tank volume and the structure arrangement is reached as a result of rapid iterations of alternative designs.

As recommendations:

- Same assessment to be performed using FEM in order to validate applicability of super-element theory in the A.D.N procedure
- Implementation of inland vessel lines/bow shapes in SHARP library

- Development of new super-elements to allow better/more realistic modelling of inland vessel hull structure (e.g. corrugated bulkheads)

Indeed, the super-element method preserves a potential, and within the further development of the SHARP Tool, it might be an effective substitution for the finite-element method in terms of rapidity and simplicity in the evaluation of the crash-worthiness within the procedure of *the A.D.N. Section 9.3.4 Alternative Constructions*.

## **9 ACKNOWLEDGEMENTS**

First of all, I would like to give my special thanks to Mr. Nzengu Wa Nzengu, my supervisor in Bureau Veritas Inland Navigation Management. From the beginning, he shared his knowledge, experience to perform a successful study. Also, I would like to express my cordial gratitude to Prof. Maciej Taczala, my supervisor in West Pomeranian University of Technology. Then, I would like to Prof. Hervé Le Sourne for reviewing my thesis.

I would like to thank my colleagues in Bureau Veritas for their friendliness and support, especially Mr. Hoang Tri Tran for his guidance and sharing his practical insight throughout my internship. In addition, I would like to thank Mr. Stéphane Paboeuf from Bureau Veritas Marine & Offshore Division for his hospitality during my stay in Nantes and his valuable help for my thesis. Moreover, I would like to convey my regards to Mr. Jean Michel Chatelier for providing me the opportunity to pursue this internship.

I would express my sincere appreciation to Prof. Philippe Rigo for his great efforts for the EMSHIP program.

Finally, my deepest gratitude goes to my beloved family for their endless support and encouragement.

This thesis was developed in the frame of the European Master Course in "Integrated Advanced Ship Design" named "EMSHIP" for "European Education in Advanced Ship Design", Ref.: 159652-1-2009-1-BE-ERA MUNDUS-EMMC.

## REFERENCES

16th International Ship and Offshore Structures Congress. (2006) 20-25 August Southampton, UK. Volume 2

Bai, Y., Bendiksen, E., Pedersen, P.T., (1993). Collapse Analysis of Ships, Marine Structures 6.

Brown, A. J., (2001). Collision Scenarios and Probabilistic Collision Damage. ICCGS 2nd International Conference on Collision and Grounding of Ships, Copenhagen.

Buldgen, L., Le Sourne, H., Besnard, N., Rigo, P., (2012). Extension of the super-elements method to the analysis of oblique collision between two ships, Marine Structures, 22-57.

Buldgen, L., Le Sourne, H., Pire, T., (2014). Extension of the super-elements method to the analysis of a jacket impacted by a ship, Marine Structures, 44-71.

Chen, D., (2000). Simplified Ship Collision Model. Dissertation submitted to the faculty of Virginia Polytechnic Institute and State University.

Giannotti, J.G., Johns, N., Genalis, P. And Van Mater, P.R. (1979). Critical Evaluations of Low-Energy ship Collision Vol. I - Damage theories and Design Methodologies, Ship Structure Committee Report No. SSC-284.

Jones, N. (2012). Structural impact. Second Edition Cambridge: Cambridge University Press.

Klanac, A., Ehlers, S., Tabri, K., Rudan, S., and Broekhuijsen, J., (2005). Qualitative design assessment of crashworthy structures. In Proceedings of the 11th International Congress of the International Maritime Association of the Mediterranean (IMAM 2005), Lisbon, Portugal, September

Le Sourne, H., et al. (2001). External Dynamics of Ship-Submarine Collisions. Preprints of 2nd International Conference on Collision and Grounding of Ships, Copenhagen

Le Sourne, H., Couty, N., Besnieret, F., et al. (2003). LS-DYNA Applications in Shipbuilding. 4th European LS-DYNA Users Conference - Plenary Session II, Ulm



Le Sourne, H., Besnard, N., Cheylan, C., Buannic, N. (2012). A Ship Collision Analysis Program Based on Upper Bound Solutions and Coupled with a Large Rotational Ship Movement Analysis Tool, Journal of Applied Mathematics.

Minorsky, V.U., (1959). An Analysis of Ship Collisions with Reference to Protection of Nuclear Power Plants, Journal of Ship Research.

NORSOK Standards, The Norwegian Oil Industry Association (OLF) Federation of Norwegian Manufacturing Industries (TBL), (2004). Rev. 2.

Paboeuf, S., Le Sourne, H., Broschard, K., Besnard, N., (2015). A Damage Assessment Tool in Ship Collisions, Damaged Ship III, London.

Paik, J.K. and Pedersen, P.T., (1996). "Modeling of the Internal Mechanics in Ship Collisions", Ocean Engineering, Vol. 23, No. 2, pp. 107-142.

Paik, J.K., ( 1994). Cutting of a Longitudinally Stiffened Plate by a Wedge, Journal of Ship Research, Vol.38, No.4, pp.340-348.

Paik, J.K., et al. (1999). "On Rational Design of Double Hull Tanker Structures against Collision, 1999 SNAME Annual Meeting.

Pedersen, P. T. (1995): "Collision and Grounding Mechanics". Proceedings WEMT '95. West European Confederation of Maritime Technology Societies. Ship Safety and Protection of the Environment. From a Technical Point-of-view. Copenhagen: The Danish Society of Naval Architecture and Marine Engineering.

Pedersen, P. T. (2010). Review and Application of Ship Collision and Grounding Analysis Procedures. Marine Structures, 23, 241-262. 10.1016/j.marstruc.2010.05.001

Pedersen, P. T., & Zhang, S. (1998). Absorbed Energy in Ship Collisions and Grounding: Revising Minorsky's Empirical Method.

Pedersen, P.T., Zhang, S., (1998). On Impact Mechanics in Ship Collisions, Marine Structures.

- Sajdak J. A.W., Brown A.J. (2005). Modeling longitudinal damage in ship collisions. Ship Structure Committee; 2005. SSC-437.
- Samuelides, E., & Frieze, P., (1984). Fluid-structure interaction in ship-ship collisions. Glasgow: Dept. of Naval Architecture & Ocean Engineering, University of Glasgow.
- Simonsen, B.C., (1999). Theory and Validation for the Collision Module, Joint MIT-Industry Program on Tanker Safety, Report no 66.
- Simonsen, B.C., Ocakli, H.(1999). Experiments and theory on deck girder crushing, Thin-Walled Structures
- United Nations Economic Commission for Europe, European Agreement concerning the International Carriage of Dangerous Goods by Inland Waterways (ADN), Volume I. 2015.
- Wierzbicki, T. (1995). Concertina Tearing of Metal Plates, Solid Structures
- Woisin, G. (1979). Design against collision. Schiff and Hafen Vol 31 No 2. Germany.
- Yamada, Y., Endo, H., & Pedersen, P. T. (2008). Effect of Buffer Bow Structure in Ship-Ship Collision. International Journal of Offshore and Polar Engineering
- Yamada, Y., Endo, H., Pedersen, P. T., (2005). Numerical Study on the Effect of Buffer Bow Structure in Ship-to-ship Collisions. Proceedings of the 15th International Offshore and Polar Engineering Conference (ISOPE) Seoul, Korea, June 19 24
- Zhang, S., (1999). The Mechanics of Ship Collisions, Department of Naval Architecture and Ocean Engineering, Technical University of Denmark.

## **A APPENDIX: RULE STRENGTH CHECK**

### Local Rule Requirements - Stiffener

N°	WGActu.		H <sub>1</sub>	E <sub>1</sub>	H <sub>2</sub>	E <sub>2</sub>	Mat	Spac	Span	Bend.Eff.
CAdd	WNetActu.	WNetRule	SigX1	ps	pw		Case			
	ANetActu.	ANetRule		ps	pw		Case			
		SigU	SigX1	ps	pw		Case			

#### 1 - Outer<sub>s</sub>hell

1	86.65		140.0	8.0	0.0	0.0	ST235	0.470	1.590	100
1.00	74.09	57.43	96.57	57.14	17.85		SEABAL 2-N			
	8.96	2.11		57.14	17.85		SEABAL 2-N			
		235.00	162.15	57.14	17.85		SEABAL 2-N			
2	86.65		140.0	8.0	0.0	0.0	ST235	0.470	1.590	100
1.00	74.09	57.43	96.57	57.14	17.85		SEABAL 2-N			
	8.96	2.11		57.14	17.85		SEABAL 2-N			
		235.00	162.15	57.14	17.85		SEABAL 2-N			
3	86.65		140.0	8.0	0.0	0.0	ST235	0.470	1.590	100
1.00	74.09	57.43	96.57	57.14	17.85		SEABAL 2-N			
	8.96	2.11		57.14	17.85		SEABAL 2-N			
		235.00	162.15	57.14	17.85		SEABAL 2-N			
4	86.65		140.0	8.0	0.0	0.0	ST235	0.470	1.590	100
1.00	74.09	57.43	96.57	57.14	17.85		SEABAL 2-N			
	8.96	2.11		57.14	17.85		SEABAL 2-N			
		235.00	162.15	57.14	17.85		SEABAL 2-N			
5	86.65		140.0	8.0	0.0	0.0	ST235	0.470	1.590	100
1.00	74.09	57.43	96.57	57.14	17.85		SEABAL 2-N			
	8.96	2.11		57.14	17.85		SEABAL 2-N			
		235.00	162.15	57.14	17.85		SEABAL 2-N			
6	86.65		140.0	8.0	0.0	0.0	ST235	0.470	1.590	100
1.00	74.09	57.43	96.57	57.14	17.85		SEABAL 2-N			
	8.96	2.11		57.14	17.85		SEABAL 2-N			
		235.00	162.15	57.14	17.85		SEABAL 2-N			

Figure 54: Rule check for stiffeners (Part 1)

**Local Rule Requirements - Stiffener**

N°	WGActu.	H <sub>1</sub>	E <sub>1</sub>	H <sub>2</sub>	E <sub>2</sub>	Mat	Spac	Span	Bend.Eff.
CAdd	WNetActu.	WNetRule	SigX1	ps	pw	Case			
	ANetActu.	ANetRule		ps	pw	Case			
		SigU	SigX1	ps	pw	Case			

1 - Outer<sub>s</sub>hell

7	86.65	140.0	8.0	0.0	0.0	ST235	0.470	1.590	100
1.00	74.09	57.43	96.57	57.14	17.85	SEABAL 2-N			
	8.96	2.11		57.14	17.85	SEABAL 2-N			
		235.00	162.15	57.14	17.85	SEABAL 2-N			
8	86.65	140.0	8.0	0.0	0.0	ST235	0.470	1.590	100
1.00	74.09	57.43	96.57	57.14	17.85	SEABAL 2-N			
	8.96	2.11		57.14	17.85	SEABAL 2-N			
		235.00	162.15	57.14	17.85	SEABAL 2-N			
9	86.61	140.0	8.0	0.0	0.0	ST235	0.466	1.590	100
1.00	74.06	56.94	96.57	57.14	17.85	SEABAL 2-N			
	8.96	2.10		57.14	17.85	SEABAL 2-N			
		235.00	161.42	57.14	17.85	SEABAL 2-N			
10	78.37	140.0	7.0	0.0	0.0	ST235	0.250	1.590	100
1.00	67.03	18.11	50.28	50.52	9.86	SEABAL 2-N			
	7.84	0.98		50.52	9.86	SEABAL 2-N			
		235.00	75.74	50.52	9.86	SEABAL 2-N			
11	200.48	140.0	10.0	100.0	10.0	ST235	0.500	1.590	100
1.00	161.01	30.04	33.14	45.62	9.35	SEABAL 2-N			
	11.34	1.63		45.62	9.35	SEABAL 2-N			
		235.00	53.96	45.62	9.35	SEABAL 2-N			
12	81.50	140.0	7.0	0.0	0.0	ST235	0.500	1.590	100
1.00	69.40	24.87	16.00	40.71	8.85	SEABAL 2-N			
	7.84	1.47		40.71	8.85	SEABAL 2-N			
		235.00	60.57	40.71	8.85	SEABAL 2-N			

Figure 55: Rule check for stiffeners (Part 2)

## Local Rule Requirements - Stiffener

N°	WGActu.	H <sub>1</sub>	E <sub>1</sub>	H <sub>2</sub>	E <sub>2</sub>	Mat	Spac	Span	Bend.Eff.
CAdd	WNetActu.	WNetRule	SigX1	ps	pw	Case			
	ANetActu.	ANetRule	SigX1	ps	pw	Case			
		SigU	SigX1	ps	pw	Case			

1 - Outer<sub>s</sub>hell

13	81.50	140.0	7.0	0.0	0.0	ST235	0.500	1.590	100
1.00	69.40	20.68	0.94	35.81	8.34	SEABAL 2-N			
	7.84	1.31		35.81	8.34	SEABAL 2-N			
		235.00	39.89	35.81	8.34	SEABAL 2-N			
14	81.50	140.0	7.0	0.0	0.0	ST235	0.500	1.590	100
1.00	69.40	19.35	15.02	30.90	7.84	SEABAL 2-N			
	7.84	1.15		30.90	7.84	SEABAL 2-N			
		235.00	57.95	30.90	7.84	SEABAL 2-N			
15	81.50	140.0	7.0	0.0	0.0	ST235	0.500	1.590	100
1.00	69.40	17.84	29.10	26.00	7.33	SEABAL 2-N			
	7.84	0.99		26.00	7.33	SEABAL 2-N			
		235.00	76.03	26.00	7.33	SEABAL 2-N			
16	94.07	140.0	7.0	0.0	0.0	ST235	0.500	1.590	100
1.00	79.85	16.10	43.18	21.09	6.83	SEABAL 2-N			
	7.84	0.83		21.09	6.83	SEABAL 2-N			
		235.00	97.87	21.09	6.83	SEABAL 2-N			
17	58.74	120.0	7.0	0.0	0.0	ST235	0.500	1.590	100
1.00	50.22	14.06	57.26	16.19	6.32	SEABAL 2-N			
	6.72	0.67		16.19	6.32	SEABAL 2-N			
		235.00	125.62	16.19	6.32	SEABAL 2-N			
18	56.68	120.0	7.0	0.0	0.0	ST235	0.250	1.590	100
1.00	48.64	5.83	71.34	11.28	5.82	SEABAL 2-N			
	6.72	0.28		11.28	5.82	SEABAL 2-N			
		235.00	114.89	11.28	5.82	SEABAL 2-N			

Figure 56: Rule check for stiffeners (Part 3)

**Local Rule Requirements - Stiffener**

N°	WGActu.		H <sub>1</sub>	E <sub>1</sub>	H <sub>2</sub>	E <sub>2</sub>	Mat	Spac	Span	Bend.Eff.
CAdd	WNetActu.	WNetRule	SigX1	ps	pw		Case			
	ANetActu.	ANetRule		ps	pw		Case			
		SigU	SigX1	ps	pw		Case			

2 - Inner<sub>bottom</sub>

1	107.14		160.0	7.0	0.0	0.0	ST235	0.470	1.590	100
1.00	94.32	71.22	57.49	110.72	10.40		LIQ 1-N			
	8.97	3.42		110.72	10.40		LIQ 1-N			
		235.00	111.59	56.16	10.44		BAL 2-N			
2	107.14		160.0	7.0	0.0	0.0	ST235	0.470	1.590	100
1.00	94.32	70.95	57.07	110.57	10.39		LIQ 1-N			
	8.97	3.41		110.57	10.39		LIQ 1-N			
		235.00	110.96	56.01	10.43		BAL 2-N			
3	107.14		160.0	7.0	0.0	0.0	ST235	0.470	1.590	100
1.00	94.32	70.68	56.64	110.42	10.37		LIQ 1-N			
	8.97	3.41		110.42	10.37		LIQ 1-N			
		235.00	110.33	55.87	10.41		BAL 2-N			
4	107.14		160.0	7.0	0.0	0.0	ST235	0.470	1.590	100
1.00	94.32	70.41	56.22	110.28	10.36		LIQ 1-N			
	8.97	3.40		110.28	10.36		LIQ 1-N			
		235.00	109.71	55.72	10.40		BAL 2-N			
5	107.14		160.0	7.0	0.0	0.0	ST235	0.470	1.590	100
1.00	94.32	70.14	55.80	110.13	10.34		LIQ 1-N			
	8.97	3.40		110.13	10.34		LIQ 1-N			
		235.00	109.08	55.57	10.38		BAL 2-N			
6	107.14		160.0	7.0	0.0	0.0	ST235	0.470	1.590	100
1.00	94.32	69.87	55.37	109.98	10.33		LIQ 1-N			
	8.97	3.39		109.98	10.33		LIQ 1-N			
		235.00	108.45	55.43	10.37		BAL 2-N			

Figure 57: Rule check for stiffeners (Part 4)

**Local Rule Requirements - Stiffener**

N°	WGActu.		H <sub>1</sub>	E <sub>1</sub>	H <sub>2</sub>	E <sub>2</sub>	Mat	Spac	Span	Bend.Eff.
CAdd	WNetActu.	WNetRule	SigX1	ps	pw		Case			
	ANetActu.	ANetRule		ps	pw		Case			
		SigU	SigX1	ps	pw		Case			

2 - Inner<sub>ottom</sub>

7	107.14		160.0	7.0	0.0	0.0	ST235	0.470	1.590	100
	94.32	69.60	54.95	109.84	10.31		LIQ 1-N			
	8.97	3.39		109.84	10.31		LIQ 1-N			
1.00		235.00	107.83	55.28	10.35		BAL 2-N			
8	107.14		160.0	7.0	0.0	0.0	ST235	0.470	1.590	100
	94.32	69.34	54.53	109.69	10.30		LIQ 1-N			
	8.97	3.38		109.69	10.30		LIQ 1-N			
1.00		235.00	107.20	55.13	10.34		BAL 2-N			
9	107.10		160.0	7.0	0.0	0.0	ST235	0.467	1.590	100
	94.29	68.66	54.11	109.54	10.28		LIQ 1-N			
	8.97	3.36		109.54	10.28		LIQ 1-N			
1.00		235.00	106.28	54.98	10.32		BAL 2-N			

Figure 58: Rule check for stiffeners (Part 5)



**Local Rule Requirements - Stiffener**

N°	WGActu.	H <sub>1</sub>	E <sub>1</sub>	H <sub>2</sub>	E <sub>2</sub>	Mat	Spac	Span	Bend.Eff.
CAdd	WNetActu.	WNetRule	SigX1	ps	pw	Case			
	ANetActu.	ANetRule	SigX1	ps	pw	Case			
		SigU	SigX1	ps	pw	Case			

3 - Deck

1	81.23	140.0	7.0	0.0	0.0	ST235	0.470	1.590	100
0.75	69.28	47.04	91.10	58.96	5.07	LIQ 1-N			
	7.84	1.81		58.96	5.07	LIQ 1-N			
		235.00	200.50	58.96	5.07	LIQ 1-N			
2	81.23	140.0	7.0	0.0	0.0	ST235	0.470	1.590	100
0.75	69.28	47.07	91.56	58.79	5.05	LIQ 1-N			
	7.84	1.80		58.79	5.05	LIQ 1-N			
		235.00	201.12	58.79	5.05	LIQ 1-N			
3	81.23	140.0	7.0	0.0	0.0	ST235	0.470	1.590	100
0.75	69.28	47.10	92.03	58.63	5.03	LIQ 1-N			
	7.84	1.80		58.63	5.03	LIQ 1-N			
		235.00	201.73	58.63	5.03	LIQ 1-N			
4	81.23	140.0	7.0	0.0	0.0	ST235	0.470	1.590	100
0.75	69.28	47.13	92.49	58.47	5.02	LIQ 1-N			
	7.84	1.79		58.47	5.02	LIQ 1-N			
		235.00	202.35	58.47	5.02	LIQ 1-N			
5	81.23	140.0	7.0	0.0	0.0	ST235	0.470	1.590	100
0.75	69.28	47.16	92.96	58.31	5.00	LIQ 1-N			
	7.84	1.79		58.31	5.00	LIQ 1-N			
		235.00	202.96	58.31	5.00	LIQ 1-N			
6	81.23	140.0	7.0	0.0	0.0	ST235	0.470	1.590	100
0.75	69.28	47.20	93.42	58.15	4.98	LIQ 1-N			
	7.84	1.78		58.15	4.98	LIQ 1-N			
		235.00	203.58	58.15	4.98	LIQ 1-N			

Figure 59: Rule check for stiffeners (Part 6)

**Local Rule Requirements - Stiffener**

N°	WGActu.		H <sub>1</sub>	E <sub>1</sub>	H <sub>2</sub>	E <sub>2</sub>	Mat	Spac	Span	Bend.Eff.
CAdd	WNetActu.	WNetRule	SigX1	ps	pw		Case			
	ANetActu.	ANetRule		ps	pw		Case			
		SigU	SigX1	ps	pw		Case			

3 - Deck

7	81.23		140.0	7.0	0.0	0.0	ST235	0.470	1.590	100
0.75	69.28	47.23	93.89	57.98	4.97		LIQ 1-N			
	7.84	1.77		57.98	4.97		LIQ 1-N			
		235.00	204.19	57.98	4.97		LIQ 1-N			
8	81.23		140.0	7.0	0.0	0.0	ST235	0.470	1.590	100
0.75	69.28	47.26	94.35	57.82	4.95		LIQ 1-N			
	7.84	1.77		57.82	4.95		LIQ 1-N			
		235.00	204.80	57.82	4.95		LIQ 1-N			
9	81.21		140.0	7.0	0.0	0.0	ST235	0.467	1.590	100
0.75	69.26	47.04	94.82	57.66	4.93		LIQ 1-N			
	7.84	1.76		57.66	4.93		LIQ 1-N			
		235.00	204.89	57.66	4.93		LIQ 1-N			

Figure 60: Rule check for stiffeners (Part 7)

**Local Rule Requirements - Stiffener**

N°	WGActu.	H <sub>1</sub>	E <sub>1</sub>	H <sub>2</sub>	E <sub>2</sub>	Mat	Spac	Span	Bend.Eff.
CAdd	WNetActu.	WNetRule	SigX1	ps	pw	Case			
	ANetActu.	ANetRule		ps	pw	Case			
		SigU	SigX1	ps	pw	Case			

**4 - Inner<sub>ide</sub>**

1	76.28	140.0	7.0	0.0	0.0	ST235	0.250	1.590	100
1.00	65.19	32.79	41.30	105.08	9.82	LIQ 1-N			
	7.84	1.86		105.08	9.82	LIQ 1-N			
		235.00	76.36	50.52	9.86	BAL 2-N			
2	196.32	140.0	10.0	100.0	10.0	ST235	0.500	1.590	100
1.00	157.53	58.06	27.22	100.17	9.32	LIQ 1-N			
	11.34	3.25		100.17	9.32	LIQ 1-N			
		235.00	54.20	45.62	9.35	BAL 2-N			
3	79.74	140.0	7.0	0.0	0.0	ST235	0.500	1.590	100
1.00	67.90	51.54	13.14	95.27	8.81	LIQ 1-N			
	7.84	3.09		95.27	8.81	LIQ 1-N			
		235.00	61.30	40.71	8.85	BAL 2-N			
4	79.74	140.0	7.0	0.0	0.0	ST235	0.500	1.590	100
1.00	67.90	46.25	1.15	90.36	8.31	LIQ 1-N			
	7.84	2.93		90.36	8.31	LIQ 1-N			
		235.00	40.86	35.81	8.34	BAL 2-N			
5	79.74	140.0	7.0	0.0	0.0	ST235	0.500	1.590	100
1.00	67.90	47.32	18.29	85.46	7.80	LIQ 1-N			
	7.84	2.77		85.46	7.80	LIQ 1-N			
		235.00	58.30	30.90	7.84	BAL 2-N			
6	79.74	140.0	7.0	0.0	0.0	ST235	0.500	1.590	100
1.00	67.90	48.59	35.44	80.55	7.29	LIQ 1-N			
	7.84	2.61		80.55	7.29	LIQ 1-N			
		235.00	75.74	26.00	7.33	BAL 2-N			

Figure 61: Rule check for stiffeners (Part 8)

### Local Rule Requirements - Stiffener

N°	WActu.		H <sub>1</sub>	E <sub>1</sub>	H <sub>2</sub>	E <sub>2</sub>	Mat	Spac	Span	Bend.Eff.
CAdd	WNetActu.	WNetRule	SigX1	ps	pw		Case			
	ANetActu.	ANetRule		ps	pw		Case			
		SigU	SigX1	ps	pw		Case			

#### 4 - Inner<sub>ide</sub>

7	79.74		140.0	7.0	0.0	0.0	ST235	0.500	1.590	100
1.00	67.90	50.11	52.58	75.65	6.79		LIQ 1-N			
	7.84	2.45		75.65	6.79		LIQ 1-N			
		235.00	93.18	21.09	6.83		BAL 2-N			
8	79.74		140.0	7.0	0.0	0.0	ST235	0.500	1.590	100
1.00	67.90	51.96	69.72	70.74	6.28		LIQ 1-N			
	7.84	2.28		70.74	6.28		LIQ 1-N			
		235.00	110.63	16.19	6.32		BAL 2-N			
9	76.28		140.0	7.0	0.0	0.0	ST235	0.250	1.590	100
1.00	65.19	27.13	86.87	65.84	5.78		LIQ 1-N			
	7.84	1.16		65.84	5.78		LIQ 1-N			
		235.00	111.28	65.84	5.78		LIQ 1-N			

Figure 62: Rule check for stiffeners (Part 9)

**Local Rule Requirements - Strake**

N°	tGActu.	tGRule				Mat	Spac	Span	Bend.Eff.
CAdd	tNetActu.	tLoad	SigX1	ps	pw	Case			
		tTest	$\sigma_N$ Actu.	$\sigma_N$ Rule		Case	$\sigma_{Ap}$ Buck	$\sigma_{CRIT}$ Buck	t3
		tMini							
<b>1 - Outer<sub>shell</sub></b>									
1	11.00	10.00				ST235	0.530	2.186	100
	9.50	7.20	96.57	57.14	17.85				
1.50		4.43	111.59	192.00			-79.31	-142.72	8.43
		6.64							
2	13.00	10.00				ST235	0.530	2.186	100
	11.50	7.20	96.57	57.14	17.85				
1.50		4.43	111.59	192.00			-79.31	-170.23	8.43
		6.64							
3	11.00	10.00				ST235	0.530	2.186	100
	9.50	6.48	76.01	57.14	11.36				
1.50		4.24	87.83	192.00			-79.31	-142.72	8.43
		6.64							
4	25.00	7.00				ST235	0.500	1.590	100
	23.50	3.18	35.44	26.00	7.33				
1.50		2.81	70.65	192.00			-69.72	-209.82	4.82
		5.49							
5	11.00	7.00				ST235	0.500	1.590	100
	9.50	2.96	52.58	21.09	6.83				
1.50		2.58	100.37	192.00			-86.87	-204.48	5.44
		5.49							
6	25.00	20.50				ST235	0.530	0.650	100
	23.50	2.58	86.87	11.28	5.82				
1.50		1.68	126.13	192.00			-109.16	-209.82	6.81
		18.93							

Figure 63: Rule check for strakes (Part 1)

### Local Rule Requirements - Strake

N°	tGActu.	tGRule	Mat	Spac	Span	Bend.Eff.
	tNetActu.	tLoad	SigX1	ps	pw	Case
CAdd		tTest	$\sigma_N$ Actu.	$\sigma_N$ Rule		Case
		tMini				$\sigma_{Ap}$ Buck $\sigma_{CRIT}$ Buck t3

#### 2 - Inner<sub>p</sub>ottom

7	9.00	7.50				ST235 0.470 1.590 100
	7.25	5.91	70.51	110.87	10.42	
		5.14	81.48	192.00		-57.91 -166.64
1.75		5.14				4.38

Figure 64: Rule check for strakes (Part 2)

### Local Rule Requirements - Strake

N°	tGActu.	tGRule	Mat	Spac	Span	Bend.Eff.
	tNetActu.	tLoad	SigX1	ps	pw	Case
CAdd		tTest	$\sigma_N$ Actu.	$\sigma_N$ Rule		Case
		tMini				$\sigma_{Ap}$ Buck $\sigma_{CRIT}$ Buck t3

#### 3 - Deck

8	11.00	11.00				ST235 0.530 1.009 100
	9.50	2.44	110.36	4.56	5.12	
		1.51	127.52	192.00		-110.36 -146.17
1.50		6.96				9.38
9	11.00	7.50				ST235 0.470 1.590 100
	9.75	4.59	110.92	58.96	5.07	
		3.85	134.06	192.00		-115.45 -205.73
1.25		6.04				6.22

Figure 65: Rule check for strakes (Part 3)

**Local Rule Requirements - Strake**

N°	tGActu.	tGRule				Mat	Spac	Span	Bend.Eff.
	tNetActu.	tLoad	SigX1	ps	pw	Case			
CAdd		tTest	$\sigma_N$ Actu.	$\sigma_N$ Rule		Case	$\sigma_{Ap}$ Buck	$\sigma_{CRIT}$ Buck	t3
		tMini							

4 - Inner<sub>ide</sub>

10	9.00	9.50				ST235	0.000	0.000	100
	7.20	0.00							
1.80		0.00	111.59	192.00			-79.31	-120.16	
		0.00					*	7.77	
11	9.00	9.50				ST235	0.500	1.590	100
	7.50	5.98	50.28	105.08	9.82				
		5.34	127.52	192.00			-110.36	-141.37	
1.50		4.40					*	7.92	

Figure 66: Rule check for strakes (Part 4)

**Local Rule Requirements - Strake**

N°	tGActu.	tGRule				Mat	Spac	Span	Bend.Eff.
	tNetActu.	tLoad	SigX1	ps	pw	Case			
CAdd		tTest	$\sigma_N$ Actu.	$\sigma_N$ Rule		Case	$\sigma_{Ap}$ Buck	$\sigma_{CRIT}$ Buck	t3
		tMini							

5 - Long<sub>B</sub>ulkhead

12	7.00	6.00				ST235	0.000	0.000	0
	5.60	0.00							
1.40		0.00	0.00	192.00			0.00	0.00	
		0.00						0.00	
13	7.00	46.00				ST235	5.440	1.590	0
	6.00	* 45.10	0.00	110.87	10.42				
		* 41.67	0.00	192.00			0.00	0.00	
1.00		* 22.29						0.00	

Figure 67: Rule check for strakes (Part 5)

## **B APPENDIX: DEFORMATION ENERGIES**



**Descriptive information for the graphs:**

**SCENARIO I:** Push barge striking bow with an impact angle of 55 deg.

**SCENARIO II:** V-shaped striking bow with an impact angle of 90 deg.

**Case 1:** above deck collision

**Case 2:** sheerstrake collision

**Case 3:** mid-depth collision

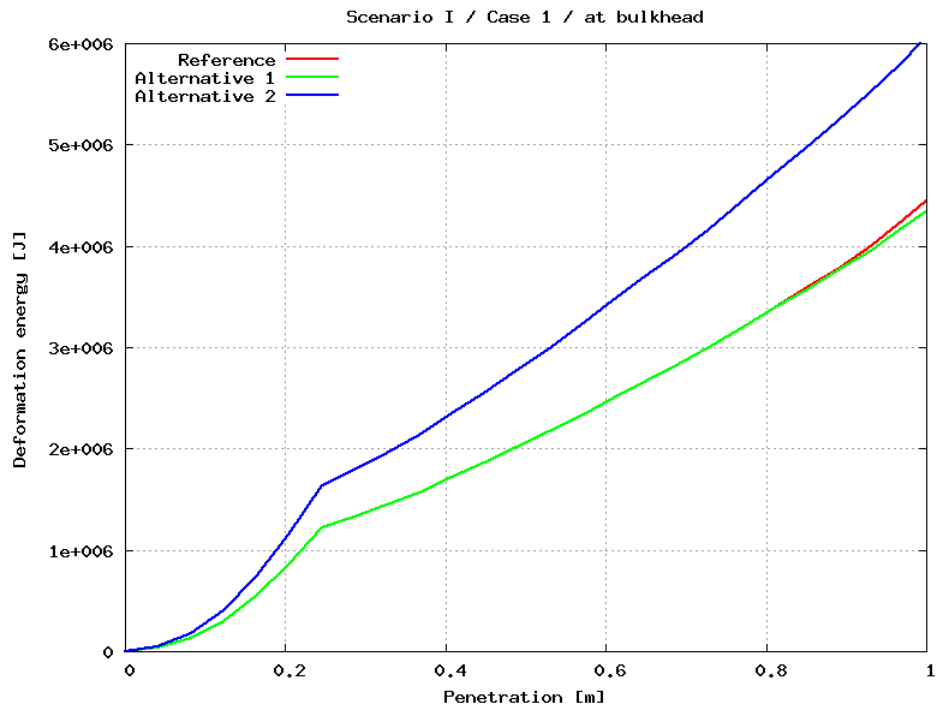


Figure 68: Scenario I, Case 1 - at bulkhead

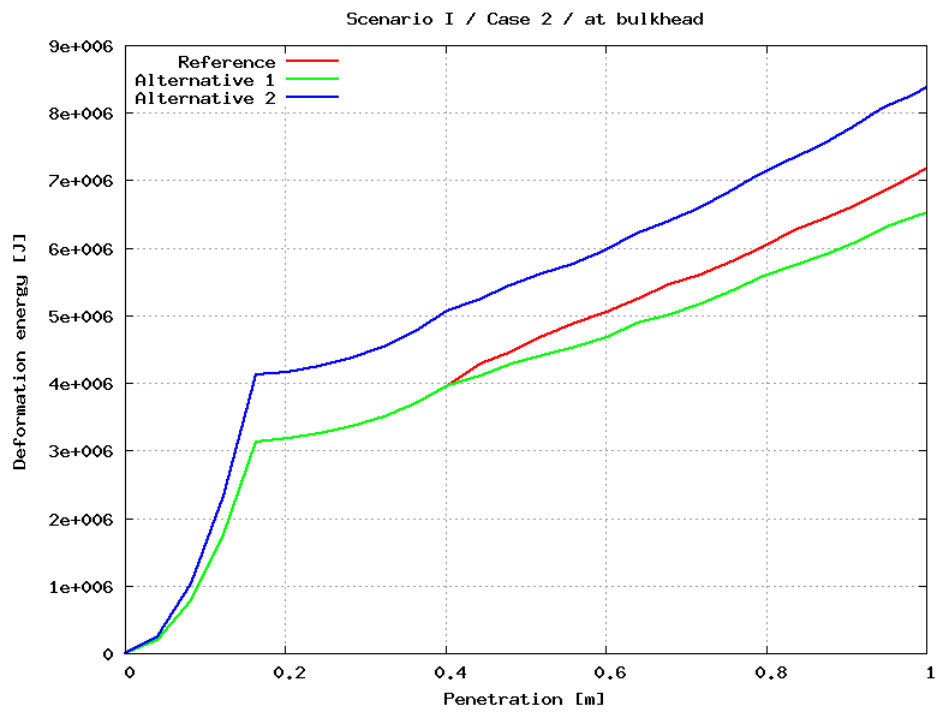


Figure 69: Scenario I / Case 2 / at bulkhead

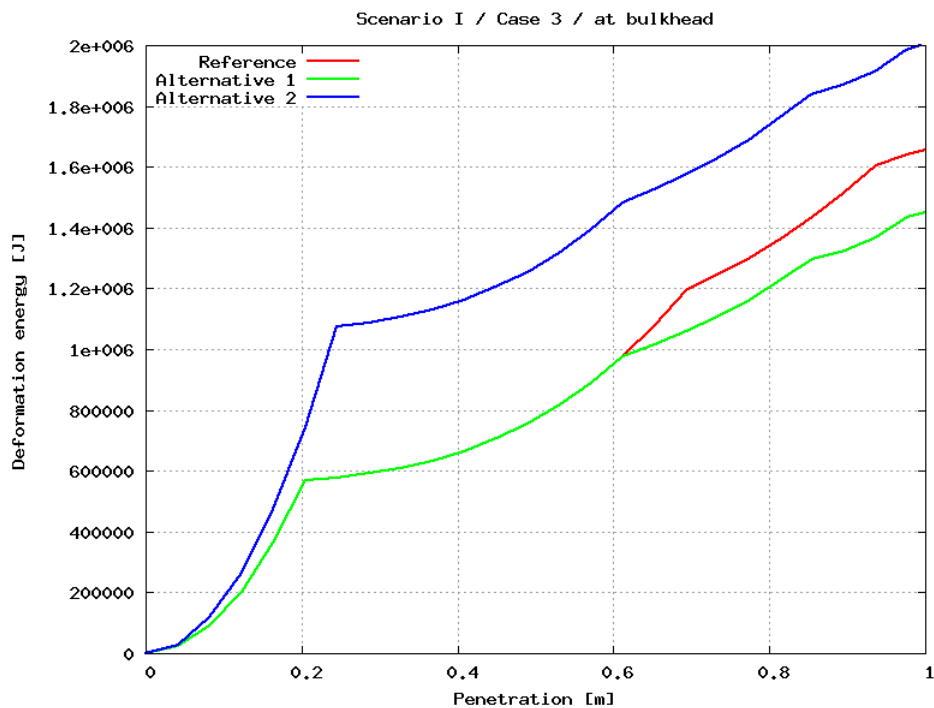


Figure 70: Scenario I / Case 3 / at bulkhead

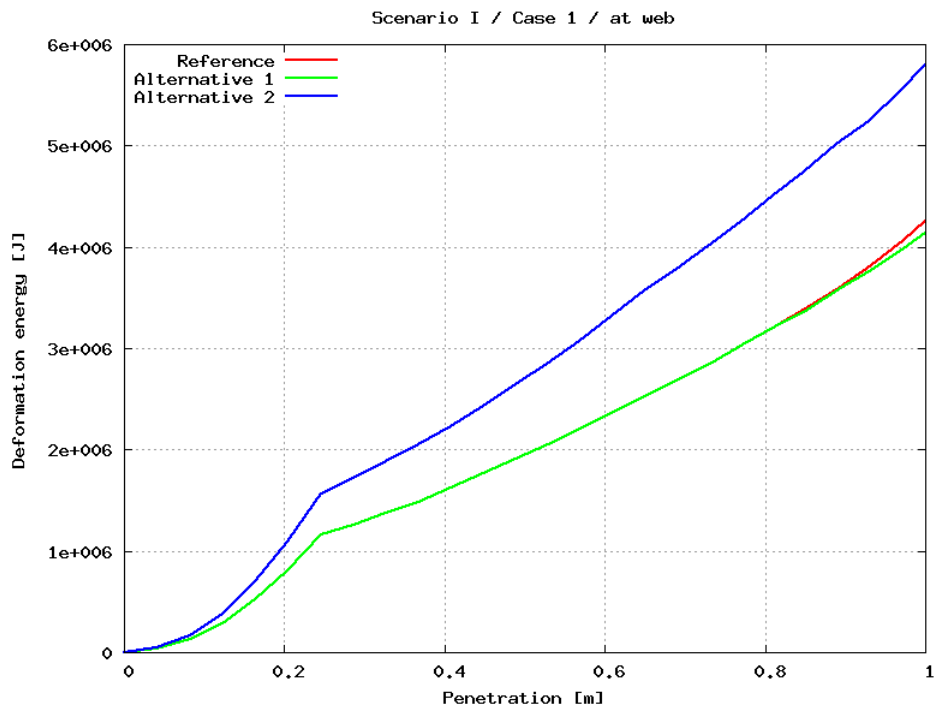


Figure 71: Scenario I, Case 1 - at web

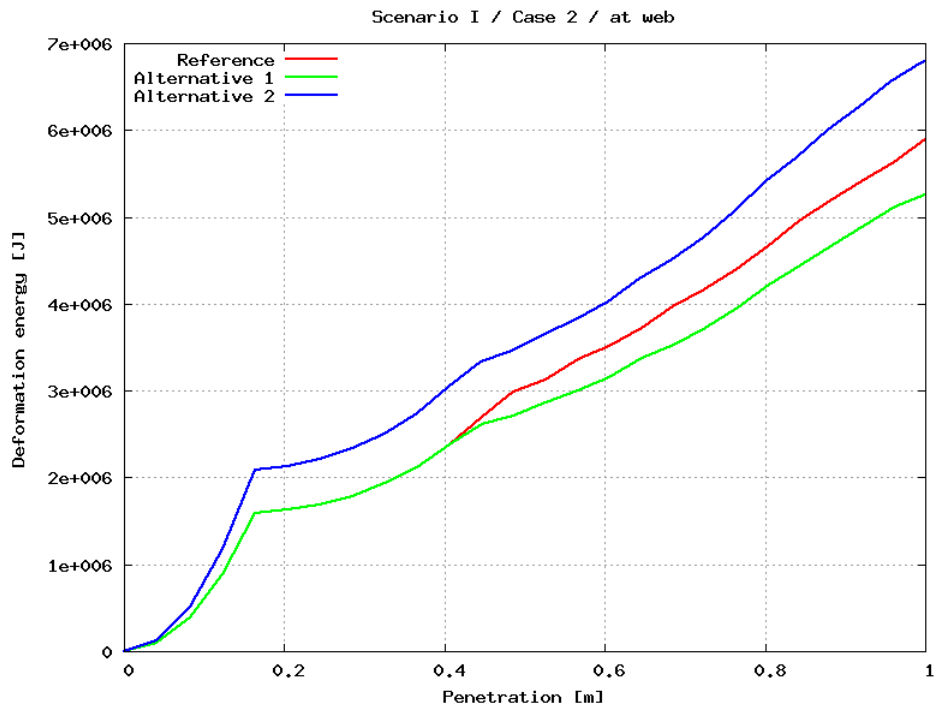


Figure 72: Scenario I / Case 2 / at web

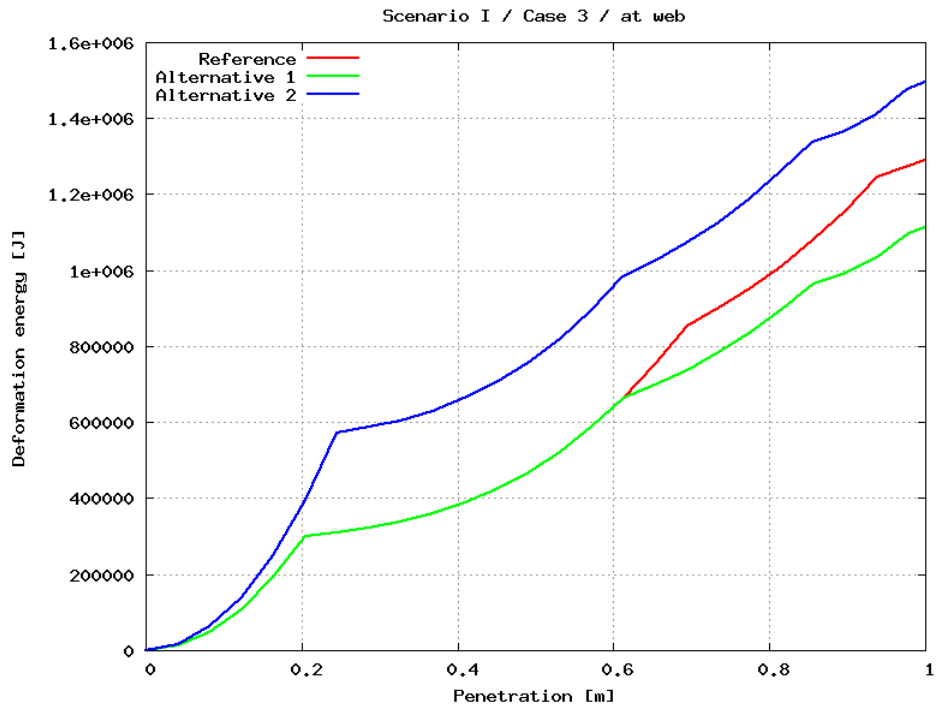


Figure 73: Scenario I / Case 3 / at web

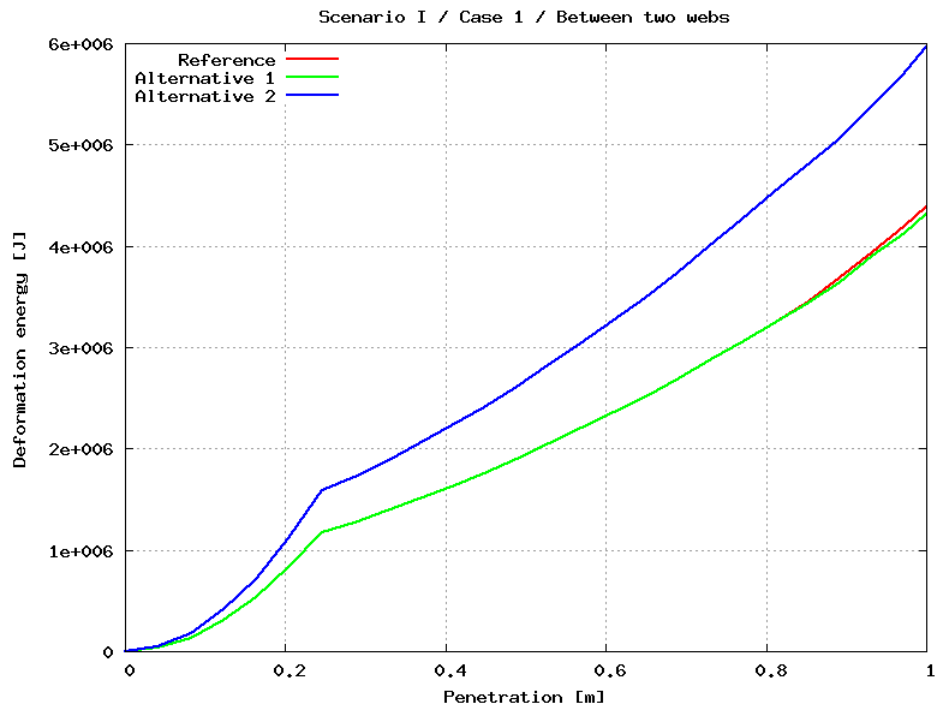


Figure 74: Scenario I, Case 1 - between webs

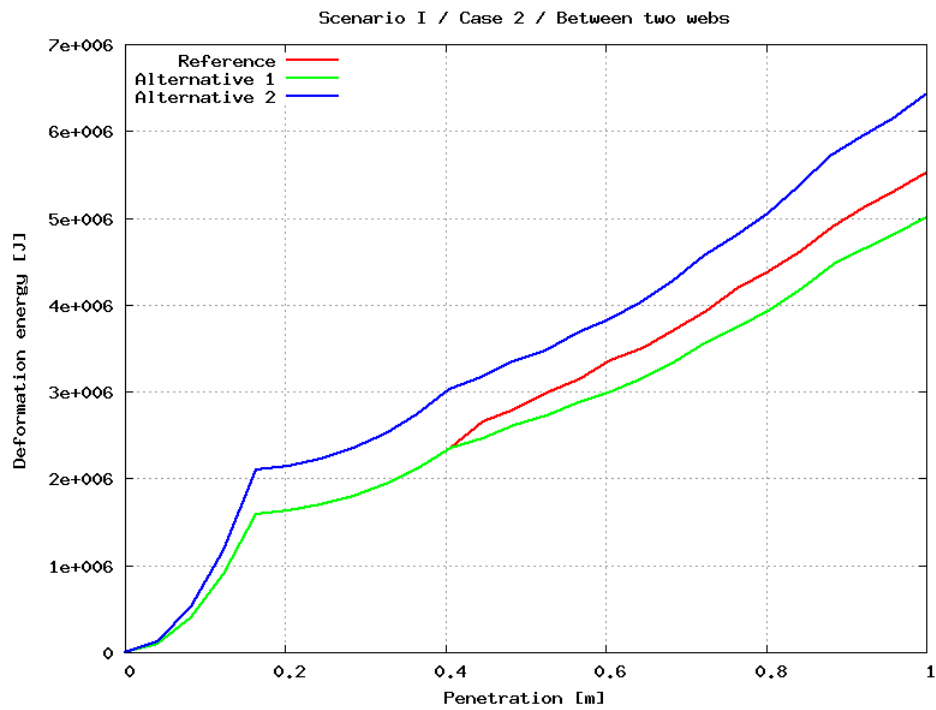


Figure 75: Scenario I / Case 2 / between webs

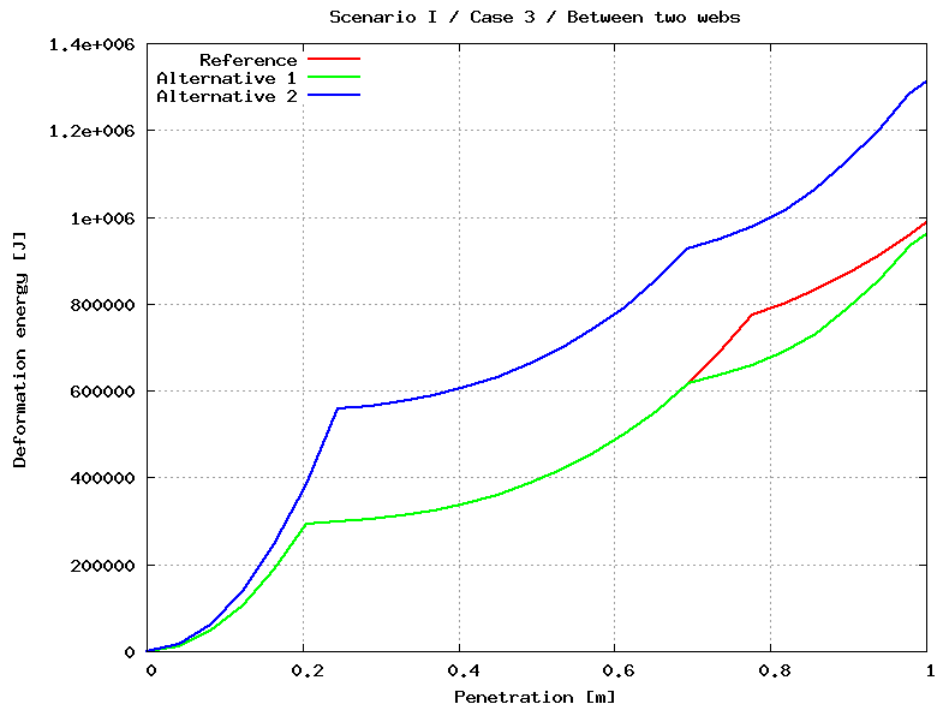


Figure 76: Scenario I / Case 3 / between webs

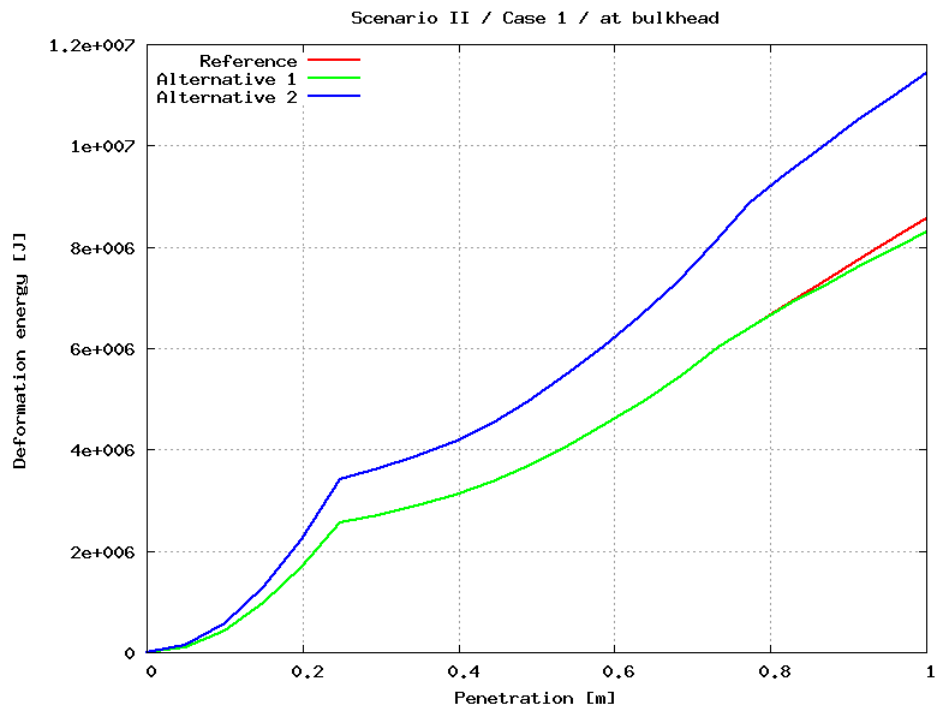


Figure 77: Scenario II, Case 1 - at bulkhead

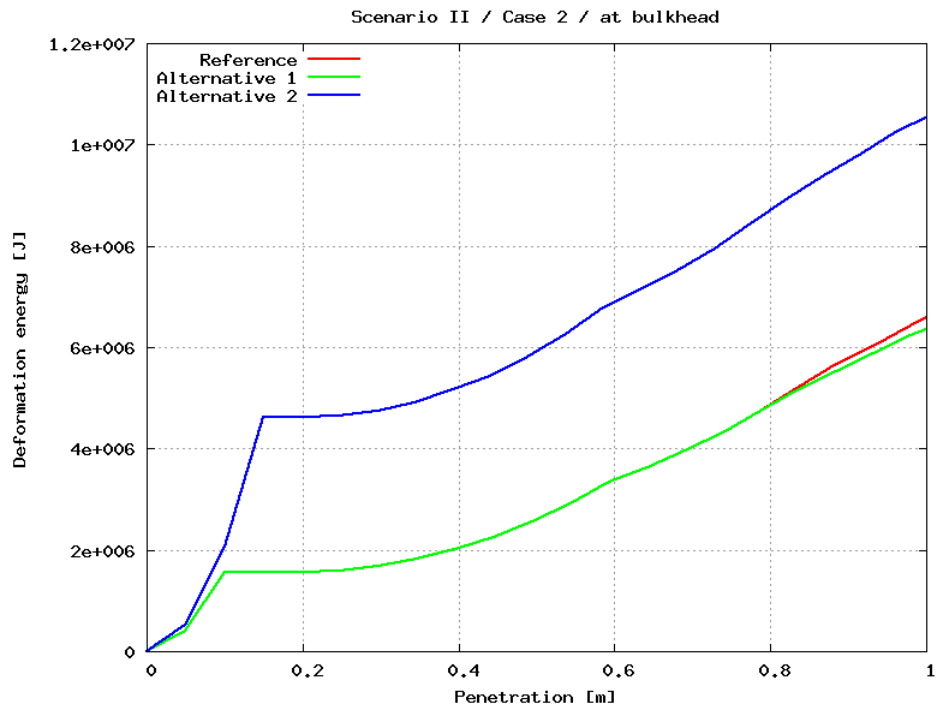


Figure 78: Scenario II / Case 2 / at bulkhead

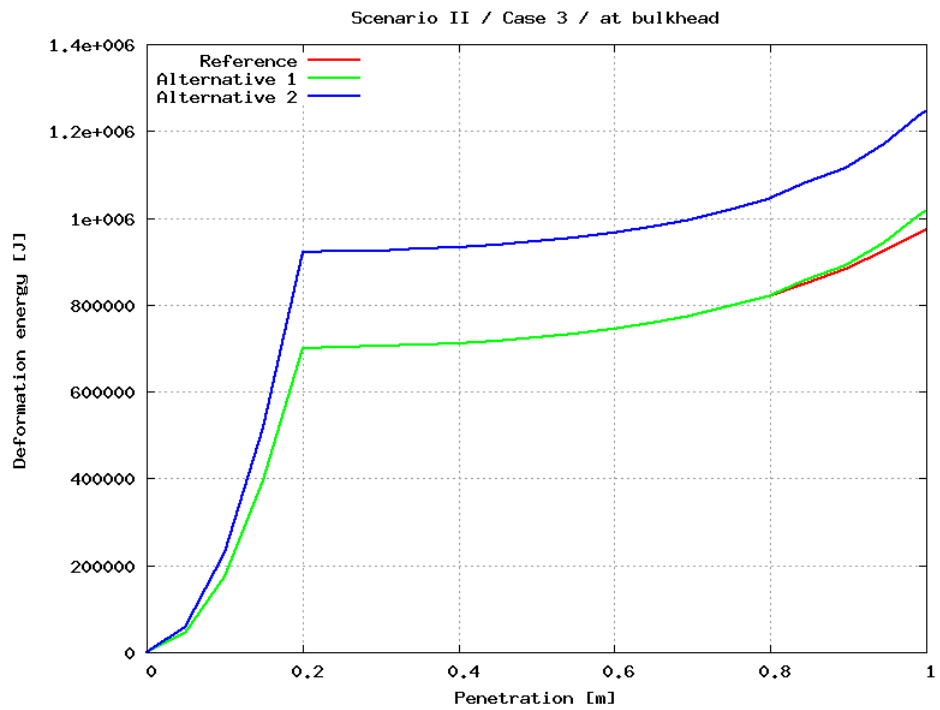


Figure 79: Scenario II / Case 3 / at bulkhead

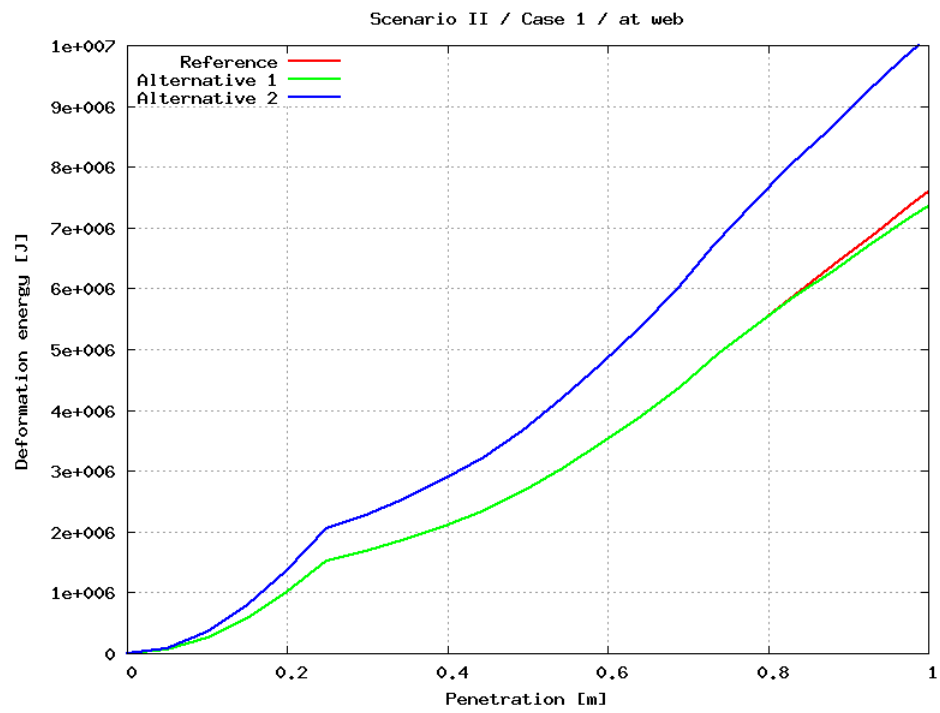


Figure 80: Scenario II, Case 1 - at web

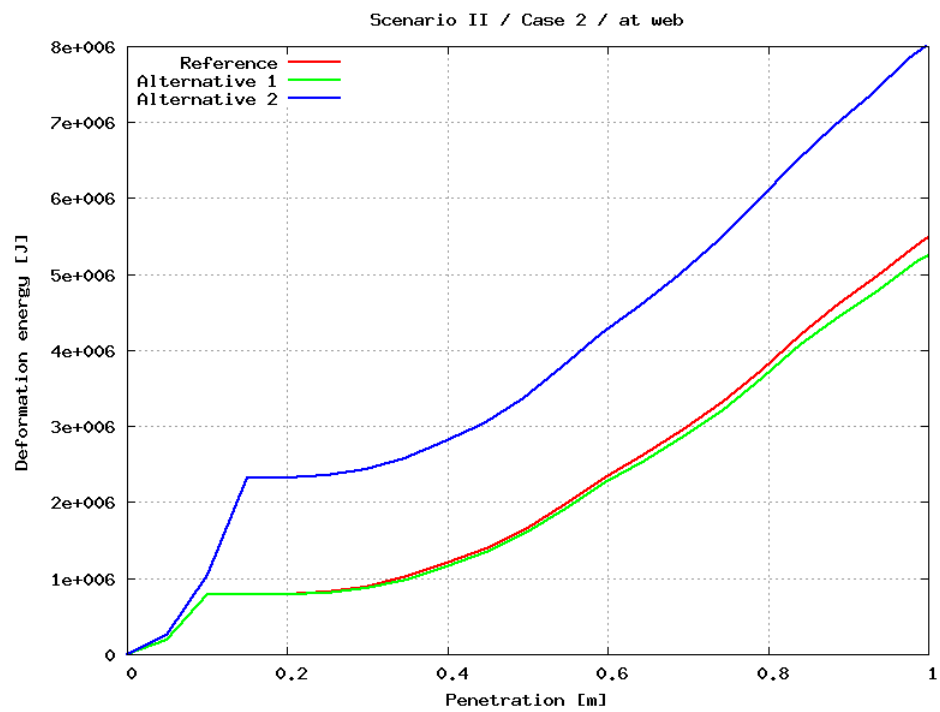


Figure 81: Scenario II / Case 2 / at web



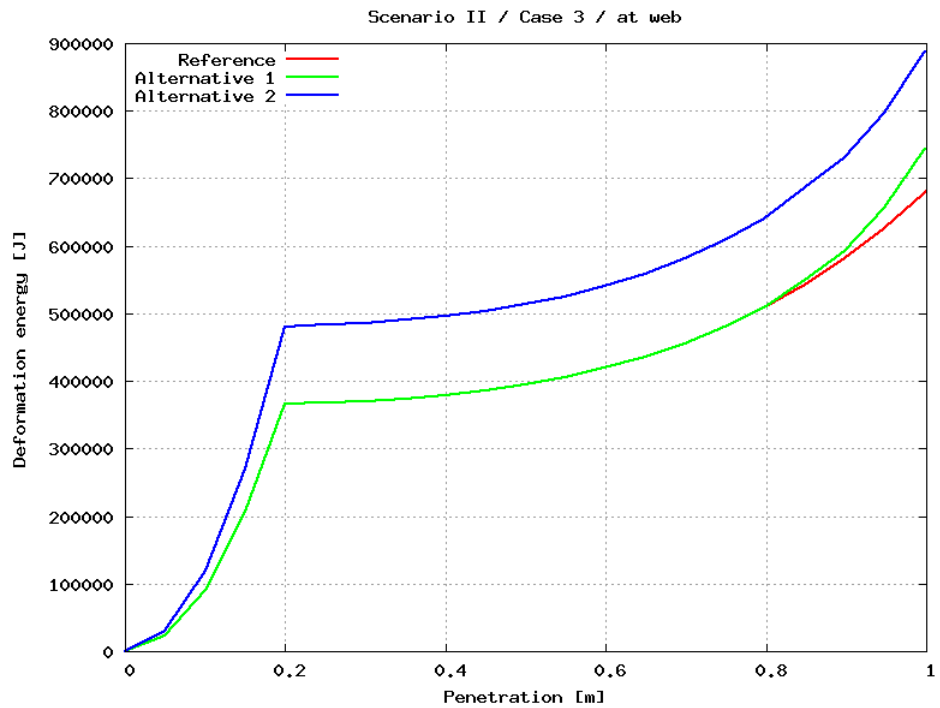


Figure 82: Scenario II / Case 3 / at web

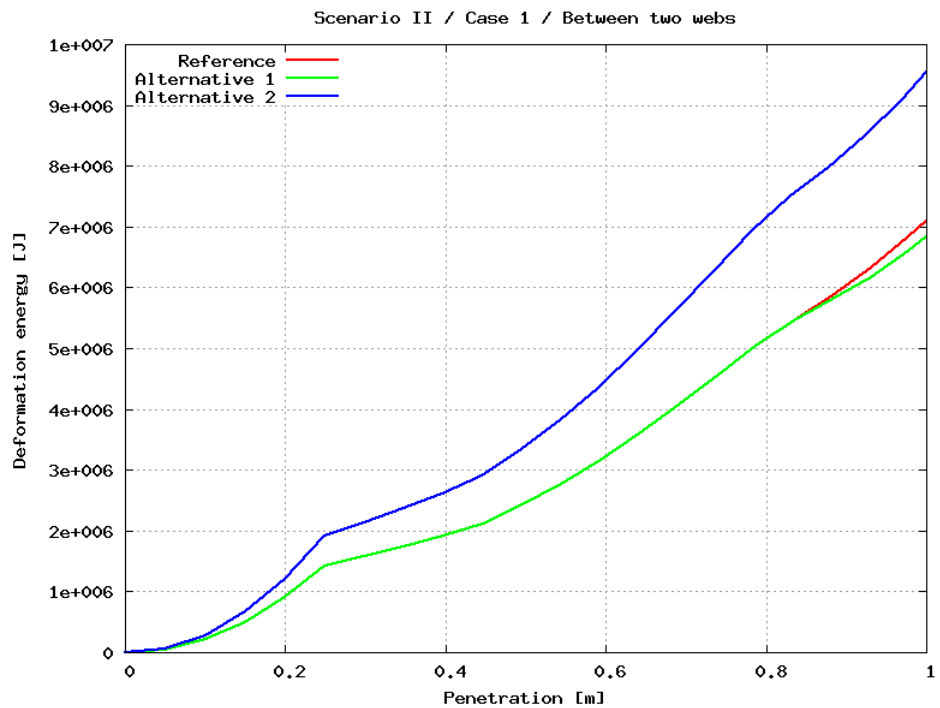


Figure 83: Scenario II, Case 1 - between webs

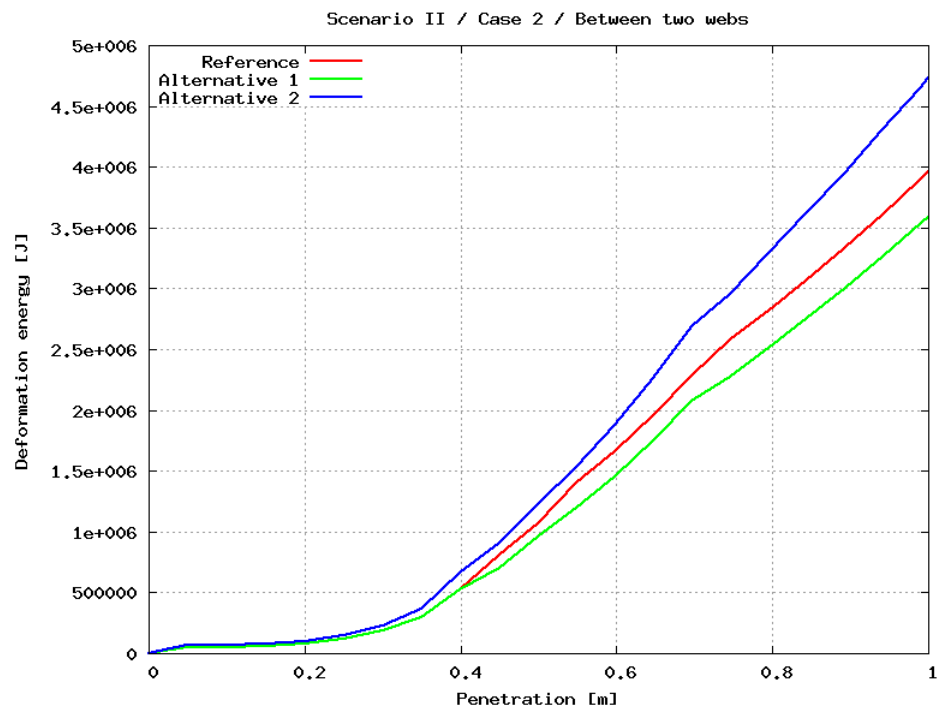


Figure 84: Scenario II / Case 2 / between webs

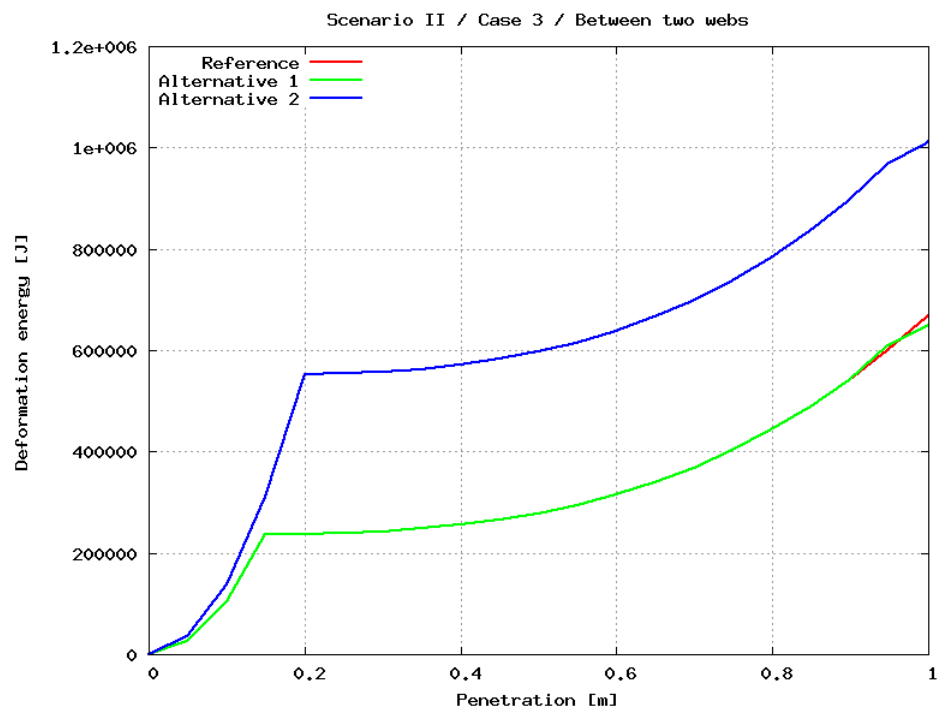


Figure 85: Scenario II / Case 3 / between webs

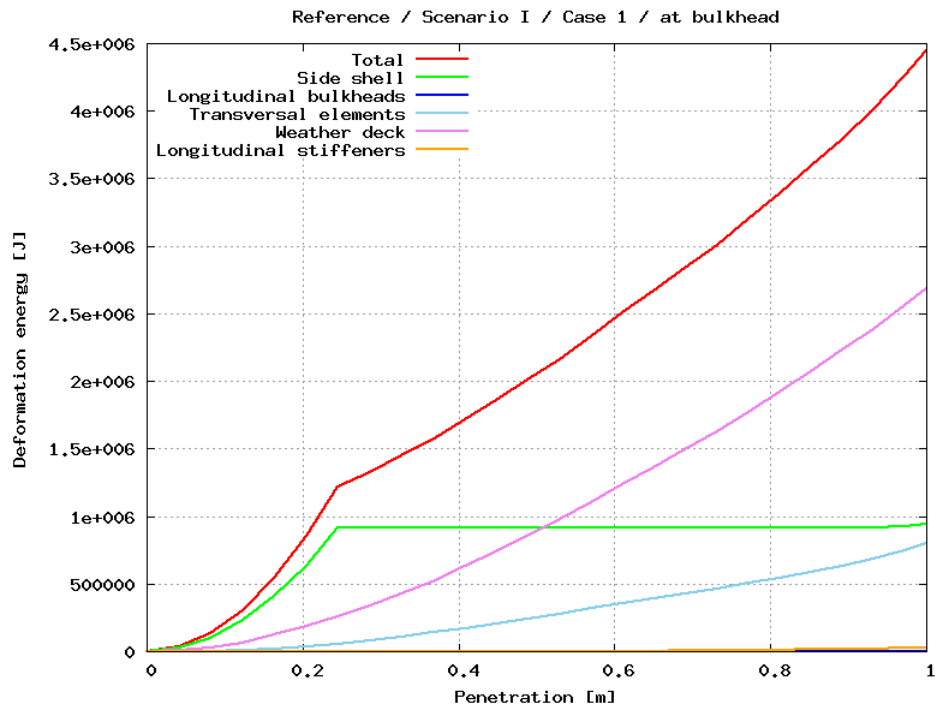


Figure 86: Scenario I, Case 1 - at bulkhead

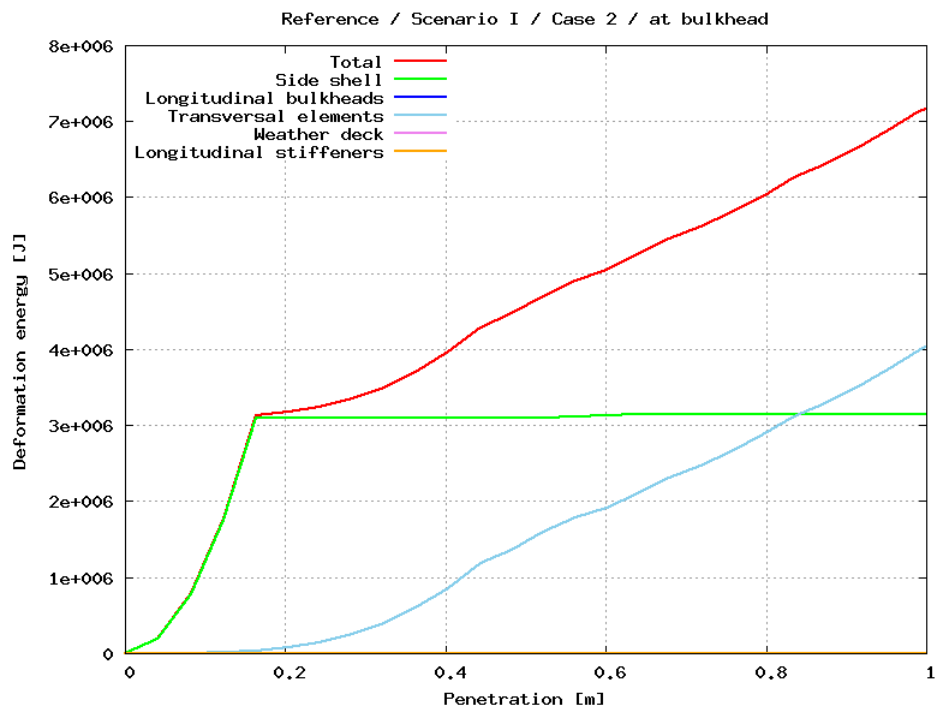


Figure 87: Scenario I / Case 2 / at bulkhead

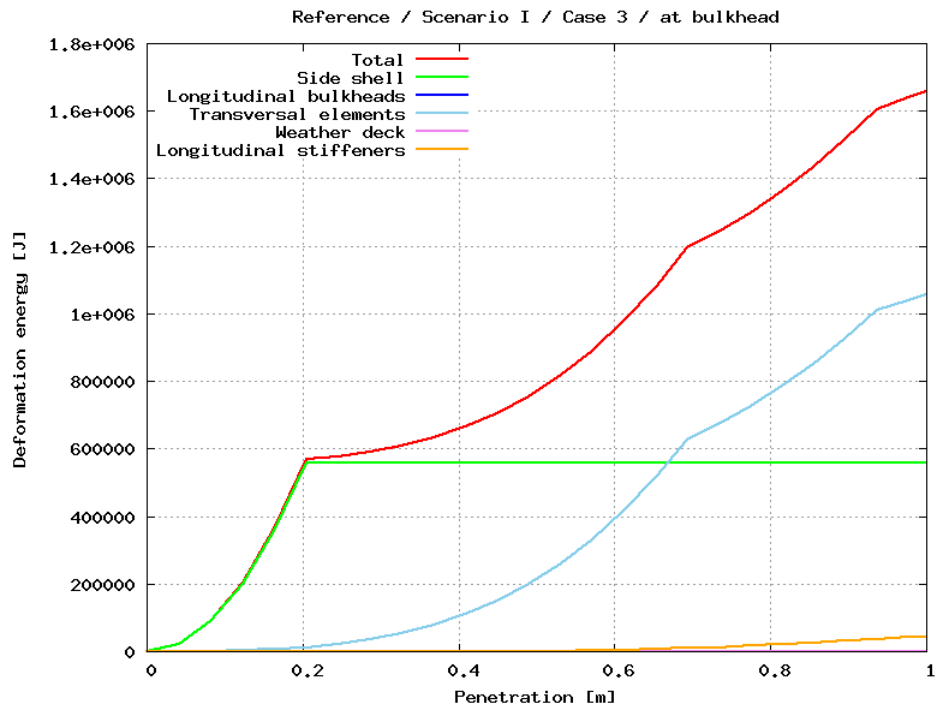


Figure 88: Scenario I / Case 3 / at bulkhead

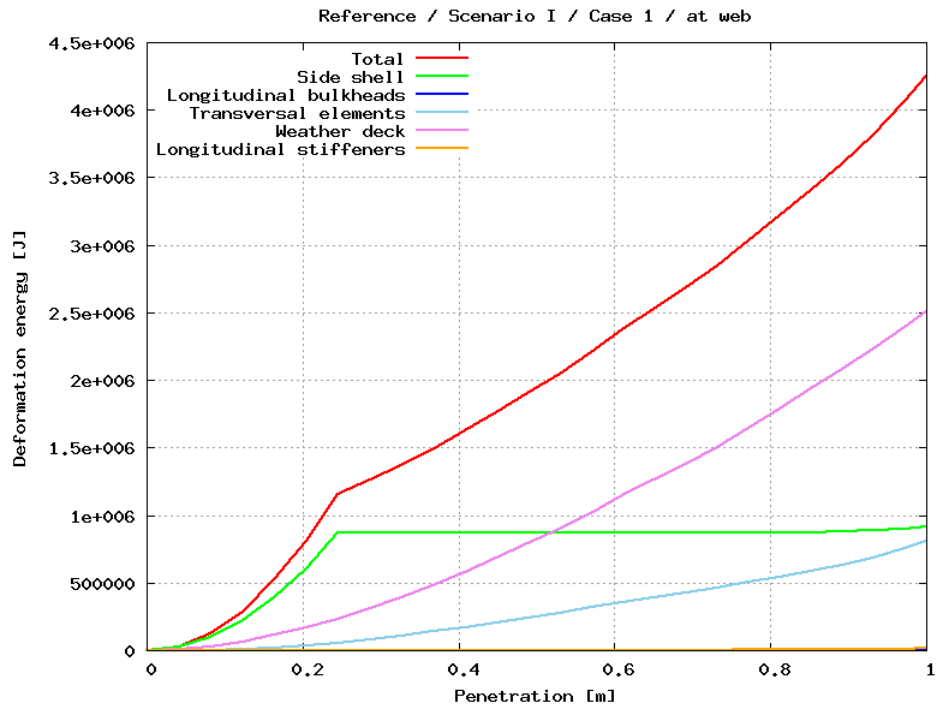


Figure 89: Scenario I, Case 1 - at web

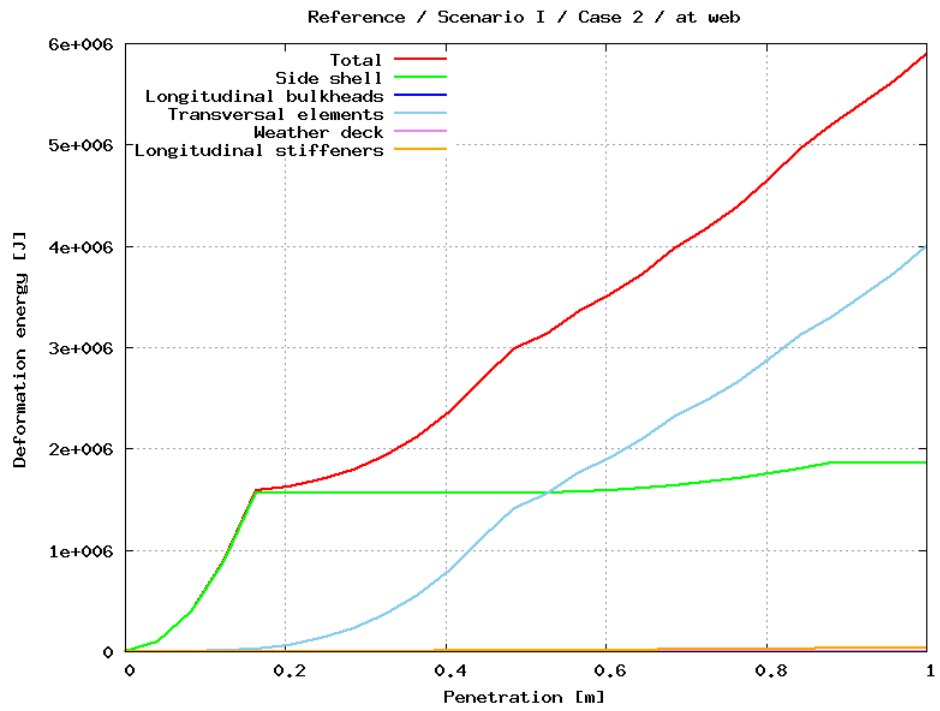


Figure 90: Scenario I / Case 2 / at web

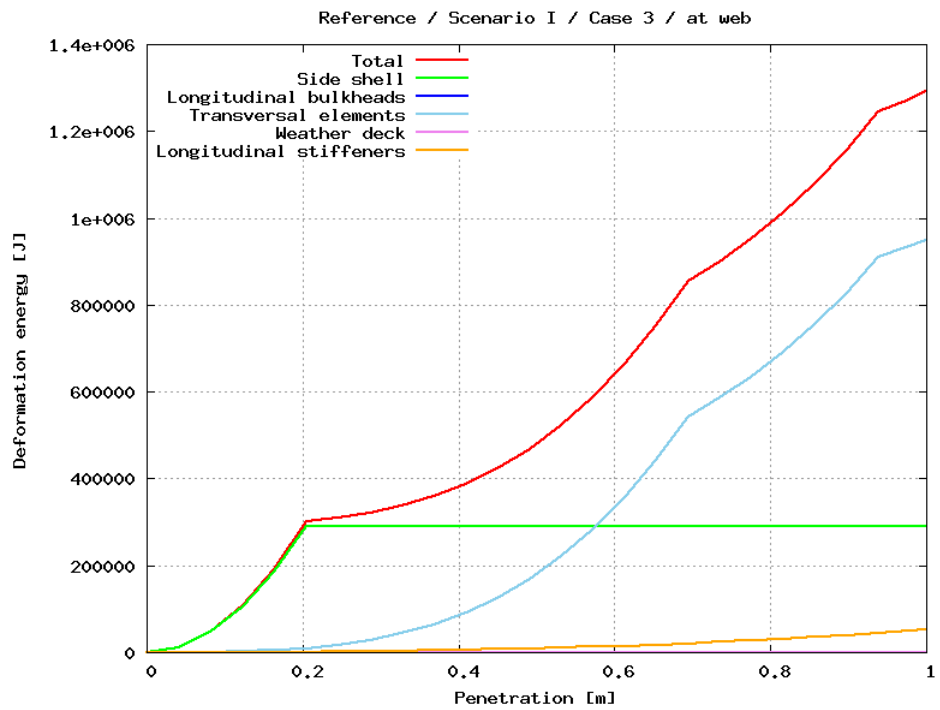


Figure 91: Scenario I / Case 3 / at web

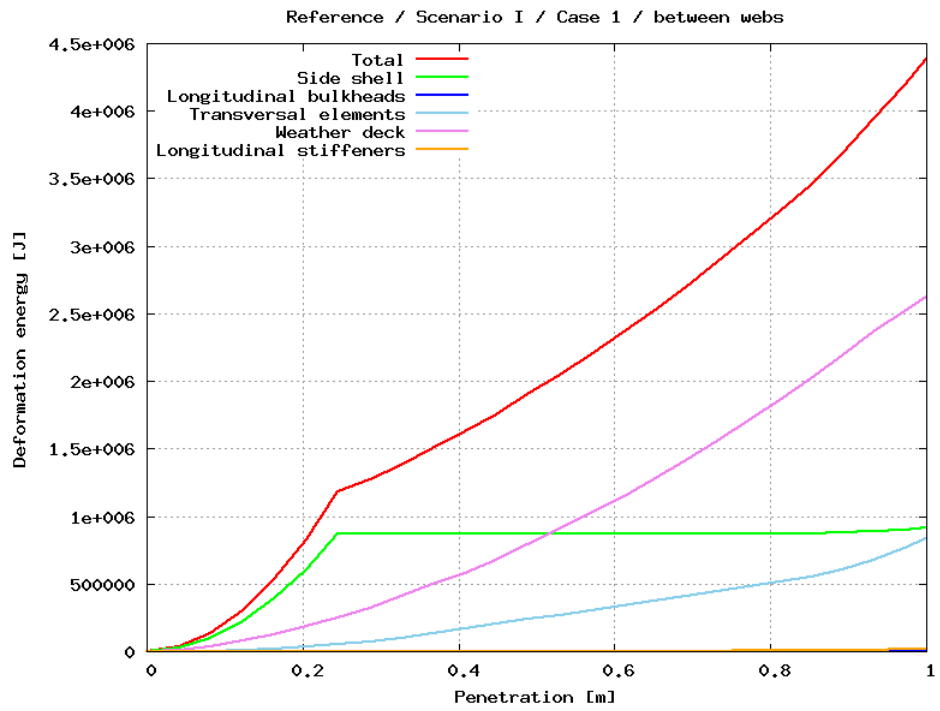


Figure 92: Scenario I, Case 1 - between webs

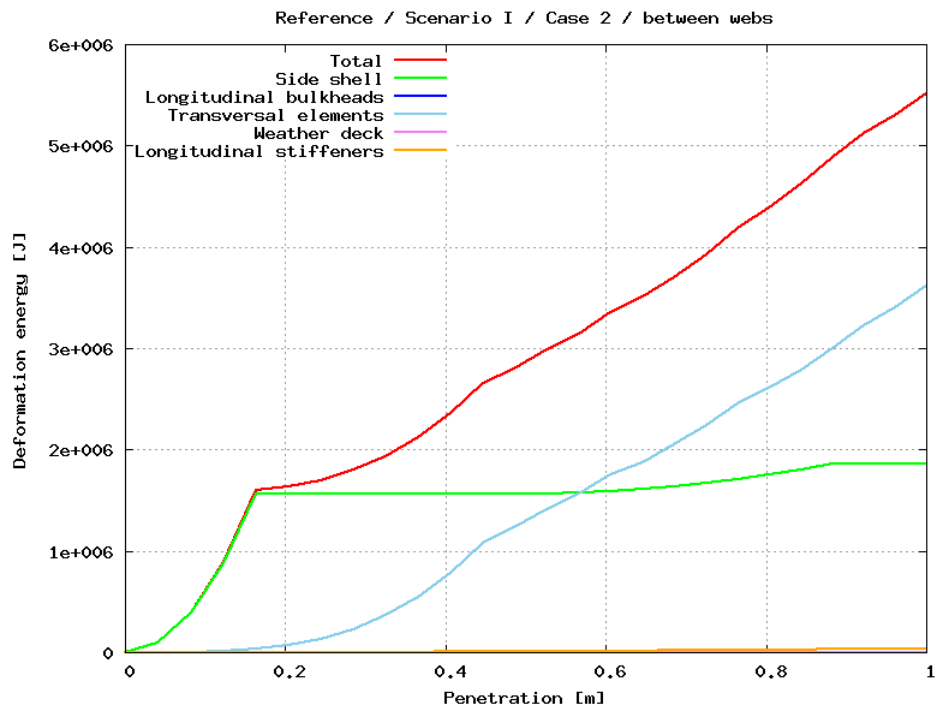


Figure 93: Scenario I / Case 2 / between webs

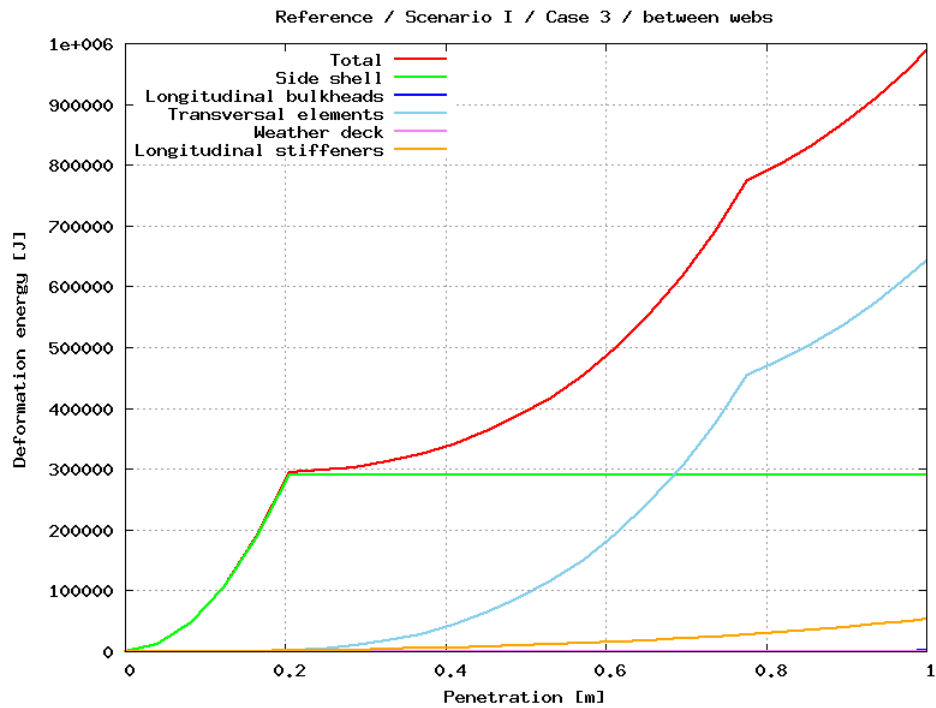


Figure 94: Scenario I / Case 3 / between webs

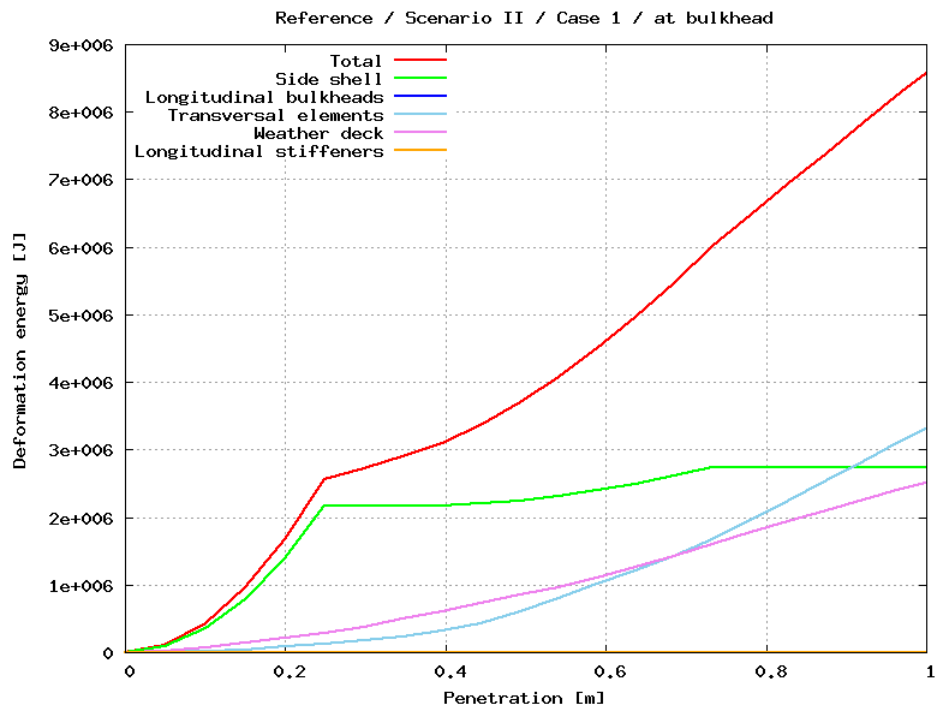


Figure 95: Scenario I, Case 1 - at bulkhead

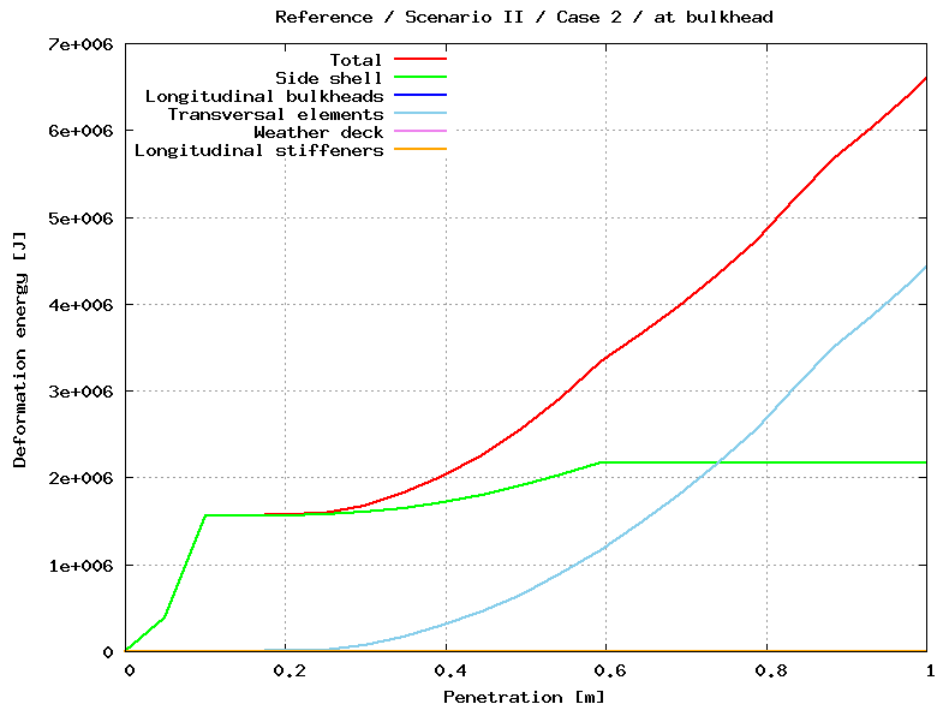


Figure 96: Scenario I / Case 2 / at bulkhead

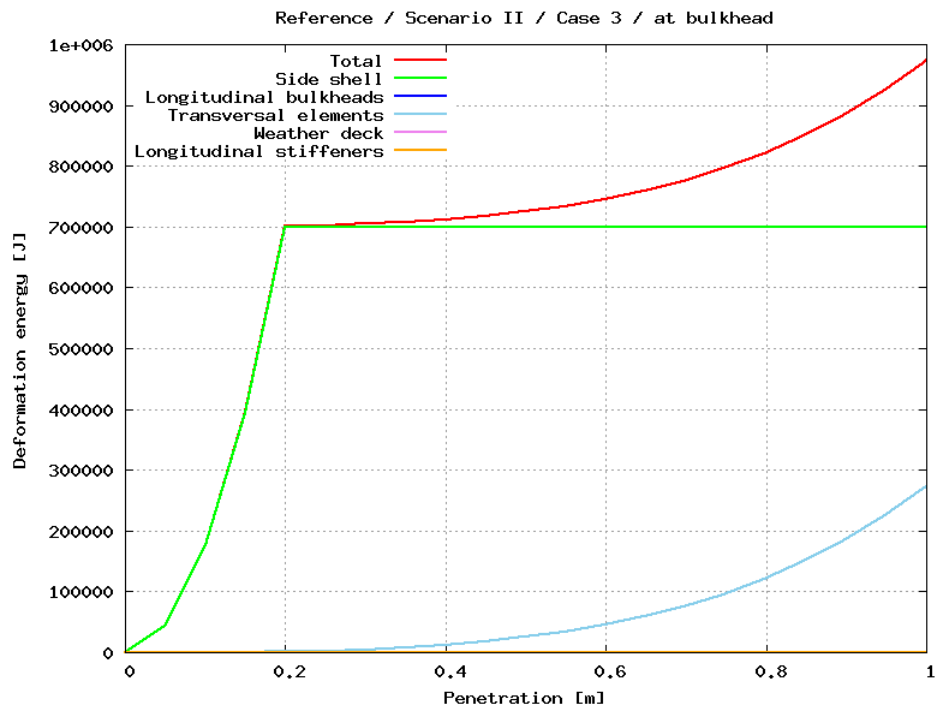


Figure 97: Scenario I / Case 3 / at bulkhead



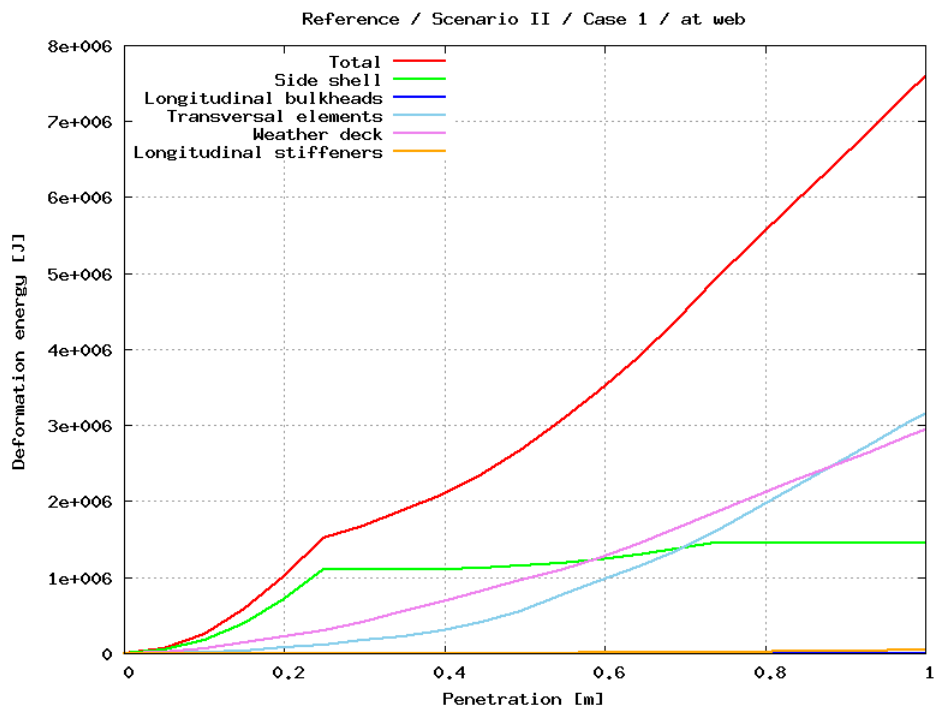


Figure 98: Scenario I, Case 1 - at web

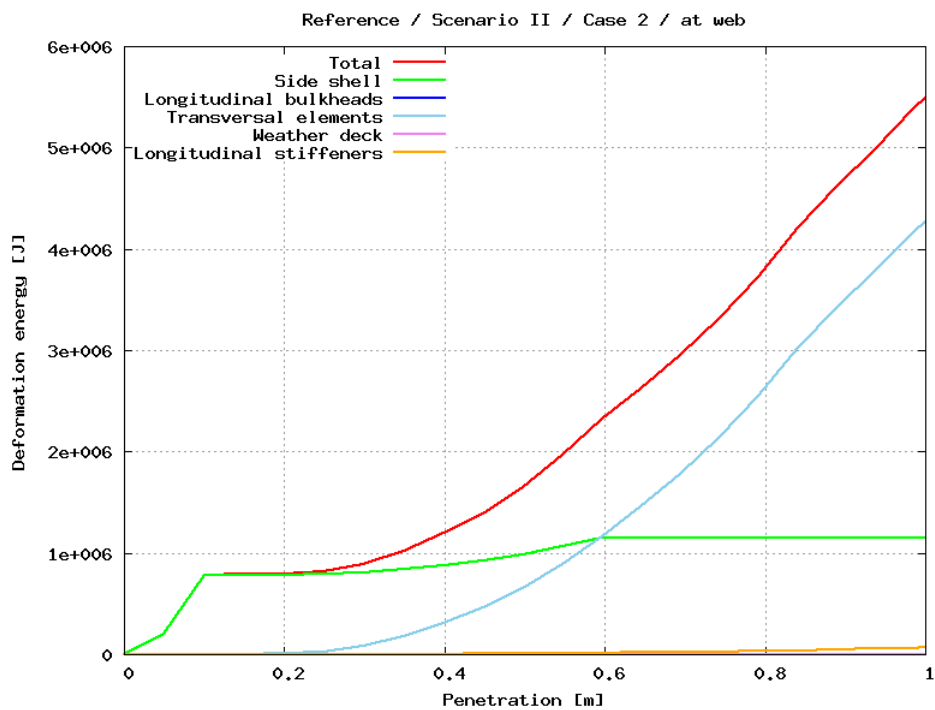


Figure 99: Scenario I / Case 2 / at web

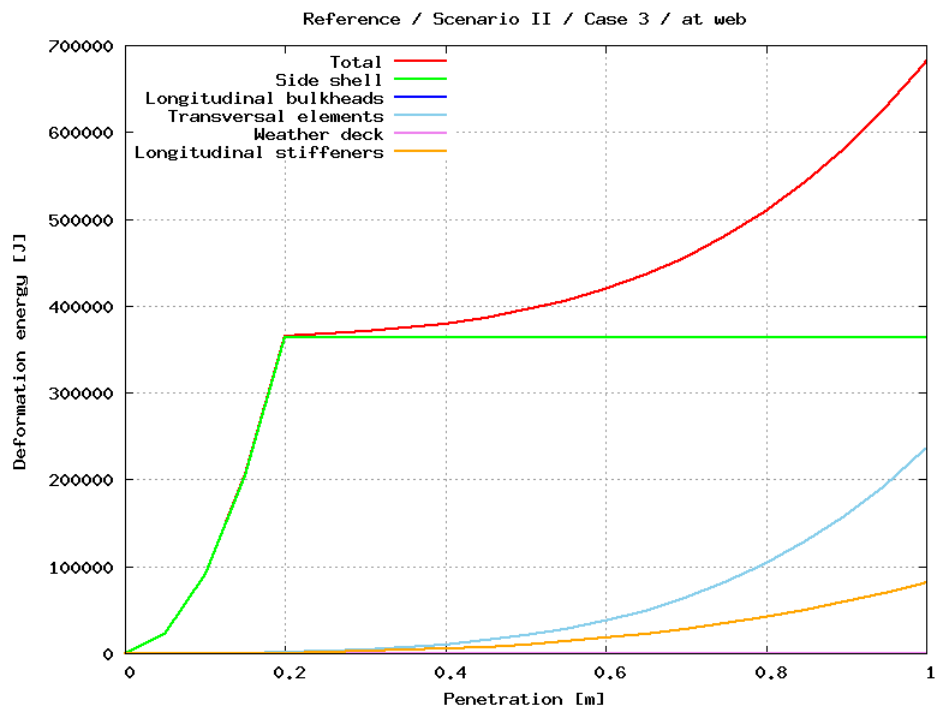


Figure 100: Scenario I / Case 3 / at web

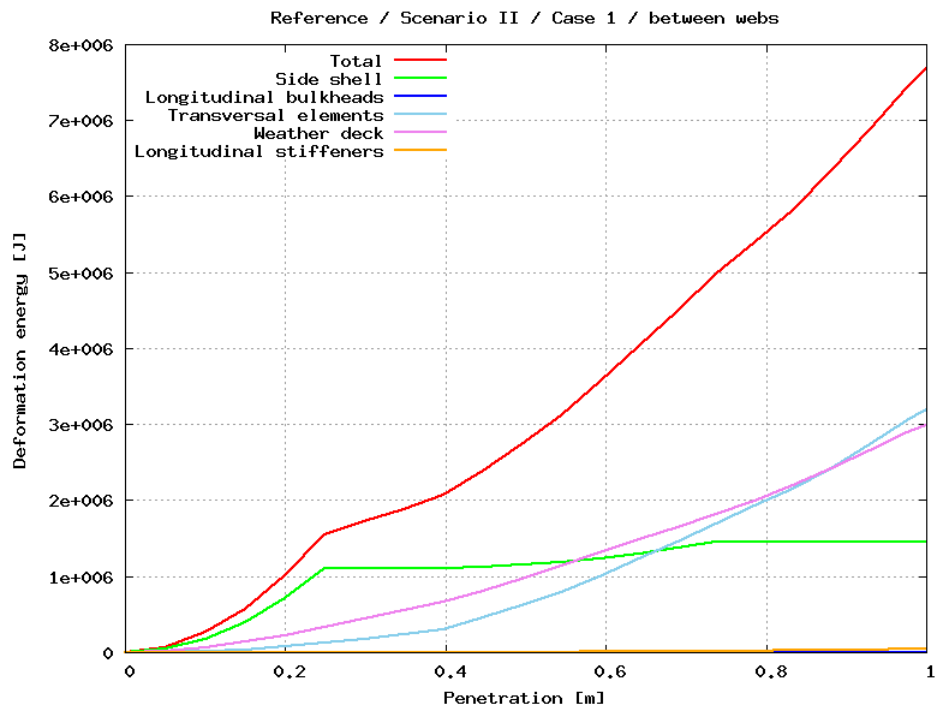


Figure 101: Scenario I, Case 1 - between webs

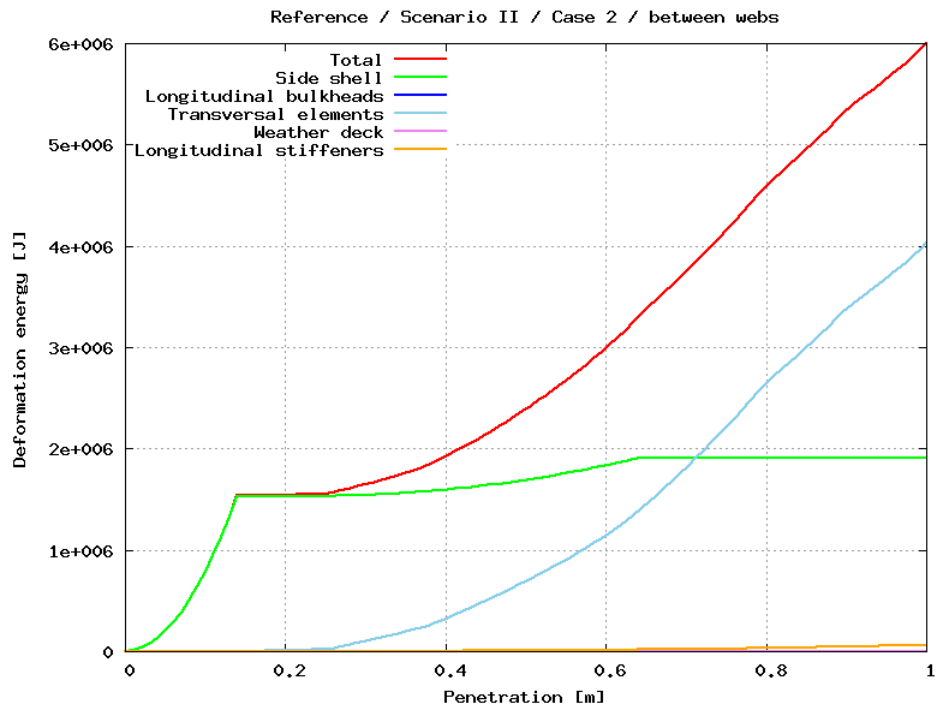


Figure 102: Scenario I / Case 2 / between webs

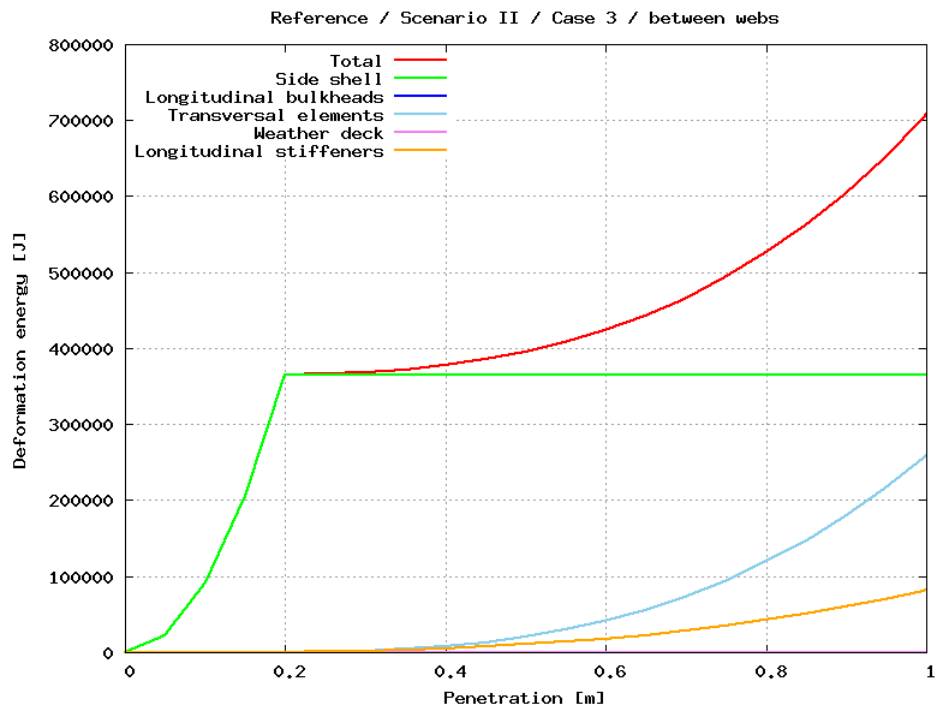


Figure 103: Scenario I / Case 3 / between webs

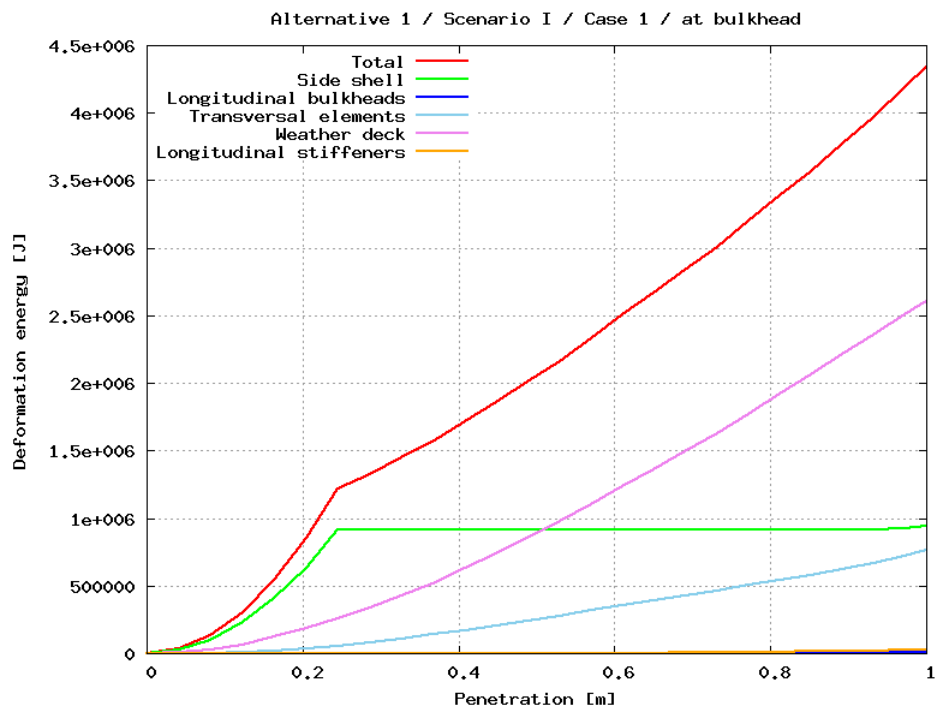


Figure 104: Scenario I, Case 1 - at bulkhead

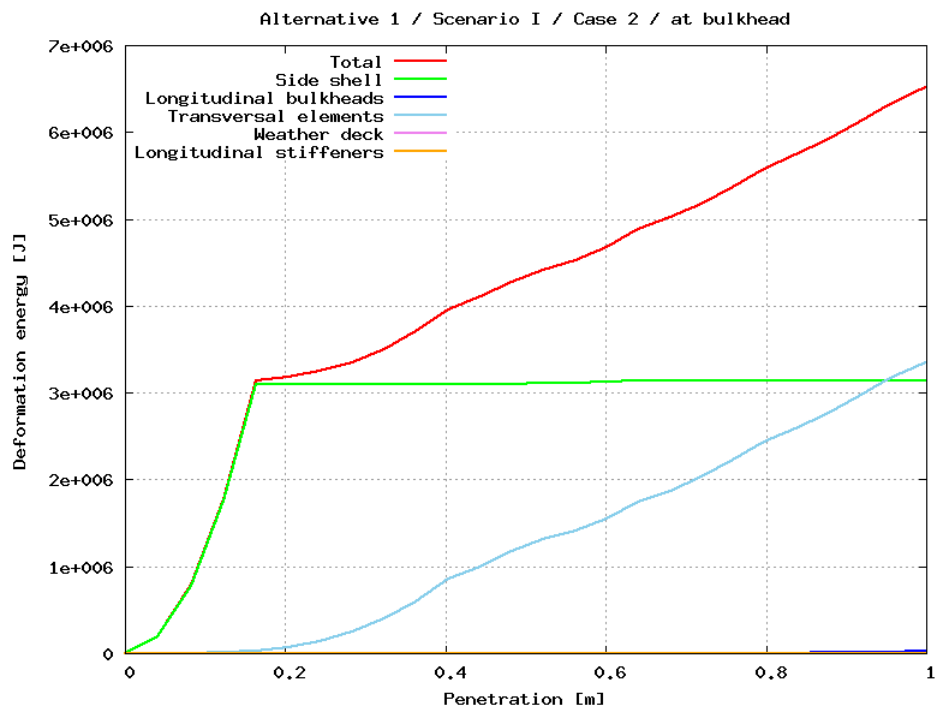


Figure 105: Scenario I / Case 2 / at bulkhead

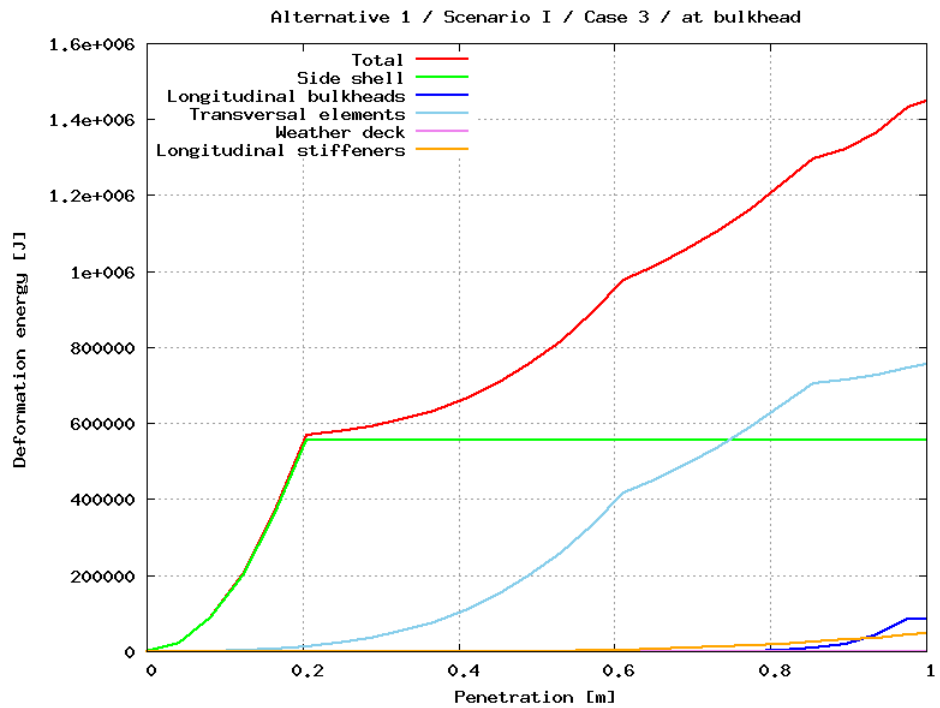


Figure 106: Scenario I / Case 3 / at bulkhead

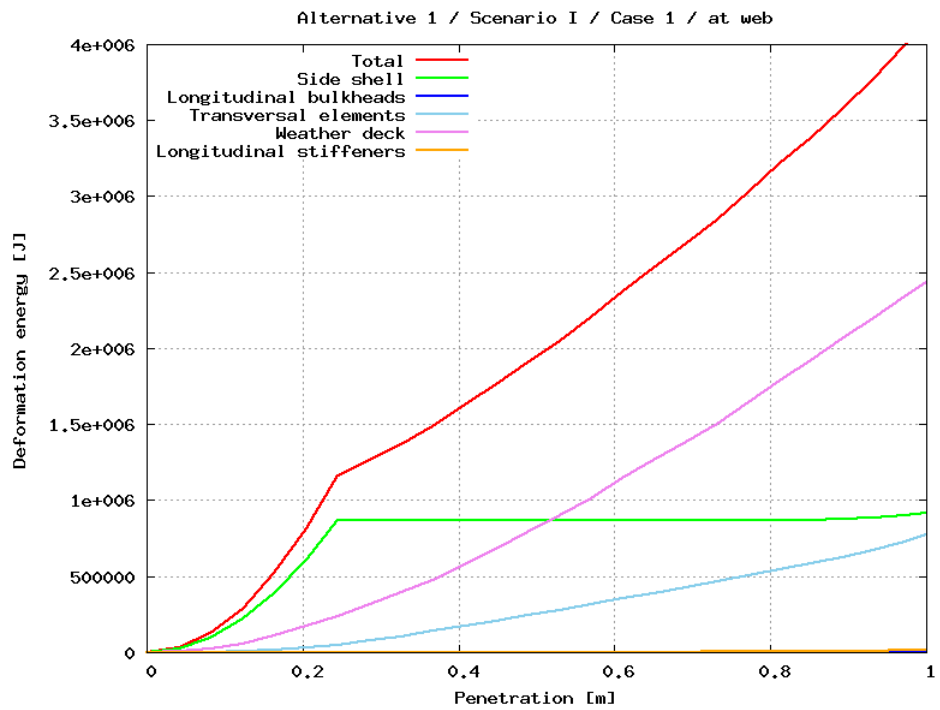


Figure 107: Scenario I, Case 1 - at web

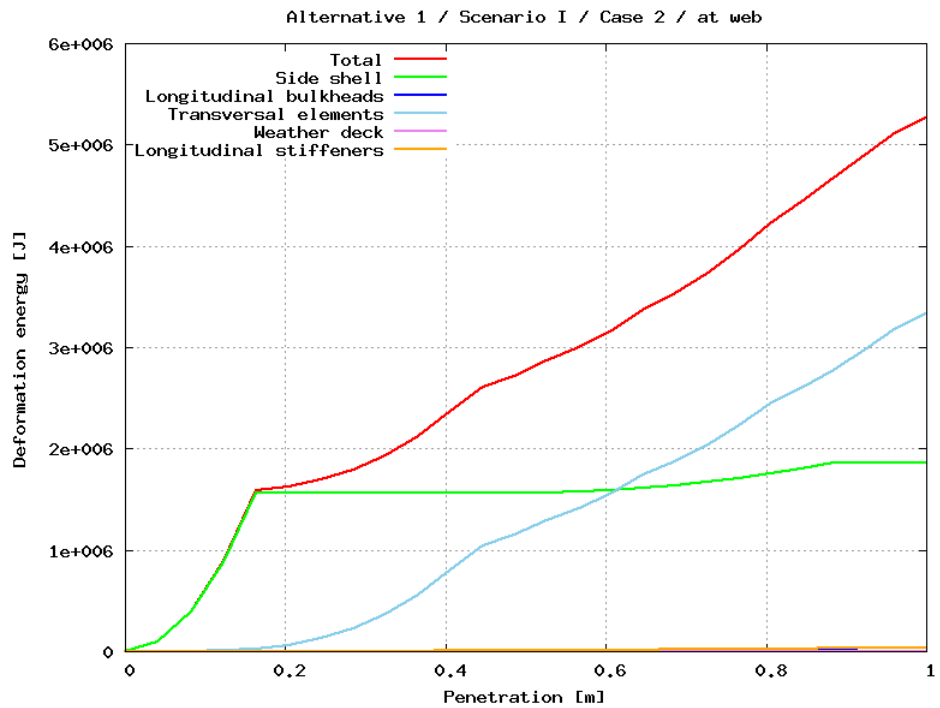


Figure 108: Scenario I / Case 2 / at web

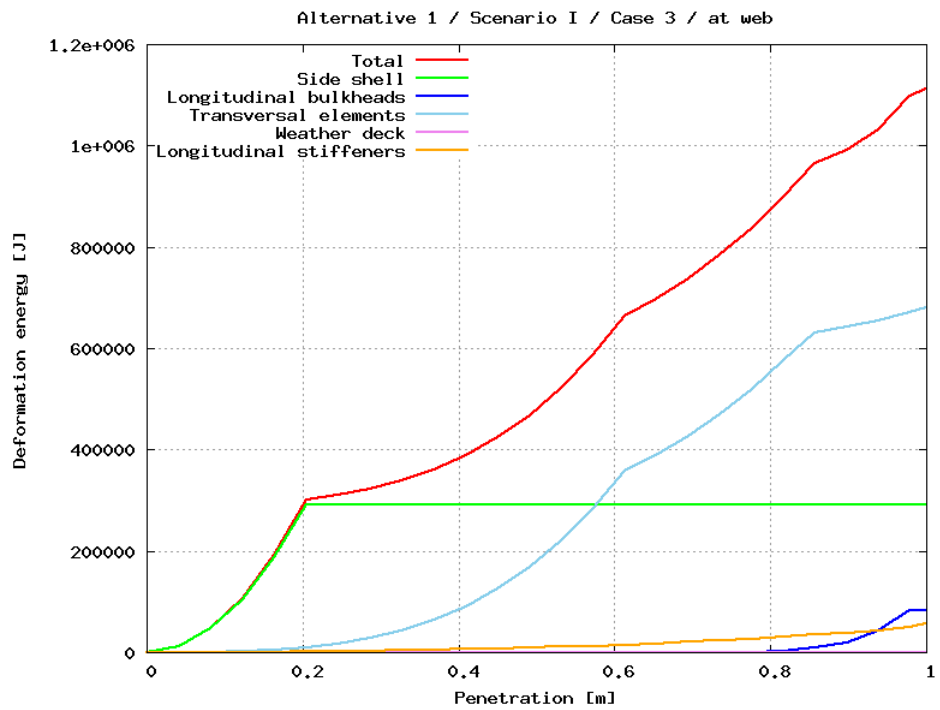


Figure 109: Scenario I / Case 3 / at web

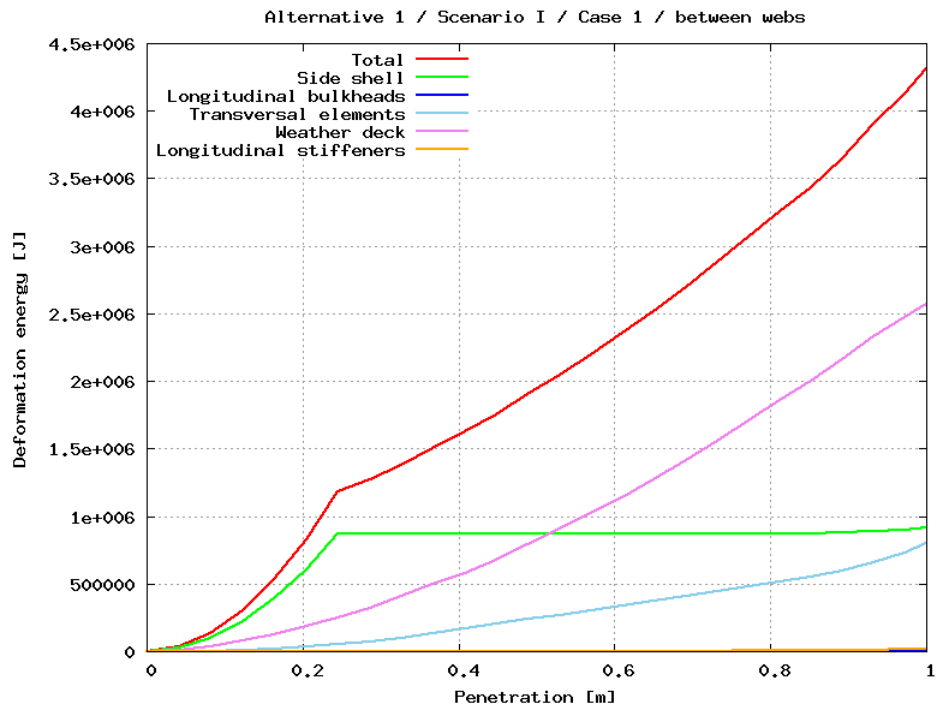


Figure 110: Scenario I, Case 1 - between webs

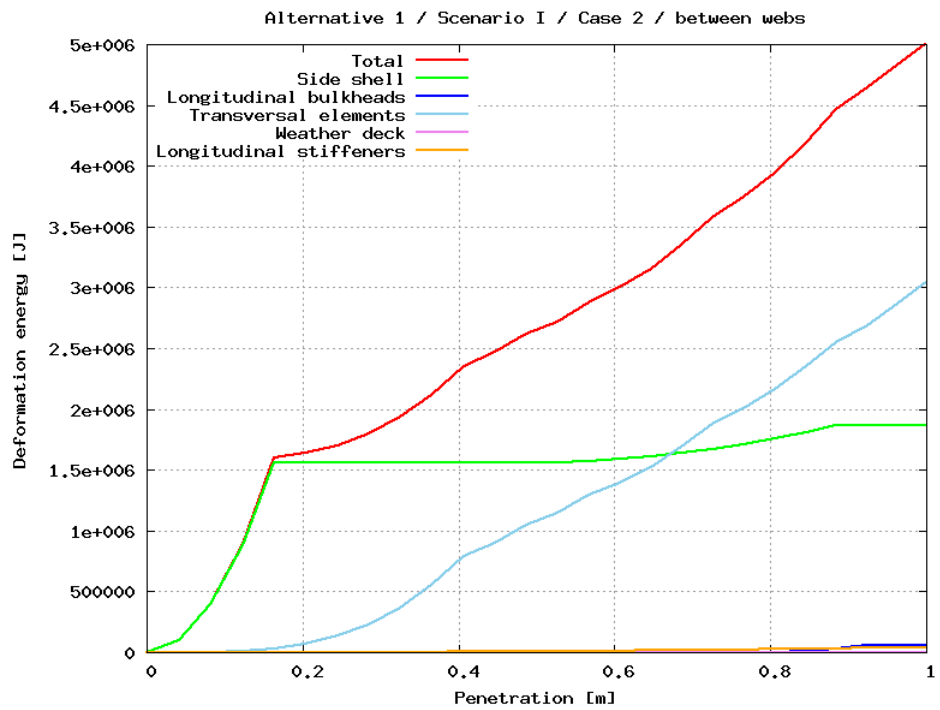


Figure 111: Scenario I / Case 2 / between webs

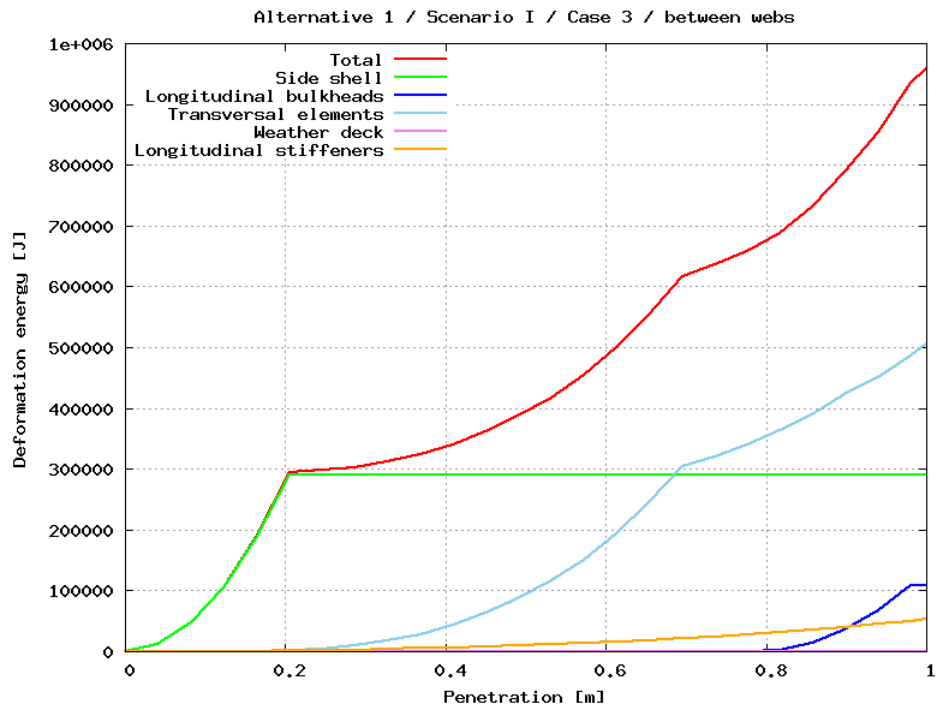


Figure 112: Scenario I / Case 3 / between webs

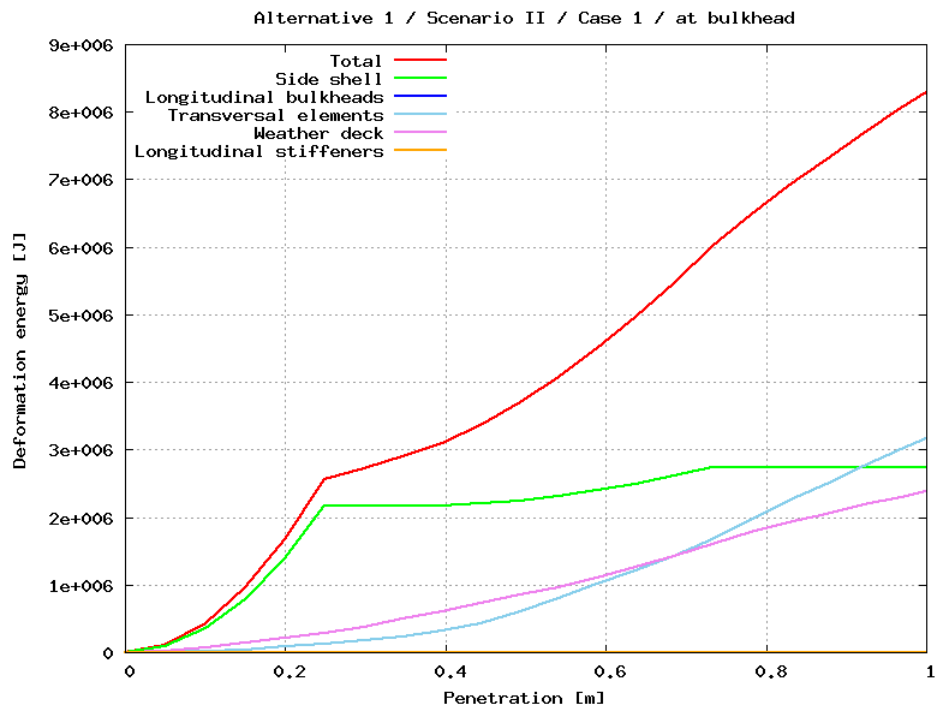


Figure 113: Scenario I, Case 1 - at bulkhead



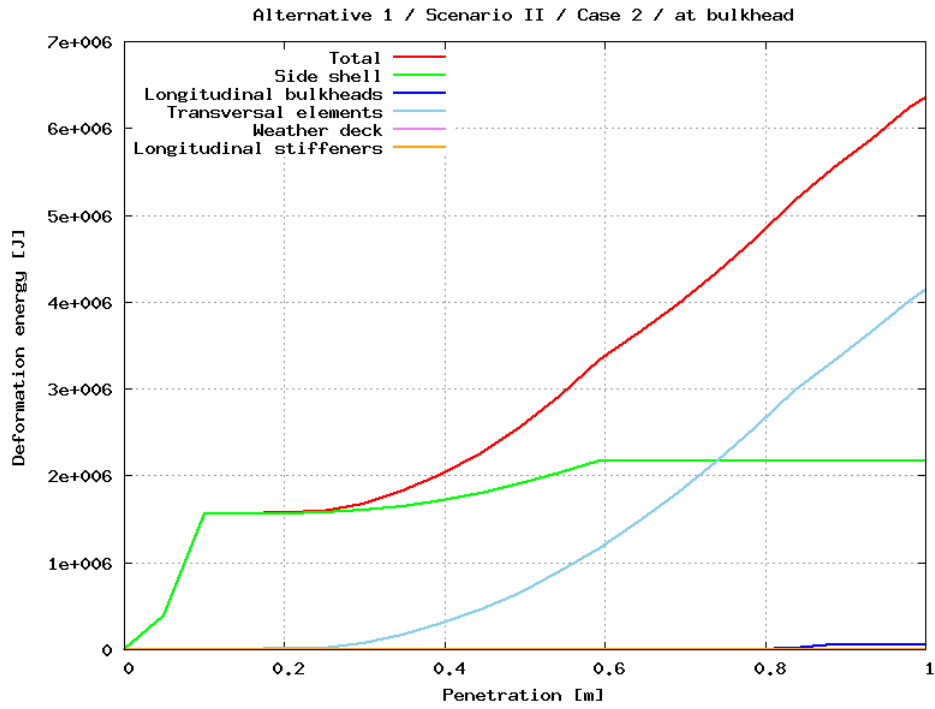


Figure 114: Scenario I / Case 2 / at bulkhead

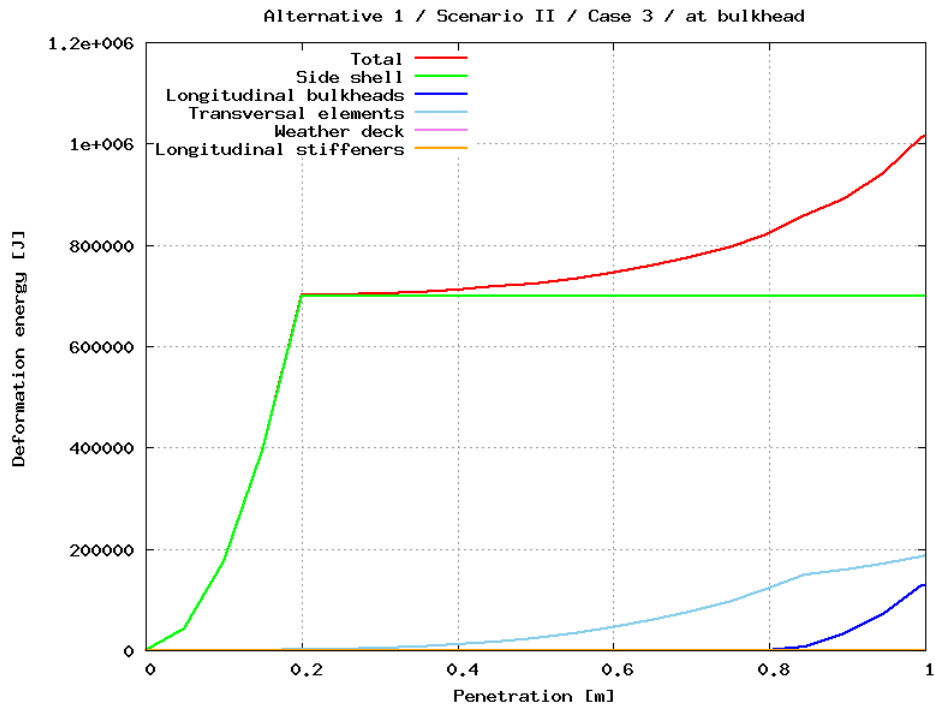


Figure 115: Scenario I / Case 3 / at bulkhead

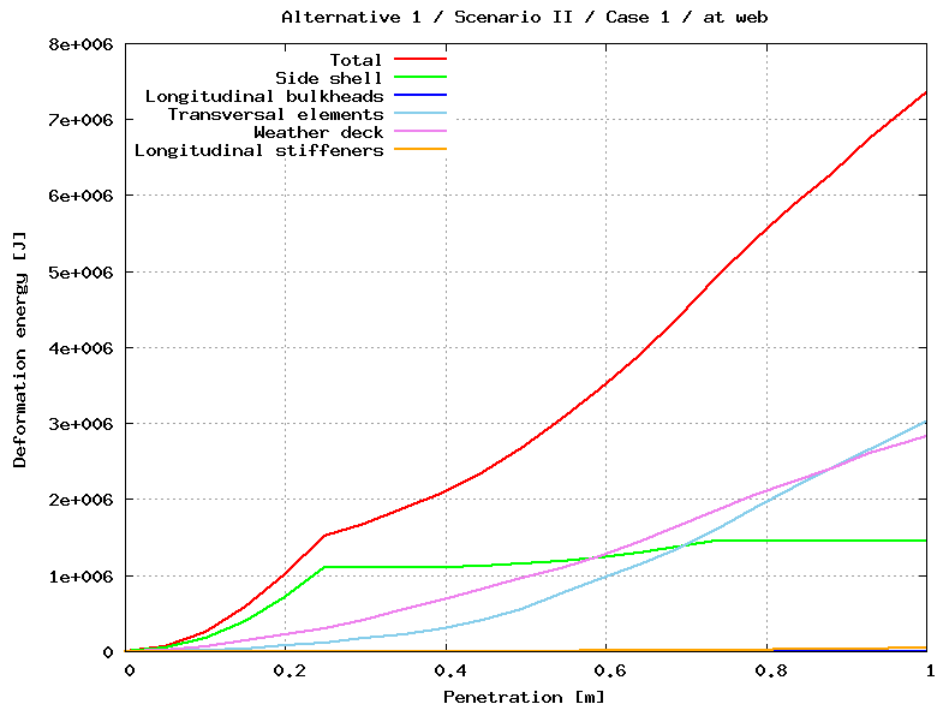


Figure 116: Scenario I, Case 1 - at web

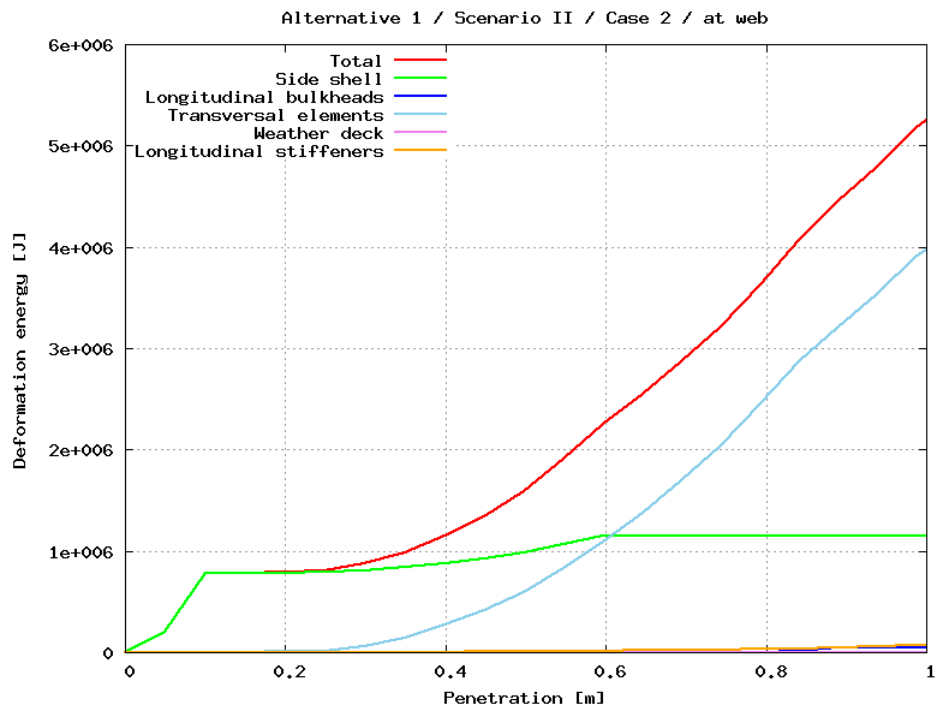


Figure 117: Scenario I / Case 2 / at web

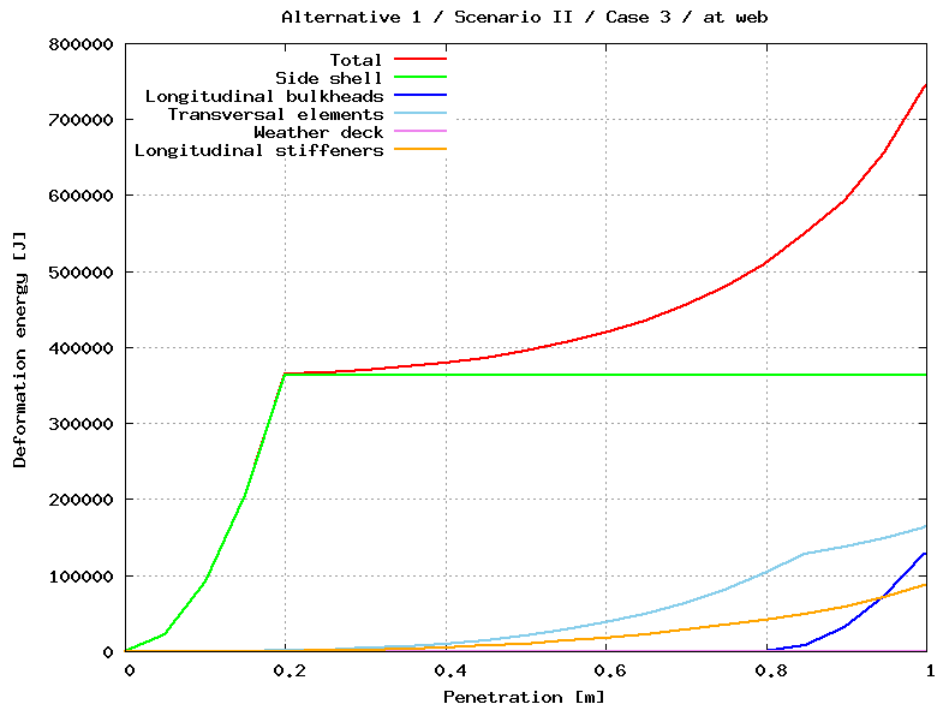


Figure 118: Scenario I / Case 3 / at web

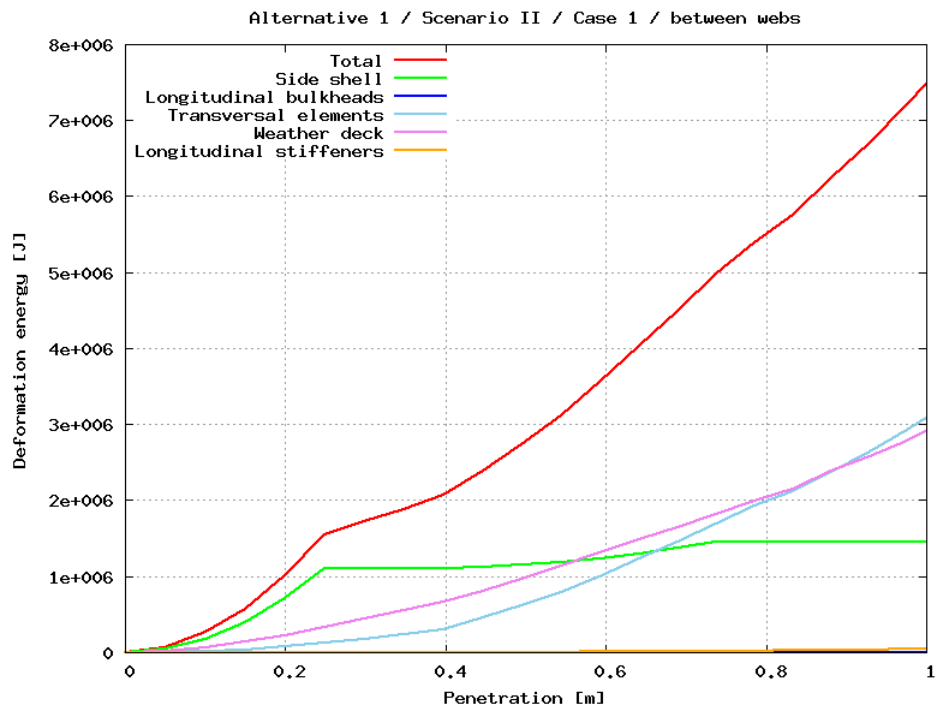


Figure 119: Scenario I, Case 1 - between webs

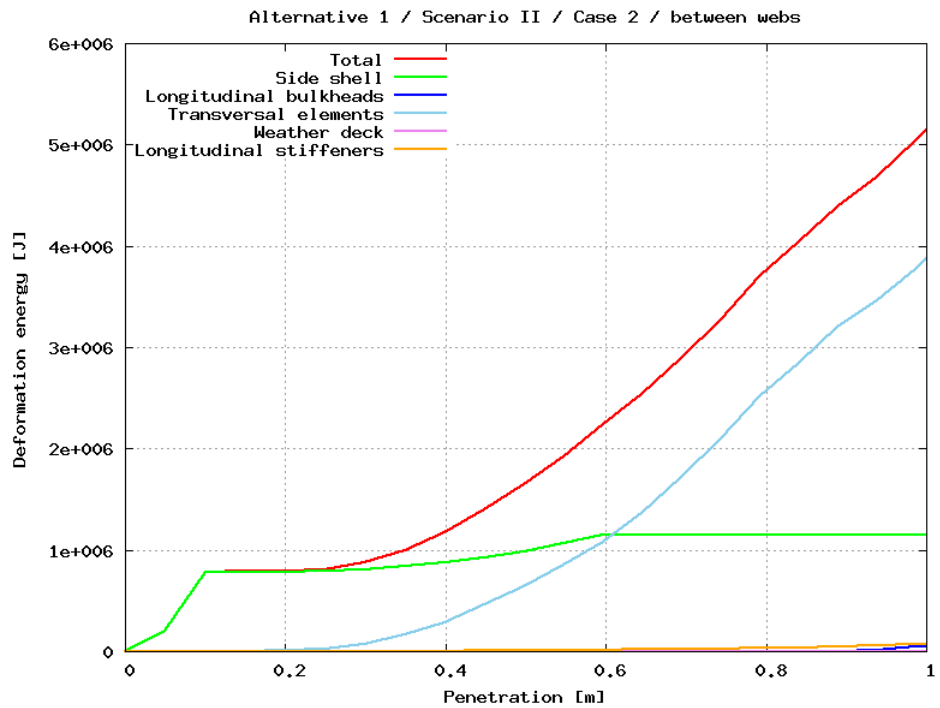


Figure 120: Scenario I / Case 2 / between webs

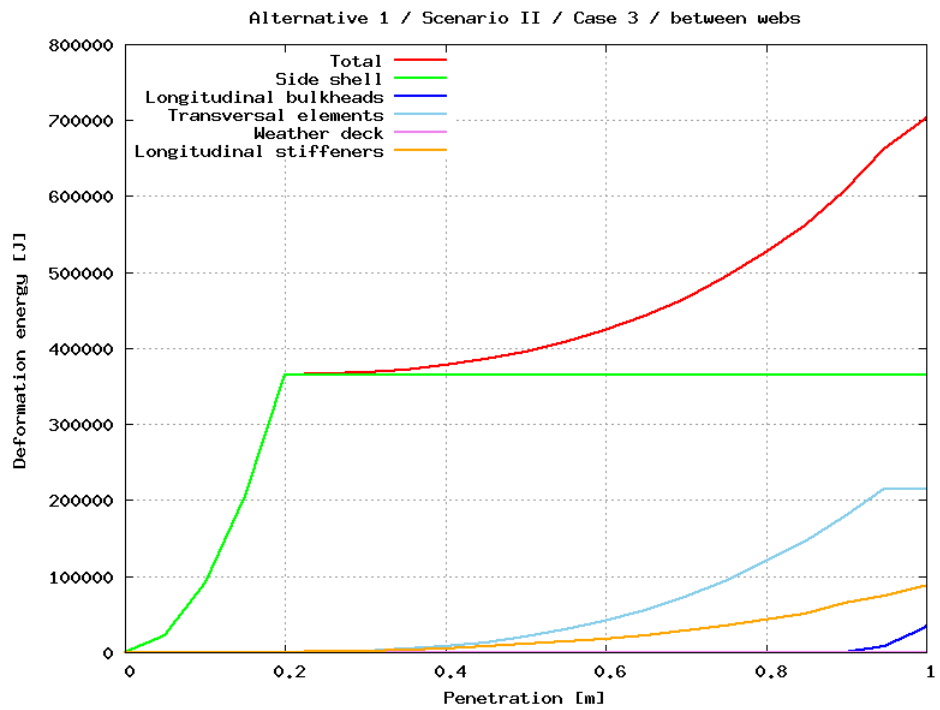


Figure 121: Scenario I / Case 3 / between webs

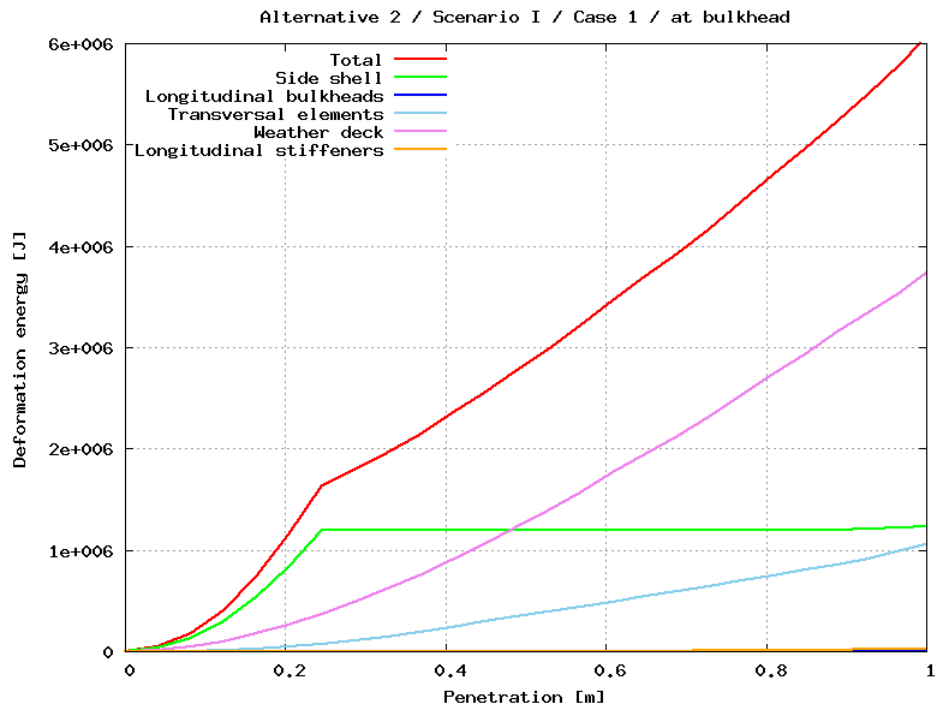


Figure 122: Scenario I, Case 1 - at bulkhead

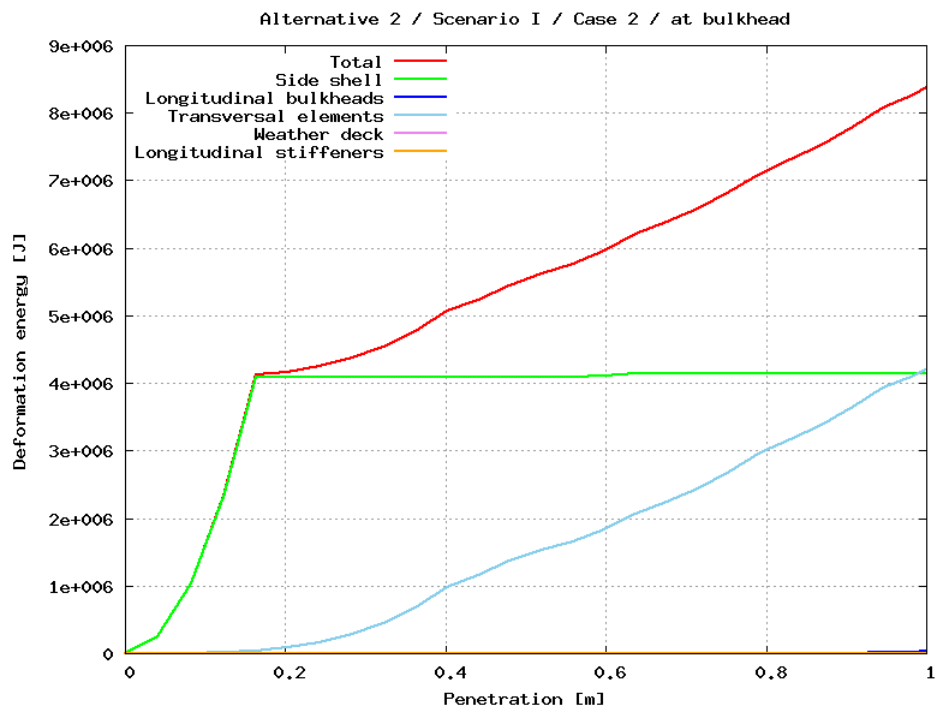


Figure 123: Scenario I / Case 2 / at bulkhead

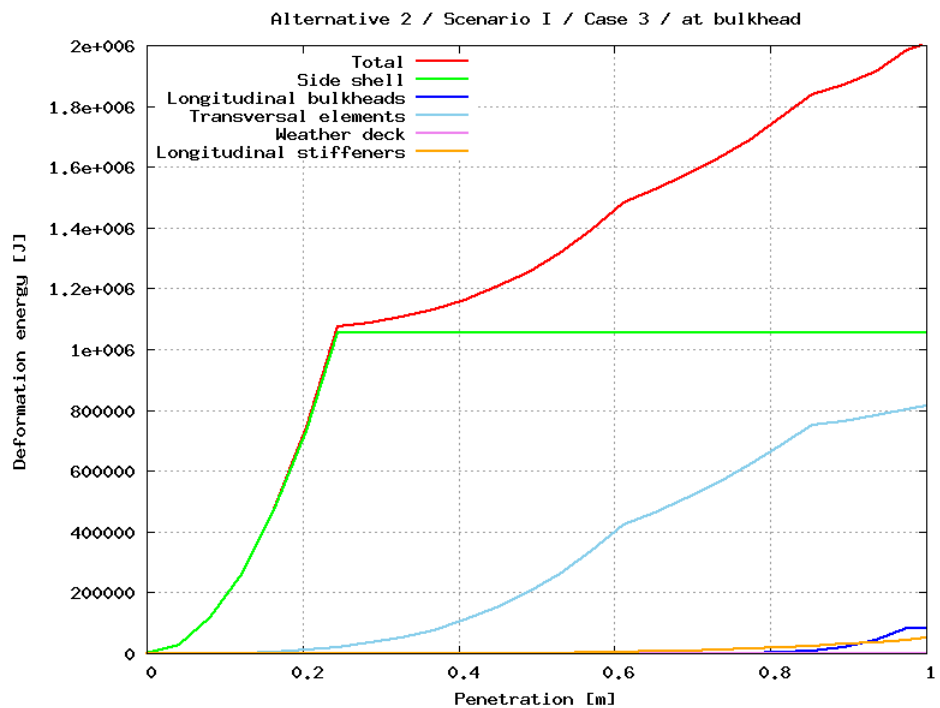


Figure 124: Scenario I / Case 3 / at bulkhead

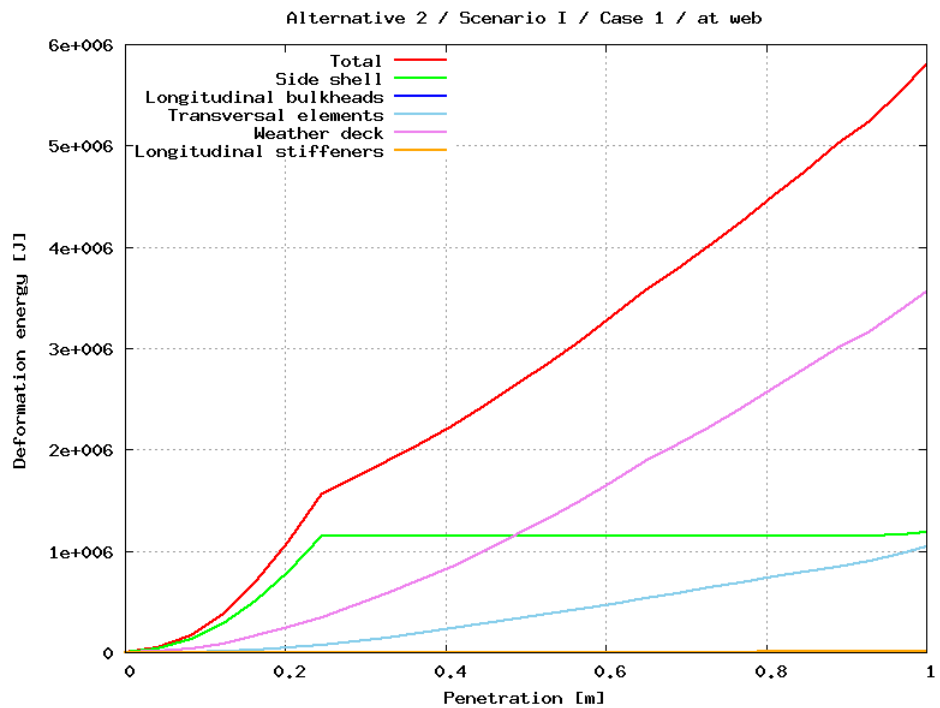


Figure 125: Scenario I, Case 1 - at web

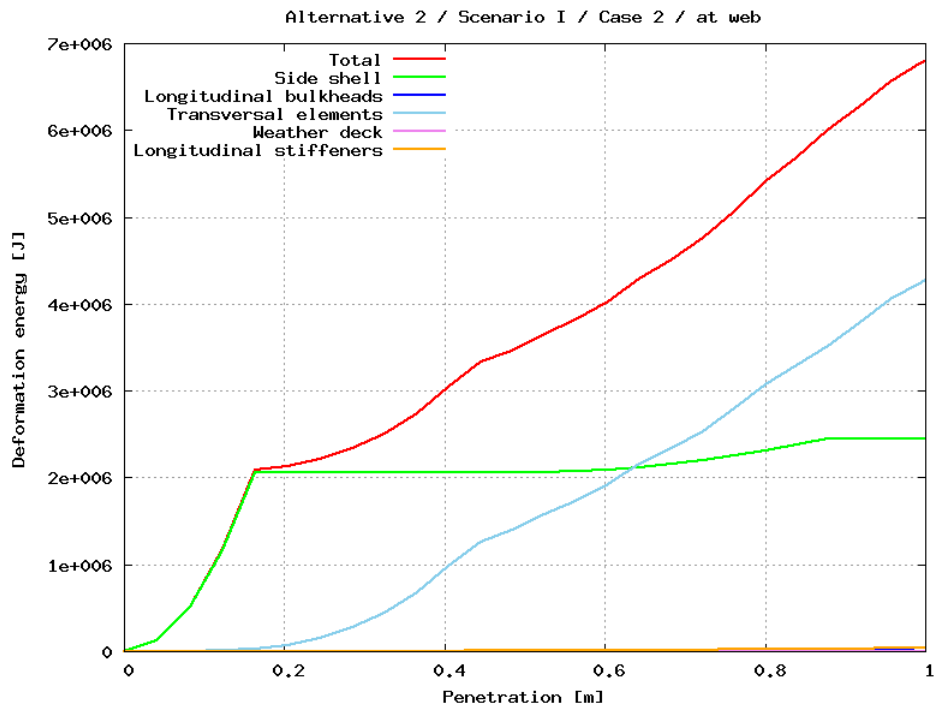


Figure 126: Scenario I / Case 2 / at web

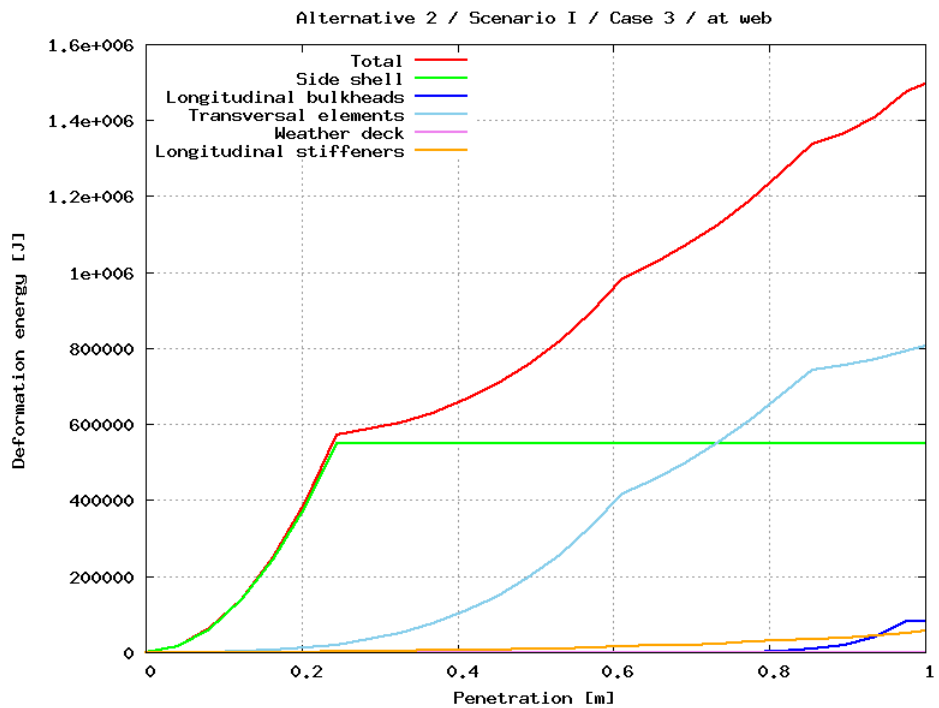


Figure 127: Scenario I / Case 3 / at web

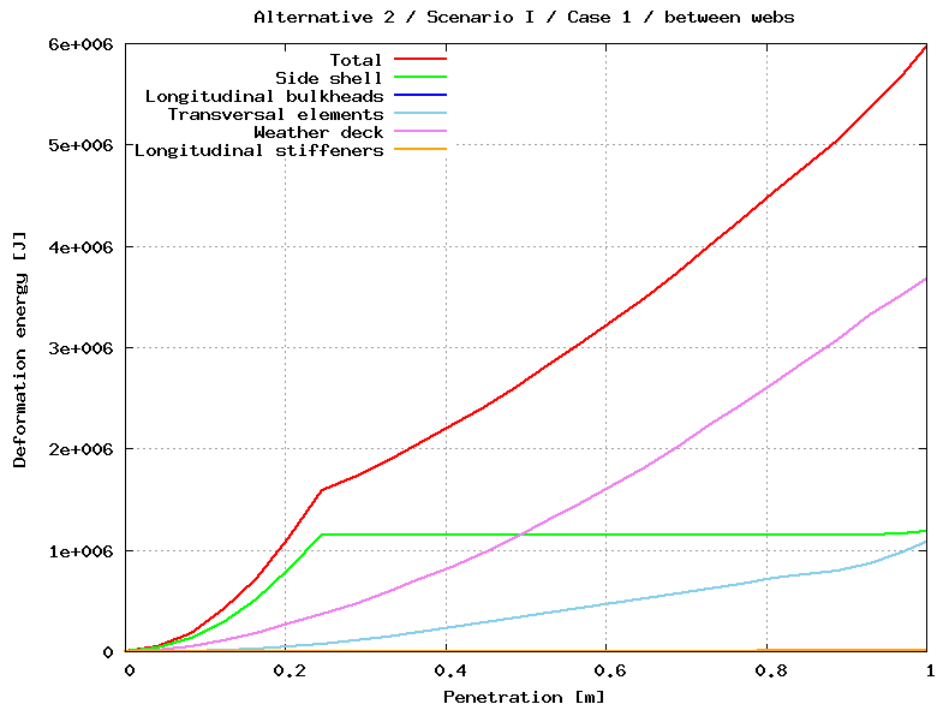


Figure 128: Scenario I, Case 1 - between webs

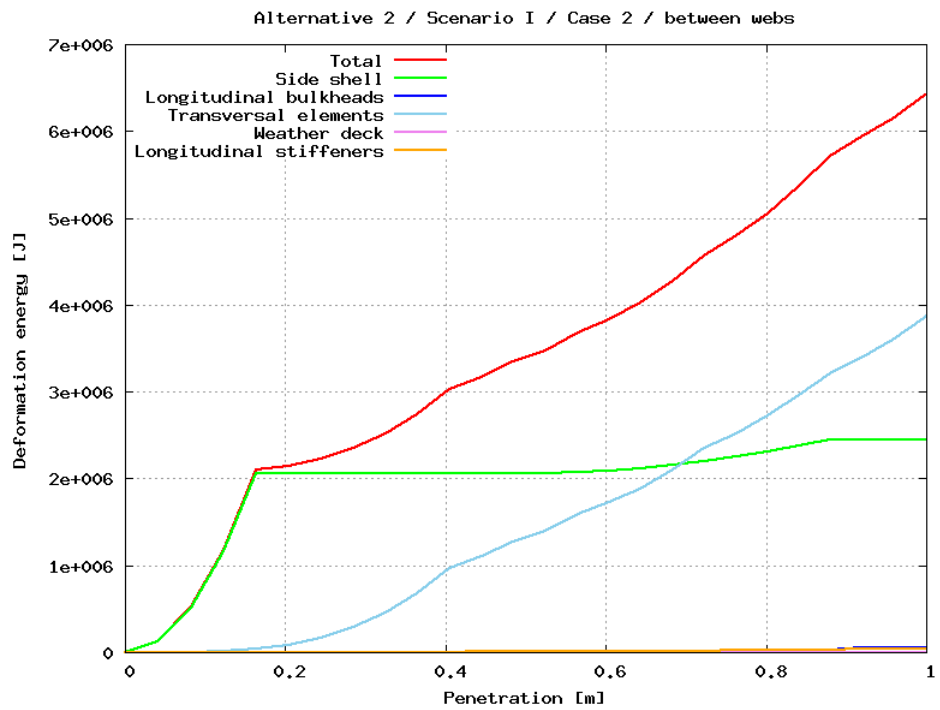


Figure 129: Scenario I / Case 2 / between webs



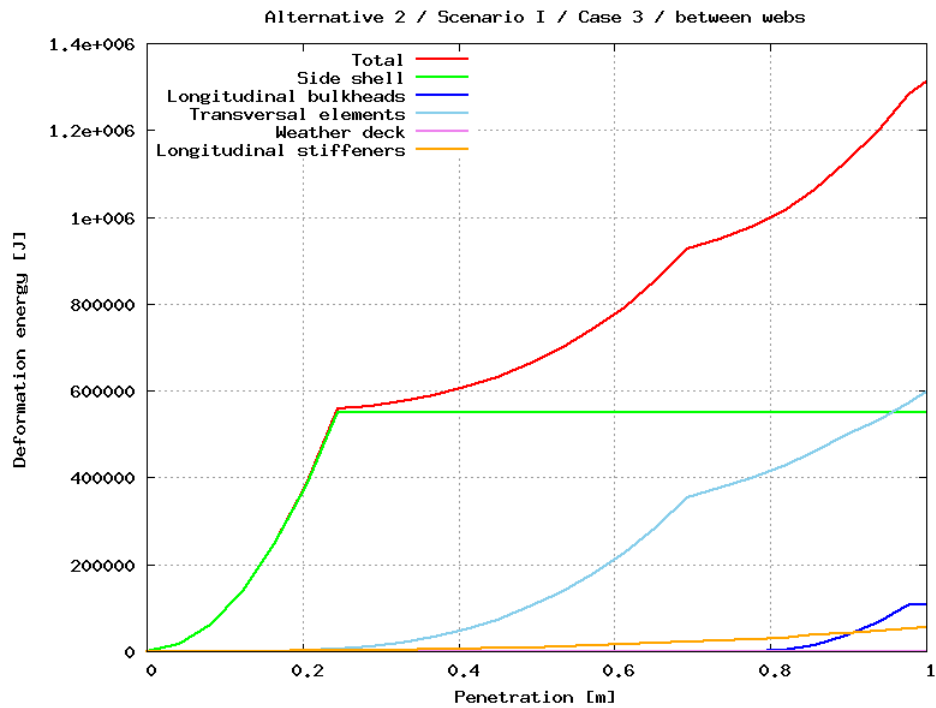


Figure 130: Scenario I / Case 3 / between webs

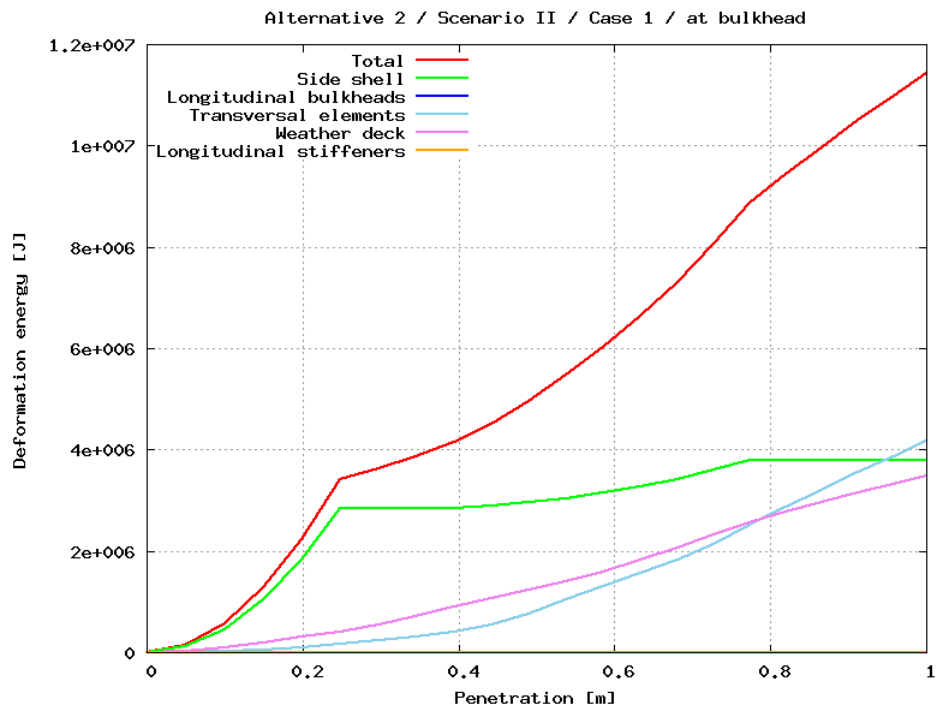


Figure 131: Scenario I, Case 1 - at bulkhead

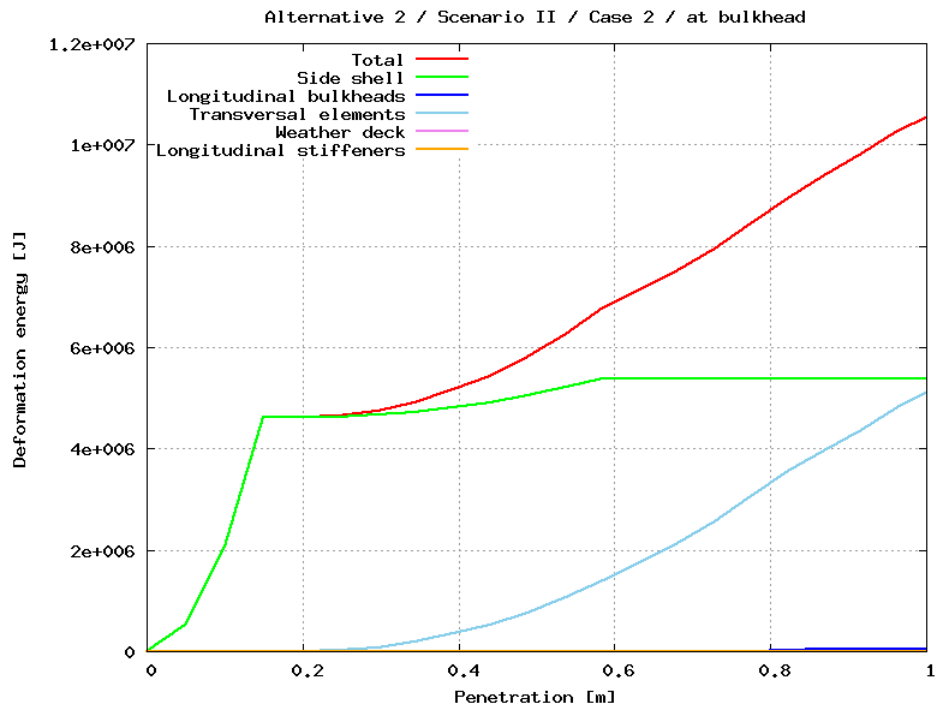


Figure 132: Scenario I / Case 2 / at bulkhead

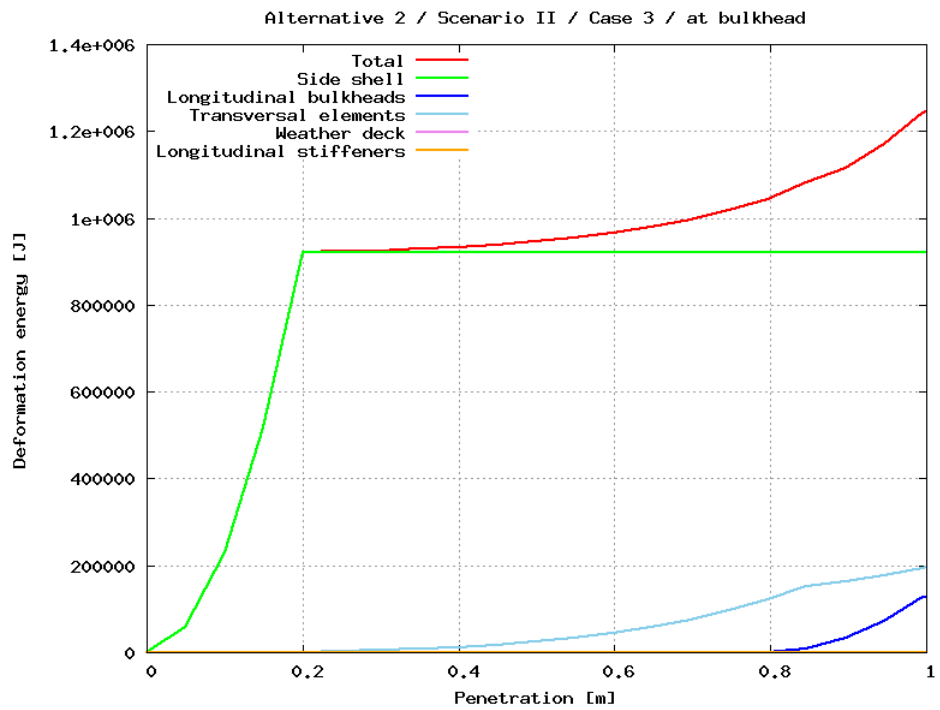


Figure 133: Scenario I / Case 3 / at bulkhead

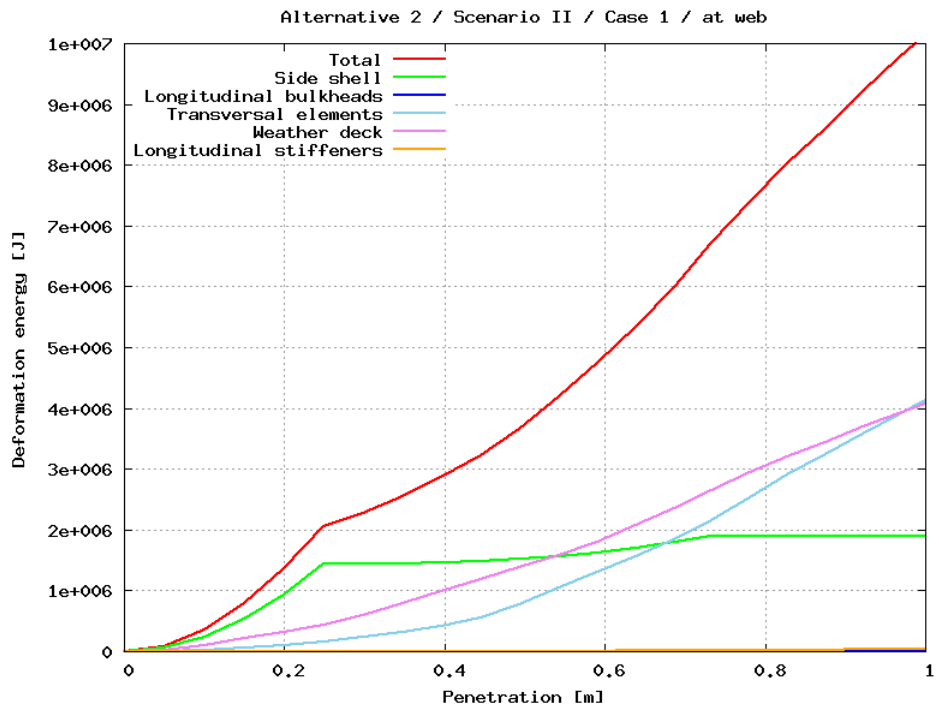


Figure 134: Scenario I, Case 1 - at web

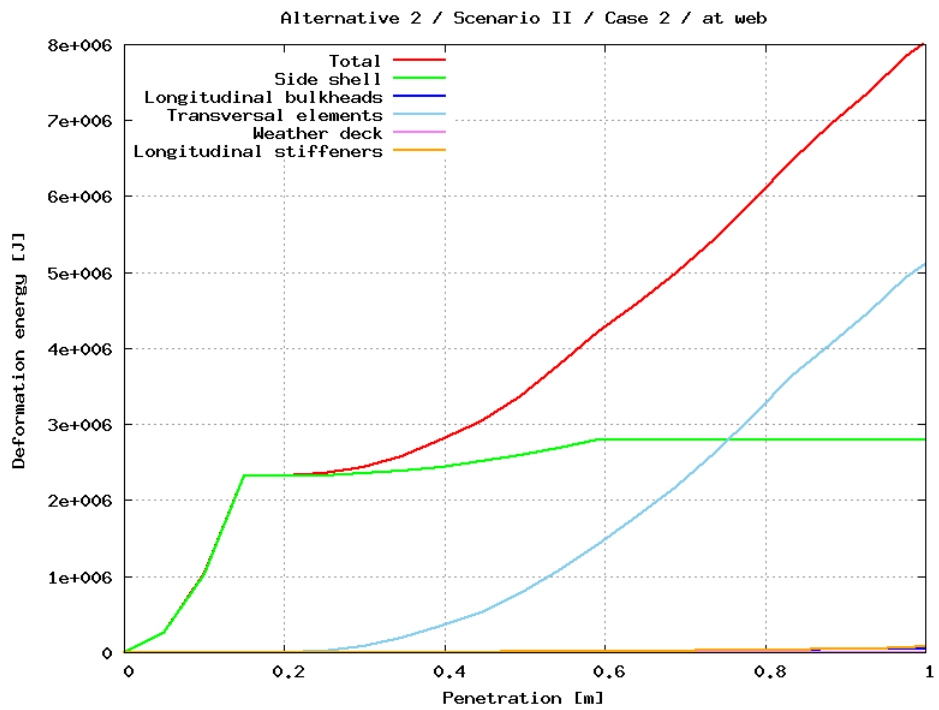


Figure 135: Scenario I / Case 2 / at web

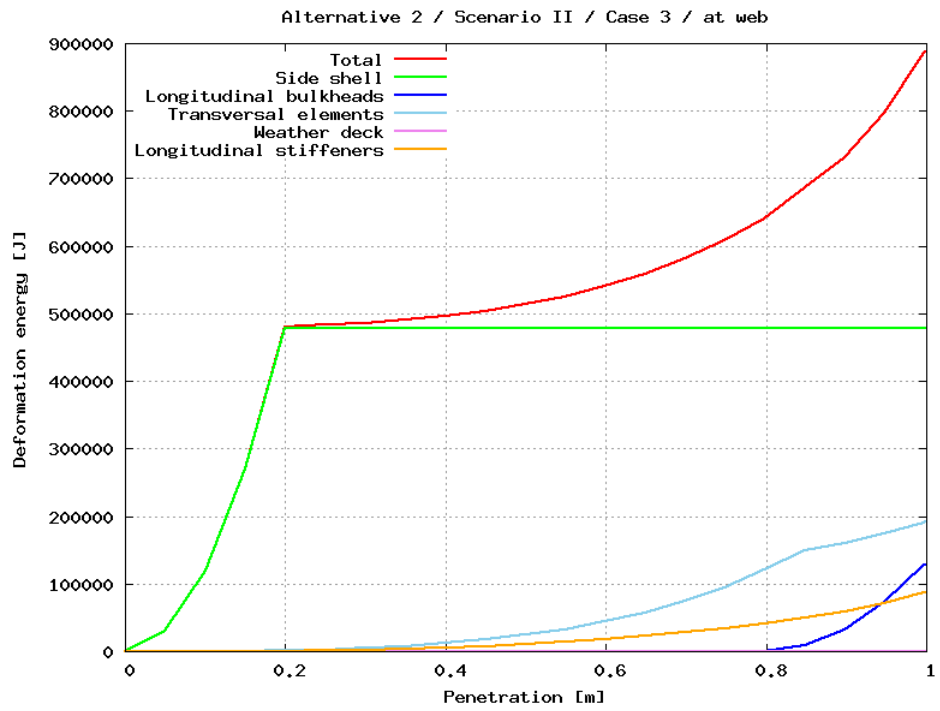


Figure 136: Scenario I / Case 3 / at web

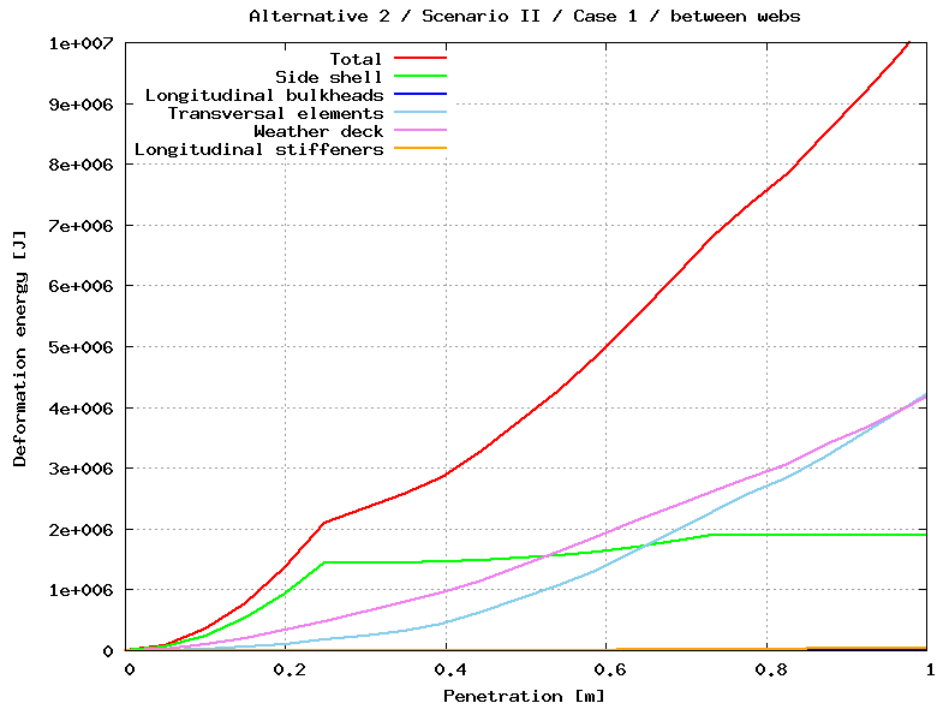


Figure 137: Scenario I, Case 1 - between webs

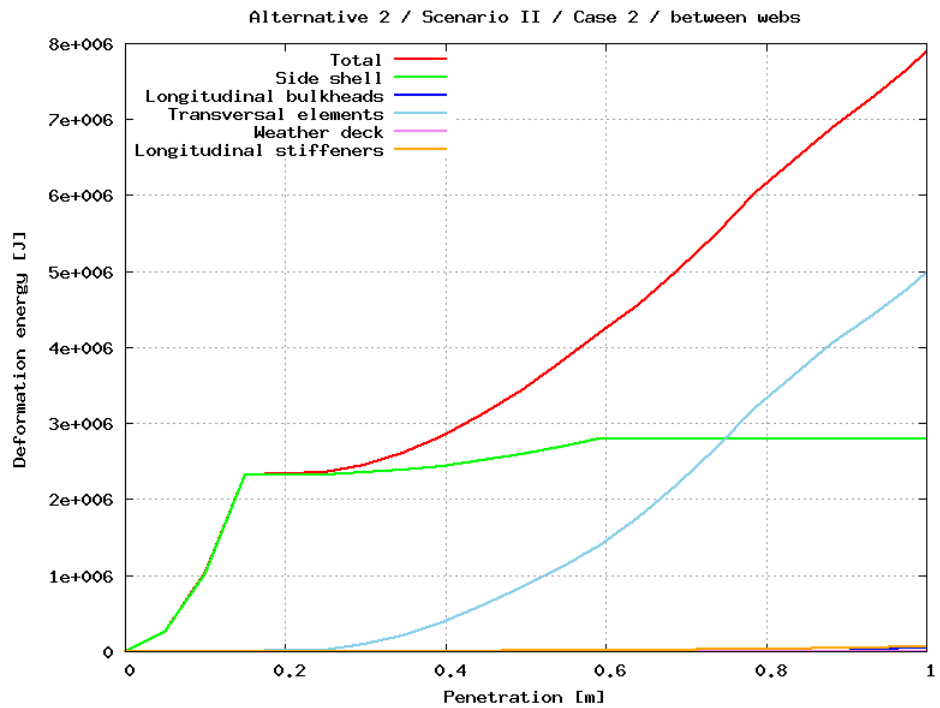


Figure 138: Scenario I / Case 2 / between webs

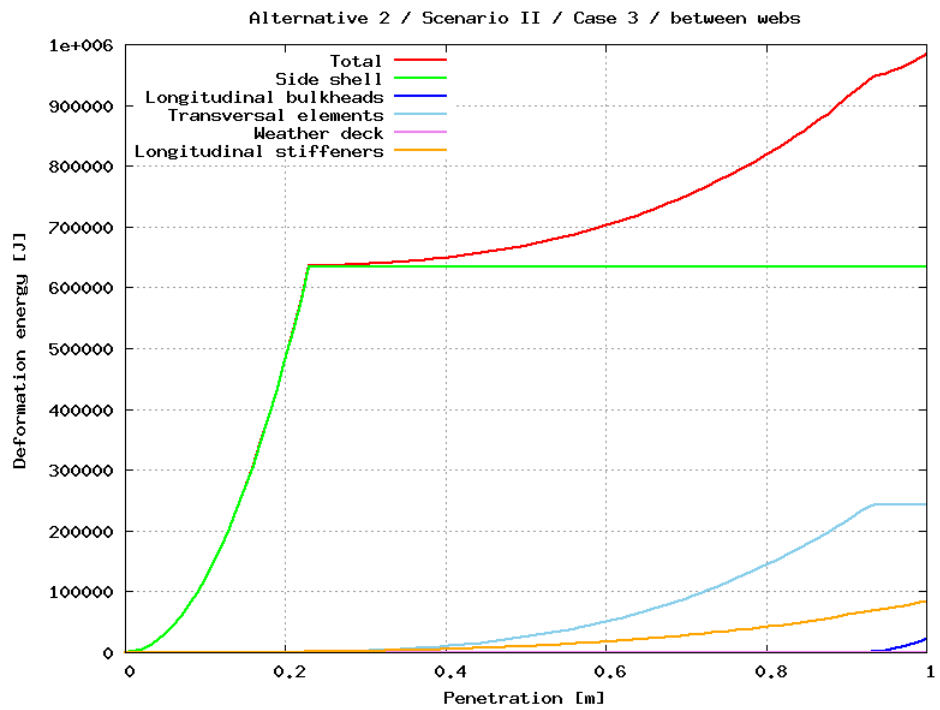


Figure 139: Scenario I / Case 3 / between webs

## **C APPENDIX: EQUIVALENT THICKNESS FOR THE PLATINGS WITH HOLES**

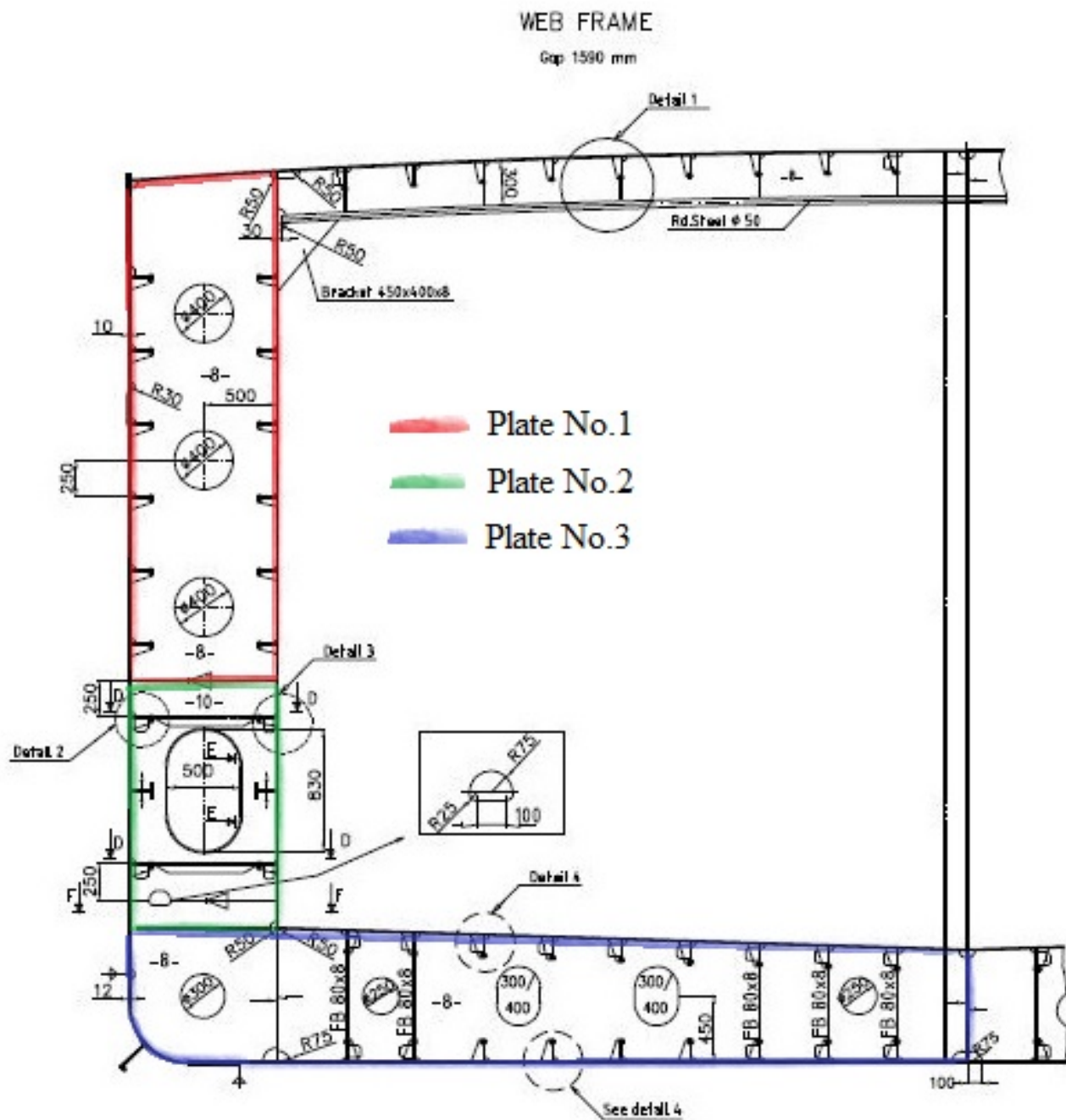


Figure 140: Web frame section

Table 34: Equivalent thickness calculations for web frame  
**Conventional structure** **Reinforced structure**

<b>Plate No. 1</b>			<b>Plate No. 1</b>		
t_actual	6.40	mm	t_actual	8.00	mm
A_gross	3400000	mm <sup>2</sup>	A_gross	3400000	mm <sup>2</sup>
A_hole	376991	mm <sup>2</sup>	A_hole	376991	mm <sup>2</sup>
A_net	3023009	mm <sup>2</sup>	A_net	3023009	mm <sup>2</sup>
<b>Plate No. 2</b>			<b>Plate No. 2</b>		
t_actual	8.00	mm	t_actual	8.00	mm
A_gross	1450000	mm <sup>2</sup>	A_gross	1450000	mm <sup>2</sup>
A_hole	361350	mm <sup>2</sup>	A_hole	361350	mm <sup>2</sup>
A_net	1088650	mm <sup>2</sup>	A_net	1088650	mm <sup>2</sup>
<b>Joint Plate No. 1-2 (web)</b>			<b>Joint Plate No. 1-2 (web)</b>		
t_eq (No. 1 &2)	<b>5.785</b>	mm	t_eq (No. 1 &2)	<b>6.782</b>	mm
<b>Plate No. 3</b>			<b>Plate No. 3</b>		
t_actual	6.40	mm	t_actual	6.40	mm
A_gross	5187000	mm <sup>2</sup>	A_gross	5187000	mm <sup>2</sup>
A_hole	370232	mm <sup>2</sup>	A_hole	370232	mm <sup>2</sup>
A_net	4816768	mm <sup>2</sup>	A_net	4816768	mm <sup>2</sup>
A_net/A_gross	0.929		A_net/A_gross	0.929	
t_eq	<b>5.943</b>	mm	t_eq	<b>5.943</b>	mm

Plate No.1 and No.2 are merged into one plating in order to model the web as a single element in SHARP.



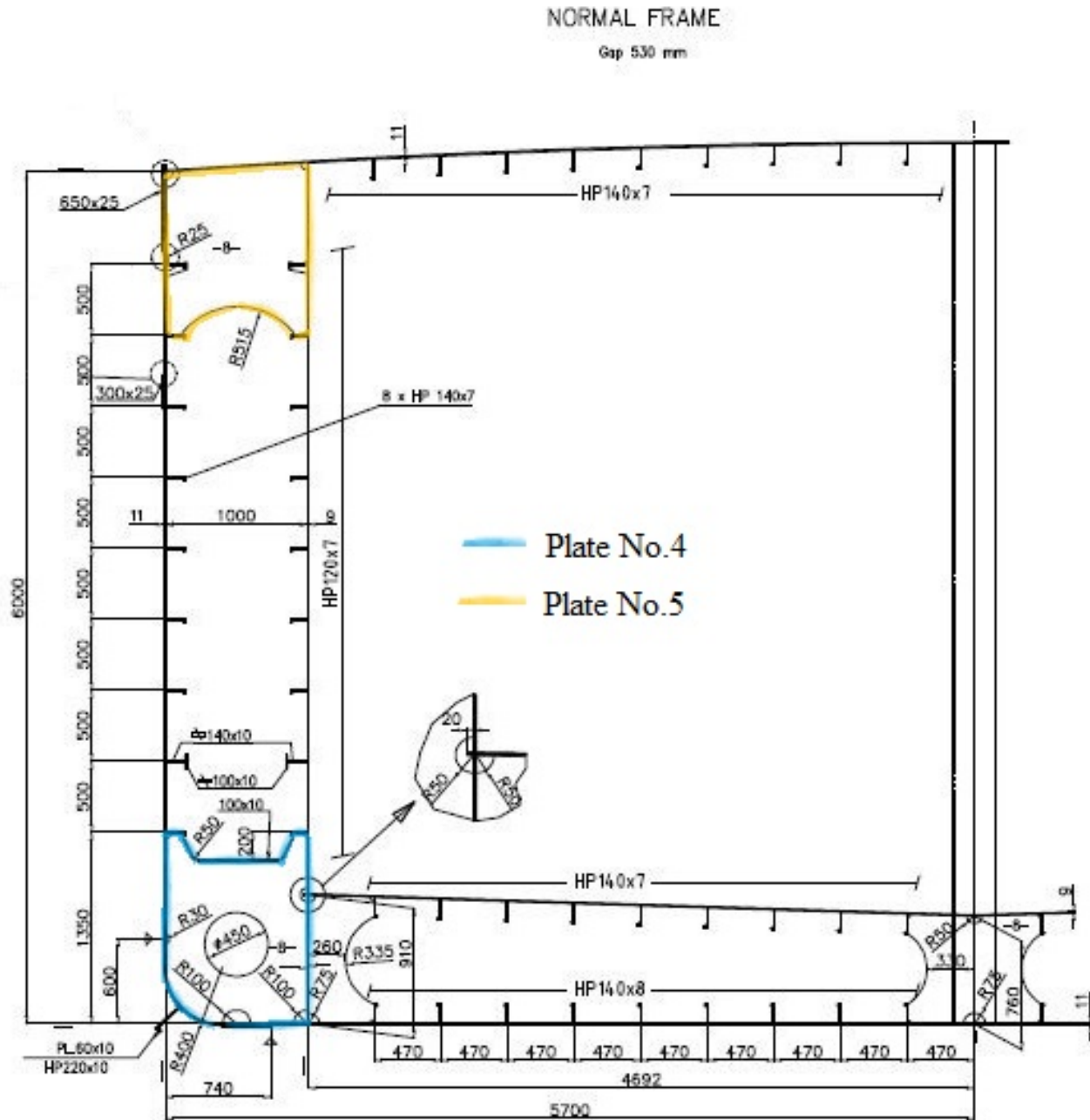


Figure 141: Ordinary frame section

Table 35: Equivalent thickness calculations for ordinary frame  
**Conventional structure**                      **Reinforced structure**

**Plate No. 4**

t_actual	6.40	mm
A_gross	1150000	mm <sup>2</sup>
A_hole	159043	mm <sup>2</sup>
A_net	990957	mm <sup>2</sup>
A_net/A_gross	0.862	
t_eq	<b>5.515</b>	mm

**Plate No. 4**

t_actual	6.40	mm
A_gross	1150000	mm <sup>2</sup>
A_hole	159043	mm <sup>2</sup>
A_net	990957	mm <sup>2</sup>
A_net/A_gross	0.862	
t_eq	<b>5.515</b>	mm

**Plate No. 5**

t_actual	<b>6.400</b>	mm
----------	--------------	----

**Plate No. 5**

t_actual	<b>7.600</b>	mm
----------	--------------	----

## **D APPENDIX: VBA CODES FOR .MCO FILES**

---

```
1 ' --- Create matrices in an excel sheet from HydroStar output ---
2
3 Sub LoadFiles_all()
4
5 Dim myFile, URL, text, row, textline, posLat, posLong As Integer
6 Dim fileNameN, FolderName, directory, info As String
7
8 directory = pickFolder()
9
10 'File name styles
11 Dim fileTypes(1 To 2) As String
12 fileTypes(1) = "ADM_0_"
13 fileTypes(2) = "DMP_0_"
14
15 row = 2 'Row to add the info
16
17 'Loop between different file name styles
18 For fileNameN = 1 To 2
19 fileN = 1
20 'Loop through the file names
21 While fileN <= 66
22 'Error handling to avoid missing file names:
23 errorH:
24 If Err.Number = 53 Then
25 Resume 1
26 ElseIf Err.Number <> 0 Then
27 Err.Raise Err.Number
28 End If
29
30 'Creating the file name
31 myFile = fileTypes(fileNameN) & fileN & ".DAT"
32 URL = directory & myFile
33
34 On Error GoTo errorH
35 Open URL For Input As #1
36
37 Do Until EOF(1)
38 Line Input #1, textline
```

```
39 If InStr(textline, "#") = 0 Then
40 col = 2
41 Do Until InStr(textline, " ") = 0
42 Cells(row, 1) = myFile
43 Do Until InStr(textline, " ") > 1 Or InStr(textline, " ") = 0
44 textline = Mid(textline, 2, Len(textline))
45 Loop
46 ind = InStr(textline, " ")
47 If ind = 0 Then ind = Len(textline)
48 info = Mid(textline, 1, ind)
49 Cells(row, col) = info
50 col = col + 1
51 textline = Mid(textline, ind + 1, Len(textline) - ind)
52 Loop
53 row = row + 1
54 End If
55 Loop
56 Close #1
57
58 1:         fileN = fileN + 1
59 Wend
60 Next
61
62 End Sub
63
64 Function pickFolder() As String
65 With Application.FileDialog(msoFileDialogFolderPicker)
66 .AllowMultiSelect = False
67 If .Show = -1 Then
68 pickFolder = .SelectedItem(1) & "\"
69 ' "
70 End If
71 End With
72 End Function
```

---

---

```

1 ' --- Export information to .mco file ---
2 Sub export()
3 Dim strFileName As String
4
5 strFileName = Application.GetSaveAsFilename_
6 (fileFilter:="MCO Files (*.mco), *.mco")
7 Open strFileName For Output As #1
8
9 'Write the other coefficients to file
10 Dim strText As String
11
12 Sheets("Other_coef").Select
13 For i = 1 To 23
14 strText = ""
15 For j = 1 To 6
16 If Not IsEmpty(Cells(i, j)) Then
17 If IsNumeric(Cells(i, j)) Then
18 If Cells(i, j) >= 0 Then
19 strText = strText & " " & Format(CDbl(Val(Cells(i, j))), "0.0000E+00")
20 Else
21 strText = strText & "" & Format(CDbl(Val(Cells(i, j))), "0.0000E+00")
22 End If
23 Else
24 strText = strText & "" & Cells(i, j)
25 End If
26 End If
27 Next
28 Print #1, strText 'Print to file without quotation marks
29 Next
30
31 'Write the number of additional static info
32 Print #1, "006$nb surf and viscous damping surfaces_
33 (rho, dCl/dalpa, Cd, A, nx, ny, nz, xc, yc, zc) "
34 Print #1, "000"
35 Print #1, "007$parameter for checking convergence (gosa0, accl) "
36 Print #1, " 0.1000E-03 0.1000E+01"
37 Print #1, "008$nb omega, omega and wave damping matrixes [C(w)] "
38 Print #1, "022"

```

```
39
40 'Write the damping coeffcients to file
41 Sheets("Damping").Select
42 For i = 1 To 154
43 strText = ""
44 For j = 5 To 10
45 If Not IsEmpty(Cells(i, j)) Then
46 If IsNumeric(Cells(i, j)) Then
47 If Cells(i, j) >= 0 Then
48 strText = strText & " " & Format(CDbl(Val(Cells(i, j))), "0.0000E+00")
49 Else
50 strText = strText & "" & Format(CDbl(Val(Cells(i, j))), "0.0000E+00")
51 End If
52 Else
53 strText = strText & "" & Cells(i, j)
54 End If
55 End If
56 Next
57 Print #1, strText
58 Next
59 Close #1
60
61 Sheets("Other_coef").Select
62
63 MsgBox ("File saved")
64 End Sub
65
66
67 Sub LoadFiles()
68
69 Dim myFile, directory, URL, text, textline, posLat As Integer, _
70 posLong As Integer
71
72 directory = "G:\Data\DNI\INTERNSHIPS\Hasan_Ozgur_Uzoguten_
73 \4_Hydrodynamics\Conventional\rao\"
74 ' "
75 Dim row As Integer
76 Dim info As String
77
```

```
78 'File name styles
79 Dim fileTypes(1 To 2) As String
80 fileTypes(1) = "ADM_0_"
81 fileTypes(2) = "DMP_0_"
82
83 row = 2 'Row to add the info
84
85 'Loop between different file name styles
86 For fileNameN = 1 To 2
87 fileN = 1
88 'Loop through the file names
89 While fileN <= 66
90 'Error handling to avoid missing file names:
91 errorH:
92 If Err.Number = 53 Then
93 Resume 1
94 ElseIf Err.Number <> 0 Then
95 Err.Raise Err.Number
96 End If
97
98 'Creating the file name
99 myFile = fileTypes(fileNameN) & fileN & ".DAT"
100 URL = directory & myFile
101
102 On Error GoTo errorH
103 Open URL For Input As #1
104
105
106 Do Until EOF(1)
107 Line Input #1, textline
108 If InStr(textline, "#") = 0 Then
109 col = 2
110 Do Until InStr(textline, " ") = 0
111 Cells(row, 1) = myFile
112 Do Until InStr(textline, " ") > 1 Or InStr(textline, " ") = 0
113 textline = Mid(textline, 2, Len(textline))
114 Loop
115 ind = InStr(textline, " ")
116 If ind = 0 Then ind = Len(textline)
```



```
117 info = Mid(textline, 1, ind)
118 Cells(row, col) = info
119 col = col + 1
120 textline = Mid(textline, ind + 1, Len(textline) - ind)
121 Loop
122 row = row + 1
123 End If
124 Loop
125 Close #1
126
127 1:          fileN = fileN + 1
128 Wend
129 Next
130
131 End Sub
```

---